UNIVERSITY OF BIRMINGHAM

Development of novel emulsion-based liquid pharmaceutical formulations to enable combination drug therapy

by

Georgia Ioanna Sakellari

A thesis submitted to
The University of Birmingham
for the degree of
DOCTOR OF PHILOSOPHY

School of Chemical Engineering
College of Engineering and Physical Sciences
University of Birmingham
March 2023

Abstract

In recent years, major healthcare and social challenges have made it even more apparent that there is a growing need for the design and development of pharmaceutical modalities with patient centricity as their mainstay. Amongst these approaches, combination drug therapy has been endorsed for the aptitude to achieve improved clinical outcomes and consolidate the patient adherence to treatment regimes. Although technological strategies that enable the co-encapsulation and co-delivery of actives from within a sole microstructure have been realised for solid dosage forms, the liquid-based co-delivery formulations portfolio remains hitherto limited.

This thesis proposes the utilisation of lipid particle-stabilised (Pickering) emulsions as a promising liquid-based structuring strategy for the segregated co-encapsulation and subsequent independent co-delivery of two active ingredients. The impact of varying lipid particle formulation characteristics and encapsulation of a hydrophobic active (curcumin) on key indicators of Pickering behaviour were initially scrutinised. Compatibility between the lipid matrix constituents was suggested as a factor greatly affecting the particles' characteristics, particularly their crystallinity. The capacity of the particles to serve as colloidal dual functional species was demonstrated, by acting as effective active carriers and release regulators of curcumin, and simultaneously stabilising o/w emulsion droplets through a Pickering mechanism. The particles maintained their dual role, irrespectively of changes in their structural properties. Alterations to the particles' formulation parameters were shown as a useful means of tuning the release performance both within dispersion and emulsion settings. Part of their functionality as Pickering stabilisers was manifested through their capacity to serve as an interfacial barrier regulating the release of an additional hydrophobic active (cinnamaldehyde)

encapsulated within the emulsion droplets. Co-encapsulation of the two hydrophobic actives did not compromise the co-delivery performance of the system, thus corroborating the appealing potential of the developed novel co-delivery formulation approach.

Acknowledgements

Reaching the end of this 4.5 year-long journey, which at times really felt impossible, I am realising how full of life-long experiences, lessons and memories this time was. It was truly one of the most mentally, physically and emotionally challenging periods of my life, but also thrilling and defining, rich with inexplicably rewarding adventures! This journey would not be the same without the people in my life, people that were there before, people I met along the way, people I hope will be with me forever.

Firstly, I would like to thank my supervisors Dr. Fotis Spyropoulos, Prof. Hannah Batchelor and for the first years of this project Dr. Ioanna Zafeiri. Fotis, you took me under your wing at a time, when giving up felt like the only option. Thank you for trusting me with such an exciting and creative project and for providing me with all these amazing opportunities I never thought were possible. You were there to listen to me, guide and advise me, at times more than just a supervisor, and for that I am forever grateful. Ioanna, my Post-Doctoral supervisor and friend, thank you for always being there for me. Your genuine love for science and research is truly inspiring. I consider myself extremely lucky to have come across such wonderful scientists and mentors, whose examples I will always seek to follow.

I would also like to acknowledge the MIBTP for accepting me into the programme and the BBSRC for the generous financial support, that not only allowed me to complete this project, but also participate in conferences and research activities that would not have been possible otherwise.

A huge thank you goes to my friends for all the good times, laughs and memorable moments, and for bearing with me during this time. My friends in Athens Antonis, Despina, Sofia, Alexandra, Nikos, Penny, Melina and my friends here Charlotte, Tom, Adam, Vini, Vasilis, and of course…. Marina. My time in Birmingham would truly not have been the same without

you my long-lost twin sister from different parents, my lab and venting buddy, my lobster. I could also not forget to mention Conor, Dom, Joe, Philip and James for keeping me company day and night throughout this project.

To my mum and dad. Your unconditional love and willingness to do anything humanly possible to always support me has been an endless source of strength for me. You taught me to always follow my dreams no matter how crazy they are, and that with hard work and perseverance anything is possible. A thank you is simply not enough. Σας ευχαριστώ για όλα όσα έχετε κάνει για μένα!

Lastly and mostly, a huge thank you goes to Freddie and Niko. Freddie, you came into my life the moment I needed you the most, and with you, you brought so much laughter and joy. Thank you for being the cutest distraction, and needless to say for your invaluable contribution during the writing stage of this thesis. And to Niko, who has been with me since the very beginning of this crazy journey, thank you for always supporting me and believing in me.

Table of Contents

List of Figures

List of Tables

Abbreviations & Acronyms

3D	Three dimensional
AFM	Atomic force microscopy
AI	Active ingredient
API	Active pharmaceutical ingredient
BSA	Bovine serum albumin
C888	Compritol® 888 ATO
CA	Cinnamaldehyde
CARS	Coherent anti-Stokes Raman scattering
CLSM	Confocal laser scanning microscopy
CMC	Critical micelle concentration
CRM	Curcumin
DLS	Dynamic light scattering
DSC	Differential scanning calorimetry
EE	Encapsulation efficiency
FDA	Food and Drug Administration
FDC	Fixed dose combination
FIB	Focused ion beam
HLB	Hydrophilic-lipophilic balance
HPLC	High-performance liquid chromatography
HPMC	Hydroxypropyl methylcellulose
HSP	Hansen solubility parameter
LC	Loading capacity

LD	Laser diffraction
LP	Lipid particles
M812	Miglyol® 812
MCT	Medium chain triglyceride
NLC	Nanostructured lipid carrier
o/w	oil-in-water
P188	Poloxamer 188
P5	Precirol® ATO 5
PBS	Phosphate buffer saline
PDI	Polydispersity index
PGPR	Polyglycerol polyricinoleate
PVA	Poly(vinyl alcohol)
RI	Recrystallisation index
SD	Standard deviation
SEM	Scanning electron microscopy
SLN	Solid lipid nanoparticle
T80	Tween® 80
TAG	Triacylglycerol
TEM	Transmission electron microscopy
USP	United States Pharmacopeia
UV-Vis	Ultraviolet-visible
w/o	water-in-oil
WAXS	Wide-angle X-ray scattering
XRD	X-Ray diffraction

Nomenclature

A	Surface area	m^2
γ	Interfacial tension	$N\ m^{-1}$
Γ_s	Surface load	$mg\ m^{-2}$
C	Concentration	$mol\ l^{-1}$
δ_D	Dispersion interactions	$MPa^{1/2}$
δ_H	Hydrogen bonding	$MPa^{1/2}$
δ_P	Permanent dipole forces	$MPa^{1/2}$
$\Delta\pi$	Osmotic pressure difference	Pa
ΔE	Detachment energy	J
ΔG_d	Free energy of displacement	J
ΔH	Molar melting enthalpy	$J\ g^{-1}$
ΔT	Temperature difference	°C
d	Density	$g\ ml^{-3}$
D	Diffusion coefficient	$cm^2\ s^{-1}$
$D_{3,2}$	Surface weighted (Sauter) mean diameter	nm
$D_{4,3}$	Volume weighted (de Brouckere) mean diameter	nm
$D_{SLN,NLC}$	Particle diameter	nm
E_h	Hydrogen bonding energy	$J\ mol^{-1}$
ζ-potential	Zeta potential	mV
F_d	Dispersion forces	$J^{½}\ cm^{3/2}\ mol^{-1}$
F_p	Polar forces	$J^{½}\ cm^{3/2}\ mol^{-1}$
η	Viscosity	Pa s

h	Thickness	m
θ	Contact angle	Degree
J	Molecular flux	g m^{-2} s^{-1}
J_p	Hydrostatic pressure difference	Pa
k	Interfacial rate constant	cm^2 s^{-1}
l	Length	m
l_p	Hydraulic membrane permeability	m^2
n	Number of terms in a series	
n_d	Number of droplets	
n_p	Number of particles	
N_A	Avogadro's number	6.02×10^{23} mol^{-1}
N_p	Number of particles per droplet	
N_t	Number of particles required to cover a droplet	
P	Partition coefficient	
r	Particle radius	nm
R	Gas constant	8.31 J K^{-1} mol
R^2	Coefficient of determination	
R_0	Radius of interaction	$MPa^{1/2}$
R_a	Distance in the HSP space	$MPa^{1/2}$
σ	Reflection coefficient	
S_d	Surface area of a lipid particle	m^2
S_p	Surface area of an emulsion droplet	m^2
t	Time	s
T	Temperature	°C

$\Phi_{SLN,NLC}$	Volume fraction	
V	Volume	cm^3
V_m	Molar volume	$cm^3\,mol^{-1}$
W	Weight	g

Chapter 1

General Introduction

1.1 Thesis background and motivation

Whether it is relevant to the collaboration between two people to accomplish a task or the combination of two technological strategies to achieve an improved outcome, the philosophy "two is better than one" has broad relevance. In this regard, within the pharmaceutical industry, specifically in the context of devising new strategies to overcome the challenges associated with diseases that are classed as difficult to treat, the benefits of combining two drugs have attracted increased interest in the last couple of decades. This treatment modality, widely known as combination drug therapy, has in many instances substituted the use of conventional single drug approaches, thereby improving treatment response, minimising drug resistance, diminishing adverse effects and enhancing patient treatment compliance. As of 2019, the Food and Drug Administration (FDA) was anticipating an ever-increasing number of combination products to be submitted for review, owing to the rapid scientific and technological advances, thus providing an impetus to overcome challenges concomitant with their regulatory and policy requirements [1].

Within the combination therapy arena, fixed dose combination (FDC) drugs, where two active ingredients are combined within the same formulation vehicle, have emerged as attractive alternatives to traditional treatment methods. Particularly in the case of infectious diseases such as human immunodeficiency virus [2], tuberculosis [3] and malaria [4], they even constitute the primary treatment route. As with any other drug development pathway, the overarching rationale is to target and address all patients' needs, entailing the minimisation of the demands' diversity and added complexity of formulating two or more active ingredients into a single dose. In the interest of pharmaceutical companies and FDC product developers to be able to develop effective and efficient business models to tackle these impediments, but also of shortening the

prolonged approval times (12–15 years [5]) of new active pharmaceutical ingredients (APIs) and providing patients promptly with efficacious treatment options, the focus has shifted towards the development of new technologies and methodologies to combine already existing and pre-approved APIs [6].

Amongst these tactics are processing methods and formulation strategies, that have hitherto been predominantly realised for solid dosage forms (i.e. tablets, pills, capsules) and significantly less so for liquid-based formulations (i.e. solutions, suspensions, emulsions), omitting to meet a considerable market need. Paediatric and geriatric patient populations, along with people that struggle to adhere to solid dosage forms (e.g. patients with dysphagia) represent a big portion of said market. The lack of suitable dosage forms in tandem with the risks bestowed by using existing formulations, the latter arising from the practice of crushing tablets and splitting pills to prepare suspensions of appropriate dose [7], have made it apparent that there is a momentous drive towards the adoption of a patient-centric and patient-tailored formulation development viewpoint.

Regardless of whether it is relevant to single or multiple encasement of actives, current approaches employed in liquid formulations that contain a lipid phase play a principal role, as they can be used to address hurdles commonly encountered with the encapsulation and subsequent delivery of poorly water-soluble actives. Considering that the vast majority of APIs are small hydrophobic molecules, and aiming to devise strategies that can enable their enhanced adsorption and improved bioavailability, emulsions are microstructures that have over the years manifested their appropriateness as active carriers and delivery systems in a plethora of already marketed products. Although their attributes extend even further than the ease of preparation and multiphase features, there are still issues related to destabilisation phenomena and short

shelf-life of the formed systems. Additionally, pertaining to their utilisation within FDC drugs, it is envisaged that the developed emulsion-based formulation can facilitate the compartmentalised encapsulation of the two (or more) actives, to diminish any detrimental interactions between them, and potentially and more crucially to accommodate their independently controlled delivery.

To this end, emulsion stabilisation by colloidal solid particles (Pickering emulsions), rather than conventional emulsifiers, can not only convey superior protection against destabilisation mechanisms, but also it can introduce into the system the co-presence of two physically different phases (i.e. the liquid phase as a result of the emulsion droplet presence and a crystalline phase on account of the solid particle existence). The utilisation of such a platform, whereby the two segregated actives are contained within two phases with varying structural characteristics could potentially enable the independently tuned performance of each segment, and consequently of each active encapsulated within them. Such novel structuring strategies employing biorelevant Pickering particles, have already demonstrated their aptitude in expanding current liquid-based formulation portfolios [8,9], although still at an exploratory level.

Designing, fabricating and understanding the behaviour of these complex emulsion architectures at all stages of the formulation process, to contrive the tools to ultimately appropriately manipulate and control their performance as a co-encapsulation and co-delivery platform was the pivotal driver of this project.

1.2 Aims and objectives

The overall aim of this project was to design and instigate a structuring strategy that could be utilised to enable the segregated co-encapsulation and subsequent independent co-delivery of two active ingredients from a liquid-based formulation system. The approach adopted was lipid particle-stabilised o/w emulsions, with a large portion of the work focusing on the capacity of the developed lipid particulates to manifest the dual functionality of concurrently stabilising o/w emulsion droplets through a Pickering mechanism and acting as effect active carriers and release regulators of an active.

This project was realised through the delivery of the following objectives:

- Fabricating and characterising lipid particles with varying formulation parameters and studying how these parameters affect characteristics associated with their active carrying and Pickering functionalities;
- Confirming the Pickering stabilisation capacity of the lipid particles and understanding how changes in their formulation aspects influence said performance;
- Exploring the capability of the previously developed particles to regulate the release of a model hydrophobic active encapsulated within them, while attempting to propose a mechanism for their behaviour;
- Investigating the ability of the particles to control the co-encapsulation and co-release behaviour of two model hydrophobic actives encapsulated within the two physical different compartments offered by the developed approach (i.e. lipid particles and emulsion droplets), and devising approaches to tune the attained release profiles.

1.3 Thesis layout

This thesis is organised into seven chapters. The four experimental chapters (Chapters 3, 4, 5 and 6) are written in the style of peer-reviewed publications, and are composed of an introduction, materials and methods, results and discussion and conclusions section. An appendix including supportive data is also provided where necessary, at the end of the chapter. A synopsis of each chapter is presented below:

Chapter 1: General Introduction

The chapter introduces the background and motivation, along with the aims and objectives of the work presented in this thesis. An outline of the chapters to follow is also presented, and information regarding the dissemination of this work is provided.

Chapter 2: Literature Review

This chapter provides an overview of the scientific knowledge and current understanding of the design and development of formulations utilised for co-encapsulation and co-delivery purposes. This review specifically focuses on Pickering emulsions and lipid particle dispersions and the characteristics that can render them effective carrier and delivery systems, as this was the premise for the work that follows.

Chapter 3: Formulation design and development of lipid particles loaded with a hydrophobic active

The work in this chapter explores the design and fabrication of solid lipid nanoparticles and nanostructured lipid carriers used as carriers of a model hydrophobic active. The effect of

different formulation variables on lipid particle characteristics that are associated with both their Pickering functionality and active carrying capacity is considered.

Chapter 4: Lipid particles of dual functionality at emulsion interfaces. Part I: Pickering functionality

This chapter is the first segment of a two-part study that investigates the aptitude of solid lipid nanoparticles and nanostructured lipid carriers to exhibit the dual functionality of simultaneously acting as Pickering stabilisers and as active carriers/release regulators of a model hydrophobic active. Part I focuses on the Pickering stabilisation capability of the lipid particles and how certain formulation parameters can impact upon the particle properties that endow this functionality.

Chapter 5: Lipid particles of dual functionality at emulsion interfaces. Part II: active carrying/delivery functionality

In this chapter, the second part of the aforementioned study is presented. The focus shifts on confirming the second concurrent active carrying and delivery functionality of both solid lipid nanoparticles and nanostructured lipid carriers. The influence of lipid particle formulation parameters on said capacity is investigated, and a mechanism relevant to the release regulation capability of the particles once introduced within the emulsion setting is proposed.

Chapter 6: The impact of the interfacial architecture on the release and co-release from lipid particle-stabilised emulsions

The final experimental chapter assesses how certain lipid particle compositional changes can influence the release behaviour of both particle types within dispersion and emulsion settings. It then proceeds to study the co-release performance of two model hydrophobic actives

separately encapsulated within the particle-stabilised o/w emulsions, and scrutinise approaches to regulate the active release rate.

Chapter 7: Concluding remarks and future recommendations

This chapter summarises the conclusions drawn from the results presented throughout the thesis, and deliberates future work on the basis of potential applications.

1.4 Dissemination of research work

The research presented in this thesis has been disseminated through a variety of mechanisms, including conference oral and poster presentations, and publications. Details for each of these dissemination activities are given below:

Presentations:

- G.I. Sakellari, I. Zafeiri, H. Batchelor, F. Spyropoulos. "A study of lipid-based systems with potential application in multiple delivery in pharmaceutical formulations". Oral presentation for the *Young Lipid Scientist Award*, SCI, virtual participation, June 2020
- G.I. Sakellari, I. Zafeiri, H. Batchelor, F. Spyropoulos. "Formulation development of lipid nanoparticles with potential application in multiple delivery in pharmaceutical formulations". Oral presentation at the *International Conference on Formulations in Food and Healthcare*, virtual participation, March 2021
- G.I. Sakellari, I. Zafeiri, H. Batchelor, F. Spyropoulos. "Lipid nanoparticles for the development of liquid pharmaceutical formulations able to carry/deliver multiple

actives". Oral presentation at the *35th Conference of the European Colloid & Interface Society*, virtual participation, September 2021

- G.I. Sakellari, I. Zafeiri, H. Batchelor, F. Spyropoulos. "Lipid nanoparticles of dual functionality for the development of emulsion formulations able to carry/deliver multiple actives". Poster presentation at the *Formulating colloids – innovation and disruption (Graham Award Symposium 2021)*, SCI, London, April 2022
- G.I. Sakellari, I. Zafeiri, H. Batchelor, F. Spyropoulos. "Lipid nanoparticles of dual functionality for the development of multiple delivery formulations". Oral presentation for the *Young Lipid Scientist Award*, SCI, London, June 2022
- G.I. Sakellari, I. Zafeiri, H. Batchelor, F. Spyropoulos. "Lipid nanoparticles of dual functionality for the development of multiple delivery formulations". Oral presentation at the *2nd Edible Soft Matter Workshop & Conference*, Wageningen, July 2022
- G.I. Sakellari, I. Zafeiri, H. Batchelor, F. Spyropoulos. "The role of lipid nanoparticles in the development of liquid formulations able to carry/deliver multiple actives". Oral presentation at the *8th International Conference on Food Chemistry and Technology*, Rome, October 2022

Publications:

- G.I. Sakellari, I. Zafeiri, H. Batchelor, F. Spyropoulos, Formulation design, production and characterisation of solid lipid nanoparticles (SLN) and nanostructured lipid carriers (NLC) for the encapsulation of a model hydrophobic active, *Food Hydrocolloids for Health*. (2021) 100024

- G.I. Sakellari, I. Zafeiri, H. Batchelor, F. Spyropoulos, Solid lipid nanoparticles and nanostructured lipid carriers of dual functionality at emulsion interfaces. Part I: Pickering stabilisation functionality, *Colloids and Surfaces A: Physicochemical Engineering Aspects*. (2022) 130135
- G.I. Sakellari, I. Zafeiri, H. Batchelor, F. Spyropoulos, Solid lipid nanoparticles and nanostructured lipid carriers of dual functionality at emulsion interfaces. Part II: active carrying/delivery functionality, *Colloids and Surfaces A: Physicochemical Engineering Aspects*. (2023) 130787
- G.I. Sakellari, I. Zafeiri, H. Batchelor, F. Spyropoulos, The impact of interfacial architecture on the release and co-release from lipid-particle stabilised emulsions, *Journal of Controlled Release*, in preparation

References

[1] U.S. Food & Drug Administration, About Combination Products, (2019). https://www.fda.gov/combination-products/about-combination-products (accessed February 17, 2023).

[2] L. Oversteegen, M. Shah, H. Rovini, HIV combination products, Nat Rev Drug Discov. 6 (2007) 951–952. https://doi.org/10.1038/nrd2448.

[3] World Health Organisation, WHO consolidated guidelines on tuberculosis. Module 4: treatment - drug-resistant tuberculosis treatment, 2022 update, (2022). https://www.who.int/publications/i/item/9789240063129 (accessed February 17, 2023).

[4] World Health Organization, Artemisinin resistance and artemisinin-based combination therapy efficacy (December 2018), 2018.

[5] J.P. Hughes, S.S. Rees, S.B. Kalindjian, K.L. Philpott, Principles of early drug discovery, Br J Pharmacol. 162 (2011) 1239. https://doi.org/10.1111/j.1476-5381.2010.01127.x.

[6] Pfizer, Making a case for a fixed dose combination drug strategy, (2016). https://www.pfizercentreone.com/insights-resources/articles/making-case-fixed-dose-combination-drug-strategy (accessed February 17, 2023).

[7] H.K. Batchelor, J.F. Marriott, Formulations for children: problems and solutions, Br J Clin Pharmacol. 79 (2015) 405–418. https://doi.org/10.1111/bcp.12268.

[8] F. Spyropoulos, D. Kurukji, P. Taylor, I.T. Norton, Fabrication and Utilization of Bifunctional Protein/Polysaccharide Coprecipitates for the Independent Codelivery of Two Model Actives from Simple Oil-in-Water Emulsions, Langmuir. 34 (2018) 3934–3948. https://doi.org/10.1021/acs.langmuir.7b04315.

[9] G.I. Sakellari, I. Zafeiri, A. Pawlik, D. Kurukji, P. Taylor, I.T. Norton, F. Spyropoulos, Independent co-delivery of model actives with different degrees of hydrophilicity from oil-in-water and water-in-oil emulsions stabilised by solid lipid particles via a Pickering mechanism: a-proof-of-principle study, J Colloid Interface Sci. 587 (2021) 644–649. https://doi.org/10.1016/j.jcis.2020.11.021.

Chapter 2

Literature Review

Synopsis

This chapter outlines the main considerations implicated in the design and formulation of vehicles used for co-encapsulation and co-delivery purposes. Solid and liquid state approaches currently utilised are presented, and the underlying mechanisms involved in their employment as encapsulants and controlled delivery systems are discussed. Special focus is paid to liquid formulations and particularly to Pickering emulsion systems. Therein, the requirements concerned in providing effective Pickering stabilisation with respect to the particles are examined, along with the current trends in their utilisation as delivery and co-delivery systems. Part of this literature review is dedicated to solid lipid nanoparticles and nanostructured lipid carriers, two lipid particle counterparts. The formulation parameters, defining characteristics and performance as carrying and delivery systems are delineated, in an endeavour to set the scene for the experimental Chapters 3, 4, 5 and 6.

2.1 Co-encapsulation and co-delivery

The terms co-encapsulation and co-delivery are predominantly used to describe the inclusion and subsequent release, respectively, of more than one active ingredients from within the same microstructure. The design and development of vehicles that can enable the co-encapsulation and co-delivery of multiple actives have gained increased research interest in the last few decades, with the developed formulations finding a wide range of applications in various sectors. Although the mechanisms and approaches to successfully encapsulate and control the release of a single active have been extensively studied within the formulation research field, inclusion of a secondary species can introduce further hurdles to such endeavour. Said challenges could relate to either of the two aspects involved in this approach. Referring to encapsulation as the first facet, the development of the carrier structure should ensure that the enclosed species are incorporated in such way, either co-localised or segregated, that the optimal interactions between the actives are permitted. Correspondingly, the second element of the succeeding active delivery has to also be considered, as each of the encapsulated species needs to be individually released in a controllable and independent manner.

With the recent emergence in the range of applications requiring the employment of formulations that can accommodate these co-encapsulation and co-delivery demands, the different types of formulation platforms have also expanded to include both solid and liquid dosage forms. The applications portfolio, the types of co-encapsulation, along with currently available multiple encapsulation and delivery platforms are delineated in the following sections, where special attention is given on the use of liquid formulations as carrier and delivery systems.

2.2 Applications of co-encapsulation and co-delivery systems

Although deep-rooted in pharmaceutical applications [1,2], the benefits proffered by multiple encapsulation and delivery systems have been discerned and harnessed by other adjacent industries that utilise formulation design to deliver active ingredients, such as agrochemicals [3–5], cosmetics [6] and food products [7,8]. The advantages of the utilisation of a single multi-active delivery formulation extend further to the apparent ease conferred by the concurrent delivery of more than one active ingredients (AIs). The co-existence of multiple actives within a sole vehicle has been shown to give rise to synergistic or additive effects between the encapsulated species, thereby enhancing their bioactivity and overall efficacy of the formulation [9,10]. Therefore, considering the overarching aspiration of designing and developing products of high value that can bestow the highest efficiency on the encapsulated actives, the fundamental understanding and formulation knowhow of an effective multiple encapsulation and delivery system development has been a cross-sectoral venture.

In pharmaceuticals, the use of fixed dose combination (FDC) drugs, where multiple therapeutic cargos are combined within the same carrier, as a treatment modality in combination therapy, has proven to be an effective substitute of single therapeutics that fail to demonstrate the desired clinical outcomes and treatment compliance, by minimising adverse reactions and drug resistance [11]. Estimating the timescales over which a newly designed drug is expected to enter the pharmaceutical market (approximately 15 years) [12], along with the cost of new AI development [13] has led an increasing number of treatment regimen to turn into FDC therapy usage. More specifically, FDCs are currently used in the treatment of a wide range of diseases to achieve better therapeutic effects and surmount treatment resistance, along with providing better tolerability, elongated product life-cycle management and cost savings, including but not

limited to cancer [14], cardiovascular diseases [15], viral infections [16] and type 2 diabetes [17]. In agrochemicals, the simultaneous delivery of AIs, such as multiple fungicides [18] or pesticides [4] to mitigate long term single active resistance or to diminish the excessive use of AIs that can cause harm to human health or the natural ecosystems [19] has already been utilised as a successful approach. Similarly in cosmetics and personal care products, the combination of two or more AIs of the same or different classes that can however demonstrate synergistic effects has been employed for the development of a safer and more efficient sunscreen [20], skin protecting [21], anti-aging [6] and hair regrowth [22] products. Lastly, within foods the employment of co-delivery systems is gaining a growing interest, particularly due to the rise of nutraceuticals and functional foods that have been proposed as nature-derived alternatives to traditional medicinal methods of treating diseases [23,24], while also serving personalised nutrition needs [25].

The range and effectiveness of multiple delivery applications has extensively expanded with the utilisation of a greater range of active types, as the level of synergy and overall functionality of the formulation greatly depends on the selection of the right combination of compounds (e.g. inclusion of a second active that minimises the adverse effects or enhances the benefits of the first), that also have the optimal concentration to show positive associations [7]. As mentioned above, a single co-delivery vehicle can contain two or more AIs of the same or even different classes. Within the former category, multiple active pharmaceutical ingredients (APIs), such as isoniazid and rifampicin have been used in dual combination formulations for the treatment of tuberculosis [26], and doxorubicin and verapamil acting as chemosensitizers [27], among a myriad of examples. Analogously, two microbial agents, nisin and garlic extract were co-encapsulated and assessed for their potential application as biopreservatives in the food industry [28], as were two phenolic antioxidant compounds, curcumin and resveratrol with capacity to

prevent and treat diseases associated with oxidative stress within functional foods [29]. As for the latter class, the combination of different classes of AIs, such as doxorubicin, an effective anti-cancer agent used in chemotherapy and an antioxidant such as curcumin [30,31], or plasmid DNA and bovine serum albumin (BSA) protein for co-delivery to plant cells [32] has also been widely explored. The diversity in AIs can stretch between lower (e.g. terpenes) commonly used as flavourings and odour masking agents [33] to considerably higher molecular weight (e.g. siRNA, plasmid DNA [34]) molecules, from hydrophobic [35] to hydrophilic [36] compounds or even combinations of them [9]. However, apart from the specific AI selection, it is also the interplay between the formulation components/type and the encapsulated cargos that can dictate the overall performance of the final system.

2.3 Types of single and multiple active encapsulation

Regardless of whether it is relevant to single or multi-active incorporation, encapsulation is generally used to describe the encasement of an active ingredient within a carrier structure [37]. The purpose of encapsulation is not only to preserve the entrapped AIs' properties and protect them from physical or chemical degradation processes that may occur during the manufacturing, storage or end-use stage, but also to deliver them in a controlled and potentially triggered and targeted manner. Additionally in many industrial applications, encapsulation is used as a means of hiding/masking undesirable AI characteristics [38], or even changing the physical attributes of the resulting formulation [39]. In terms of the techniques utilised, chemical and physical encapsulation are the two main categories, with the key differentiation lying on the design at a chemistry basis versus the mechanical processing involved, respectively. Briefly, the chemical encapsulation includes methods such as coacervation [40], molecular inclusion [41], solvent evaporation [42] and co-crystallisation [43], while the

physical or otherwise known as mechanical encapsulation encompasses processes like spray-drying [44], extrusion [45], freeze-drying [46] and fluidised bed coating [47], among others [48]. In some instances, these techniques have been used in pairs, usually employing the secondary technique as a method to eliminate the disadvantages of the first, while still exploiting its benefits. For example, emulsification and spray drying have been explored for their potential to overcome known instability issues of double emulsions for the encapsulation of naturally derived polyphenols from rosemary leaves [49]. In another study [50], emulsification/internal gelation followed by spray/freeze-drying exhibited capacity to enhance the stability of anthocyanins and their post-treatment retention.

A general description of the location of the active agent(s) in relation to the matrix components is provided in Fig. 2.1, where three types of encapsulation are illustrated [51]. In the reservoir type, also known as core-shell type, a shell of the carrier material is created around the AI, that functions as a barrier against the release and/or exposure of the active to the surroundings. Multiple reservoir chambers can co-exist within the same particle. In contrast, the AI is more homogeneously dispersed in the carrier material or even at the surface, in the matrix type. The amalgamation of these two forms of encapsulation results in the coated matrix type, where the AI is dispersed in the carrier material, while an additional external coating is also present. The resultant morphology in respect of the encapsulation type, but also the particle size and encapsulation load expressing the percentage of AI entrapped within the microstructure, are greatly reliant on the encapsulation technology and the specific materials used.

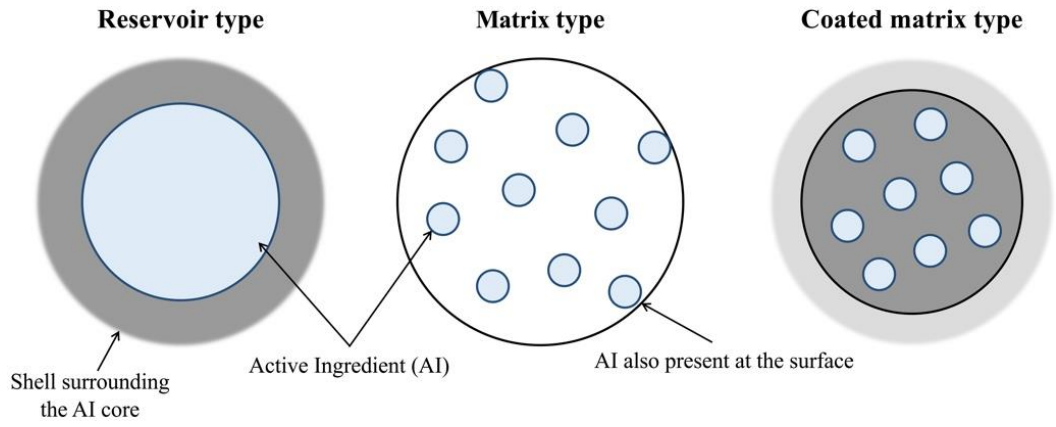

Fig. 2.1. Types of encapsulation in colloidal systems (adapted from Zuidman *et al.* [51]).

The terms co-encapsulation, multiple encapsulation or multi-active encapsulation are merely used to describe the entrapment of multiple actives within the same formulation. The encapsulation techniques mentioned above can also be applied for co-encapsulation, though, different ones might be employed for each active, which will depend on the specific physicochemical characteristics of the components, among other reasons. Regarding the relative arrangement of the AIs within the microstructure, the various species can either be co-localised within the same area of the structure or contained separately, which is commonly referred to as segregated or compartmentalised co-encapsulation. The chemical compatibility between the carrier materials and the AIs, but also the AIs themselves is a crucial parameter that can dictate their relative placement, and in turn control aspects ranging from how efficiently the encapsulated species will be retained to what is the mechanism that these enclosed agents will be released under defined conditions. Therefore, segregation of the functional molecules is usually the preferred method, as it eradicates detrimental interactions between the entrapped species. Although fine tuning of the processes involved in the development of a carrier system appear as a relatively straightforward task when it comes to single encapsulation/delivery, introduction of a second (or even more) active(s) can present further challenges. Amongst these

is the divergence in the physicochemical properties of the AIs (e.g. hydrophobicity, polarity, solubility, molecular weight), which as mentioned earlier is quite a frequent phenomenon (Section 2.2). Lopes *et al.* [52] co-encapsulated lysozyme and nisin in liposomes coated with polysaccharides, and reported that interactions such as H-bonding, hydrophobic and electrostatic interactions are occurring for both actives, implying that the two AIs were co-localised in the hydrophobic portion of the microstructure. In contrast, Liu *et al*. [53] harnessed the co-existence of the lipid bilayer (hydrophobic part) and the aqueous cavity (hydrophilic part) in liposomes to co-encapsulate *β*-carotene (hydrophobic AI) and vitamin C (hydrophilic AI) in the respective environments. In another study [54], a relatively large molecule (siRNA) and a smaller anticancer drug (paclitaxel) were co-entrapped in cationic liposomes, with the former being stabilised via electrostatic interactions in the hydrophilic cores and the latter located in the hydrophobic fraction of the liposomes. Chen *et al*. [55] developed a triple emulsion (water-in-oil-in-(oil-in-water)) with a highly compartmentalised structure for the segregated co-encapsulation of three photosensitive compounds with varying degrees of hydrophobicity. These are typical examples of co-localised or segregated encasing of AIs, and although all could potentially lead to triggered and controlled release, given suitable formulation design, the AIs are limited to either simultaneous or sequential delivery rather than independently modulated and/or triggered [56]. Thus, it is apparent that the dominating factor that will control the location and underlying mechanism of the actives' partitioning within the microstructure, and ultimately their delivery under defined conditions, is the finetuning between formulation design and processing. The choice of formulation type and method used will have to serve constraints set by the scale and cost of production, accommodate the physicochemical requirements of the specific AIs, as well as fulfil the delivery performance and final product application needs.

2.4 Mechanisms to control delivery

The delivery of the encapsulated active species to the target site (e.g. specific organ, tissue, cell) in a controlled and, if desirable, in a triggered and targeted manner is a crucial aspect in the formulation development process. Depending on the type and intended function of the active agent, the objectives of the delivery system relevant to the AI, can include controlling the temporal exposure, facilitating physiological barrier crossing, protecting from untimely elimination, minimising undesired exposure and guiding the AI to the target location. Fulfilment of these objectives can enhance the performance of the system and lead to improved efficacy and treatment results. The strategies devised to attain triggered and controlled release of the single or multiple encapsulated species, in a temporal and/or spatial manner, can be of biological, physicochemical and/or mathematical basis [57].

Before delving into the mechanisms that can control the active release, either solely or jointly, a clear distinction between the terms commonly deployed to describe release needs to be made. The terms controlled or modified are used, most of the times interchangeably, to characterise release systems, where the active discharge is occurring in an altered rate (faster or more sustained) compared to the control formulation. In regard to the course of co-delivery, AIs can either be delivered simultaneously or sequentially, in an independent or interlinked mode. Concerning the latter, the occurrence of co-dependence in the co-release profiles of multiple actives is usually a facet attributed to the delivery vehicle, that could subsequently result in issues with distinct controlled/triggered release of the individual AIs [58]. Lastly, targeted and triggered active discharge, although broadly fall into the controlled release category, they in fact refer to more specific concepts. Targeted release is related to the transport and deposition of the AIs to a specific target site, while triggered delivery delineates the release of the AIs as

a response to changes in the environmental conditions (e.g. pH, temperature, solvent). The above-outlined terms could be illustrated in a co-encapsulation/co-delivery concept of two AIs from a formulation intended for oral drug delivery would be a microstructure, that can release a taste masking agent (first active) as a response to temperature in the oral cavity immediately after administration, and an anti-inflammatory drug (second active) in a sustained manner in the upper small intestine. This practical example showcases the range of functionalities of a co-delivery system, whereby both actives are delivered at different targeted sites in a temporally controlled way, having independent and separately triggered release profiles.

The main mechanisms that can be implemented to control the AI release from a delivery or multi-delivery system are outlined below [59,60].

2.4.1 Dissolution

The dissolution process entails the transfer of molecules from the core of the delivery vehicle (i.e. dispersed phase) to the surrounding phase (i.e. continuous phase), due to solubilisation of the wall material in the dissolution medium, resulting in the release of the AI contained within the core structure. As more core material is solubilised in the dissolution medium solvent, the concentration of AI in the medium also increases, thus creating a boundary layer around the solid core. This boundary layer is characterised by an increased dissolution rate and solubility concentration close to saturation. Elimination of the boundary layer causes solvent renewal, ultimately increasing the dissolution rate, which is calculated as follows:

$$\frac{dC}{dt} = \frac{D\,A}{Vl}(C_l - C_s) \qquad (2.1)$$

where D is the diffusion coefficient of the AI, A is the surface area of the core, l is the thickness of the boundary layer, V is the volume of solution, C_l is the inner portion of the boundary layer concentration, and C_s is the concentration at the outer portion of the boundary layer (Fig. 2.2). Consequently, the dissolution rate is dependent on the size of the delivery vehicle, the characteristics of the dissolution medium (e.g. viscosity and temperature) and kinetic properties occurring during dissolution, such as agitation conditions. Additionally, the affinity and solubilisation capacity of the dissolution medium for the AI can also affect the dissolution rate [59]. Particles coated with low solubility polymeric membranes or effervescent tables are characteristic dissolution-controlled delivery systems [61].

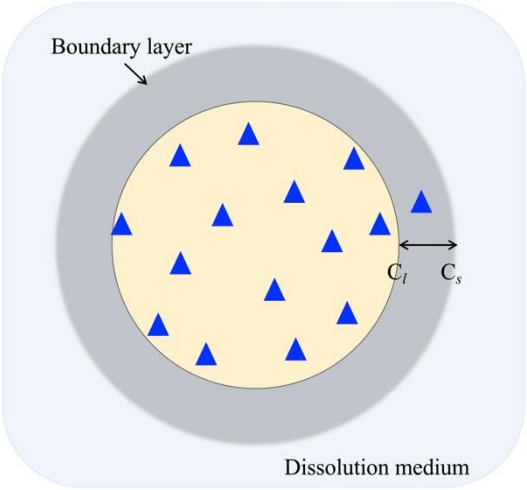

Fig. 2.2. Dissolution process from a solid core to the outer dissolution phase, depicting the formation of a boundary layer around the core of the matrix and the presence of two AI concentration areas; C_l: inner portion of the boundary layer and C_s: outer portion of the boundary layer (adapted from Siepmann *et al.* [62]).

2.4.2 Diffusion

The concentration gradient between two areas of a system can give rise to mass transfer phenomena of AI molecules from one area to the other, through spontaneous mass flux (Fig. 2.3). This kinetic process, where molecules move in random directions is known as diffusion, and it can take place in systems that are not in equilibrium. According to Fick's laws, the molecular flux is proportional to the gradient concentration:

Fick's 1st law $$J = -D\frac{dC}{dx} \quad (2.2)$$

Fick's 2nd law $$\frac{dC}{dt} = -D\frac{d^2C}{dx^2} \quad (2.3)$$

where *J* is the rate of transfer per unit area of the section, *C* is the concentration of the AI diffusing, *x* is the distance between two points and *D* is the diffusion coefficient. When the diffusion from a system follows Fick's laws is called Fickian diffusion, while in the opposite case, it is classified as non-Fickian or anomalous diffusion. *D* is the measure of the AI molecule's mobility within the system, and is affected by external conditions, such as temperature, pressure, solvent characteristics, AI concentration and chemical interactions, as it is driven by Brownian motion. In very diluted solutions, *D* can be considered as constant, otherwise it depends on concentration [63]. The diffusion coefficient can be calculated using the Stokes-Einstein equation with appropriate adjustments to account for changes in the shape of the particle/molecule. For spherical particles/molecules:

$$D = \frac{RT}{6\pi\eta r C N_A} \quad (2.4)$$

where R is the gas constant, T is temperature, η is viscosity, r is the particle radius and N_A is Avogadro's number. According to the above, the diffusion coefficient of a molecule within a system is highly dependent on the properties of the vehicle, with *Crank* [63] describing a wide range of initially and boundary conditions.

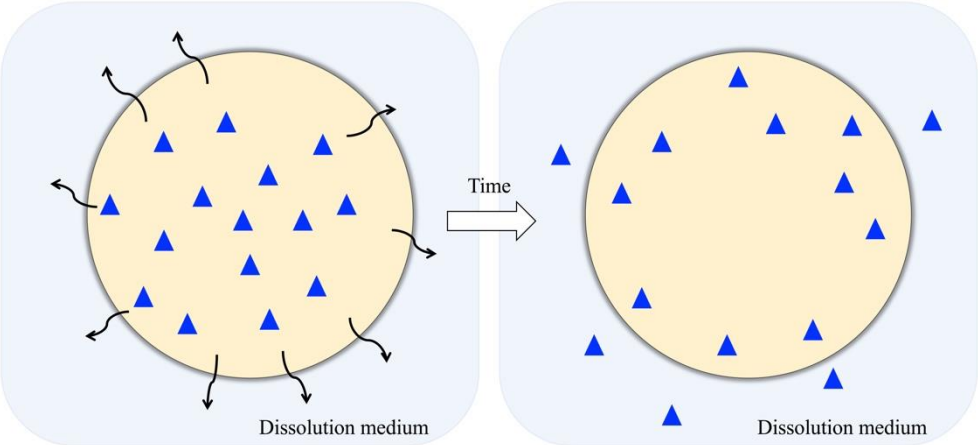

Fig. 2.3. Overtime diffusion of active molecules from within the core of a spherical vehicle to the external dissolution medium, driven by the concentration gradient.

2.4.3 Partitioning

Interfaces between two different wall materials or system phases can instigate partitioning of the active agent between the two. The distribution of a solute between the two phases is expressed as partition coefficient (P), which is essentially used as a measure of the relative affinity of the AI between the two phases and can be calculated as follows:

$$P = \frac{C_2}{C_1} \tag{2.5}$$

where C_1 and C_2 are the active concentrations in the hydrophilic and hydrophobic phases, respectively (Fig. 2.4). The partition coefficient is usually reported as log*P*. Control over the release performance can be attained by manipulating the partitioning rate of the AI within the core structure [64].

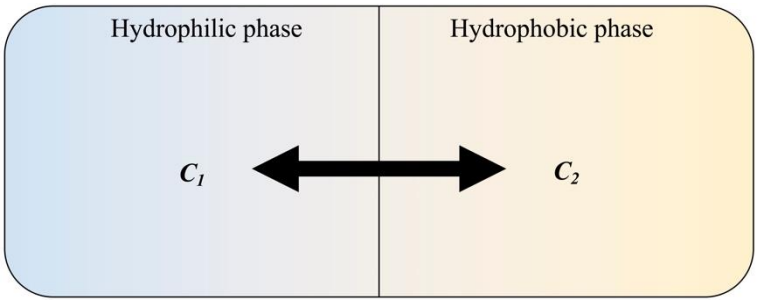

Fig. 2.4. Partitioning of active between two phases, with C_1 representing the concentration in the hydrophilic phase and C_2 the concentration in the hydrophobic phase (adapted from Bruschi *et al.* [59]).

2.4.4 Osmosis

The presence of two phases separated by a semipermeable membrane can allow the flow of solvent molecules from the more AI-concentrated side to the less concentrated one, until a concentration equilibrium is reached (Fig. 2.5). The osmotic pressure difference, which is the driver to this process is influenced by both the AI concentration and the AI/solvent compatibility. The volume flow of solvent describing the rate of transport through the membrane is given by [65]:

$$\frac{dV}{dt} = \frac{A}{h} l_p(\sigma \Delta\pi - J_p) \qquad (2.6)$$

where A is the cross-sectional area of transport, h is the membrane thickness, l_p is the hydraulic membrane permeability, σ is the reflection coefficient, $\Delta\pi$ is the osmotic pressure difference across the membrane and J_p is the hydrostatic pressure difference across the membrane. Typical examples of osmotic-controlled release are polymer coated systems, where the coating can act as a semipermeable membrane allowing the flow of solvent and subsequent dissolution of the AI, which can then be release through the pores into the dissolution medium [66].

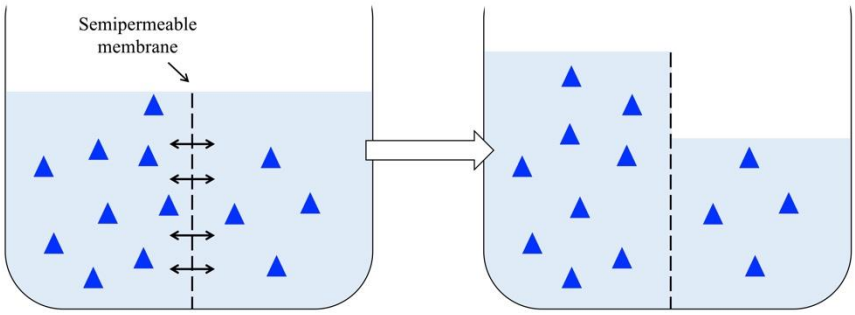

Fig. 2.5. Schematic diagram showing the osmosis induced transfer of solvent through a semipermeable membrane.

2.4.5 Swelling

Certain hydrophilic-nature wall materials, such as hydrogels, when exposed to an aqueous phase can exhibit swelling, due to the association, dissociation, and binding of various ions to polymer chains. There are two reverse forces that determine the equilibrium status of a hydrogel swollen in a fluid; the thermodynamic force of mixing governed by the compatibility between the polymer and the solvent, and the stored force, one favouring and the other hindering swelling, respectively. The degree of expansion of the polymeric network due to swelling can be utilised as a control over active release (Fig. 2.6). In some instances, swelling can be followed by dissolution depending on the relative compatibility between the used polymer and

water. In other cases, the integrity of the structure can remain intact after swelling, and the release mechanism can be a combination with diffusion of the active through the swelled network [67].

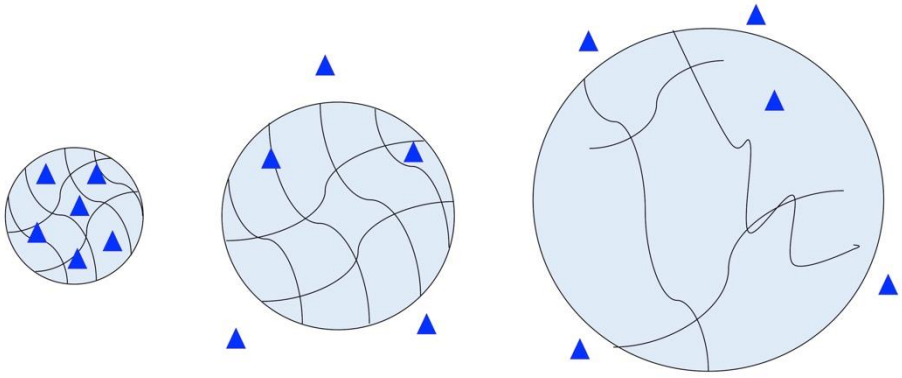

Fig. 2.6. Changes in the structure of a hydrogel due to swelling, that overtime can lead to less obstructed diffusion of the active in the dissolution medium (adapted from Sheth *et al*. [67]).

2.4.6 Erosion and degradation

Certain systems can respond to external stimuli (e.g. hydrolytic or enzymatic response) and release the encapsulated species due to erosion or degradation of the wall materials comprising the core, through a chemically induced process. For example, bioerodible systems contain hydrolytically or enzymatically labile bonds that can be cleaved by certain enzymes or chemical groups into smaller molecules that are readily water soluble. The release rate of the encapsulated species is then controlled by the hydrophilicity and porosity of the vehicle. For polymeric-based systems, erosion can be categorised into surface erosion, describing a phenomenon that begins at the surface and overtime moves towards the centre of the core, or bulk erosion that although begins at the surface, it tends to spread rapidly throughout the entire core [60]. However, due to the temporal nature of erosion/degradation, other mechanisms can

simultaneously drive release (e.g. diffusion). Apart from polymers [68], lipid-based systems can also demonstrate degradation-induced release, an example of this being the phospholipase lipid hydrolysis of ester bonds of a lipid-containing polymerosome vehicle, that could be also potentially used as a mechanism to achieve sustained release
(Fig. 2.7) [69].

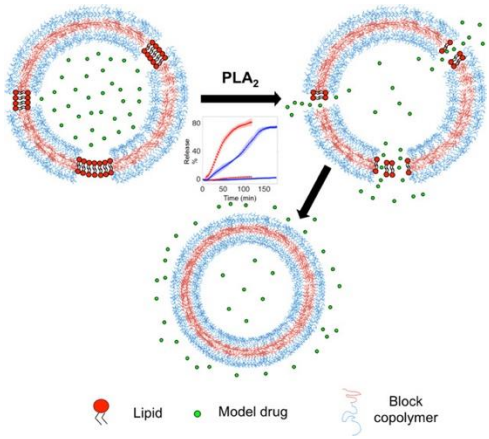

Fig. 2.7. Schematic representation of the phospholipase lipid hydrolysis of a lipid-containing polymerosome vehicle resulting in release of the encapsulated species [69].

2.4.7 Changes to environmental conditions

Manipulation of environmental conditions, including pH and temperature among others, can also be employed for the control of the obtained release profiles. Utilisation of wall materials with appropriate response to temperature increase (e.g. lipids with specific melting point [70]) or alteration in the environmental pH (e.g. protein/polysaccharide complexes [56]) can result in delivery vehicles with controlled and triggered release performance at specific target sites.

2.5 Types of formulations used for co-encapsulation and co-delivery systems

Among the formulation design and development considerations of a delivery or co-delivery system is the physical form of the final product. The majority of the formulations range from solid and semi-solid to liquid and semi-liquid forms, depending on the choice of materials and formulation techniques, but most importantly considering the end application, stability, transportation and storage conditions. Research efforts have primarily focused on solid formulations due to the advantages of longer shelf life, accurate dosage and ease of manipulation [71,72]. Thus, there is growing evidence supporting the realisation of co-encapsulation and co-delivery in these systems, using various approaches, like 3D printing [73]. Conversely, liquid formulations tend to be less favoured, although they can offer benefits such as dosage flexibility, rapid absorption and better patient compliance when used in pharmaceuticals and nutraceuticals [74–76] and easier scale-up and applicability for agrochemicals [77]. The challenges that liquid formulations are associated with are usually relevant to compromised stability, manufacturing complexity and cost [78,79]. However, given the appropriate formulation development, said hurdles could be overcome and outbalanced by the aforementioned merits. In the following sections, co-encapsulation and co-delivery approaches from both types of forms will be presented and discussed, with special attention given on the liquid counterparts.

2.5.1 Solid formulations

Herein, typical examples of solid co-delivery formulations, encompassing forms in a solid physical state (e.g. tablets, dried particulates), will be presented. These formulations are usually

found in pharmaceuticals, although not just limited to them. Despite being among the most established dosage forms when it comes to pharmaceutical applications, they still face issues with AI stability, optimising release kinetics and bioavailability limitations [80,81].

2.5.1.1 Multi-layered tablets

Multi-layer or more frequently bi-layer tablets are commonly used to combine incompatible AIs within separated layers that are pressed together to form a single tablet [82], either through simple compression or 3D printing technologies [83,84]. The layers can be sequentially applied one on top of the other as shown in Fig. 2.8, or an intermediate layer could be included to separate actives that show incompatibility issues, allowing for separated delivery of each active in a controlled manner [82]. Additionally, the use of different matrices (e.g. polymers) on each layer can potentially allow for different release patterns (immediate or sustained) for the AI contained in each layer [84].

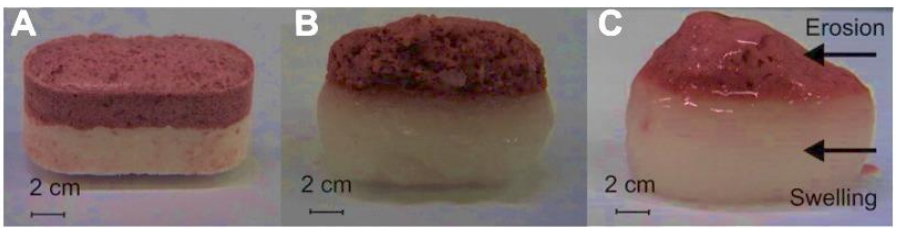

Fig. 2.8. Images of a bilayer tablet containing two active pharmaceutical ingredients fesoterodine fumarate (bottom white layer) and mirabegron (top red layer) before (A), and after 60 (B) and 240 min (C) of dissolution testing [85].

2.5.1.2 Polymeric-based systems

Polymeric-based systems, in the form of dried microspheres, nanospheres and microcapsules have also been utilised [86,87]. Microspheres and nanospheres (differing in their size range, 1–1000 μm and 100–1000 nm, respectively) can entrap AIs in their continuous matrix or have the actives adsorbed on their surface [88,89], while dried microcapsules consist of a solid or liquid phase encased within a thin polymeric membrane or coating, with the overall microstructure ranging between 0.2 and 5 μm [90]. The microcapsules can be freeze-dried to obtain an overall solid formulation [91,92], or the dried microcapsules can contain an aqueous core [93], with coating providing a means of attaining more sustained release. Examples of their utilisation in multi-active delivery formulations include nanospheres for the combination of an anti-cancer drug (tamoxifen) and an antioxidant (quercetin) in the work by Jain *et al*. [94]. Shi *et al*. [95] co-encapsulated antioxidants, *β*-carotene and anthocyanins, in pH-responsive polymeric microspheres demonstrating great potential for specific delivery and enhanced stability (Fig. 2.9).

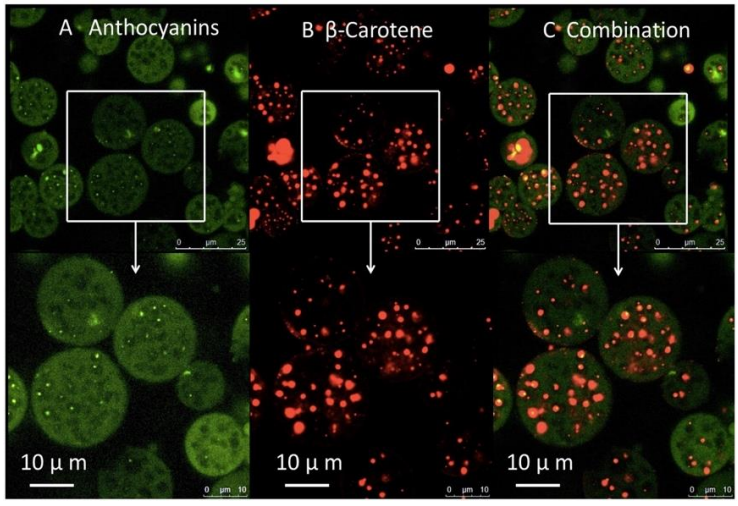

Fig. 2.9. CLSM images showing the distribution of hydrophobic (Nile Red) and hydrophilic (SUPER Green I) dyes representing antioxidants of similar properties in microspheres [95].

2.5.1.4 Protein-based particulates

Another type of solid co-encapsulation vehicle that have gained increased interest for their stability and biodegradability, is protein-based particles [96]. Protein molecules have the ability to self-assemble, cross-link and rearrange to form carrier structure, due to the presence of specific functional groups (e.g. disulphide, carbonyl and amide groups) [97,98]. Xiao *et al*. [99] co-loaded two antimicrobial agents (thymol and nisin) in zein-based particulates (Fig. 2.10), while an anticancer API (doxorubicin) and antioxidant (curcumin) were co-encapsulated in albumin nanoparticle blocks [31]. Both animal [31,100] and plant [99] derived proteins have been employed as co-delivery systems, with the methods used to acquire the solid particulate formulations including spray- or freeze-drying [100].

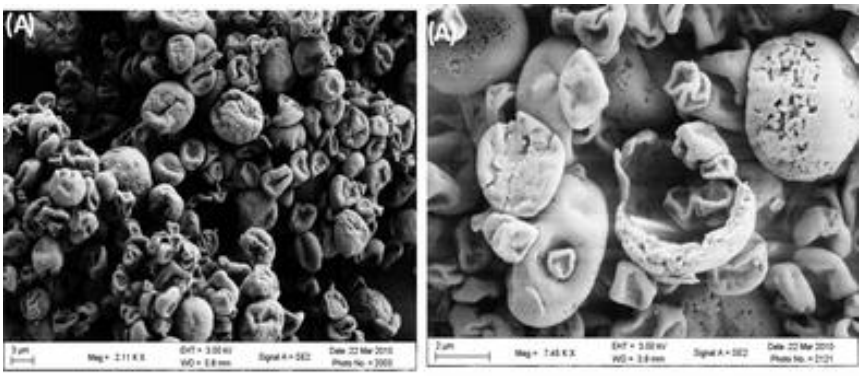

Fig. 2.10. SEM images showing surface morphology (left) and fractured structure (right) of nisin and thymol co-loaded zein capsules [99].

2.5.1.5 Polysaccharide-based nanocomplexes

Similarly to protein-based carriers, polysaccharide-based complexes that are obtained through spray- or freeze-drying have been explored for their usage in solid formulations [101]. In these structures, encapsulation is achieved via chemical linking of the AIs between the spacings

creating within the complexes [101]. Di Martino *et al*. [102] studied the co-encapsulation and potential of controlled co-release of two antineoplastic drugs (5-fluorouracil and temozolomide) through swelling of the chitosan-based structure.

2.5.1.6 Emulsion-gel hybrid systems

An emulsion gel, or otherwise known as "emulgel" is a hybrid emulsion and gel system, where gelling agents are added within the continuous phase of the initially produced emulsion to enhance the overall stability of the system. As carrier and delivery systems, emulsion gels have been investigated for their ability to carry multiple actives within the emulsion phase, that can potentially be a multiple emulsion [103], but also within both the emulsion and gel phases [104,105]. This type of carriers, as well as potentially their oleogel (oil-continuous phase) counterpart seem to be emerging as promising delivery and co-delivery systems, due to the co-existence of the two phases providing the ability to independently control the AI release.

2.5.2 Liquid formulations

The liquid formulations category encompasses systems that could be classed among the most widely explored and researched when it comes to delivery and co-delivery vehicles, such as emulsions, dispersions and suspensions. The development of a liquid formulation that could substitute the solid co-delivery system usage and overcome their slow absorption and dosage flexibility shortcomings [71,106,107], is still an area of ongoing research. Previously presented solid state vehicles can also be exploited while still in their liquid state before further processing is performed (e.g. drying), that is usually applied to enhance the long-term stability of the

formulation. In the following sections, the most extensively studied co-delivery liquid platforms will be outlined.

2.5.2.1 Emulsion-based systems

Emulsions are multiphase systems that contain two immiscible phases that have been combined via the contribution of energy [108]. The dispersed phase in the form of liquid droplets can be stabilised by surface active species (e.g. emulsifiers, surfactants), colloidal particles, or combination of the two (i.e. mixed particle-surfactant systems [109]). As carrier and delivery systems, emulsions offer the flexibility and versatility of being compatible with different types of actives, including both hydrophobic and hydrophilic molecules depending on the dispersed phase, oil-in-water (o/w) or water-in-oil (w/o) types, respectively. Notably, their co-encapsulation and co-delivery attributes are further enhanced, owing to their ability to provide segregated encasing of AIs within different compartments, i.e. the dispersed and continuous phases, adsorbed at the interface, or even within the colloidal particles used as emulsion stabilisers.

Among the emulsion structuring approaches that have been utilised for multi-encapsulation, particle-stabilised and multiple emulsions are among the most attractive systems (Fig. 2.11). Regarding particle-stabilised emulsions, also known as Pickering emulsions, a variety of diverse particles have been utilised as Pickering stabilisers, ranging from inorganic to organic entities. Although when it comes to the development of delivery systems the choice of materials is largely focused on biological or biocompatible sources, such as starch [110], chitosan [111] and lipids [112], among others. Compartmental encapsulation is realised by encasing one of the AIs within the Pickering particles and the other within the emulsion droplets, with both

hydrophobic/hydrophilic [113,114] and hydrophobic/hydrophobic [114,115] combinations of actives having been explored. What is particularly attractive about these platforms, is that the diverse properties of the two compartments (i.e. the colloidal particles and the emulsion droplets) offer the tools to achieve controlled and triggered release for each AI, through manipulation of the features of each separate compartment [56].

Within multiple emulsions, and predominantly double emulsions, where a dispersed phase is contained within another dispersed phase [116], active molecules can either be co-localised or separately incorporated. Comparably to the Pickering emulsions, the type of emulsion can be tailored to the properties of the AIs, so that they can be both efficiently encased and protected from external conditions that might compromise their integrity. Certain studies have reported that incorporation of the secondary active within the same phase can significantly change the co-release performance compared to the individual profiles [117,118], whereas segregated co-encapsulation in different phases has led to reverse results [119]. A hierarchical triple emulsion (water-in-oil-in-(oil-in-water)) was also utilised for the compartmentalised co-encapsulation of actives with varying degrees of hydrophobicity [55], thereby improving the physicochemical stability of the incorporated molecules. In some instances, Pickering particles are used in conjunction with double emulsions, with the former serving the role of improving the storage life and bio-accessibility of the developed structure [120,121]. Lastly, segregated co-encapsulation of AIs within simple emulsions (e.g. o/w or w/o) is accomplished by binding/associating one of the active agents with the surface active species (e.g. through hydrophobic interactions [122] or electrostatic adsorption [123]) and the secondary being carried within the emulsion droplets [122–125] (Fig. 2.11).

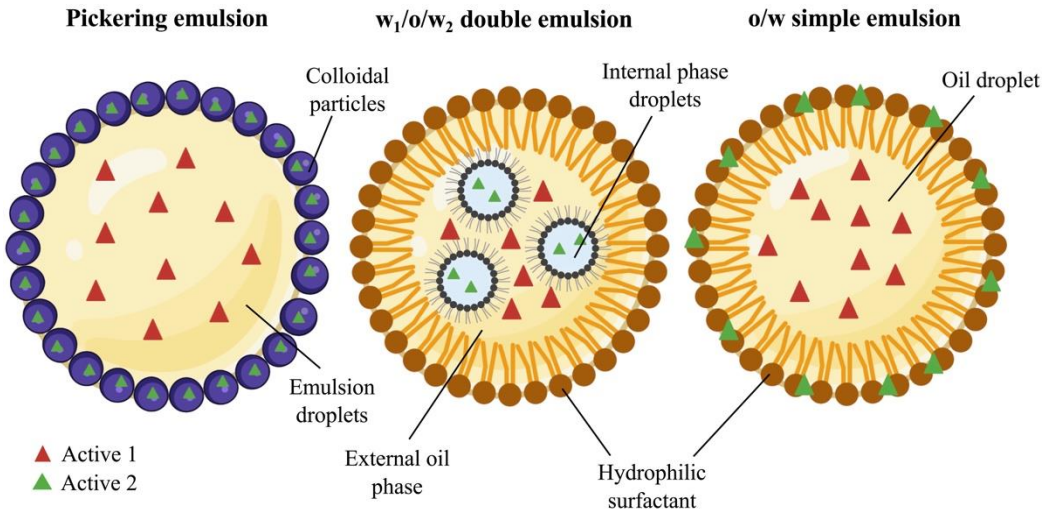

Fig. 2.11. Schematic representation of the segregated co-encapsulation of AIs within Pickering, double and simple emulsions.

2.5.2.2 Lipid-based systems

Another prominent category within the liquid formulations span is lipid-based systems, which due to their primarily hydrophobic character constitute a promising route for the encapsulation and delivery of poorly water-soluble active ingredients (Fig. 2.12). The aptitude of these carriers to enhance the solubility and bioavailability of said actives, due to active molecules being able to pass readily through the cell membrane, while simultaneously offering improved long-term storage stability has marked them out as attractive platforms, particularly for bioactive carrier systems within pharmaceuticals, cosmeceuticals and nutraceuticals [126–129]. Within this class of vehicles, lipid colloidal particles including solid lipid nanoparticles (SLNs) and nanostructured lipid carriers (NLCs) have emerged into versatile nanocarriers due to their complementary attribute of shielding actives prone to degradation (e.g. chemical, photochemical, oxidative, thermal) [130,131]. The main difference between the two lies in their lipid core composition, with the latter being composed of both solid and liquid lipids at room temperature, compared to the solely solid lipid-composed matrix of SLNs. Their lipophilic

nature has been predominantly harnessed for hydrophobic active encapsulation [132,133], though through the versatility offered by the active species and liquid lipid variations, hydrophilic molecules have also been explored [134,135]. Due to their relatively simple microstructure (lipid matrix stabilised by surface active species), the possibilities of AI co-loading are either co-localised within the lipid matrix [136,137] or segregated with one active associated with the surface and the other entrapped within the matrix [138] (Fig. 2.12). As co-delivery systems, they can provide fast (within a couple of hours) or sustained (over the course of a few days) release, depending on the choice of materials used; something that will be further considered in a later section.

Lipid-based vesicular dispersions, such as liposomes and niosomes, have also been explored for the co-encapsulation of hydrophobic/hydrophilic combinations of AIs. Liposomes consisting of a phospholipid bilayer membrane enclosing an aqueous core can entrap in a compartmentalised approach hydrophobic actives in the former and hydrophilic agents in the latter [53]. Niosomes on the other hand, are similarly structured, but with the bilayer membrane being composed of non-ionic surfactants [9]. Co-encapsulation of the secondary hydrophobic active has been shown to affect the co-release performance of the structure due to changes in the fluidity and permeability of the bilayer [9], hence posing issues with the level of control over the release performance.

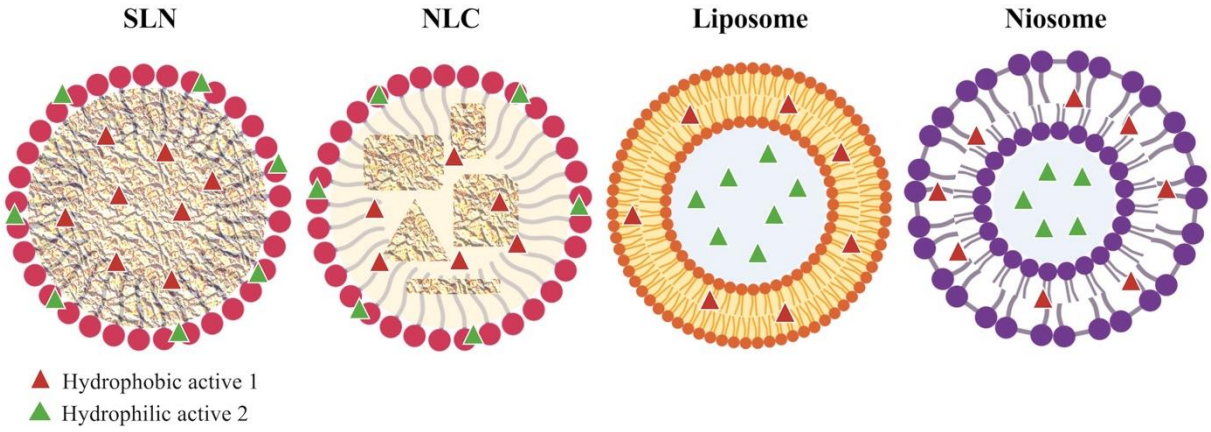

Fig. 2.12. Schematic representation of the segregated co-encapsulation of hydrophobic/hydrophilic AIs within the SLN, NLC, liposome and noisome microstructures

2.5.2.3 Polymer-based dispersions

Polymer-based platforms, principally in the form of particle/nanoparticle dispersions, polymerosomes or polymeric nanocapsules have been explored for both hydrophobic and hydrophilic types of actives, among others. Their pH responsiveness, due to the presence of acidic or basic groups in their structure, renders them attractive systems for the triggered and controlled AI delivery, by manipulating the charges along the polymer backbone or electrolyte concentration that could result in changes in the hydrodynamic volume of the polymer. (transition between coiled and expanded state) [74,139,140]. The relative active positioning within the polymeric particle structure, the matching of active/core material properties and any additional functionalisation of the particle surface can be used as tools for controlling the release rate [1,141,142]. In polymeric nanocapsules, where a liquid core is surrounded by a polymeric exterior layer [29], an additional barrier over the release performance of the internally encapsulated active is provided by the external layer, while allowing for a more burst release for the secondary layer-associated species [143].

2.5.2.4 Protein-based systems

The utilisation of protein-based systems has been widely investigated as a delivery approach for food and nutraceutical applications, in the form of protein particles/nanoparticles or protein/polysaccharide complexes, allowing for more naturally derived core materials to be exploited. Particles comprised of just the protein isolate [144], or covered in polysaccharides to provide further protection to the structure [145] have been quite recently studied. In the form of coacervates with phenols [146], polysaccharides [147] or mixtures of protein and polysaccharides [148], protein-based vehicles have shown promising stability results. However, research is still focusing on the co-encapsulation and synergism potential rather than exploring and developing approaches to trigger or control the release from these structures [147].

2.6 Pickering emulsions as co-encapsulation and co-delivery microstructures

In recent years, particle-stabilised emulsions have transpired to be promising delivery systems, owing to their evidenced capacity to manifest segregated co-encapsulation and independently controlled delivery potential, in combination with their ability to confer improved emulsion stabilisation. Originally described in the works by Ramsden [149] and Pickering [150] in the beginning of the 20th century, solid particles were shown to provide effective emulsion stabilisation through a Pickering mechanism (inheriting the term from the latter), thereby posing an alternative to conventional emulsifiers. In classical emulsions, referring to emulsions where stability is provided by the adsorption of amphiphilic molecules (either low molecular weight surfactants or larger biopolymers) at the oil/water interface, emulsifiers serve a dual purpose. During and/or post the emulsion formation process, the surface active species which can be

ionic or non-ionic, synthetically or naturally derived, are expected to move to the newly formed interfaces and lower the interfacial tension by adsorbing onto them, while also forming a protective layer surrounding the droplets that prevents destabilisation phenomena. On the contrary, Pickering particles not having any interfacial tension reduction capabilities, bestow stabilisation by creating a steric and/or electrostatic barrier around the liquid/liquid interfaces. The improved stabilisation compared to emulsifier-stabilised emulsions is attributed to the high detachment energy (ΔE) of small particles (less than a few microns in diameter) from the interface, which is given by:

$$\Delta E = \pi r^2 \gamma_{ow} (1 - |\cos\theta|)^2 \qquad (2.7)$$

where r is the particle radius (if spherical), γ_{ow} is the oil/water interfacial tension and θ is the contact angle of the three phases defined by oil, water and the solid particles. The commonly occurring emulsion destabilisation phenomena, along with how the particle characteristics in relation to their physicochemical properties can affect the emulsion formation and stability are further explored in the following paragraphs.

2.6.1 Destabilisation mechanisms

Even though emulsion destabilisation is more common in simple emulsions, Pickering stabilised emulsions can also be affected by physical breakdown mechanisms. These phenomena, as presented in Fig. 2.13, tend to occur during storage and can be influenced by both the emulsion processing method and the type of stabilising particles.

Flocculation occurs when the repulsive long-distance interactions between droplets are overcome by attractive van der Waals forces, that results in droplets/particles to come in close

proximity forming weaker or stronger flocs, although still maintaining their physical integrity. Overtime and with enhanced flocculation, gravitational separation can take over, with either creaming or sedimentation, depending on the dispersed/continuous phase density difference. Although creaming/sedimentation are reversible phenomena and do not bestow physical destabilisation, they can potentially impair certain functionalities of the system (i.e. delivery capacity) [151]. The phenomenon by which two or more droplets will come together, rupture and merge to form a single droplet of larger dimensions is known as coalescence, and the reduction of interfacial area is the driving force behind it. Coalescence is an irreversible process, and it can lead to phase separation overtime, where the system will separate into two distinct oil and water phases [152]. Finally, Ostwald ripening driven by the Laplace pressure difference between droplets of different sizes, is the process by which mass is transferred from smaller droplets, diffuses through the continuous phase and deposits onto larger droplets [153].

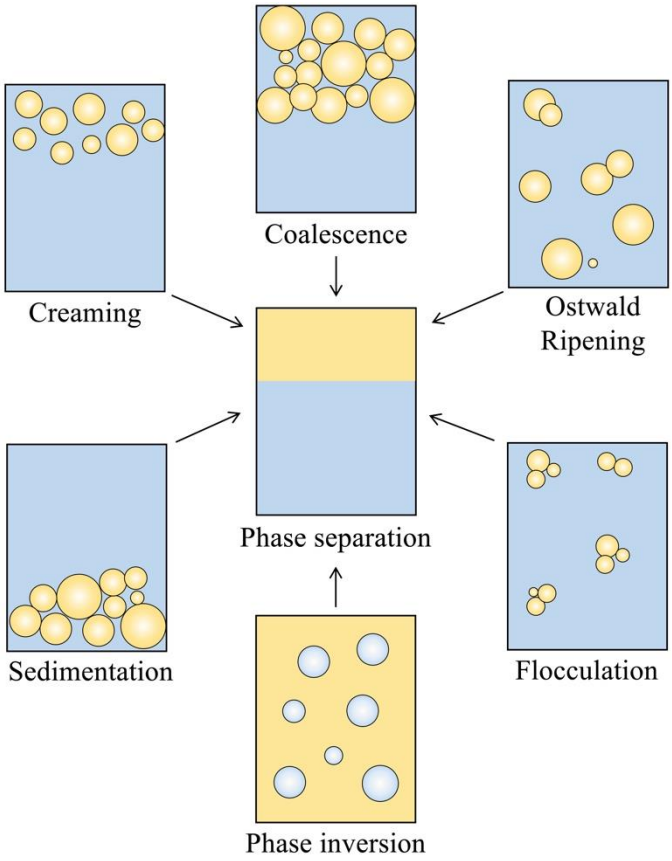

Fig. 2.13. The main emulsion destabilisation mechanisms.

In Pickering emulsions, the presence of solid particles at the droplet interface can in most instances act as an effective barrier against coalescence by preventing droplet merging [154,155]. However, during emulsion formation the specific particle type/characteristics can in some cases induce coalescence, such as when particles with different stabilisation capacity are used within the same formulation [156]. Partially coated droplets are also prone to coalescence, particularly when the covering particles are poorly wetted by the continuous phase [157], or when the processing method used does not allow sufficient time for the interfacial particle adsorption [158,159]. Flocculation is a common destabilisation mechanism in particle-stabilised emulsions, with inter-particle network formation (bridging) due to lack of sufficient particle concentration to cover the droplet interfacial area [160], and strong particle flocculation eventually leading to coalescence [161]. In cases where flocculated droplets are in close

proximity, mainly in o/w emulsions, oil transfer phenomena can occur from smaller to larger droplets, with the destabilisation being triggered by a combination of flocculation and ripening [162]. The characteristics of the emulsion in regard to the stabilising entities can either induce or halt the occurrence of specific destabilisation mechanisms as will be discussed later on.

2.6.2 Effect of particle characteristics on emulsion formation

2.6.2.1 Particle wettability

One of the most important particle characteristics that dictates not only the adsorption at the liquid/liquid interface, but also the stability of the resulting emulsion is the particle wettability [163]. The relative hydrophobicity/hydrophilicity of the particles, which is expressed through their multiphase contact angle θ, will affect how strongly they adsorb at the interface and subsequently their detachment energy (ΔE) (*Equation 2.7*). Particles with a contact angle < 90º are hydrophilic and are therefore preferentially wetted by the aqueous phase, which will be the continuous phase of the resulting o/w emulsion (Fig. 2.14). Conversely, a contact angle > 90º indicates a stronger hydrophobic character, and these particles will end up stabilising w/o emulsions. At θ = 90º the particles are most strongly held at the interface, while at extreme contact angle values (i.e. < 20º or > 160 º) the ΔE gets quite small and the particles remain dispersed in the phase they are most akin to, thus leading to emulsion instability issues [164]. The particle wettability can be traditionally controlled through surface modification using surfactants, or as more recently described by Xiao *et al*. [165] through alteration of the surface chemistry and surface roughness. Several examples exist in literature, where different types of particles ranging from organic (e.g. carbon nanotubes [166]) to inorganic (e.g. silica [167]) species were modified in regard to their wettability via surfactant utilisation. The synergy

between solid particles and surfactants in emulsion stabilisation is further discussed later on (Section 2.6.2.7).

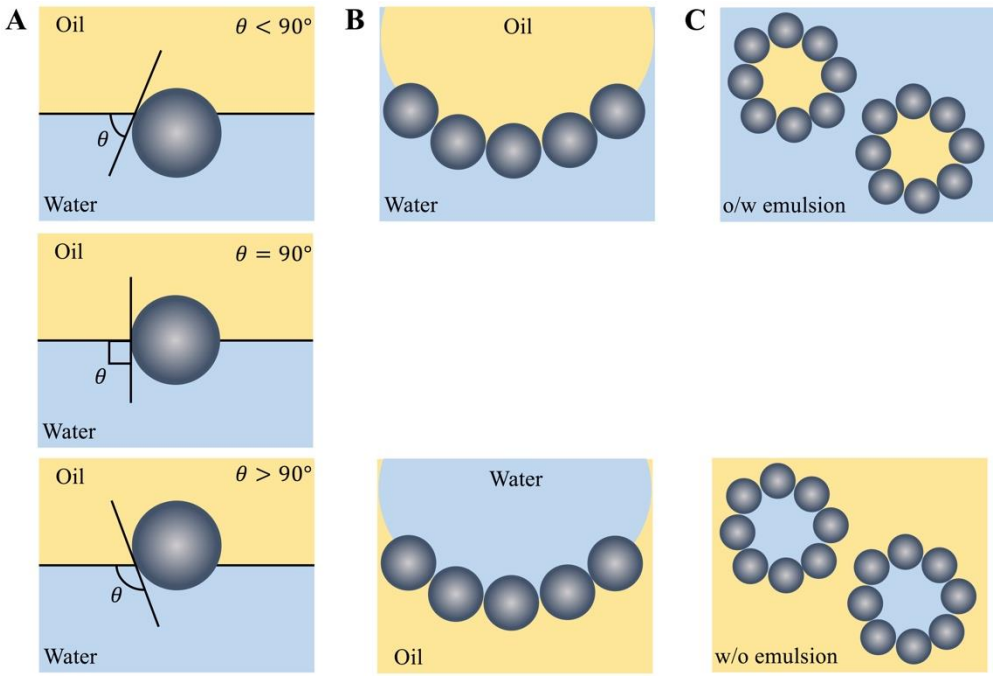

Fig. 2.14. Positioning of small spherical particles depending on the contact angle (θ) at a planar (A) and curved (B) oil-water interface, and the resulting emulsion type (adapted from Binks [163]).

2.6.2.2 Particle size

Since one of the parameters defining the detachment energy is the particle radius, the particle size is another characteristic affecting the Pickering performance. According to *Equation 2.7*, small particles (in the nm range) will have a very large binding energy, and thus will be irreversible adsorbed, due to that being considerably higher than the thermal energy (kT) [163]. Additionally, the particle diameter will determine the droplet surface coverage [168], while softer than more rigid/hard particles will show better emulsifying performance owing to their ability to deform/stretch at the interface providing better coverage [169]. Regarding the droplet

characteristics, the particle size needs to be at least an order of magnitude smaller than the droplet to achieve effective Pickering stabilisation [170]. Binks *et al*. [171] underlined the effect of particle size on the emulsion physical stability, by demonstrating that increasing silica particle diameter led to increasing droplet size, that eventually resulted in sedimentation.

2.6.2.3 Particle shape

Besides size, another Pickering particle morphology aspect that plays a crucial role on their interfacial behaviour and as such also on their overall emulsion stabilisation performance, is their shape. The use of spherical particles that offer the possibility of achieving the highest packing density (i.e. hexagonal packing) at the interface and hence the lower possibility of destabilisation phenomena, has been widely explored for Pickering stabilisation of emulsions and foams [172]. Apart from spherical particles, other non-spherical structures have been investigated for their stabilisation capability, their contribution in regulating the emulsion type (i.e. o/w or w/o) and effect on the Pickering emulsion behaviour. The primary difference between spherical and non-spherical particles is the driving forces dominating their formation at the interface, with the former being governed mainly by particle interactions and the latter by capillary forces [173,174]. Despite hurdles associated with the production of specific anisotropic particles [173] and the obtained packing density once at the interface [175], anisotropic particles can potentially provide stronger materials and be used to tune the rheology and performance of the final microstructure [176]. Therefore, various shapes including rods [177], ellipsoids [178], disc- [179] and fibrous-like [180], cubes [181], peanuts [181] and cylinders [182] have been explored for their Pickering stabilisation capacity. Although shape appears to influence the aforementioned parameters, there is strong evidence to support the use

of diverse particle morphologies to acquire physically stable emulsions with tuneable properties, provided that certain packing and self-assemble requirements can be met [173].

2.6.2.4 Particle type

There is a mountain of research regarding the utilisation of different types of colloidal particles as Pickering stabilisers, including both inorganic- and organic-based materials; though when it comes to the use of Pickering emulsions in pharmaceutical or food applications, the focus shifts to biodegradable and biocompatible particles that primarily tend to be organic-based. Among the advantages that inorganic particles can offer, with representative examples being silica [183,184] and clay particles [185], are the increased stability, easily controllable size, structure and surface modification. More recently, magnetic/paramagnetic particles have also been investigated for their de-emulsification capacity that overall can lead to recyclable and reusable systems [186,187], as well as microbial cells (from bacteria and yeast) to serve clean label purposes in food applications [188]. Carbon nanotubes that offer high number of exposed active sites and large surface area [189,190], and cyclodextrins with the ability to enclose lipophilic moieties in their central cavity [191] have been also utilised for emulsion stabilisation. Among naturally derived materials that possess biocompatibility and biodegradability properties with attractive prospects in both the delivery field (e.g. pharmaceuticals) and as Pickering stabilisers are chitosan [111], starch [110], chitin [192], zein [193], cellulose [194], lignin [195] and lipid particles [112].

The lipid-based particle platform constitutes a relatively underexplored area when it comes to their Pickering stabilisation capacity. Ranging from fats and waxes to glycerides and fat-soluble vitamins among others, lipids are a large and diverse group of organic compounds. In Pickering

stabilisation, fat crystals are the most widely used type, with the hydrophobic character of the crystals resulting in the stabilisation of w/o emulsion systems [196–198]. Stabilisation can occur by adsorption at the oil/water interface, surface templated crystallisation or shearing-induced agglomeration [196]. Although effective stabilisation can be achieved, the *in-situ* formation of the crystals during the emulsification step limits the control over attaining specific crystal characteristics (e.g. size). On the contrary, both the wettability and desired properties of lipid-based particles can be easily manipulated when using lipid particulates. Specifically, solid lipid nanoparticles (SLNs) have shown potential to stabilise both o/w and w/o emulsions by manipulating the particle wettability through the use of hydrophilic compounds (e.g. surface active species) or exclusively lipophilic molecules that contain polar groups [199,200]. With the majority of the research primarily dated in the last decade [70,112,200–206] SLNs are emerging as promising Pickering stabilisers, not only due to their strong interfacial adsorption and proven stabilisation capability, but also for their diverse functionalities allowing them to serve more than one role while at the droplet interface. From acting as antioxidant reservoirs for o/w emulsion droplets [207] to controlling the release of actives encapsulated within o/w droplets in response to temperature stimuli [70], lipid colloidal particles offer a range of functionalities, some of which are yet to be explored.

2.6.2.5 Particle concentration

Considering that one aspect governing the physical integrity of the resulting Pickering emulsion is the surface coverage provided by the particles [208], the concentration of solid particles greatly influences the emulsion stability. It has been demonstrated that with increasing particle concentration [209] and the formation of a tightly packed particle layer around the interface [210], improved stability against droplet coalescence phenomena can be attained. Similar

behaviour was described for emulsions stabilised by fat crystals, where the stabilisation at higher fat concentration was explained by fat bridging formation between droplets, acting as protective layers thereby hindering coalescence [211]. On that basis, Binks *et al*. [212] revealed that this can be equally achieved using solid particles. The usage of particle excess in relation to the dispersed phase surface would ensure enough particles are present to form at least a monolayer around the droplets, thus providing enough surface coverage; although the latter is also controlled by the dispersed phase volume fraction and processing conditions used.

2.6.2.6 Particle-particle interactions

Although the formation of at least a tightly packed particle monolayer could potentially appear as the most straightforward way to impart increased emulsion stabilisation potential, it has been experimentally shown that sufficient stabilisation can be provided without full coverage [213,214]. What is more, for solid particles of small dimensions (nm range), the attainment of a truly monodisperse system is quite challenging, even when high intensity techniques are used (e.g. ultrasonication), constituting the formation of a uniform particle monolayer even more improbable [215]. Creation of bridging layers between droplets as a result of interactions between the particles can prevent droplet coalescence due to steric hindrance effects [215]. Additionally, in instances where there is strong particle adsorption at the droplet interface leading to aggregated particles stabilising the droplets, rigid disordered particle/droplet networks can be generated, again favouring steric coalescence barriers through attractive interparticle forces [215,216]. Even more interestingly, it was recently revealed [217] that interactions between particles can lead to their interfacial displacement and positional exchange between droplets, when particles are shared between droplets through bridging.

Depending on the type of particle employed, different types of interactions ranging between repulsive or attractive, hydrophobic, steric or electrostatic have been reported. The interplay between van der Waals and capillary forces and particle aggregation/concentration has been explored using theoretical approximations [218] and surface modification [219] or salt concentration [220] of silica particle-stabilised o/w emulsions. Several studies have attempted to tune the repulsive/attractive forces between silica particles at droplet interfaces [221–223], with some more recent ones modifying their surface using silane agents and sodium alginate to not only improve their stabilisation, but also to enhance their functionality employing attractive interactions [224]. Zembyla *et al*. [225] reported that the presence of attractive electrostatic interactions and/or hydrogen bonding between polyphenol crystals present in the oil continuous phase and whey protein microgels stabilising the water droplets of an w/o emulsion, improved the stability of the system via a "double Pickering" mechanism. Addition of surface active species that can modify the hydrophobicity of the interface through altering the wettability of the particles themselves [226], or through directly adsorbing at the droplet interface can induce further interactions, aiding the persistence of physical droplet stability.

2.6.2.7 Particle-surfactant co-presence and interactions

Emulsion systems where the stabilisation is due to the combined effect of both colloidal particles and surfactant molecules, also commonly described as mixed-emulsifier stabilised emulsions [167], have been utilised to overcome the short comings (e.g. stability) of the sole use of either one of them. The co-presence of particles and surfactants at the droplet interface has been investigated in terms of the adsorption mechanism involved and any synergistic/antagonistic effects between the two species [167], and in relation to the influence of particle/surfactant characteristics on the combined stabilisation [227–229]. In a mixed

emulsifier system, surfactant molecules (or vice versa) can either be introduced by addition of a mixed aqueous surfactant/particle solution, or they can come into the system as remnants from the particulates preparation process.

In most cases, co-presence of the two leads to improved emulsion stability [227,230,231], albeit the opposite has also been reported and appears to be dependent on the type/characteristics of the species (e.g. charge state [212], concentration) used and experimental conditions. When synergistic emulsification arises, surfactant molecules promptly move to the interface thereby minimising coalescence phenomena, while particles that diffuse more slowly are responsible for the long-term stability [167]. Conversely, antagonistic effects relevant to their interfacial adsorption can result in interfacial displacement, and eventually to de-stabilisation. A major role in that is played by the surfactant concentration, as it has been reported that at high surfactant concentration [109] or more specifically at concentration above the critical micelle concentration (CMC) [232] particle displacement is pronounced, occasionally even leaving the interface solely stabilised by surfactant molecules. Another prospect is the preferential adsorption of surfactant molecules on the particles' surfaces rather than the emulsion interface [233], thus affecting not only the particles' wettability but also the overall interfacial tension reduction ability of the particle/surfactant mixture [234]. Occurrence of the aforementioned behaviour can compromise the stabilisation performance, although the mechanism of adsorption in mixed emulsifier systems is not well established.

The behaviour of composite particle and surfactant system has been shown to differ from that of a sole surfactant, both in terms of the equilibrium interfacial tension values and the interfacial tension reduction profile. Zafeiri *et al*. [230] demonstrated that the interfacial tension of the composite particle/surfactant systems (comprised of hydroxypropyl methylcellulose (HPMC)

particles and either Tween® 80 or polyglycerol polyricinoleate (PGPR) as surfactants) was lower than that of particle dispersions alone, with the concentration and hydrophilic-lipophilic balance (HLB) value of the surfactant employed playing an important role in the system's stability. The latter was attributed to changes in the particles' hydrophobicity, particularly when the lower HLB value surfactant (PGPR) was used at low concentration. Pichot *et al*. [109] utilised scanning electron microscopy (SEM) coupled with droplet size measurements to demonstrate that even though at low concentrations the surfactant molecules aid the droplet break-up by interfacial tension reduction, at higher concentrations they tend towards particle displacement. Understanding the underlying mechanisms involved can become even more convoluted, when the presence of surface active species is due to excess concentration remnant from the colloidal particle formation step, or even when the surface active species adsorbed at the particles' surfaces interact with the droplet interface. When studying the interfacial behaviour of dialysed SLNs (processed to remove excess surfactant from the aqueous dispersion phase before emulsification), Dieng *et al*. [70] ascribed the recorded interfacial tension reduction to release of surface active species from the SLNs' surface to the droplet interface, followed by succeeding interfacial tension increase owing to diffusion to the bulk continuous phase.

2.6.3 Pickering emulsions as active encapsulation and delivery systems

As discussed previously, particle-stabilised emulsions represent an incipient research area for their application as carrier and delivery systems. The prolonged physical stability bestowed by the presence of particles at the droplet interface [235], in combination with the versatility proffered by the potential utilisation of copious types of colloidal particles [236] signify them as promising systems for the controlled and/or triggered delivery of active ingredients.

Compared to conventional emulsions, particle-stabilised emulsions provide a dynamic interface that can correspond and/or adapt to environmental changes. Thus, the employment of a diverse portfolio of particles and actives, along with mechanisms to control/trigger the release of the encapsulated species have attracted increased research interest.

By virtue of their multi-compartmental structure, it is feasible for the active entrapment to occur within or in close association with either of the discrete sections, namely the emulsion droplets and the colloidal particles, or in the case of co-encapsulation systems within both. With respect to the former, o/w emulsions allow the encapsulation of hydrophobic moieties, which constitute the most commonly encountered type of AIs, while w/o emulsion are attractive systems for the encasing of hydrophilic molecules. When compared to simple emulsions, Pickering particles have been shown to impart better control over the release performance of the species encapsulated within the emulsion droplets, by delaying the release rate. Moreover, the use of the appropriate emulsion type can potentially provide greater loading efficiency and protection against varying environmental conditions, as shown by Yi *et al*. [237]. Xiao *et al*. [238] demonstrated that kafirin nanoparticle-stabilised o/w emulsions offer improved stability to curcumin against processing conditions and UV radiation, while compared to Tween® 80 or no surfactant emulsions the release rate was reduced. Hydrophilic caffeine and hydrophobic retinol encapsulated in w/o and o/w silica-stabilised emulsions, respectively, showed enhanced skin penetration and more sustained release compared to surfactant-stabilised or emulsions fabricated without any surfactant, in the studies by Frelichowska *et al*. [239,240].

The effect of the compatibility between the used active and the carrier oil was highlighted in the work of Shah *et al*. [241], where the release of vitamin D3 from o/w emulsions stabilised by zein/chitosan complexes in both acidic and basic conditions and at elevated temperature

(37°C) was reported to be diffusion controlled. Analogously the impact of the stabilising particles' characteristics on the release performance was underlined in the work by Li *et al*. [242], who used both hydrophobic and hydrophilic silica particles to study the effect on the release of essential oils. The specific response of the particles to environmental conditions is another parameter that can dictate the Pickering particle selection, as shown by the different release rates from phosphatidylcholine-kaolinite-stabilised emulsions in simulated gastric and intestinal conditions, in the work by Tang *et al*. [243]. Last but not least, the deployment of temperature as a mechanism to trigger release constitutes a widely investigated tool. Thermo-responsive particles, such as fat crystals [198,244,245] and lipid colloidal particles [70] have been utilised to show that temperature increase can induce partial or complete melting of the interfacial layer thus provoking faster release of the encapsulated active. Conversely, Dai *et al*. [246] reported that temperature increase can also result in release inhibition, that was attributed to coalescence, deformation or changes in the coverage density of lignin-stabilised emulsions.

When the Pickering particles act as the active carriers/delivery control component, the AI can either be included/associated with the particles' structure or bioactive ingredients can comprise the building materials of the particles. Representative examples of the latter are flavonoid [247], protein [248] and polyphenol [225] particles, among others. The use of particles with antioxidant properties has been reported to have a beneficial effect against the emulsions' oxidative instability [247,249,250]. As a pharmaceutically relevant delivery system, Yi *et al*. [251] developed silybin nanocrystal self-stabilised Pickering o/w emulsions for the enhanced bioavailability of silybin. In the same study [251], it was suggested that the desirable faster release of silybin from the Pickering emulsion system compared to silybin coarse powder or silybin nanocrystalline suspension, was due to partial dissolution of silybin to the oil phase. For Pickering particles used as active carriers, Zhang *et al*. [252] employed zein nanoparticles

loaded with epigallocatechin gallate and Li *et al*. [253] utilised zein/gum arabic nanoparticles encasing thymol to demonstrate that the developed formulations had a more sustained release compared to pure active solutions or solely loaded particle dispersion systems, respectively. In the work by Schröder *et al*. [207], SLNs acting as antioxidant reservoirs for lipophilic substances (α-tocopherol and carnosic acid) at the o/w interface were shown to increase the antioxidant activity, and also that dynamic transfer of the lipophilic compounds to the droplets occurs over short timescales. Loading of Pickering particles with AIs renders the particles with the dual functional role of stabilising the droplets and enhancing the active functionality, whether that is focused on the antioxidant activity or even the controlled/triggered delivery of the active. The contribution of the particles to delaying or accelerating the release rate is an area with scarce investigation that only very recently has attracted research attention [254], particularly concerning the effect of the oil phase presence on the particles' carrying/releasing performance. Based on the above, the control/trigger over the Pickering emulsions' release behaviour is largely provided by structure rupturing strategies (e.g. melting, deformation), which albeit offering the desired release kinetic results can impede other functionalities of the system (e.g. stability) that may be required when the Pickering emulsion is serving more than one purpose. Therefore, part of the research efforts should focus on developing alternative approaches to control release, while maintaining the integrity of the structure, such as interfacial particle aggregation as was recently suggested by Ming *et al*. [255].

2.6.3.1 Pickering emulsions as co-encapsulation and co-delivery systems

In the context of the dual functionality of Pickering emulsions, one of their roles as dual functional systems is their ability to facilitate the co-encapsulation and co-delivery of multiple actives in a controlled and according to the intended application, potentially an independent

manner. However, this concept is still at its infancy with the vast majority of the available research focusing on characterising the microstructure and establishing the co-encapsulation potential of the systems. Limited focus is put on scrutinising the release and co-release performance under different formulation, processing or environmental conditions, and devising approaches to control/trigger it.

Among the existing literature, Pickering emulsions have exhibited aptitude for the segregated co-encapsulation of actives with varying degrees of hydrophobicity [115,256], thereby demonstrating that the choice of Pickering stabilisers can serve different active delivery needs. In the study by Sun *et al*. [257] the co-encapsulation of three AIs with different solubilities, namely vitamin B_2, vitamin E and *β*-carotene was achieved by developing a liposome-stabilised emulsion. Within this work, the effect of the microstructural components' composition was underlined, as in the presence of phospholipids in the oil phase the encapsulation efficiency of *β*-carotene was higher. More complex systems, utilising double emulsions stabilised by Pickering particles have also been employed to accommodate specific requirements of the active, or of the overall delivery system (e.g. synergistic hypolipidemic effect [120] or enhanced bioavailability [243]). Improved physicochemical stability against environmental stresses (e.g. pH, radiation, ionic strength, heat) [258] due to structural protection, and enhanced stability of the actives due to synergistic effects [258] have also been reported.

In terms of the effect of co-encapsulation on the properties of blank emulsions, Chen *et al*. [113] showed very subtle changes on the size distribution and better stability after co-encapsulation of chlorogenic acid and *β*-carotene in shrimp ferritin nanocage-stabilised emulsions. The impact of the particles' characteristics on the release performance of the co-encapsulated AIs was highlighted in the study by Spyropoulos *et al*. [58], where two independent release profiles

were achieved for a hydrophobic/hydrophilic active combination. More specifically, the model hydrophilic active associated with the sodium caseinate/chitosan co-precipitated complexes was released faster through a pH-responsive triggered mechanism, compared to the sustained release of the model hydrophobic active encased within the (unaffected by pH changes) o/w emulsion droplets. Similarly, the release of quercetin-loaded black bean protein-based nanocomplexes was more sustained compared to that of perilla oil of the emulsion droplets, accentuating the protection over environmental conditions offered by the Pickering particles [122]. In the same work, the influence of the secondary active addition (referring to that enclosed within the particles) on the release performance of perilla oil was underlined, as its co-presence hindered the release further, due to the creation of a thicker interfacial coating compared to blank particles. Relevant to the contribution of the surface properties to the co-release performance either from the droplets or the particles, when a bulkier surface active species (whey protein isolate) was used in the preparation of SLNs, the release from particles was insignificant, while sintering of SLNs at the emulsion interface also led to minimal percentage of active release from the oil droplets [114]. Consequently, understanding the impact of AIs addition on the physicochemical properties and stability of these multi-compartmental systems, but also the effect of the formulation aspects on the co-delivery behaviour is imperative in maintaining a balance between the practicality and complexity involved in developing co-delivery systems for targeted applications.

2.7 Solid lipid nanoparticles (SLNs) and nanostructured lipid carriers (NLCs) as co-encapsulation and co-delivery microstructures

Since their introduction in 1991 [259], solid lipid nanoparticles (SLNs) have surfaced as promising carrying and delivery systems, owing to their auspicious attributes of long-term physicochemical stability and affinity for hydrophobic molecules, that can be hosted within their lipophilic core. After the first description of their preparation by Eldem *et al*. [260], numerous reports have experimented with their production methods, building materials and ability to carry both lipophilic and hydrophilic compounds.

The basic components of an aqueous SLNs dispersion are the lipid core composed of lipids that are solid at room and body temperature, a surface active species that is used to stabilise the particles and water. The compositional percentage of either can vary, provided that the percentage of surfactant used relative to the lipid phase is sufficient to produce a stable system. They can be made up by materials with varying characteristics, which if appropriately selected can facilitate improved loading capacities for actives with diverse properties and allow a level of control over the attained release profiles [132,261–263]. They are characterised by small sizes (50–1000 nm) and have large surface areas, both of which are important factors in serving as delivery systems and being able to achieve cell membrane permeation and site-specific drug targeting. Collectively, SLNs have shown the ability to address issues commonly encountered with drug encapsulation and delivery, such as solubility and bioavailability of poorly water-soluble actives [264,265], improved stability and shielding of actives prone to degradation (e.g.

chemical, photochemical, oxidative, thermal) [130,131], and ease of preparation and scale-up processes [266].

Regardless of the promising potential embodied by SLNs and the plethora of studies utilising them as delivery systems, overtime their highly ordered crystalline structure revealed its demerits that entailed limited space for drug encapsulation, and drug expulsion due to polymorphic transitions arising during storage [267–269]. To overcome said issues, the nanostructure lipid carriers (NLCs) were developed shortly afterwards [270]. In these colloidal dispersions, the lipid phase is composed of both solid and liquid lipids at room temperature, albeit the final lipid core remains solid. The creation of more imperfect crystals and overall amorphous structures, leaves more available space for drug loading, and simultaneously polymorphic transitions of the pure solid lipid caused by re-crystallisation phenomena are prevented [271,272]. Substitution of the solid lipid by the oil (i.e. liquid lipid) results in suppression of the melting point and alters the crystallisation process, thus rendering the NLCs more physically stable than the SLNs.

Although relatively simple in composition, both SLNs and NLCs bear characteristics that are crucial for their capacity to carry and deliver actives, which will be discussed in the following section.

2.7.1 Formulation parameters

The interplay between formulation parameters and lipid particle characteristics is critical in designing SLNs or NLCs with desirable and at the same time predictable performance in regard to their stability and carrying/delivery capacity. Amongst the formulation aspects that have been

investigated in literature and in this work are the lipid type, the surfactant type and concentration, and for NLCs specifically the solid-to-liquid lipid mass ratio.

With respect to the type of lipid materials used, whether that refers to the solid or liquid lipids, copious different lipids have been utilised, including triglycerides, fatty acids, waxes, phospholipids, steroids and mixtures of partial glycerides (mono-, di- and tri-substituted esters of glyceryl) [273], as the solid components. On the other hand, oleic acid, caprylic/capric triglycerides (also known as medium chain triglycerides, MCTs) and squalene are among the most commonly employed liquid lipids [274]. The chemical composition and structure of the lipids greatly influences their physicochemical properties, including their thermal behaviour and capacity to entrap and carry actives, with lipid mixtures containing fatty acids with different alkyl chain lengths being able to accommodate higher active loading capacities [275]. The impact of the lipid composition relative to the number of carbon atoms and polarity on the particle size was underlined in the work by Boonme *et al*. [276]. Further to that, the use of triglycerides compared to a hard fat resulted in significantly smaller SLN particle sizes, which was ascribed to the surface active properties of mono- and diglycerides contained in the former [277]. Schröder *et al*. [205] demonstrated that tailored particles in terms of their crystalline structure and morphology can be attained by altering the type of solid lipid (tripalmitin, palm stearin) used or substituting part of it with a liquid lipid (tripalmitin with the liquid lipid tricaprylin, 4:1 w/w). Specifically with respect to the solid-to-liquid lipid mass ratio selected in the NLCs' composition, it has been widely reported that the use of higher liquid lipid percentages, sometimes reaching up to 20 or 30% of the total lipid phase has led to improved active loadings and smaller particle sizes [278,279]. A number of studies have also highlighted the importance of choosing lipid combinations with good miscibility/compatibility, as this can play a role in the matrix arrangement, loading capacity, release performance and ultimately in

the active bioavailability if used for delivery [262,280–283]. Therefore, miscibility studies through visual observations and thermal behaviour of the bulk lipids have been also employed as part of the formulation design [281,284,285].

Apart from the lipid materials, a key compositional component of the lipid structure is the surface active species. Their main function is to reduce the interfacial tension between the lipid and aqueous phase during preparation, subsequently causing particle size reduction, while also forming a layer around the particles that contributes to their long-term storage stability. Commonly used emulsifiers are phospholipids like lecithin, polymers (e.g. poloxamers) and polysorbates, with some studies reporting the use of combinations of them to attain improved stability and smaller particle sizes [266,286]. Given that an enormous surface area is generated by the nm size ranged lipid particles, a sufficient concentration of surfactant is required, that can move promptly and cover the newly formed surfaces. High concentration of surfactant (Tween® 80) resulted in more stable SLN dispersions, while the molecular weight also contributed, with bulkier poloxamers stabilising larger particles than polysorbates [287]. Zafeiri *et al*. [202] demonstrated that compared to sodium caseinate (a high molecular weight protein), Tween® 80 was able to lower the interfacial tension much more efficiently leading to smaller particle formation, though better long-term stability was granted by sodium caseinate due to the thicker interfacial film around the particles. Furthermore, in the same work, the significance of the selection of surface active species relative to the lipid materials (and vice versa) was emphasised, as cetyl palmitate particles required a higher concentration of Tween® 80 to achieve the same particle size as tristearin. Moreover, the surface active species have been found to influence the polymorphic transitions and crystalline behaviour of the lipids [282,286–290]. The compatibility between the surfactant and the lipids used can determine the degree of participation of the former in the lipid crystalline lattice [202] and the promotion of

polymorphic transition [289], jointly influencing the particles' internal structure, that consequently impacts upon their functionalities.

2.7.2 Lipid particle characteristics

According to the discussion presented above, evaluation of the lipid particles' structure is imperative to characterise and understand their performance as active carriers and as Pickering emulsion stabilisers. Certain challenges are associated with their characterisation, arising from the small particle size and physical state of the system [291]. Commonly assessed properties are the particle size, electrokinetic potential, thermal behaviour, encapsulation efficiency and loading capacity.

2.7.2.1 Size, morphology and electrokinetic potential

The particle size is one of the main parameters controlling the suitability of a colloidal particle as Pickering stabiliser and its efficacy as a delivery system. It is usually measured immediately after preparation and over storage time to determine stability. Commonly used techniques to characterise the particle size include laser diffraction (LD), and the most frequently used dynamic light scattering (DLS). In these methods, a laser beam illuminates the sample, and the fluctuations of the scattered light are interpreted using different theories to determine the particle size; in the former size is determined from variation in the intensity of scattered light as a function of a scattering angle, while in the latter particle motion causes intensity fluctuations of the scattered light which are used to convert to particle size. Complementary to the size information, the polydispersity index (PDI) is also provided by these techniques as a means of interpreting the size distribution. DLS is deemed more suitable for smaller particle

sizes, and it was therefore the method of choice in this work for the characterisation of the SLNs and NLCs prepared using ultrasonication. Emulsification by ultrasound is a high energy method, where the droplet breakage is driven by acoustic cavitation. The underlying principle is related to the formation, growth and collapse of bubbles in the liquid medium, that consequently produces a shock wave that creates local pressure gradient and fluid shear leading in droplet size reduction [292]. Parameters that can be adjusted include the frequency, residence time, energy density and acoustic intensity and power. Following the emulsification step, the sample is rapidly cooled down below the crystallisation point of the lipid phase to obtain the crystalline particles. The rate of crystallisation can be tuned, though extremely rapid cooling can cause the particles to experience delayed polymorphic transitions and eventual destabilisation [293].

In cases where the particle size is large enough (μm range), optical microscopy can be used to determine the particle size and morphology [294]. With respect to the morphology, scanning electron microscopy (SEM), transmission electron microscopy (TEM) and atomic force microscopy (AFM) can provide information regarding the shape, and in some studies the distribution of materials within the lipid matrix [205,295,296], as will be discussed later.

The electrokinetic potential, also known as zeta potential (ζ-potential), is used as a measure of particle surface charge in the aqueous dispersion systems and comprises a useful tool for predicting long-term stability. Depending on size, DLS and LD can enable the determination of ζ-potential by means of the electrophoretic mobility of the particles. Zeta potential values more than 30 mV in absolute value have been considered as required to ensure stability, albeit particles with smaller values have exhibited good long-term stability owing to combination of steric and electrostatic effects [282]. Thus, environmental conditions including the pH, ionic

strength, type of solvent and nature and concentration of electrolytes need to be considered, as these will greatly affect the surface charge of the particles [297].

2.7.2.2 Crystallinity and polymorphism

A simplified description of the lipid particle structure could be given by the lipid core constituting the internal fragment and the surfactant layer comprising the external portion of the particle. The specific organisation and interaction between these two parts together with the active ingredient define the active carrying/release capabilities, and are greatly affected by the crystalline behaviour of the lipids. The crystallisation of the lipids is a process that largely occurs after emulsification during the cooling step, though part of it continues during storage. The lipid matrix composition (encompassing the solid and liquid lipid, AI and surfactant), size of the melted droplets and cooling rate play a major role in the crystallisation of the solid lipid [298]. Throughout the main portion of crystallisation, the shape, organisation and relative location of each component is established, and therefore it is crucial for the subsequent particle behaviour.

It has been extensively reported that re-crystallisation taking place during storage can give rise to detrimental phenomena, including active expulsion and agglomeration due to shape changes [282,299,300]. These alterations are induced by polymorphic transitions, which are reversible transitions of a solid crystalline phase to different arrangements [301]. Control over this, can allow for higher AI loadings by selecting metastable polymorphic forms [272], or improved stability by opting for a stable state [293]. A typical example used to describe variations in the packing and inclination angle between different polymorphic states is that of triglycerides (TAGs). TAGs can exist in three main polymorphic forms, namely α (hexagonal subcell), β'

(orthorhombic-perpendicular subcell) and β (triclinic-parallel subcell), as shown in Fig. 2.15. The α form is metastable and has the tendency to rapidly transform into forms with improved packing density, β' is a form with intermediate stability, while β is the form with the highest stability. The transition from the least stable to the most stable form follows the sequence depicted in Fig. 2.15, although the transformation from one form to another is not always complete, leading to mixtures of different polymorphic forms. For instance, crystals that during crystallisation remained in the β' form have been shown to transition to more stable states during storage, resulting in changes in the shape and stability of the particles [302,303]. With respect to the polymorphic forms influence on the SLNs/NLCs shape, particles of spherical or almost spherical shapes have been ascribed to the α polymorph, while platelet, needle- or lath-like shapes have been described for crystalline states that contain β' and β forms [205,288,304].

The length and characteristics of the alkyl chain, saturation/unsaturation and *cis*/*trans* configurations of the lipids participating can affect the specific behaviour, as well as the rate of nucleation which is dictated by the rate of cooling or shear applied during crystallisation [305]. The co-presence of lower molecular weight, amphiphilic (e.g. monoacylglycerols, diacylglycerols), liquid or lipids of higher polarity can induce further polymorphic transitions and post-crystallisation phenomena, usually towards less stable forms, together with a suppression of the melting temperature [281,306]. Relative to the active loading capacity, the use of mixtures of lipids with vastly different alkyl chain lengths or addition of liquid lipids, could potentially create imperfections in the crystalline lattices or provoke crystallisation in less stable polymorphs with lower packing densities that can in turn increase the loading efficiency [307]. Additionally, the use of stabilising agents with some affinity/compatibility for the lipid core can contribute to polymorphic transitions to some extent [202], albeit they can also have an effect without participation in the crystalline lattice [308].

Therefore, it is crucial to characterise the crystalline structure of the bulk lipid blends and lipid particles. The techniques frequently utilised for that purpose are differential scanning calorimetry (DSC) and X-ray diffraction (XRD), solely or in combination.

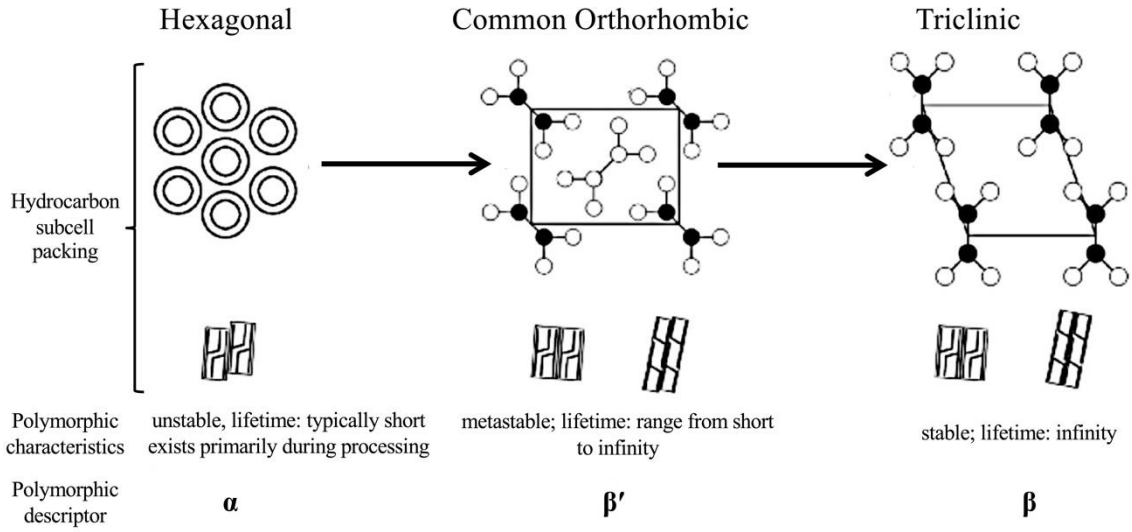

Fig. 2.15. Polymorphic forms of fat crystals, polymorphic transitions, subcell packing structures, stability characteristics and TAG stacking conformations (adapted from Rogers *et al*. [309]).

2.7.2.3 Encapsulation efficiency and loading capacity

Thus far the terms encapsulation efficiency and loading capacity have been used almost interchangeably, and although they are calculated differently, they indeed describe the same attribute, which is the aptitude of the particles' structure to encase an active. The encapsulation efficiency (EE), also referred to as entrapment efficiency, describes the amount of active present in the particles in comparison to the amount of active that came in the dispersion during preparation. The loading capacity (LC) conveys the amount of active present in relation to the amount of lipid phase in the particles.

In most cases, the method used for their determination is the same (despite alteration in the calculation step), and could be ranging from ultrafiltration and centrifugation to dialysis. The values usually reported for EE are above 70%, while LC can range between 0.1 and 80% [310]. The variance in the latter could be attributed to differences in the active solubilisation method used. Compared to simple solubilisation of the active in the lipid melt, which was the process used in this work, the employment of organic solvents (e.g. ethanol, chloroform) has been shown to lead to higher LC values [311,312]. Considering the drug expulsion phenomena during crystallisation and storage that were described above, it is paramount to quantify the percentage of active remaining associated with the particles' structure, as this will then influence interpretation of the dispersions' release performance. It is expected that the solubility of the active in the lipids will decrease after crystallisation, and thus maintaining the concentration of the active close to the solubility threshold defined during preliminary solubility and screening studies could potentially grant that the highest proportion of the active quantity will remain associated with the particles. A few studies have utilised lipid screening as a tool to predict the active loading, and additionally to eliminate the need of experimental screening which can be tedious [284,313,314]. Undoubtedly, the compatibility and affinity of the active for the lipid matrix components, encompassing both lipids and surface active species, can greatly impact upon the loading capacities and lipid matrix arrangements ultimately achieved [262,280–283].

2.7.2.4 Proposed lipid structure and active location

Differences in the morphology of SLNs can be relatively simply assigned to changes in the type of lipid and surfactant used, and in most cases they are relevant to the shape of the structure, which is defined by the parameters described above. However, once the liquid lipid is

introduced things get a bit more complicated. As illustrated in Fig. 2.16A, the classical approach to the NLCs type identification entails three classes; namely, the imperfect, amorphous and multiple types. Müller *et al*. [275] has paralleled the SLNs internal structure to that of a 'brick wall', whereas this is overcome with the creation of imperfections caused by the liquid lipid incorporation in NLCs. According to the authors [275], the generation of the imperfect type has been attributed to mixing of two very different types of fatty acid glycerides in terms of their spatial differences. Attainment of the amorphous type can be accomplished by mixing solid lipids and special liquid lipids, such as medium chain triglycerides. The multiple type is essentially an oil-in fat-in water system, formed when the concentration of the liquid lipid exceeds the solubility limit of the solid fat, thereby forming oil nano-compartments in the fat core.

Since that classification, several other studies have attempted to provide a description for the NLCs' internal arrangement, by corroborating information from the use of several different techniques, including cryo-TEM [315,316], NMR [317–319], DSC [315,318] and X-Ray diffraction [317,319]. Galeano *et al*. [273] has created a schematic synopsis of the reported structures based on literature data, that is depicted in Fig. 2.16B. Predominantly dictated by the solid-to-liquid lipid ratio used and the formed polymorphic states, 5 types of NLCs are presented, with differences between them lying on the particle shape and location of the liquid lipid. First described by the group of Jores *et al*. [316,318,320] in a series of studies regarding the structure of NLCs, was the creation of liquid lipid spots at the surface of NLCs that get increasingly bigger with increasing liquid lipid concentration. Only when the liquid lipid is used in very low concentrations (<10%) there is a possibility of acquiring the uniformly dispersed model [321], while at intermediate concentration and depending on the compatibility between the two lipid, the oil nano-compartment model can exist [270]. Keck *et al*. [322], emphasised

the influence of the solid-to-liquid lipid relative arrangement on the active delivery performance, by exhibiting that as the matrix organisation changes so does the release performance and dermal penetration efficacy of the SLNs and NLCs.

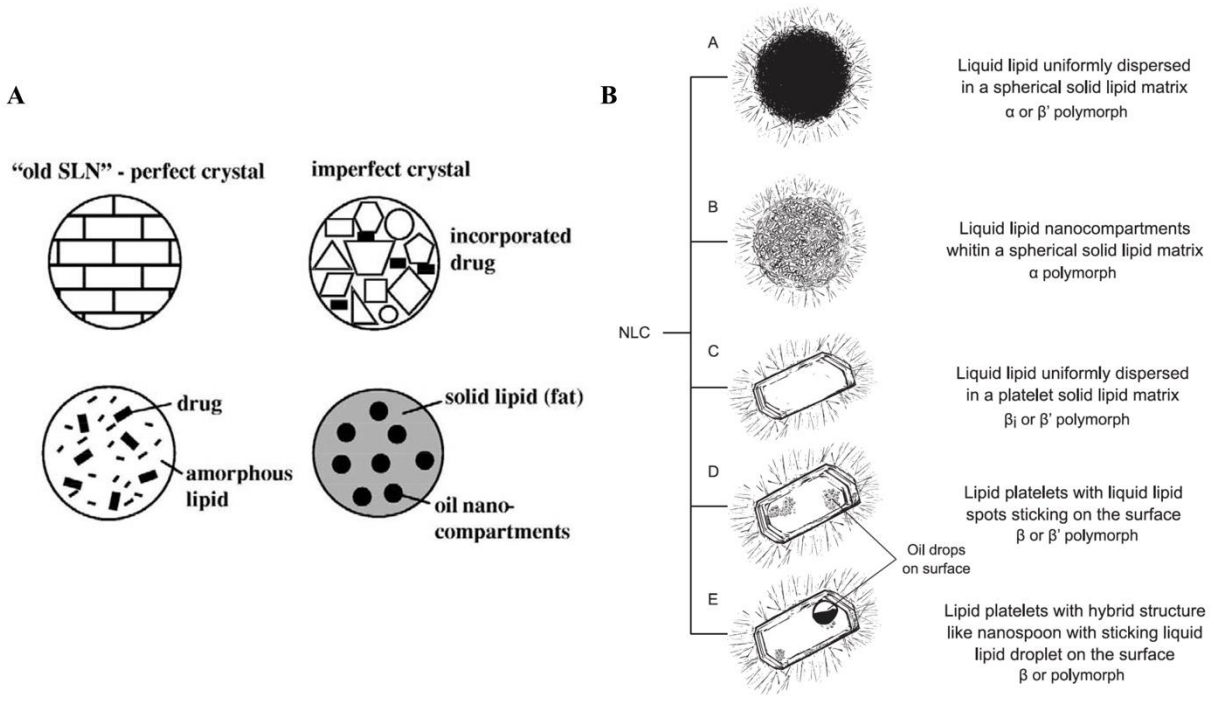

Fig. 2.16. (A) Proposed structure of SLNs and three types of NLCs for comparison purposes. The NLCs types as described by Müller et al. [275] are the imperfect type (upper right), amorphous type (lower left), multiple type (lower right). (B) Schematic representation of the NLCs models according to their shape and liquid lipid distribution as summarised by Galeano et al. [273].

As deliberated throughout this section, the characterisation of the lipid particles' structure is a challenging endeavour not only due to their small size, but also due to the liquid physical state of the particle dispersions. Besides the determination of the solid and liquid lipid arrangement, this engenders complexities with devising tools to predict the localisation of the encapsulated active molecule, as the majority of the techniques utilised cannot provide definitive

conclusions. Therefore, in most studies the release behaviour is corroborated with physicochemical characterisation to postulate about the relative location of the active molecule.

Based on the positioning of the active, three models have been described for SLNs; the homogeneous matrix, the active-enriched shell and the active-enriched core models (Fig. 2.17). In the homogeneous matrix model, uniform particle crystallisation owing to the process used, or entrapment of a highly lipophilic active can lead to a homogeneously dispersed active throughout the core, with this model having been linked to prolonged release profiles [135]. On the contrary, in the active-enriched shell model, the active is mainly located in the outer shell of the particles with little or no presence in the core. Rapid cooling of an active-loaded lipid melt, or higher affinity of the active for the surface agent than the lipids can generate this model, that has been associated with burst release profiles [42,323]. Finally, the active-enriched core model can be attained when the active has a higher crystallisation point than the lipids, causing supersaturation in the lipid melt mixture as it cools down, resulting in crystallisation of the active in the core of the particle. Suitably controlled and prolonged release rates have been ascribed to this model [135,324].

In addition to the aforementioned explanations, significant contribution to the drug location also has the polymorphic state at which the lipids exist as was discussed above, the distribution coefficient [310], the affinity/solubility [325] and any interactions [326,327] of the active with the lipid matrix components. In cases where the α polymorphic state is predominant in the lipid matrix, allowing for more space for active encasement, the homogeneous active model described the developed systems [286,328]. Although in SLNs the active tends to be found near the surface, associated with the surfactant [329–332], in NLCs a big contributing factor is the liquid lipid, particularly with lipophilic actives [280,320,333]. Specifically for hydrophilic

species [334,335] or when the amount of active used exceeds the limit that the particles' surface area [336] can incorporate, the actives would be preferentially located at the surface. Using state of the art techniques, like coherent anti-Stokes Raman scattering (CARS), Christophersen *et al*. [337] was able to visualise the internal structure of lipid microparticles and concluded that the active location is dictated by the preparation method and lipid excipients used.

As deduced based on the range of factors that can potentially contribute to the ultimate active location, this is a topic that has not been fully elucidated yet, and its intricacy requires further investigations.

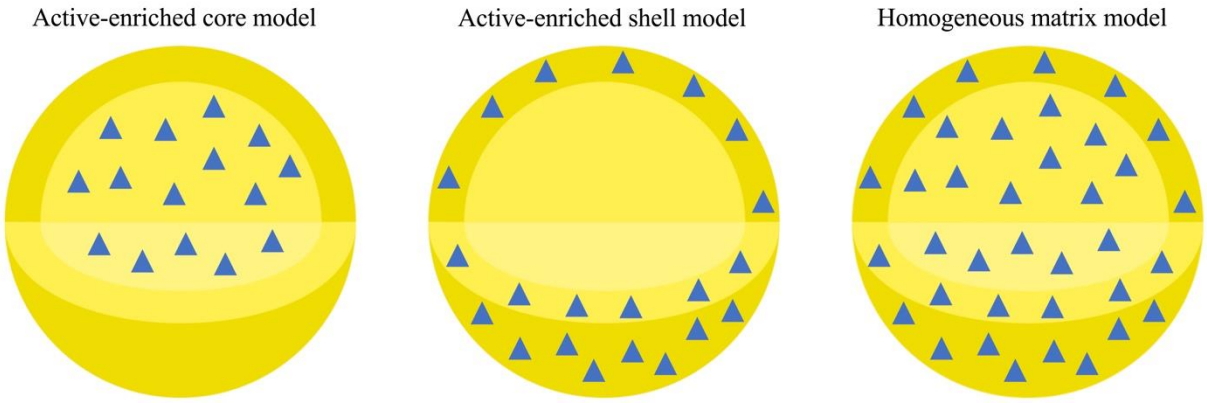

Fig. 2.17. Schematic representation of the active incorporation models in SLNs (adapted from Müller et al. [275]).

2.7.3 SLNs and NLCs as active encapsulation and delivery systems

Numerous works have utilised SLNs and NLCs for the encapsulation and delivery of active ingredients of diverse properties, relevant to a plethora of applications [135,338,339]. Investigation of their *in vitro* release performance is a useful tool for predicting their *in vivo* performance, and therefore an abundance of release data is available in literature. However,

some of the studies are only reporting the optimised performance without disclosing the parameters that were altered to achieve said release profiles, or there is a lack of comparison to either control formulations or systems that examine the effect of modifying formulation parameters. What is more, understanding the level of control over the active release performance that the formulation itself can provide is impeded, when vastly different experimental conditions and formulation aspects are used throughout the studies, that may be interfering with the physical stability of the structure.

A big portion of the literature at hand is comparing the SLNs release behaviour to that of NLCs, with contradictory conclusions drawn on their performance, which is centred around the effect of the liquid lipid addition in NLCs on either accelerating [269,278,340–343] or decelerating [344–346] the release rate. Some reports are reinforcing even further the conflicting results, by showing that there are no differences between the release control capability of the two counterparts [347], or variations are only observed at the rate of release and not at the overall percentage released at the same timescales [348]. The release pattern, whether that is monophasic or biphasic, burst or prolonged, the overall percentage released and the perpetuation of that performance over time are among the characteristics examined when comparing the release profiles [349].

Regardless of the deduction, there are certain factors that need to be deliberated when trying to find explanations for these observations. Amongst these are the release conditions (e.g. type of solvent in the dissolution medium, pH, temperature), active concentration, encapsulation efficiency and whether that is accounted when reporting release results, particle morphology (e.g. shape, size), lipid phase concentration, particle composition (e.g. type and concentration of lipids and surface agents), interactions/affinity between the active and the lipid matrix

components and particle preparation method. Gonçalves *et al*. [350] presented the significance of the dissolution medium's nature relative to the active employed, with lipophilic curcumin showing faster release in the lipophilic than the hydrophilic media. Das *et al*. [349] attributed the hindered release rate when a higher active concentration was used (8% compared to 4% active to lipid ratio), to the absence of true sink conditions, an effect that was eliminated when the particle dispersion was diluted before release measurement. The influence of the active concentration has been also discussed in relation to the formed active distribution model, with lower concentration leading to active-enriched shell and consequently slow diffusion [269].

In fact, a correlation between some of the aforementioned factors, their impact on the internal lipid matrix arrangement and consequent release performance has been attempted in several studies. In a recent work by Galeano *et al.* [310], the degree of the active solubility in the lipid phase and overall distribution coefficient in the lipid matrix components was shown to lead to burst release of parabens from SLNs, NLCs and nano-emulsions, that was explained by the active preferential partition to the surfactant layer of the structures. Mura *et al*. [351] ascribed the hindered release rate from SLNs compared to NLCs to the denser packing of the internal lipid structure, which results in reduced active mobility; an argument also made in the study by Andrade *et al*. [346] and Keck *et al*. [322]. Zoubari *et al*. [352] further accentuated the feature of burst release from a highly disordered internal lattice, by employing two solid lipids in the NLCs core. More specifically on the effect of the liquid lipid concentration in NLCs, in two studies by the same authors [278,343] it was demonstrated that increasing liquid lipid concentration led to increased release percentage. The authors discerned that the liquid lipid presence influenced only the initial burst release phase due to the heterogeneous liquid lipid distribution resulting in an active-rich layer towards the edge of the core, while also in one of the studies the particles had significantly smaller particle sizes [278]. It was also discussed that

the reason behind attaining such internal core arrangement was the processing method used, which once altered (from solvent evaporation performed at 70°C to high pressure homogenisation performed at 0°C) an almost linear release rate was acquired, due to homogeneous liquid lipid distribution [343]. The impact of the processing method utilised on the particle formulation characteristics, and particularly on the percentage of active encapsulated and thus released rate has also been documented [323]. In another work comparing between emulsions, SLNs and NLCs, the importance over the ability to control the release behaviour was assigned to the location and distribution of the liquid lipid in NLCs rather than its concentration [353]. In the same study [353], it was suggested that this can be achieved by deliberate selection of the formulation and processing parameters.

Galeano *et al*. [273] endeavoured to provide a comprehensive review of the different processing, formulation and experimental aspects influence on the release behaviour of paclitaxel, a hydrophobic chemotherapy drug, for which SLNs and NLCs are widely employed as carrier and delivery vehicles. In this summary, tens of research papers are discussed, and the release data are presented in the same graph to enable comparison purposes. The attempt to unravel the underlying mechanisms of the release performance is also reflected by the utilisation of release model fitting in copious studies [322,349,351]. However, in the same review it is also highlighted [273], that no definite conclusions can be made regarding the contribution of each factor, due to the variations in the composition and experimental conditions employed throughout the studies, that would in turn result in different underlying mechanisms driving the dissolution kinetics (e.g. active partition coefficients and internal particle arrangement).

2.7.3.1 SLNs and NLCs as co-encapsulation and co-delivery systems

The exploitation of SLNs and NLCs as encapsulants and delivery vehicles is not just limited to a single AI, on the contrary it extends to two or even more active molecules [137]. A wide range of compounds spanning from lipophilic APIs and antioxidants [354] to siRNA [355] and DNA [356] have been combined in SLNs [357] and NLCs [136,358–361], but primarily in the latter.

In terms of the co-encapsulation behaviour, studies reporting the EE and LC values show that there are no significant differences between the two AIs [136,356,361–363], as well as that any active expulsion phenomena over time are not induced by their co-entrapment [359]. Although, no information is provided regarding the EE or LC values before encapsulation of the secondary active. With respect to the release behaviour, the co-release profiles of the AIs can be completely different (one active showing biphasic and the other linear release rate [360]) or the two actives can share the same profile [354], depending on the specific formulation, processing and experimental conditions, as was discussed in the previous sections. Andrade *et al*. [363] discussed the effect of the relative affinity between the used actives (tacrolimus and clobetasol) and the lipids comprising the NLCs. They attributed the more sustained release of tacrolimus to its higher affinity for the solid lipid, and the faster release of clobetasol to its association with the liquid lipid localised towards the outer layer of the particles. Vitorino *et al*. [362] examined the influence of ethanol and limonene utilised as chemical enhancers for transdermal formulations on the EE and release profile of simvastatin and olanzapine from NLCs. It was shown that the chemical enhancers slightly increased the release rate of the two actives, that already had different release profiles, while the EE values decreased with ethanol and increased with limonene.

Overall, due to the relatively limited number of studies in this area, or the fact that the available literature focuses on the application testing rather than on formulation design aspects and detailed characterisation of the co-encapsulated microstructures, there is a lack of investigation regarding the effect of the co-presences of the AIs on the performance of the formulation. In the future, approaches to allow the independent control of the release profiles need to be explored, along with methods to enable the segregated co-encapsulation in SLN/NLC dispersions. That could be potentially achieved by mixing two aqueous lipid particle dispersions, one containing lipid particles loaded with 'active A' and the other particles loaded with 'active B' into the same formulation, and studying its performance as a co-encapsulation and co-delivery system.

2.8 Conclusions

The quest for a structuring strategy that can enable the segregated co-encapsulation and independent, and potentially triggered co-delivery of multiple active ingredients from Pickering emulsions is an area still in its infancy, as evidenced by the only recently published and at exploratory-level studies presented in this review. Lipid particles with varying microstructural characteristics, namely SLNs and NLCs, show great potential for acting as dual functional species, thereby acting as active carriers and delivery systems for an active, while in tandem stabilising emulsion droplets encasing a secondary active. Such a liquid-based formulation approach requires diligent design to subdue the inherent complexity of combining two distinctive phases (i.e. crystalline particles and liquid oil droplet) and ratify that microstructural characteristics governing their carrying and delivery functionalities remaining intact. In the subsequent experimental chapters, formulation parameters that impact upon the performance of the envisaged structuring approach will be scrutinised.

References

[1] M.R. Kim, T. Feng, Q. Zhang, H.Y.E. Chan, Y. Chau, Co-Encapsulation and Co-Delivery of Peptide Drugs via Polymeric Nanoparticles, Polymers (Basel). 11 (2019). https://doi.org/10.3390/polym11020288.

[2] N. Kolishetti, S. Dhar, P.M. Valencia, L.Q. Lin, R. Karnik, S.J. Lippard, R. Langer, O.C. Farokhzad, Engineering of self-assembled nanoparticle platform for precisely controlled combination drug therapy, Proc Natl Acad Sci U S A. 107 (2010) 17939–17944. https://doi.org/10.1073/pnas.1011368107.

[3] F. Graily Moradi, M.J. Hejazi, H. Hamishehkar, A.A. Enayati, Co-encapsulation of imidacloprid and lambda-cyhalothrin using biocompatible nanocarriers: Characterization and application, Ecotoxicol Environ Saf. 175 (2019) 155–163. https://doi.org/10.1016/j.ecoenv.2019.02.092.

[4] C. An, J. Cui, Q. Yu, B. Huang, N. Li, J. Jiang, Y. Shen, C. Wang, S. Zhan, X. Zhao, X. Li, C. Sun, B. Cui, C. Wang, F. Gao, Z. Zeng, H. Cui, R. Zhang, Y. Wang, Polylactic acid nanoparticles for co-delivery of dinotefuran and avermectin against pear tree pests with improved effective period and enhanced bioactivity, Int J Biol Macromol. 206 (2022) 633–641. https://doi.org/10.1016/j.ijbiomac.2022.02.182.

[5] Y. Ji, S. Ma, S. Lv, Y. Wang, S. Lü, M. Liu, Nanomaterials for Targeted Delivery of Agrochemicals by an All-in-One Combination Strategy and Deep Learning, ACS Appl Mater Interfaces. 13 (2021) 43386. https://doi.org/10.1021/acsami.1c11914/.

[6] F. Han, D. Luo, W. Qu, D. Chen, Y. Hong, J. Sheng, X. Yang, W. Liu, Nanoliposomes codelivering bioactive peptides produce enhanced anti-aging effect in human skin, J Drug Deliv Sci Technol. 57 (2020) 101693. https://doi.org/10.1016/j.jddst.2020.101693.

[7] P.J. Chawda, J. Shi, S. Xue, S. Young Quek, Co-encapsulation of bioactives for food applications, Food Quality and Safety. 1 (2017) 302–309. https://doi.org/10.1093/fqsafe/fyx028.

[8] Y. Wei, Z. Yu, K. Lin, S. Yang, K. Tai, J. Liu, L. Mao, F. Yuan, Y. Gao, Fabrication, Physicochemical Stability, and Microstructure of Coenzyme Q10 Pickering Emulsions Stabilized by Resveratrol-Loaded Composite Nanoparticles, J Agric Food Chem. 68 (2020) 1405–1418. https://doi.org/10.1021/acs.jafc.9b06678/.

[9] L. Tavano, R. Muzzalupo, N. Picci, B. de Cindio, Co-encapsulation of antioxidants into niosomal carriers: gastrointestinal release studies for nutraceutical applications, Colloids Surf B Biointerfaces. 114 (2014) 82–88. https://doi.org/10.1016/j.colsurfb.2013.09.058.

[10] J. Liu, D. Chi, S. Pan, L. Zhao, X. Wang, D. Wang, Y. Wang, Effective co-encapsulation of doxorubicin and irinotecan for synergistic therapy using liposomes prepared with triethylammonium sucrose octasulfate as drug trapping agent, Int J Pharm. 557 (2019) 264–272. https://doi.org/10.1016/j.ijpharm.2018.12.072.

[11] S. Bangalore, G. Kamalakkannan, S. Parkar, F.H. Messerli, Fixed-Dose Combinations Improve Medication Compliance: A Meta-Analysis, American Journal of Medicine. 120 (2007) 713–719. https://doi.org/10.1016/j.amjmed.2006.08.033.

[12] J.A. DiMasi, R.W. Hansen, H.G. Grabowski, The price of innovation: new estimates of drug development costs, J Health Econ. 22 (2003) 151–185. https://doi.org/10.1016/s0167-6296(02)00126-1.

[13] S. Rennane, L. Baker, A. Mulcahy, Estimating the Cost of Industry Investment in Drug Research and Development: A Review of Methods and Results, INQUIRY: The Journal of Health Care Organization, Provision, and Financing. 58 (n.d.) 1–11. https://doi.org/10.1177/00469580211059731.

[14] J. Woodcock, J.P. Griffin, R.E. Behrman, Development of Novel Combination Therapies, New England Journal of Medicine. 364 (2011) 985–987. https://doi.org/10.1056/NEJMp1101548.

[15] A.N. de Cates, M.R.B. Farr, N. Wright, M.C. Jarvis, K. Rees, S. Ebrahim, M.D. Huffman, Fixed-dose combination therapy for the prevention of cardiovascular disease, Cochrane Database of Systematic Reviews. 2014 (2014). https://doi.org/10.1002/14651858.cd009868.pub2.

[16] X. Zhang, Anti-retroviral drugs: current state and development in the next decade, Acta Pharm Sin B. 8 (2018) 131–136. https://doi.org/10.1016/j.apsb.2018.01.012.

[17] G. Schernthaner, Fixed-dose combination therapies in the management of hyperglycaemia in Type 2 diabetes: An opportunity to improve adherence and patient care, Diabetic Medicine. 27 (2010) 739–743. https://doi.org/10.1111/j.1464-5491.2010.03000.x.

[18] H. Chen, Y. Shan, L. Cao, P. Zhao, C. Cao, F. Li, Q. Huang, Enhanced Fungicidal Efficacy by Co-Delivery of Azoxystrobin and Diniconazole with Cauliflower-Like Metal–Organic Frameworks NH2-Al-MIL-101, International Journal of Molecular Sciences 2021, Vol. 22, Page 10412. 22 (2021) 10412. https://doi.org/10.3390/ijms221910412.

[19] K.A. Molla, S. Karmakar, J. Molla, P. Bajaj, R.K. Varshney, S.K. Datta, K. Datta, Understanding sheath blight resistance in rice: the road behind and the road ahead, Plant Biotechnol J. 18 (2020) 895–915. https://doi.org/10.1111/pbi.13312.

[20] G. Badea, N. Badea, L.I. Brasoveanu, M. Mihaila, R. Stan, D. Istrati, T. Balaci, I. Lacatusu, Naringenin improves the sunscreen performance of vegetable nanocarriers, New Journal of Chemistry. 41 (2017) 480–492. https://doi.org/10.1039/c6nj02318e.

[21] L.D. di Filippo, J.L. Duarte, C.A. Roque-Borda, F.R. Pavan, A.B. Meneguin, M. Chorilli, A. Melero, A.J. Guillot, C.M. Spagnol, M.A. Correa, In Vitro Skin Co-Delivery and Antibacterial Properties of Chitosan-Based Microparticles Containing Ascorbic Acid and Nicotinamide, Life. 12 (2022) 1049. https://doi.org/10.3390/life12071049/s1.

[22] L.W. Tian, D. Luo, D. Chen, H. Zhou, X.C. Zhang, X.L. Yang, Y.L. Wang, W. Liu, Co-delivery of bioactive peptides by nanoliposomes for promotion of hair growth, J Drug Deliv Sci Technol. 72 (2022) 103381. https://doi.org/10.1016/j.jddst.2022.103381.

[23] P. Daliu, A. Santini, E. Novellino, From pharmaceuticals to nutraceuticals: bridging disease prevention and management, Expert Rev Clin Pharmacol. 12 (2019) 1–7. https://doi.org/10.1080/17512433.2019.1552135.

[24] A. Bergamin, E. Mantzioris, G. Cross, P. Deo, S. Garg, A.M. Hill, Nutraceuticals: Reviewing their Role in Chronic Disease Prevention and Management, Pharmaceut Med. 33 (2019) 291–309. https://doi.org/10.1007/S40290-019-00289-w.

[25] S.G.J. van Breda, T.M.C.M. de Kok, Smart Combinations of Bioactive Compounds in Fruits and Vegetables May Guide New Strategies for Personalized Prevention of Chronic Diseases, Mol Nutr Food Res. 62 (2018). https://doi.org/10.1002/mnfr.201700597.

[26] A. Gürsoy, E. Kut, S. Özkirimli, Co-encapsulation of isoniazid and rifampicin in liposomes and characterization of liposomes by derivative spectroscopy, Int J Pharm. 271 (2004) 115–123. https://doi.org/10.1016/j.ijpharm.2003.10.033.

[27] N. Li, P. Zhang, C. Huang, Y. Song, S. Garg, Y. Luan, Co-delivery of doxorubicin hydrochloride and verapamil hydrochloride by pH-sensitive polymersomes for the reversal of multidrug resistance, RSC Adv. 5 (2015) 77986–77995. https://doi.org/10.1039/c5ra15313a.

[28] C.M.B. Pinilla, A. Brandelli, Antimicrobial activity of nanoliposomes co-encapsulating nisin and garlic extract against Gram-positive and Gram-negative bacteria in milk, Innovative Food Science & Emerging Technologies. 36 (2016) 287–293. https://doi.org/10.1016/j.ifset.2016.07.017.

[29] K. Coradini, F.O. Lima, C.M. Oliveira, P.S. Chaves, M.L. Athayde, L.M. Carvalho, R.C.R. Beck, Co-encapsulation of resveratrol and curcumin in lipid-core nanocapsules improves their in vitro antioxidant effects, European Journal of Pharmaceutics and Biopharmaceutics. 88 (2014) 178–185. https://doi.org/10.1016/j.ejpb.2014.04.009.

[30] A. Sesarman, L. Tefas, B. Sylvester, E. Licarete, V. Rauca, L. Luput, L. Patras, S. Porav, M. Banciu, A. Porfire, Co-delivery of curcumin and doxorubicin in PEGylated liposomes favored the antineoplastic C26 murine colon carcinoma microenvironment, Drug Deliv Transl Res. 9 (2019) 260–272. https://doi.org/10.1007/s13346-018-00598-8.

[31] S.M. Motevalli, A.S. Eltahan, L. Liu, A. Magrini, N. Rosato, W. Guo, M. Bottini, X.-J. Liang, S.M. Motevalli, A.S. Eltahan, L. Liu, A. Magrini, N. Rosato, W. Guo, M. Bottini, X.-J. Liang, Co-encapsulation of curcumin and doxorubicin in albumin nanoparticles blocks the adaptive treatment tolerance of cancer cells, Biophysics Reports, 2019, Vol. 5, Issue 1, Pages: 19-30. 5 (2019) 19–30. https://doi.org/10.1007/S41048-018-0079-6.

[32] S. Martin-Ortigosa, J.S. Valenstein, V.S.Y. Lin, B.G. Trewyn, K. Wang, Gold functionalized mesoporous silica nanoparticle mediated protein and DNA codelivery to plant cells via the biolistic method, Adv Funct Mater. 22 (2012) 3576–3582. https://doi.org/10.1002/adfm.201200359.

[33] L. Han, Y. Fu, A.J. Cole, J. Liu, J. Wang, Co-encapsulation and sustained-release of four components in ginkgo terpenes from injectable PELGE nanoparticles, Fitoterapia. 83 (2012) 721–731. https://doi.org/10.1016/j.fitote.2012.02.014.

[34] G. Navarro, J. Pan, V.P. Torchilin, Micelle-like Nanoparticles as Carriers for DNA and siRNA, Mol Pharm. 12 (2015) 301. https://doi.org/10.1021/mp5007213.

[35] A.P. Acharya, J.S. Lewis, B.G. Keselowsky, Combinatorial co-encapsulation of hydrophobic molecules in poly(lactide-co-glycolide) microparticles, Biomaterials. 34 (2013) 3422–3430. https://doi.org/10.1016/j.biomaterials.2013.01.032.

[36] L. Miao, S. Guo, J. Zhang, W.Y. Kim, L. Huang, Nanoparticles with Precise Ratiometric Co-Loading and Co-Delivery of Gemcitabine Monophosphate and Cisplatin for Treatment of Bladder Cancer, Adv Funct Mater. 24 (2014) 6601–6611. https://doi.org/10.1002/adfm.201401076.

[37] N.J. Zuidam, V.A. Nedović, Encapsulation technologies for active food ingredients and food processing, Encapsulation Technologies for Active Food Ingredients and Food Processing. (2010) 1–400. https://doi.org/10.1007/978-1-4419-1008-0.

[38] T.A. Comunian, M. Thomazini, A.J.G. Alves, F.E. de Matos Junior, J.C. de Carvalho Balieiro, C.S. Favaro-Trindade, Microencapsulation of ascorbic acid by complex coacervation: Protection and controlled release, Food Research International. 52 (2013) 373–379. https://doi.org/10.1016/j.foodres.2013.03.028.

[39] L.C.M. Cunha, M.L.G. Monteiro, B.R.C. Costa-Lima, J.M. Guedes-Oliveira, V.H.M. Alves, A.L. Almeida, R. v. Tonon, A. Rosenthal, C.A. Conte-Junior, Effect of microencapsulated extract of pitaya (Hylocereus costaricensis) peel on color, texture and oxidative stability of refrigerated ground pork patties submitted to high pressure processing, Innovative Food Science & Emerging Technologies. 49 (2018) 136–145. https://doi.org/10.1016/j.ifset.2018.08.009.

[40] B. Wang, T.O. Akanbi, D. Agyei, B.J. Holland, C.J. Barrow, Coacervation Technique as an Encapsulation and Delivery Tool for Hydrophobic Biofunctional Compounds, Role of Materials Science in Food Bioengineering. (2018) 235–261. https://doi.org/10.1016/b978-0-12-811448-3.00007-3.

[41] Y.H. Cho, J. Park, Encapsulation of flavors by molecular inclusion using β-cyclodextrin: Comparison with spray-drying process using carbohydrate-based wall materials, Food Sci Biotechnol. 18 (2009) 185–189.

[42] M. Li, O. Rouaud, D. Poncelet, Microencapsulation by solvent evaporation: State of the art for process engineering approaches, Int J Pharm. 363 (2008) 26–39. https://doi.org/10.1016/j.ijpharm.2008.07.018.

[43] C.I. Beristain, A. Vazquez, H.S. Garcia, E.J. Vernon-Carter, Encapsulation of Orange Peel Oil by Co-crystallization, LWT - Food Science and Technology. 29 (1996) 645–647. https://doi.org/10.1006/fstl.1996.0098.

[44] A. Gharsallaoui, G. Roudaut, O. Chambin, A. Voilley, R. Saurel, Applications of spray-drying in microencapsulation of food ingredients: An overview, Food Research International. 40 (2007) 1107–1121. https://doi.org/10.1016/j.foodres.2007.07.004.

[45] M.P. Silva, F.L. Tulini, E. Martins, M. Penning, C.S. Fávaro-Trindade, D. Poncelet, Comparison of extrusion and co-extrusion encapsulation techniques to protect Lactobacillus acidophilus LA3 in simulated gastrointestinal fluids, LWT. 89 (2018) 392–399. https://doi.org/10.1016/j.lwt.2017.11.008.

[46] Z. Fang, B. Bhandari, Spray drying, freeze drying and related processes for food ingredient and nutraceutical encapsulation, Encapsulation Technologies and Delivery Systems for Food Ingredients and Nutraceuticals. (2012) 73–109. https://doi.org/10.1533/9780857095909.2.73.

[47] C. Frey, Fluid Bed Coating-Based Microencapsulation, Microencapsulation in the Food Industry. (2014) 65–79. https://doi.org/10.1016/b978-0-12-404568-2.00007-8.

[48] S.H. Sonawane, B.A. Bhanvase, M. Sivakumar, S.B. Potdar, Current overview of encapsulation, Encapsulation of Active Molecules and Their Delivery System. (2020) 1–8. https://doi.org/10.1016/b978-0-12-819363-1.00001-6.

[49] A. Bušić, D. Komes, A. Belščak-Cvitanovic, A.V. Cebin, I. Špoljarić, G. Mršić, S. Miao, The Potential of Combined Emulsification and Spray Drying Techniques for Encapsulation of Polyphenols from Rosemary (Rosmarinus officinalis L.) Leaves, Food Technol Biotechnol. 56 (2018) 494–505. https://doi.org/10.17113/ftb.56.04.18.5680.

[50] R. Zhang, L. Zhou, J. Li, H. Oliveira, N. Yang, W. Jin, Z. Zhu, S. Li, J. He, Microencapsulation of anthocyanins extracted from grape skin by emulsification/internal gelation followed by spray/freeze-drying techniques: Characterization, stability and bioaccessibility, LWT. 123 (2020) 109097. https://doi.org/10.1016/j.lwt.2020.109097.

[51] N.J. Zuidam, E. Shimoni, Overview of microencapsulates for use in food products or processes and methods to make them, Encapsulation Technologies for Active Food Ingredients and Food Processing. (2010) 3–29. https://doi.org/10.1007/978-1-4419-1008-0_2.

[52] N.A. Lopes, C.M. Barreto Pinilla, A. Brandelli, Antimicrobial activity of lysozyme-nisin co-encapsulated in liposomes coated with polysaccharides, Food Hydrocoll. 93 (2019) 1–9. https://doi.org/10.1016/j.foodhyd.2019.02.009.

[53] X. Liu, P. Wang, Y.X. Zou, Z.G. Luo, T.M. Tamer, Co-encapsulation of Vitamin C and β-Carotene in liposomes: Storage stability, antioxidant activity, and in vitro gastrointestinal digestion, Food Research International. 136 (2020) 109587. https://doi.org/10.1016/j.foodres.2020.109587.

[54] R. Zhang, S. bin Wang, A.Z. Chen, W.G. Chen, Y.G. Liu, W.G. Wu, Y.Q. Kang, S.F. Ye, Codelivery of paclitaxel and small interfering RNA by octadecyl quaternized carboxymethyl chitosan-modified cationic liposome for combined cancer therapy, 30 (2015) 351–360. https://doi.org/10.1177/0885328215579297.

[55] X.W. Chen, X.Y. Ning, X.Q. Yang, Fabrication of Novel Hierarchical Multicompartment Highly Stable Triple Emulsions for the Segregation and Protection of Multiple Cargos by Spatial Co-encapsulation, J Agric Food Chem. 67 (2019) 10904–10912. https://doi.org/10.1021/acs.jafc.9b03509.

[56] F. Spyropoulos, D. Kurukji, P. Taylor, I.T. Norton, Fabrication and Utilization of Bifunctional Protein/Polysaccharide Coprecipitates for the Independent Codelivery of Two Model Actives from Simple Oil-in-Water Emulsions, Langmuir. 34 (2018) 3934–3948. https://doi.org/10.1021/acs.langmuir.7b04315.

[57] M.L. Bruschi, Main mechanisms to control the drug release, in: Strategies to Modify the Drug Release from Pharmaceutical Systems, Woodhead Publishing, 2015: pp. 37–62. https://doi.org/10.1016/b978-0-08-100092-2.00004-7.

[58] D. Kurukji, I. Norton, F. Spyropoulos, Fabrication of sub-micron protein-chitosan electrostatic complexes for encapsulation and pH-Modulated delivery of model hydrophilic active compounds, Food Hydrocoll. 53 (2016) 249–260. https://doi.org/10.1016/j.foodhyd.2015.02.021.

[59] M. Bruschi, Mathematical models of drug release, in: Strategies to Modify the Drug Release from Pharmaceutical Systems, Elsevier, 2015: pp. 63–86. https://doi.org/10.1016/b978-0-08-100092-2.00005-9.

[60] R.A. Siegel, M.J. Rathbone, Overview of controlled release mechanisms, Fundamentals and Applications of Controlled Release Drug Delivery. (2012) 19–43. https://doi.org/10.1007/978-1-4614-0881-9_2.

[61] S. Adepu, S. Ramakrishna, Controlled Drug Delivery Systems: Current Status and Future Directions, Molecules. 26 (2021). https://doi.org/10.3390/molecules26195905.

[62] J. Siepmann, F. Siepmann, Mathematical modeling of drug dissolution, Int J Pharm. 453 (2013) 12–24. https://doi.org/10.1016/j.ijpharm.2013.04.044.

[63] J. Crank, The Mathematics of Diffusion, 2nd Edition, Oxford University Press, London, 1975.

[64] S.K. Tiwari, R. Tzezana, E. Zussman, S.S. Venkatraman, Optimizing partition-controlled drug release from electrospun core–shell fibers, Int J Pharm. 392 (2010) 209–217. https://doi.org/10.1016/j.ijpharm.2010.03.021.

[65] F. Theeuwes, Evolution and design of 'rate controlled'' osmotic forms, 8 (2008) 20–27. https://doi.org/10.1185/03007998309109820.

[66] Y. Zhang, Z. Zhang, F. Wu, A novel pulsed-release system based on swelling and osmotic pumping mechanism, Journal of Controlled Release. 89 (2003) 47–55. https://doi.org/10.1016/S0168-3659(03)00092-0.

[67] S. Sheth, E. Barnard, B. Hyatt, M. Rathinam, S.P. Zustiak, Predicting Drug Release From Degradable Hydrogels Using Fluorescence Correlation Spectroscopy and

Mathematical Modeling, Front Bioeng Biotechnol. 7 (2019) 410. https://doi.org/10.3389/fbioe.2019.00410.

[68] S. Zuleger, B.C. Lippold, Polymer particle erosion controlling drug release. I. Factors influencing drug release and characterization of the release mechanism, Int J Pharm. 217 (2001) 139–152. https://doi.org/10.1016/S0378-5173(01)00596-8.

[69] M. Mumtaz Virk, E. Reimhult, Phospholipase A2-Induced Degradation and Release from Lipid-Containing Polymersomes, Langmuir. 34 (2018) 395–405. https://doi.org/10.1021/acs.langmuir.7B03893.

[70] S.M. Dieng, N. Anton, P. Bouriat, O. Thioune, P.M. Sy, N. Massaddeq, S. Enharrar, M. Diarra, T. Vandamme, Pickering nano-emulsions stabilized by solid lipid nanoparticles as a temperature sensitive drug delivery system, Soft Matter. 15 (2019) 8164–8174. https://doi.org/10.1039/c9sm01283d.

[71] A. Lajoinie, E. Henin, B. Kassai, D. Terry, Solid oral forms availability in children: a cost saving investigation, Br J Clin Pharmacol. 78 (2014) 1080. https://doi.org/10.1111/bcp.12442.

[72] H. Wen, H. Jung, X. Li, Drug Delivery Approaches in Addressing Clinical Pharmacology-Related Issues: Opportunities and Challenges, AAPS J. 17 (2015) 1327–1340. https://doi.org/10.1208/S12248-015-9814-9.

[73] S.A. Khaled, J.C. Burley, M.R. Alexander, J. Yang, C.J. Roberts, 3D printing of tablets containing multiple drugs with defined release profiles, Int J Pharm. 494 (2015) 643–650. https://doi.org/10.1016/j.ijpharm.2015.07.067.

[74] N. Li, L. Zhao, L. Qi, Z. Li, Y. Luan, Polymer assembly: Promising carriers as co-delivery systems for cancer therapy, Prog Polym Sci. 58 (2016) 1–26. https://doi.org/10.1016/j.progpolymsci.2015.10.009.

[75] J. Čejková, F. Štěpánek, Compartmentalized and Internally Structured Particles for Drug Delivery - A Review, Curr Pharm Des. 19 (2013) 6298–6314. https://doi.org/10.2174/1381612811319350007.

[76] N.A. Helal, H.A. Eassa, A.M. Amer, M.A. Eltokhy, I. Edafiogho, M.I. Nounou, Nutraceuticals' Novel Formulations: The Good, the Bad, the Unknown and Patents Involved, Recent Pat Drug Deliv Formul. 13 (2019) 105–156. https://doi.org/10.2174/1872211313666190503112040.

[77] M.D. López, M. Cantó-Tejero, M.J. Pascual-Villalobos, New Insights Into Biopesticides: Solid and Liquid Formulations of Essential Oils and Derivatives, Frontiers in Agronomy. 3 (2021) 91. https://doi.org/10.3389/fagro.2021.763530.

[78] D.T. Chong, X.S. Liu, H.J. Ma, G.Y. Huang, Y.L. Han, X.Y. Cui, J.J. Yan, F. Xu, Advances in fabricating double-emulsion droplets and their biomedical applications, Microfluidics and Nanofluidics 2015 19:5. 19 (2015) 1071–1090. https://doi.org/10.1007/s10404-015-1635-8.

[79] S.G. Ingebrigtsen, N. Škalko-Basnet, C. de Albuquerque Cavalcanti Jacobsen, A.M. Holsæter, Successful co-encapsulation of benzoyl peroxide and chloramphenicol in liposomes by a novel manufacturing method - dual asymmetric centrifugation, European Journal of Pharmaceutical Sciences. 97 (2017) 192–199. https://doi.org/10.1016/j.ejps.2016.11.017.

[80] F. Kesisoglou, Y. Wu, Understanding the Effect of API Properties on Bioavailability Through Absorption Modeling, AAPS J. 10 (2008) 516. https://doi.org/10.1208/S12248-008-9061-4.

[81] L.H. Ng, J.K.U. Ling, K. Hadinoto, Formulation Strategies to Improve the Stability and Handling of Oral Solid Dosage Forms of Highly Hygroscopic Pharmaceuticals and

Nutraceuticals, Pharmaceutics 2022, Vol. 14, Page 2015. 14 (2022) 2015. https://doi.org/10.3390/pharmaceutics14102015.

[82] A. JSK, K. M, A Review on Bilayered Tablets, Res Rev J Pharm Pharm Sci. 5 (2016).

[83] T. Blicharski, K. Swiader, A. Serefko, S. Kulczycka-Mamona, M. Kolodziejczyk, A. Szopa, Challenges in technology of bilayer and multi-layer tablets: A mini-review, Current Issues in Pharmacy and Medical Sciences. 32 (2019) 229–235. https://doi.org/10.2478/cipms-2019-0039.

[84] A. Awad, F. Fina, S.J. Trenfield, P. Patel, A. Goyanes, S. Gaisford, A.W. Basit, 3D Printed Pellets (Miniprintlets): A Novel, Multi-Drug, Controlled Release Platform Technology, Pharmaceutics. 11 (2019). https://doi.org/10.3390/pharmaceutics11040148.

[85] H.G. Lee, Y.S. Park, J.H. Jeong, Y. bin Kwon, D.H. Shin, J.Y. Kim, Y.S. Rhee, E.S. Park, D.W. Kim, C.W. Park, Physicochemical properties and drug-release mechanisms of dual-release bilayer tablet containing mirabegron and fesoterodine fumarate, Drug Des Devel Ther. 13 (2019) 2459. https://doi.org/10.2147/dddt.S212520.

[86] P.P.D. Kondiah, Y.E. Choonara, P.J. Kondiah, T. Marimuthu, P. Kumar, L.C. du Toit, G. Modi, V. Pillay, Nanocomposites for therapeutic application in multiple sclerosis, Applications of Nanocomposite Materials in Drug Delivery. (2018) 391–408. https://doi.org/10.1016/b978-0-12-813741-3.00017-0.

[87] N.A. Noguez Méndez, C.T. Quirino Barreda, A.F. Vega, J.E. Miranda Calderon, C.G. Urioste, X.C. Palomec, A.R. Martínez, M.P. Díaz, Design and development of pharmaceutical microprocesses in the production of nanomedicine, Nanostructures for Oral Medicine. (2017) 669–697. https://doi.org/10.1016/b978-0-323-47720-8.00023-7.

[88] A. Zielinska, F. Carreiró, A.M. Oliveira, A. Neves, B. Pires, D. Nagasamy Venkatesh, A. Durazzo, M. Lucarini, P. Eder, A.M. Silva, A. Santini, E.B. Souto, Polymeric Nanoparticles: Production, Characterization, Toxicology and Ecotoxicology, Molecules 2020, Vol. 25, Page 3731. 25 (2020) 3731. https://doi.org/10.3390/molecules25163731.

[89] M. Lengyel, N. Kállai-Szabó, V. Antal, A.J. Laki, I. Antal, Microparticles, Microspheres, and Microcapsules for Advanced Drug Delivery, Scientia Pharmaceutica 2019, Vol. 87, Page 20. 87 (2019) 20. https://doi.org/10.3390/scipharm87030020.

[90] E. Campos, J. Branquinho, A.S. Carreira, A. Carvalho, P. Coimbra, P. Ferreira, M.H. Gil, Designing polymeric microparticles for biomedical and industrial applications, Eur Polym J. 49 (2013) 2005–2021. https://doi.org/10.1016/j.eurpolymj.2013.04.033.

[91] A.K. Biswal, S. Saha, Prolonging food shelf-life by dual actives release from multi-layered polymer particles, Colloids Surf B Biointerfaces. 175 (2019) 281–290. https://doi.org/10.1016/j.colsurfb.2018.12.004.

[92] N. Suraphan, L. Fan, B. Liu, D. Wu, Co-delivery of chlorantraniliprole and avermectin with a polylactide microcapsule formulation, RSC Adv. 10 (2020) 25418–25425. https://doi.org/10.1039/d0ra03825c.

[93] J. Wang, H. Hao, J.H. Cai, Amphiphilic Drug Delivery Microcapsules via Layer-by-Layer Self-Assembly, 58 (2019) 535–550. https://doi.org/10.1080/00222348.2019.1593640.

[94] A.K. Jain, K. Thanki, S. Jain, Co-encapsulation of tamoxifen and quercetin in polymeric nanoparticles: Implications on oral bioavailability, antitumor efficacy, and drug-induced toxicity, Mol Pharm. 10 (2013) 3459–3474. https://doi.org/10.1021/mp400311j.

[95] M. Shi, J. Bai, L. Zhao, X. Yu, J. Liang, Y. Liu, W. Nord, Y. Li, Co-loading and intestine-specific delivery of multiple antioxidants in pH-responsive microspheres

based on TEMPO-oxidized polysaccharides, Carbohydr Polym. 157 (2017) 858–865. https://doi.org/10.1016/j.carbpol.2016.10.057.

[96] S. Hong, D.W. Choi, H.N. Kim, C.G. Park, W. Lee, H.H. Park, Protein-Based Nanoparticles as Drug Delivery Systems, Pharmaceutics. 12 (2020) 1–28. https://doi.org/10.3390/pharmaceutics12070604.

[97] K. de Frates, T. Markiewicz, P. Gallo, A. Rack, A. Weyhmiller, B. Jarmusik, X. Hu, Protein Polymer-Based Nanoparticles: Fabrication and Medical Applications, International Journal of Molecular Sciences 2018, Vol. 19, Page 1717. 19 (2018) 1717. https://doi.org/10.3390/ijms19061717.

[98] W. Lohcharoenkal, L. Wang, Y.C. Chen, Y. Rojanasakul, Protein nanoparticles as drug delivery carriers for cancer therapy, Biomed Res Int. 2014 (2014). https://doi.org/10.1155/2014/180549.

[99] D. Xiao, P.M. Davidson, Q. Zhong, Spray-dried zein capsules with coencapsulated nisin and thymol as antimicrobial delivery system for enhanced antilisterial properties, J Agric Food Chem. 59 (2011) 7393–7404. https://doi.org/10.1021/jf200774v.

[100] J. Vulić, V. Šeregelj, A. Kalušević, S. Lević, V. Nedović, V.T. Šaponjac, J. Čanadanović-Brunet, G. Ćetković, Bioavailability and Bioactivity of Encapsulated Phenolics and Carotenoids Isolated from Red Pepper Waste, Molecules. 24 (2019). https://doi.org/10.3390/molecules24152837.

[101] Y. Luo, Q. Wang, Recent development of chitosan-based polyelectrolyte complexes with natural polysaccharides for drug delivery, Int J Biol Macromol. 64 (2014) 353–367. https://doi.org/10.1016/j.ijbiomac.2013.12.017.

[102] A. di Martino, A. Pavelkova, S. Maciulyte, S. Budriene, V. Sedlarik, Polysaccharide-based nanocomplexes for co-encapsulation and controlled release of 5-Fluorouracil and Temozolomide, European Journal of Pharmaceutical Sciences. 92 (2016) 276–286. https://doi.org/10.1016/j.ejps.2016.05.001.

[103] Y.; Dai, X.; Lu, R.; Li, Y.; Cao, W.; Zhou, J.; Li, B. Zheng, Y. Dai, X. Lu, R. Li, Y. Cao, W. Zhou, J. Li, B. Zheng, Fabrication and Characterization of W/O/W Emulgels by Sipunculus nudus Salt-Soluble Proteins: Co-Encapsulation of Vitamin C and & beta-Carotene, Foods 2022, Vol. 11, Page 2720. 11 (2022) 2720. https://doi.org/10.3390/foods11182720.

[104] M.A. Kamlow, T. Holt, F. Spyropoulos, T. Mills, Release and co-release of model hydrophobic and hydrophilic actives from 3D printed kappa-carrageenan emulsion gels, Food Hydrocoll. 132 (2022) 107852. https://doi.org/10.1016/j.foodhyd.2022.107852.

[105] H. Bao, Y. Ni, Wusigale, H. Dong, L. Liang, α-Tocopherol and resveratrol in emulsion-filled whey protein gels: Co-encapsulation and in vitro digestion, Int Dairy J. 104 (2020) 104649. https://doi.org/10.1016/j.idairyj.2020.104649.

[106] F.L. Lopez, T.B. Ernest, C. Tuleu, M.O. Gul, Formulation approaches to pediatric oral drug delivery: benefits and limitations of current platforms, Expert Opin Drug Deliv. 12 (2015) 1727–1740. https://doi.org/10.1517/17425247.2015.1060218.

[107] H.K. Batchelor, J.F. Marriott, Formulations for children: problems and solutions, Br J Clin Pharmacol. 79 (2015) 405–418. https://doi.org/10.1111/bcp.12268.

[108] D.J. McClements, Food Emulsions: Principles, Practices, and techniques, Food Emulsions: Principles, Practices, and Techniques, Third Edition. (2015) 1–676. https://doi.org/10.1201/b18868.

[109] R. Pichot, F. Spyropoulos, I.T. Norton, O/W emulsions stabilised by both low molecular weight surfactants and colloidal particles: The effect of surfactant type and

concentration, J Colloid Interface Sci. 352 (2010) 128–135. https://doi.org/10.1016/j.jcis.2010.08.021.
[110] A. Timgren, M. Rayner, M. Sjöö, P. Dejmek, Starch particles for food based Pickering emulsions, Procedia Food Sci. 1 (2011) 95–103. https://doi.org/10.1016/j.profoo.2011.09.016.
[111] Z. Wei, C. Wang, S. Zou, H. Liu, Z. Tong, Chitosan nanoparticles as particular emulsifier for preparation of novel pH-responsive Pickering emulsions and PLGA microcapsules, Polymer (Guildf). 53 (2012) 1229–1235. https://doi.org/10.1016/j.polymer.2012.02.015.
[112] I. Zafeiri, P. Smith, I.T. Norton, F. Spyropoulos, Fabrication, characterisation and stability of oil-in-water emulsions stabilised by solid lipid particles: The role of particle characteristics and emulsion microstructure upon Pickering functionality, Food Funct. 8 (2017) 2583–2591. https://doi.org/10.1039/c7fo00559h.
[113] H. Chen, H. Dai, H. Zhu, L. Ma, Y. Fu, X. Feng, Y. Sun, Y. Zhang, Construction of dual-compartmental micro-droplet via shrimp ferritin nanocages stabilized Pickering emulsions for co-encapsulation of hydrophobic/hydrophilic bioactive compounds, Food Hydrocoll. 126 (2022) 107443. https://doi.org/10.1016/j.foodhyd.2021.107443.
[114] G.I. Sakellari, I. Zafeiri, A. Pawlik, D. Kurukji, P. Taylor, I.T. Norton, F. Spyropoulos, Independent co-delivery of model actives with different degrees of hydrophilicity from oil-in-water and water-in-oil emulsions stabilised by solid lipid particles via a Pickering mechanism: a-proof-of-principle study, J Colloid Interface Sci. 587 (2021) 644–649. https://doi.org/10.1016/j.jcis.2020.11.021.
[115] V. Maingret, C. Chartier, J.L. Six, V. Schmitt, V. Héroguez, Pickering emulsions stabilized by biodegradable dextran-based nanoparticles featuring enzyme responsiveness and co-encapsulation of actives, Carbohydr Polym. 284 (2022) 119146. https://doi.org/10.1016/j.carbpol.2022.119146.
[116] D.J. McClements, Advances in fabrication of emulsions with enhanced functionality using structural design principles, Curr Opin Colloid Interface Sci. 17 (2012) 235–245. https://doi.org/10.1016/j.cocis.2012.06.002.
[117] E. Dluska, A. Markowska-Radomska, A. Metera, W. Tomaszewski, Drug-Core Double Emulsions for Co-release of Active Ingredients, International Journal of Chemical Engineering and Applications. 7 (2016) 428–432. https://doi.org/10.18178/ijcea.2016.7.6.619.
[118] A. Radomska-Soukharev, R.H. Müller, Chemical stability of lipid excipients in SLN-production of test formulations, characterisation and short-term stability, Pharmazie. 61 (2006) 425–430. https://doi.org/10.1016/s0168-3659(97)00046-1.
[119] N.P. Aditya, S. Aditya, H. Yang, H.W. Kim, S.O. Park, S. Ko, Co-delivery of hydrophobic curcumin and hydrophilic catechin by a water-in-oil-in-water double emulsion, Food Chem. 173 (2015) 7–13. https://doi.org/10.1016/j.foodchem.2014.09.131.
[120] Q. Wang, L. Wang, N. Abdullah, W. Tian, M. Song, Y. Cao, J. Xiao, Co-delivery of EGCG and lycopene via a pickering double emulsion induced synergistic hypolipidemic effect, Food Funct. 13 (2022) 3419–3430. https://doi.org/10.1039/d2fo00169a.
[121] X.Y. Tang, Z.M. Wang, H.C. Meng, J.W. Lin, X.M. Guo, T. Zhang, H.L. Chen, C.Y. Lei, S.J. Yu, Robust W/O/W Emulsion Stabilized by Genipin-Cross-Linked Sugar Beet Pectin-Bovine Serum Albumin Nanoparticles: Co-encapsulation of Betanin and Curcumin, J Agric Food Chem. 69 (2021) 1318–1328. https://doi.org/10.1021/acs.jafc.0C05212.

[122] L. Han, K. Lu, S. Zhou, S. Zhang, F. Xie, B. Qi, Y. Li, Development of an oil-in-water emulsion stabilized by a black bean protein-based nanocomplex for co-delivery of quercetin and perilla oil, LWT. 138 (2021) 110644. https://doi.org/10.1016/j.lwt.2020.110644.
[123] Y.P. Chuan, B.Y. Zeng, B. O'Sullivan, R. Thomas, A.P.J. Middelberg, Co-delivery of antigen and a lipophilic anti-inflammatory drug to cells via a tailorable nanocarrier emulsion, J Colloid Interface Sci. 368 (2012) 616–624. https://doi.org/10.1016/j.jcis.2011.11.014.
[124] H. Cheng, Q. Fan, T. Liu, Wusigale, L. Liang, Co-encapsulation of α-tocopherol and resveratrol in oil-in-water emulsion stabilized by sodium caseinate: Impact of polysaccharide on the stability and bioaccessibility, J Food Eng. 264 (2020) 109685. https://doi.org/10.1016/j.jfoodeng.2019.109685.
[125] H.H. Gahruie, M. Niakousari, K. Parastouei, M. Mokhtarian, I. Eş, A.M. Khaneghah, Co-encapsulation of vitamin D3 and saffron petals' bioactive compounds in nanoemulsions: Effects of emulsifier and homogenizer types, J Food Process Preserv. 44 (2020) e14629. https://doi.org/10.1111/jfpp.14629.
[126] H. Shrestha, R. Bala, S. Arora, Lipid-Based Drug Delivery Systems, J Pharm (Cairo). 2014 (2014) 1–10. https://doi.org/10.1155/2014/801820.
[127] A. Ahmad, H. Ahsan, Lipid-based formulations in cosmeceuticals and biopharmaceuticals, Biomedical Dermatology 2020 4:1. 4 (2020) 1–10. https://doi.org/10.1186/s41702-020-00062-9.
[128] P. Subramanian, Lipid-Based Nanocarrier System for the Effective Delivery of Nutraceuticals, Molecules. 26 (2021). https://doi.org/10.3390/molecules26185510.
[129] X.Q. Chen, O.S. Gudmundsson, M.J. Hageman, Application of lipid-based formulations in drug discovery, J Med Chem. 55 (2012) 7945–7956. https://doi.org/10.1021/jm3006433.
[130] S. Sapino, M.E. Carlotti, E. Pelizzetti, D. Vione, M. Trotta, L. Battaglia, Protective effect of SLNs encapsulation on the photodegradation and thermal degradation of retinyl palmitate introduced in hydroxyethylcellulose gel, J Drug Deliv Sci Technol. 15 (2005) 159–165. https://doi.org/10.1016/s1773-2247(05)50021-2.
[131] M. Geszke-Moritz, M. Moritz, Solid lipid nanoparticles as attractive drug vehicles: Composition, properties and therapeutic strategies, Materials Science and Engineering C. 68 (2016) 982–994. https://doi.org/10.1016/j.msec.2016.05.119.
[132] M. Üner, G. Yener, Importance of solid lipid nanoparticles (SLN) in various administration routes and future perspective, Int J Nanomedicine. 2 (2007) 289–300.
[133] G.I. Sakellari, I. Zafeiri, H. Batchelor, F. Spyropoulos, Formulation design, production and characterisation of solid lipid nanoparticles (SLN) and nanostructured lipid carriers (NLC) for the encapsulation of a model hydrophobic active, Food Hydrocolloids for Health. (2021) 100024. https://doi.org/10.1016/j.fhfh.2021.100024.
[134] K. Oehlke, D. Behsnilian, E. Mayer-Miebach, P.G. Weidler, R. Greiner, Edible solid lipid nanoparticles (SLN) as carrier system for antioxidants of different lipophilicity, PLoS One. 12 (2017) e0171662. https://doi.org/10.1371/journal.pone.0171662.
[135] N. Naseri, H. Valizadeh, P. Zakeri-Milani, Solid lipid nanoparticles and nanostructured lipid carriers: Structure preparation and application, Adv Pharm Bull. 5 (2015) 305–313. https://doi.org/10.15171/apb.2015.043.
[136] Y. Wang, H. Zhang, J. Hao, B. Li, M. Li, W. Xiuwen, Lung cancer combination therapy: co-delivery of paclitaxel and doxorubicin by nanostructured lipid carriers for synergistic

effect, Https://Doi.Org/10.3109/10717544.2015.1055619. 23 (2015) 1398–1403. https://doi.org/10.3109/10717544.2015.1055619.

[137] E.B. Lages, R.S. Fernandes, J. de O. Silva, Â.M. de Souza, G.D. Cassali, A.L.B. de Barros, L.A. Miranda Ferreira, Co-delivery of doxorubicin, docosahexaenoic acid, and α-tocopherol succinate by nanostructured lipid carriers has a synergistic effect to enhance antitumor activity and reduce toxicity, Biomedicine & Pharmacotherapy. 132 (2020) 110876. https://doi.org/10.1016/j.biopha.2020.110876.

[138] M. Ferreira, L. Barreiros, M.A. Segundo, T. Torres, M. Selores, S.A. Costa Lima, S. Reis, Topical co-delivery of methotrexate and etanercept using lipid nanoparticles: A targeted approach for psoriasis management, Colloids Surf B Biointerfaces. 159 (2017) 23–29. https://doi.org/10.1016/j.colsurfb.2017.07.080.

[139] J. Zhang, J. Li, Z. Shi, Y. Yang, X. Xie, S.M.Y. Lee, Y. Wang, K.W. Leong, M. Chen, pH-sensitive polymeric nanoparticles for co-delivery of doxorubicin and curcumin to treat cancer via enhanced pro-apoptotic and anti-angiogenic activities, Acta Biomater. 58 (2017) 349–364. https://doi.org/10.1016/j.actbio.2017.04.029.

[140] C. Gao, F. Tang, G. Gong, J. Zhang, M.P.M. Hoi, S.M.Y. Lee, R. Wang, pH-Responsive prodrug nanoparticles based on a sodium alginate derivative for selective co-release of doxorubicin and curcumin into tumor cells, Nanoscale. 9 (2017) 12533–12542. https://doi.org/10.1039/c7nr03611f.

[141] C. Emilienne Soma, C. Dubernet, D. Bentolila, S. Benita, P. Couvreur, Reversion of multidrug resistance by co-encapsulation of doxorubicin and cyclosporin A in polyalkylcyanoacrylate nanoparticles, Biomaterials. 21 (2000) 1–7. https://doi.org/10.1016/s0142-9612(99)00125-8.

[142] J.L. Wu, C.Q. Wang, R.X. Zhuo, S.X. Cheng, Multi-drug delivery system based on alginate/calcium carbonate hybrid nanoparticles for combination chemotherapy, Colloids Surf B Biointerfaces. 123 (2014) 498–505. https://doi.org/10.1016/j.colsurfb.2014.09.047.

[143] L.P. Mendes, M.P.N. Gaeti, P.H.M. de Ávila, M. de Sousa Vieira, B. dos Santos Rodrigues, R.I. de Ávila Marcelino, L.C.R. dos Santos, M.C. Valadares, E.M. Lima, Multicompartimental nanoparticles for Co-encapsulation and multimodal drug delivery to tumor cells and neovasculature, Pharm Res. 31 (2014) 1106–1119. https://doi.org/10.1007/s11095-013-1234-x.

[144] X. Yin, X. Fu, H. Cheng, Wusigale, L. Liang, α-Tocopherol and naringenin in whey protein isolate particles: Partition, antioxidant activity, stability and bioaccessibility, Food Hydrocoll. 106 (2020) 105895. https://doi.org/10.1016/j.foodhyd.2020.105895.

[145] F.L. Tchuenbou-Magaia, R. Tolve, U. Anyadike, M. Giarola, F. Favati, Co-encapsulation of vitamin D and rutin in chitosan-zein microparticles, Journal of Food Measurement and Characterization. 16 (2022) 2060–2070. https://doi.org/10.1007/s11694-022-01340-2.

[146] F. Liu, D. Ma, X. Luo, Z. Zhang, L. He, Y. Gao, D.J. McClements, Fabrication and characterization of protein-phenolic conjugate nanoparticles for co-delivery of curcumin and resveratrol, Food Hydrocoll. 79 (2018) 450–461. https://doi.org/10.1016/j.foodhyd.2018.01.017.

[147] S. Kharel, A. Gautam, M. Mahotra, N.M. Theniko, S.C.J. Loo, Valorizing okara waste into nutritionally rich polysaccharide/protein-extracts for co-encapsulation of β-carotene and ferrous sulphate as a potential approach to tackle micronutrient malnutrition., J Funct Foods. 87 (2021) 104749–104749. https://doi.org/10.1016/j.jff.2021.104749.

[148] D. Eratte, S. McKnight, T.R. Gengenbach, K. Dowling, C.J. Barrow, B.P. Adhikari, Co-encapsulation and characterisation of omega-3 fatty acids and probiotic bacteria in whey protein isolate–gum Arabic complex coacervates, J Funct Foods. 19 (2015) 882–892. https://doi.org/10.1016/j.jff.2015.01.037.
[149] W. Ramsden, Separation of solids in the surface-layers of solutions and 'suspensions' (observations on surface-membranes, bubbles, emulsions, and mechanical coagulation). Preliminary account, Proceedings of the Royal Society of London. 72 (1904) 156–164. https://doi.org/10.1098/rspl.1903.0034.
[150] S.U. Pickering, Emulsions, J. Chem. Soc., Trans. 91 (1907) 2001–2021. https://doi.org/10.1039/ct9079102001.
[151] J.D. Echeverri, M.J. Alhajj, N. Montero, C.J. Yarce, A. Barrera-Ocampo, C.H. Salamanca, Study of In Vitro and In Vivo Carbamazepine Release from Coarse and Nanometric Pharmaceutical Emulsions Obtained via Ultra-High-Pressure Homogenization, Pharmaceuticals. 13 (2020). https://doi.org/10.3390/ph13040053.
[152] H. Nadeem, R.D. Vigil, A. Samuel, A. Sarkar, T. Yeoh, M.G. Olsen, Coalescence-induced phase separation of an oil in water emulsion under controlled shear and temperature conditions, Chemical Engineering Research and Design. 182 (2022) 517–524. https://doi.org/10.1016/j.cherd.2022.04.024.
[153] M. Kahlweit, R. Strey, G. Busse, Microemulsions: A qualitative thermodynamic approach, Journal of Physical Chemistry®. 94 (1990) 3881–3894. https://doi.org/10.1021/j100373A006.
[154] S. Fouilloux, F. Malloggi, J. Daillant, A. Thill, Aging mechanism in model Pickering emulsion, Soft Matter. 12 (2016) 900–904. https://doi.org/10.1039/c5sm02134k.
[155] M. Pan, F. Lyu, S. Tang, Methods to coalesce fluorinated Pickering emulsions, Analytical Methods. 9 (2017) 4622–4629. https://doi.org/10.1039/c7ay01289f.
[156] C.P. Whitby, D. Fornasiero, J. Ralston, Structure of oil-in-water emulsions stabilised by silica and hydrophobised titania particles, J Colloid Interface Sci. 342 (2010) 205–209. https://doi.org/10.1016/j.jcis.2009.10.068.
[157] H. Fan, A. Striolo, Mechanistic study of droplets coalescence in Pickering emulsions, Soft Matter. 8 (2012) 9533–9538. https://doi.org/10.1039/c2sm26416a.
[158] M.S. Manga, O.J. Cayre, R.A. Williams, S. Biggs, D.W. York, Production of solid-stabilised emulsions through rotational membrane emulsification: influence of particle adsorption kinetics, Soft Matter. 8 (2012) 1532–1538. https://doi.org/10.1039/c1sm06547e.
[159] C. Priest, M.D. Reid, C.P. Whitby, Formation and stability of nanoparticle-stabilised oil-in-water emulsions in a microfluidic chip, J Colloid Interface Sci. 363 (2011) 301–306. https://doi.org/10.1016/j.jcis.2011.07.060.
[160] D.J. French, P. Taylor, J. Fowler, P.S. Clegg, Making and breaking bridges in a Pickering emulsion, J Colloid Interface Sci. 441 (2015) 30–38. https://doi.org/10.1016/j.jcis.2014.11.032.
[161] C.P. Whitby, H. Khairul Anwar, J. Hughes, Destabilising Pickering emulsions by drop flocculation and adhesion, J Colloid Interface Sci. 465 (2016) 158–164. https://doi.org/10.1016/j.jcis.2015.11.063.
[162] J.A. Juárez, C.P. Whitby, Oil-in-water Pickering emulsion destabilisation at low particle concentrations, J Colloid Interface Sci. 368 (2012) 319–325. https://doi.org/10.1016/j.jcis.2011.11.029.
[163] B.P. Binks, Particles as surfactants—similarities and differences, Curr Opin Colloid Interface Sci. 7 (2002) 21–41. https://doi.org/10.1016/S1359-0294(02)00008-0.

[164] R. Aveyard, J.H. Clint, T.S. Horozov, Aspects of the stabilisation of emulsions by solid particles: Effects of line tension and monolayer curvature energy, Physical Chemistry Chemical Physics. 5 (2003) 2398–2409. https://doi.org/10.1039/b210687f.
[165] M. Xiao, A. Xu, T. Zhang, L. Hong, Tailoring the wettability of colloidal particles for pickering emulsions via surface modification and roughness, Front Chem. 6 (2018) 225. https://doi.org/10.3389/fchem.2018.00225.
[166] N. Briggs, A. Raman, L. Barrett, C. Brown, … B.L.-C. and S.A., undefined 2018, Stable pickering emulsions using multi-walled carbon nanotubes of varying wettability, Colloids Surf A Physicochem Eng Asp. 537 (2018) 227–235. https://doi.org/10.1016/j.colsurfa.2017.10.010.
[167] R. Pichot, F. Spyropoulos, I.T. Norton, Mixed-emulsifier stabilised emulsions: Investigation of the effect of monoolein and hydrophilic silica particle mixtures on the stability against coalescence, J Colloid Interface Sci. 329 (2009) 284–291. https://doi.org/10.1016/j.jcis.2008.09.083.
[168] D. Rousseau, Fat crystals and emulsion stability - A review, Food Research International. 33 (2000) 3–14. https://doi.org/10.1016/s0963-9969(00)00017-x.
[169] R.W. Style, L. Isa, E.R. Dufresne, Adsorption of soft particles at fluid interfaces, Soft Matter. 11 (2015) 7412–7419. https://doi.org/10.1039/c5sm01743b.
[170] E. Dickinson, Use of nanoparticles and microparticles in the formation and stabilization of food emulsions, Trends Food Sci Technol. 24 (2012) 4–12. https://doi.org/10.1016/j.tifs.2011.09.006.
[171] B.P. Binks, S.O. Lumsdon, Pickering Emulsions Stabilized by Monodisperse Latex Particles: Effects of Particle Size, Langmuir. 17 (2001) 4540–4547. https://doi.org/10.1021/la0103822.
[172] R.D. Groot, S.D. Stoyanov, Close packing density and fracture strength of adsorbed polydisperse particle layers, Soft Matter. 7 (2011) 4750–4761. https://doi.org/10.1039/c0sm00859a.
[173] F. Bresme, M. Oettel, Nanoparticles at fluid interfaces, J Phys Condens Matter. 19 (2007). https://doi.org/10.1088/0953-8984/19/41/413101.
[174] J.C. Loudet, A.M. Alsayed, J. Zhang, A.G. Yodh, Capillary interactions between anisotropic colloidal particles, Phys Rev Lett. 94 (2005) 018301. https://doi.org/10.1103/physrevlett.94.018301.
[175] B. Madivala, S. Vandebril, J. Fransaer, J. Vermant, Exploiting particle shape in solid stabilized emulsions, Soft Matter. 5 (2009) 1717–1727. https://doi.org/10.1039/b816680c.
[176] B. Madivala, J. Fransaer, J. Vermant, Self-assembly and rheology of ellipsoidal particles at interfaces, Langmuir. 25 (2009) 2718–2728. https://doi.org/10.1021/la803554u.
[177] I. Capron, B. Cathala, Surfactant-free high internal phase emulsions stabilized by cellulose nanocrystals, Biomacromolecules. 14 (2013) 291–296. https://doi.org/10.1021/bm301871k.
[178] H. Lehle, E. Noruzifar, M. Oettel, Ellipsoidal particles at fluid interfaces, The European Physical Journal E 2008 26:1. 26 (2008) 151–160. https://doi.org/10.1140/epje/I2007-10314-1.
[179] N.P. Ashby, B.P. Binks, Pickering emulsions stabilised by Laponite clay particles, Physical Chemistry Chemical Physics. 2 (2000) 5640–5646. https://doi.org/10.1039/b007098j.

[180] Y. Feng, Y. Lee, Surface modification of zein colloidal particles with sodium caseinate to stabilize oil-in-water pickering emulsion, Food Hydrocoll. 56 (2016) 292–302. https://doi.org/10.1016/j.foodhyd.2015.12.030.
[181] J.W.J. de Folter, E.M. Hutter, S.I.R. Castillo, K.E. Klop, A.P. Philipse, W.K. Kegel, Particle shape anisotropy in pickering emulsions: Cubes and peanuts, Langmuir. 30 (2014) 955–964. https://doi.org/10.1021/la402427q.
[182] W. Li, T. Suzuki, H. Minami, The interface adsorption behavior in a Pickering emulsion stabilized by cylindrical polystyrene particles, J Colloid Interface Sci. 552 (2019) 230–235. https://doi.org/10.1016/j.jcis.2019.05.058.
[183] F. Macedo Fernandes Barros, C. Chassenieux, T. Nicolai, M.M. de Souza Lima, L. Benyahia, Effect of the hydrophobicity of fumed silica particles and the nature of oil on the structure and rheological behavior of Pickering emulsions, J Dispers Sci Technol. 40 (2019) 1169–1178. https://doi.org/10.1080/01932691.2018.1500480.
[184] Z. Briceño-Ahumada, J.F.A. Soltero-Martínez, R. Castillo, Aqueous foams and emulsions stabilized by mixtures of silica nanoparticles and surfactants: A state-of-the-art review, Chemical Engineering Journal Advances. 7 (2021) 100116. https://doi.org/10.1016/j.ceja.2021.100116.
[185] S. Guillot, F. Bergaya, C. de Azevedo, F. Warmont, J.F. Tranchant, Internally structured pickering emulsions stabilized by clay mineral particles, J Colloid Interface Sci. 333 (2009) 563–569. https://doi.org/10.1016/j.jcis.2009.01.026.
[186] H. Yang, S. Wang, W. Zhang, J. Wu, S. Yang, D. Yu, X. Wu, Y. Sun, J. Wang, Rapid demulsification of pickering emulsions triggered by controllable magnetic field, Scientific Reports 2020 10:1. 10 (2020) 1–7. https://doi.org/10.1038/s41598-020-73551-w.
[187] Z. Lin, Z. Zhang, Y. Li, Y. Deng, Magnetic nano-Fe3O4 stabilized Pickering emulsion liquid membrane for selective extraction and separation, Chemical Engineering Journal. 288 (2016) 305–311. https://doi.org/10.1016/j.cej.2015.11.109.
[188] H. Firoozmand, D. Rousseau, Microbial cells as colloidal particles: Pickering oil-in-water emulsions stabilized by bacteria and yeast, Food Research International. 81 (2016) 66–73. https://doi.org/10.1016/j.foodres.2015.10.018.
[189] W. Chen, X. Liu, Y. Liu, Y. Bang, H.K.-J. of I. and, undefined 2011, Preparation of O/W Pickering emulsion with oxygen plasma treated carbon nanotubes as surfactants, Elsevier. 17 (2011) 455–460. https://doi.org/10.1016/j.jiec.2010.10.027.
[190] W. Chen, X. Liu, Y. Liu, H. Kim, Novel synthesis of self-assembled CNT microcapsules by O/W Pickering emulsions, Mater Lett. 64 (2010) 2589–2592. https://doi.org/10.1016/j.matlet.2010.08.052.
[191] M. Jug, B.K. Yoon, J.A. Jackman, Cyclodextrin-based Pickering emulsions: functional properties and drug delivery applications, Journal of Inclusion Phenomena and Macrocyclic Chemistry 2021 101:1. 101 (2021) 31–50. https://doi.org/10.1007/s10847-021-01097-z.
[192] E. Perrin, H. Bizot, B. Cathala, I. Capron, Chitin nanocrystals for pickering high internal phase emulsions, Biomacromolecules. 15 (2014) 3766–3771. https://doi.org/10.1021/bm5010417.
[193] J. de Folter, M. van Ruijven, K.P. Velikov, Oil-in-water Pickering emulsions stabilized by colloidal particles from the water-insoluble protein zein, Soft Matter. 8 (2012) 6807–6815. https://doi.org/10.1039/c2sm07417f.

[194] J.O. Zoppe, R.A. Venditti, O.J. Rojas, Pickering emulsions stabilized by cellulose nanocrystals grafted with thermo-responsive polymer brushes, J Colloid Interface Sci. 369 (2012) 202–209. https://doi.org/10.1016/j.jcis.2011.12.011.
[195] H. Cuthill, C. Elleman, T. Curwen, B. Wolf, Colloidal Particles for Pickering Emulsion Stabilization Prepared via Antisolvent Precipitation of Lignin-Rich Cocoa Shell Extract, Foods. 10 (2021). https://doi.org/10.3390/foods10020371.
[196] D. Rousseau, Trends in structuring edible emulsions with Pickering fat crystals, Curr Opin Colloid Interface Sci. 18 (2013) 283–291. https://doi.org/10.1016/j.cocis.2013.04.009.
[197] V.N. Paunov, O.J. Cayre, P.F. Noble, S.D. Stoyanov, K.P. Velikov, M. Golding, Emulsions stabilised by food colloid particles: role of particle adsorption and wettability at the liquid interface, J Colloid Interface Sci. 312 (2007) 381–389. https://doi.org/10.1016/j.jcis.2007.03.031.
[198] S. Frasch-Melnik, I.T. Norton, F. Spyropoulos, Fat-crystal stabilised w/o emulsions for controlled salt release, J Food Eng. 98 (2010) 437–442. https://doi.org/10.1016/j.jfoodeng.2010.01.025.
[199] G. Li, W.J. Lee, C.P. Tan, O.M. Lai, Y. Wang, C. Qiu, Tailored rigidity of W/O Pickering emulsions using diacylglycerol-based surface-active solid lipid nanoparticles, Food Funct. 12 (2021) 11732–11746. https://doi.org/10.1039/d1fo01883c.
[200] A. Pawlik, D. Kurukji, I. Norton, F. Spyropoulos, Food-grade Pickering emulsions stabilised with solid lipid particles, Food Funct. 7 (2016) 2712–2721. https://doi.org/10.1039/c6fo00238b.
[201] R. Gupta, D. Rousseau, Surface-active solid lipid nanoparticles as Pickering stabilizers for oil-in-water emulsions, Food Funct. 3 (2012) 302–311. https://doi.org/10.1039/c2fo10203j.
[202] I. Zafeiri, J.E. Norton, P. Smith, I.T. Norton, F. Spyropoulos, The role of surface active species in the fabrication and functionality of edible solid lipid particles, J Colloid Interface Sci. 500 (2017) 228–240. https://doi.org/10.1016/j.jcis.2017.03.085.
[203] A. Schröder, J. Sprakel, W. Boerkamp, K. Schroën, C.C. Berton-Carabin, Can we prevent lipid oxidation in emulsions by using fat-based Pickering particles?, Food Research International. 120 (2019) 352–363. https://doi.org/10.1016/j.foodres.2019.03.004.
[204] A. Schröder, J. Sprakel, K. Schroën, J.N. Spaen, C.C. Berton-Carabin, Coalescence stability of Pickering emulsions produced with lipid particles: A microfluidic study, J Food Eng. 234 (2018) 63–72. https://doi.org/10.1016/j.jfoodeng.2018.04.007.
[205] A. Schröder, J. Sprakel, K. Schroën, C.C. Berton-Carabin, Tailored microstructure of colloidal lipid particles for Pickering emulsions with tunable properties, Soft Matter. 13 (2017) 3190–3198. https://doi.org/10.1039/c6sm02432g.
[206] H. Lim, M. Jo, C. Ban, Y.J. Choi, Interfacial and colloidal characterization of oil-in-water emulsions stabilized by interface-tunable solid lipid nanoparticles, Food Chem. 306 (2020) 125619. https://doi.org/10.1016/j.foodchem.2019.125619.
[207] A. Schröder, M. Laguerre, J. Sprakel, K. Schroën, C.C. Berton-Carabin, Pickering particles as interfacial reservoirs of antioxidants, J Colloid Interface Sci. 575 (2020) 489–498. https://doi.org/10.1016/j.jcis.2020.04.069.
[208] Y. Chevalier, M.A. Bolzinger, Emulsions stabilized with solid nanoparticles: Pickering emulsions, Colloids Surf A Physicochem Eng Asp. 439 (2013) 23–34. https://doi.org/10.1016/j.colsurfa.2013.02.054.

[209] A. Gelot, W. Friesen, H.A. Hamza, Emulsification of oil and water in the presence of finely divided solids and surface-active agents, Colloids and Surfaces. 12 (1984) 271–303. https://doi.org/10.1016/0166-6622(84)80105-5.
[210] D.E. Tambe, M.M. Sharma, Factors Controlling the Stability of Colloid-Stabilized Emulsions: I. An Experimental Investigation, J Colloid Interface Sci. 157 (1993) 244–253. https://doi.org/10.1006/jcis.1993.1182.
[211] D. Johansson, B. Bergenståhl, E. Lundgren, Water-in-triglyceride oil emulsions. Effect of fat crystals on stability, J Am Oil Chem Soc. 72 (1995) 939–950. https://doi.org/10.1007/bf02542072.
[212] B.P. Binks, P.D.I. Fletcher, B.L. Holt, O. Kuc, P. Beaussoubre, K. Wong, Compositional ripening of particle- and surfactant -stabilised emulsions: a comparison, Physical Chemistry Chemical Physics. 12 (2010) 2219–2226. https://doi.org/10.1039/b918812f.
[213] T.S. Horozov, B.P. Binks, Particle-Stabilized Emulsions: A Bilayer or a Bridging Monolayer?, Angewandte Chemie International Edition. 45 (2006) 773–776. https://doi.org/10.1002/anie.200503131.
[214] F. Gautier, M. Destribats, R. Perrier-Cornet, J.F. Dechézelles, J. Giermanska, V. Héroguez, S. Ravaine, F. Leal-Calderon, V. Schmitt, Pickering emulsions with stimulable particles: from highly- to weakly-covered interfaces, Physical Chemistry Chemical Physics. 9 (2007) 6455–6462. https://doi.org/10.1039/b710226g.
[215] E. Dickinson, Food emulsions and foams: Stabilization by particles, Curr Opin Colloid Interface Sci. 15 (2010) 40–49. https://doi.org/10.1016/j.cocis.2009.11.001.
[216] S. Arditty, V. Schmitt, F. Lequeux, F. Leal-Calderon, Interfacial properties in solid-stabilized emulsions, The European Physical Journal B - Condensed Matter and Complex Systems 2005 44:3. 44 (2005) 381–393. https://doi.org/10.1140/epjb/E2005-00137-0.
[217] D.J. French, A.T. Brown, A.B. Schofield, J. Fowler, P. Taylor, P.S. Clegg, The secret life of Pickering emulsions: particle exchange revealed using two colours of particle, Scientific Reports 2016 6:1. 6 (2016) 1–9. https://doi.org/10.1038/srep31401.
[218] S. Levine, B.D. Bowen, S.J. Partridge, Stabilization of emulsions by fine particles II. capillary and van der Waals forces between particles, Colloids and Surfaces. 38 (1989) 345–364. https://doi.org/10.1016/0166-6622(89)80272-0.
[219] D. Hatchell, W. Song, H. Daigle, Effect of interparticle forces on the stability and droplet diameter of Pickering emulsions stabilized by PEG-coated silica nanoparticles, J Colloid Interface Sci. 626 (2022) 824–835. https://doi.org/10.1016/j.jcis.2022.07.004.
[220] D.J. French, J. Fowler, P. Taylor, P.S. Clegg, Influence of salt concentration on the formation of Pickering emulsions, Soft Matter. 16 (2020) 7342–7349. https://doi.org/10.1039/d0sm00321b.
[221] N. Eskandar, S. Simovic, C. Prestidge, Interactions of hydrophilic silica nanoparticles and classical surfactants at non-polar oil–water interface, J Colloid Interface Sci. 358 (2011) 217–225. https://doi.org/10.1016/j.jcis.2011.02.056.
[222] S. Björkegren, L. Nordstierna, A. Törncrona, A. Palmqvist, Hydrophilic and hydrophobic modifications of colloidal silica particles for Pickering emulsions, J Colloid Interface Sci. 487 (2017) 250–257. https://doi.org/10.1016/j.jcis.2016.10.031.
[223] B. Wang, M. Wang, H. Zhang, N.S. Sobal, W. Tong, C. Gao, Y. Wang, M. Giersig, D. Wang, H. Möhwald, S.S. Adkins, D. Gohil, J.L. Dickson, S.E. Webber, K.P. Johnston, M.P. Boneva, N.C. Christov, K.D. Danov, P.A. Kralchevsky, T.S. Horozov, B.P. Binks, T. Gottschalk-Gaudig, Effect of electrolyte in silicone oil-in-water emulsions stabilised

by fumed silica particles, Physical Chemistry Chemical Physics. 9 (2007) 6398–6404. https://doi.org/10.1039/b709807n.
[224] F. Sabri, K. Berthomier, C.S. Wang, L. Fradette, J.R. Tavares, N. Virgilio, Tuning particle–particle interactions to control Pickering emulsions constituents separation, Green Chemistry. 21 (2019) 1065–1074. https://doi.org/10.1039/c8gc03007c.
[225] M. Zembyla, A. Lazidis, B.S. Murray, A. Sarkar, Water-in-oil pickering emulsions stabilized by synergistic particle-particle interactions, Langmuir. 35 (2019). https://doi.org/10.1021/acs.langmuir.9b02026.
[226] K. Lebdioua, A. Aimable, M. Cerbelaud, A. Videcoq, C. Peyratout, Influence of different surfactants on Pickering emulsions stabilized by submicronic silica particles, J Colloid Interface Sci. 520 (2018) 127–133. https://doi.org/10.1016/j.jcis.2018.03.019.
[227] B.P. Binks, C.P. Whitby, Nanoparticle silica-stabilised oil-in-water emulsions: improving emulsion stability, Colloids Surf A Physicochem Eng Asp. 253 (2005) 105–115. https://doi.org/10.1016/j.colsurfa.2004.10.116.
[228] B.P. Binks, J.A. Rodrigues, Enhanced stabilization of emulsions due to surfactant-induced nanoparticle flocculation, Langmuir. 23 (2007) 7436–7439. https://doi.org/10.1021/la700597k.
[229] B.P. Binks, J.A. Rodrigues, W.J. Frith, Synergistic interaction in emulsions stabilized by a mixture of silica nanoparticles and cationic surfactant, Langmuir. 23 (2007) 3626–3636. https://doi.org/10.1021/la0634600.
[230] I. Zafeiri, C. Horridge, E. Tripodi, F. Spyropoulos, Emulsions Co-Stabilised by Edible Pickering Particles and Surfactants: The Effect of HLB Value, Colloid Interface Sci Commun. 17 (2017) 5–9. https://doi.org/10.1016/j.colcom.2017.02.001.
[231] E. Tripodi, I.T. Norton, F. Spyropoulos, Formation of Pickering and mixed emulsifier systems stabilised O/W emulsions via Confined Impinging Jets processing, Food and Bioproducts Processing. 119 (2020) 360–370. https://doi.org/10.1016/j.fbp.2019.11.021.
[232] C. Vashisth, C.P. Whitby, D. Fornasiero, J. Ralston, Interfacial displacement of nanoparticles by surfactant molecules in emulsions, J Colloid Interface Sci. 349 (2010) 537–543. https://doi.org/10.1016/j.jcis.2010.05.089.
[233] R. Pichot, F. Spyropoulos, I.T. Norton, Competitive adsorption of surfactants and hydrophilic silica particles at the oil-water interface: Interfacial tension and contact angle studies, J Colloid Interface Sci. 377 (2012) 396–405. https://doi.org/10.1016/j.jcis.2012.01.065.
[234] B.W. Brian, J.C. Chen, Surface tension of solid-liquid slurries, AIChE Journal. 33 (1987) 316–318. https://doi.org/10.1002/aic.690330220.
[235] L.L. Dai, R. Sharma, C.Y. Wu, Self-assembled structure of nanoparticles at a liquid-liquid interface, Langmuir. 21 (2005) 2641–2643. https://doi.org/10.1021/la047256t.
[236] C.C. Berton-Carabin, K. Schroën, Pickering emulsions for food applications: background, trends, and challenges, Annu Rev Food Sci Technol. 6 (2015) 263–297. https://doi.org/10.1146/annurev-food-081114-110822.
[237] J. Yi, C. Gan, Z. Wen, Y. Fan, X. Wu, Development of pea protein and high methoxyl pectin colloidal particles stabilized high internal phase pickering emulsions for β-carotene protection and delivery, Food Hydrocoll. 113 (2021) 106497. https://doi.org/10.1016/j.foodhyd.2020.106497.
[238] J. Xiao, C. Li, Q. Huang, Kafirin Nanoparticle-Stabilized Pickering Emulsions as Oral Delivery Vehicles: Physicochemical Stability and in Vitro Digestion Profile, J Agric Food Chem. 63 (2015) 10263–10270. https://doi.org/10.1021/acs.jafc.5B04385.

[239] J. Frelichowska, M.A. Bolzinger, J. Pelletier, J.P. Valour, Y. Chevalier, Topical delivery of lipophilic drugs from o/w Pickering emulsions, Int J Pharm. 371 (2009) 56–63. https://doi.org/10.1016/j.ijpharm.2008.12.017.

[240] J. Frelichowska, M.A. Bolzinger, J.P. Valour, H. Mouaziz, J. Pelletier, Y. Chevalier, Pickering w/o emulsions: Drug release and topical delivery, Int J Pharm. 368 (2009) 7–15. https://doi.org/10.1016/j.ijpharm.2008.09.057.

[241] B.R. Shah, W. Xu, J. Mráz, Formulation and characterization of zein/chitosan complex particles stabilized Pickering emulsion with the encapsulation and delivery of vitamin D3, J Sci Food Agric. 101 (2021) 5419–5428. https://doi.org/10.1002/jfsa.11190.

[242] Z. Li, X. Jiang, H. Liu, Z. Yao, A. Liu, L. Ming, Evaluation of Hydrophilic and Hydrophobic Silica Particles on the Release Kinetics of Essential Oil Pickering Emulsions, ACS Omega. 7 (2022) 8651–8664. https://doi.org/10.1021/acsomega.1C06666.

[243] Q. Tang, X. Xie, C. Li, B. Zhen, X. Cai, G. Zhang, C. Zhou, L. Wang, Medium-chain triglyceride/water Pickering emulsion stabilized by phosphatidylcholine-kaolinite for encapsulation and controlled release of curcumin, Colloids Surf B Biointerfaces. 183 (2019) 110414. https://doi.org/10.1016/j.colsurfb.2019.110414.

[244] M. Nadin, D. Rousseau, S. Ghosh, Fat crystal-stabilized water-in-oil emulsions as controlled release systems, LWT - Food Science and Technology. 56 (2014) 248–255. https://doi.org/10.1016/j.lwt.2013.10.044.

[245] D.A. Garrec, S. Frasch-Melnik, J.V.L. Henry, F. Spyropoulos, I.T. Norton, Designing colloidal structures for micro and macro nutrient content and release in foods, Faraday Discuss. 158 (2012) 37–49. https://doi.org/10.1039/c2fd20024d.

[246] L. Dai, Y. Li, F. Kong, K. Liu, C. Si, Y. Ni, Lignin-based nanoparticles stabilized pickering emulsion for stability improvement and thermal-controlled release of trans-resveratrol, ACS Sustain Chem Eng. 7 (2019) 13497–13504. https://doi.org/10.1021/acssuschemeng.9b02966.

[247] L. Atarés, L.J. Marshall, M. Akhtar, B.S. Murray, Structure and oxidative stability of oil in water emulsions as affected by rutin and homogenization procedure, Food Chem. 134 (2012) 1418–1424. https://doi.org/10.1016/j.foodchem.2012.02.221.

[248] G. Shimoni, C. Shani Levi, S. Levi Tal, U. Lesmes, Emulsions stabilization by lactoferrin nano-particles under in vitro digestion conditions, Food Hydrocoll. 33 (2013) 264–272. https://doi.org/10.1016/j.foodhyd.2013.03.017.

[249] L.C. Ghirro, S. Rezende, A.S. Ribeiro, N. Rodrigues, M. Carocho, J.A. Pereira, L. Barros, B. Demczuk, M.F. Barreiro, A. Santamaria-Echart, Pickering Emulsions Stabilized with Curcumin-Based Solid Dispersion Particles as Mayonnaise-like Food Sauce Alternatives, Molecules 2022, Vol. 27, Page 1250. 27 (2022) 1250. https://doi.org/10.3390/molecules27041250.

[250] M.F. Li, Z.Y. He, G.Y. Li, Q.Z. Zeng, D.X. Su, J.L. Zhang, Q. Wang, Y. Yuan, S. He, The formation and characterization of antioxidant pickering emulsions: Effect of the interactions between gliadin and chitosan, Food Hydrocoll. 90 (2019) 482–489. https://doi.org/10.1016/j.foodhyd.2018.12.052.

[251] T. Yi, C. Liu, J. Zhang, F. Wang, J. Wang, J. Zhang, A new drug nanocrystal self-stabilized Pickering emulsion for oral delivery of silybin, European Journal of Pharmaceutical Sciences. 96 (2017) 420–427. https://doi.org/10.1016/j.ejps.2016.08.047.

[252] S. Zhang, W. Jiang, Z. Zhang, Y. Zhu, L. Wang, J. Fu, A nanoparticle/oil double epigallocatechin gallate-loaded Pickering emulsion: Stable and delivery characteristics, LWT. 130 (2020) 109369. https://doi.org/10.1016/j.lwt.2020.109369.
[253] J. Li, X. Xu, Z. Chen, T. Wang, Z. Lu, W. Hu, L. Wang, Zein/gum Arabic nanoparticle-stabilized Pickering emulsion with thymol as an antibacterial delivery system, Carbohydr Polym. 200 (2018) 416–426. https://doi.org/10.1016/j.carbol.2018.08.025.
[254] P. Formoso, R. Tundis, M.C. Pellegrino, M. Leporini, V. Sicari, R. Romeo, L. Gervasi, G.A. Corrente, A. Beneduci, M.R. Loizzo, Preparation, characterization, and bioactivity of Zingiber officinale Roscoe powder-based Pickering emulsions, J Sci Food Agric. 102 (2022) 6566–6577. https://doi.org/10.1002/jsfa.12022.
[255] Y. Ming, Y. Xia, G. Ma, C. Yufei Xia, Aggregating particles on the O/W interface: Tuning Pickering emulsion for the enhanced drug delivery systems, Aggregate. 3 (2022) e162. https://doi.org/10.1002/agt2.162.
[256] B. Niu, H. Chen, W. Wu, X. Fang, H. Mu, Y. Han, H. Gao, Co-encapsulation of chlorogenic acid and cinnamaldehyde essential oil in Pickering emulsion stablized by chitosan nanoparticles, Food Chem X. 14 (2022) 100312. https://doi.org/10.1016/j.fochx.2022.100312.
[257] Y. Sun, W. Tang, C. Pu, R. Li, Q. Sun, H. Wang, Improved stability of liposome-stabilized emulsions as a co-encapsulation delivery system for vitamin B2, vitamin E and β-carotene, Food Funct. 13 (2022) 2966–2984. https://doi.org/10.1039/d1fo03617c.
[258] Y. Wei, D. Zhou, A. Mackie, S. Yang, L. Dai, L. Zhang, L. Mao, Y. Gao, Stability, Interfacial Structure, and Gastrointestinal Digestion of β-Carotene-Loaded Pickering Emulsions Co-stabilized by Particles, a Biopolymer, and a Surfactant, J Agric Food Chem. 69 (2021) 1619–1636. https://doi.org/10.1021/acs.jafc.0c06409.
[259] R.H. Müller, J.-S. Lucks, Drug carrier of solid lipid particles-solid lipid nanoparticles (SLN), DE4131562A1, 1991.
[260] T. Eldem, P. Speiser, A. Hincal, Optimization of Spray-Dried and -Congealed Lipid Micropellets and Characterization of Their Surface Morphology by Scanning Electron Microscopy, Pharmaceutical Research 1991 8:1. 8 (1991) 47–54. https://doi.org/10.1023/a:1015874121860.
[261] B. Mishra, B.L. Sahoo, M. Mishra, D. Shukla, V. Kumar, Design of a controlled release liquid formulation of lamotrigine, DARU, Journal of Pharmaceutical Sciences. 19 (2011) 126–137.
[262] R.H. Müller, K. Mäder, S. Gohla, Solid lipid nanoparticles (SLN) for controlled drug delivery - A review of the state of the art, European Journal of Pharmaceutics and Biopharmaceutics. 50 (2000) 161–177. https://doi.org/10.1016/s0939-6411(00)00087-4.
[263] R.H. Müller, D. Rühl, S.A. Runge, Biodegradation of solid lipid nanoparticles as a function of lipase incubation time, Int J Pharm. 144 (1996) 115–121. https://doi.org/10.1016/s0378-5173(96)04731-x.
[264] J.S. Baek, C.W. Cho, Surface modification of solid lipid nanoparticles for oral delivery of curcumin: Improvement of bioavailability through enhanced cellular uptake, and lymphatic uptake, European Journal of Pharmaceutics and Biopharmaceutics. 117 (2017) 132–140. https://doi.org/10.1016/j.ejpb.2017.04.013.
[265] L. Hu, X. Tang, F. Cui, Solid lipid nanoparticles (SLNs) to improve oral bioavailability of poorly soluble drugs, Journal of Pharmacy and Pharmacology. 56 (2010) 1527–1535. https://doi.org/10.1211/0022357044959.

[266] W. Mehnert, K. Mäder, Solid lipid nanoparticles: Production, characterization and applications, Adv Drug Deliv Rev. 47 (2001) 165–196. https://doi.org/10.1016/s0169-409x(01)00105-3.
[267] J. Sun, C. Bi, H.M. Chan, S. Sun, Q. Zhang, Y. Zheng, Curcumin-loaded solid lipid nanoparticles have prolonged in vitro antitumour activity, cellular uptake and improved in vivo bioavailability, Colloids Surf B Biointerfaces. 111 (2013) 367–375. https://doi.org/10.1016/j.colsurfb.2013.06.032.
[268] X. Huang, Y.J. Chen, D.Y. Peng, Q.L. Li, X.S. Wang, D.L. Wang, W.D. Chen, Solid lipid nanoparticles as delivery systems for Gambogenic acid, Colloids Surf B Biointerfaces. 102 (2013) 391–397. https://doi.org/10.1016/j.colsurfb.2012.08.058.
[269] E.B. Souto, S.A. Wissing, C.M. Barbosa, R.H. Müller, Development of a controlled release formulation based on SLN and NLC for topical clotrimazole delivery, Int J Pharm. 278 (2004) 71–77. https://doi.org/10.1016/j.ijpharm.2004.02.032.
[270] V. Jenning, K. Mäder, S.H. Gohla, Solid lipid nanoparticles (SLN^{TM}) based on binary mixtures of liquid and solid lipids: a 1H-NMR study, Int J Pharm. 205 (2000) 15–21. https://doi.org/10.1016/s0378-5173(00)00462-2.
[271] R.H. Müller, M. Radtke, S.A. Wissing, Nanostructured lipid matrices for improved microencapsulation of drugs, Int J Pharm. 242 (2002) 121–128. https://doi.org/10.1016/s0378-5173(02)00180-1.
[272] K. Westesen, B. Siekmann, Investigation of the gel formation of phospholipid-stabilized solid lipid nanoparticles, Int J Pharm. 151 (1997) 35–45. https://doi.org/10.1016/s0378-5173(97)04890-4.
[273] A. Gordillo-Galeano, C.E. Mora-Huertas, Solid lipid nanoparticles and nanostructured lipid carriers: A review emphasizing on particle structure and drug release, Eur J Pharm Biopharm. 133 (2018) 285–308. https://doi.org/10.1016/j.ejpb.2018.10.017.
[274] A. Khosa, S. Reddi, R.N. Saha, Nanostructured lipid carriers for site-specific drug delivery, Biomedicine & Pharmacotherapy. 103 (2018) 598–613. https://doi.org/10.1016/j.biopha.2018.04.055.
[275] R.H. Müller, M. Radtke, S.A. Wissing, Solid lipid nanoparticles (SLN) and nanostructured lipid carriers (NLC) in cosmetic and dermatological preparations, Adv Drug Deliv Rev. 54 (2002). https://doi.org/10.1016/s0169-409x(02)00118-7.
[276] P. Boonme, E.B. Souto, N. Wuttisantikul, T. Jongjit, W. Pichayakorn, Influence of lipids on the properties of solid lipid nanoparticles from microemulsion technique, European Journal of Lipid Science and Technology. 115 (2013) 820–824. https://doi.org/10.1002/ejlt.201200240.
[277] Ahlin P, J. Kristl, J. Smid-Korbar, Optimization of procedure parameters and physical stability of solid lipid nanoparticles in dispersions, Acta Pharmaceutica (Zagreb). 48 (1998) 259–267.
[278] F.Q. Hu, S.P. Jiang, Y.Z. Du, H. Yuan, Y.Q. Ye, S. Zeng, Preparation and characterization of stearic acid nanostructured lipid carriers by solvent diffusion method in an aqueous system, Colloids Surf B Biointerfaces. 45 (2005) 167–173. https://doi.org/10.1016/j.colsurfb.2005.08.005.
[279] L.J. Jia, D.R. Zhang, Z.Y. Li, F.F. Feng, Y.C. Wang, W.T. Dai, C.X. Duan, Q. Zhang, Preparation and characterization of silybin-loaded nanostructured lipid carriers, Drug Deliv. 17 (2010) 11–18. https://doi.org/10.3109/10717540903431586.
[280] S. Anantachaisilp, S.M. Smith, A. Treetong, S. Pratontep, S. Puttipipatkhachorn, U.R. Ruktanonchai, Chemical and structural investigation of lipid nanoparticles: drug–lipid

interaction and molecular distribution, Nanotechnology. 21 (2010) 125102. https://doi.org/10.1088/0957-4484/21/12/125102.
[281] K.W. Kasongo, J. Pardeike, R.H. Müller, R.B. Walker, Selection and characterization of suitable lipid excipients for use in the manufacture of didanosine-loaded solid lipid nanoparticles and nanostructured lipid carriers, J Pharm Sci. 100 (2011) 5185–5196. https://doi.org/10.1002/jps.22711.
[282] A. Kovačević, S. Savic, G. Vuleta, R.H. Müller, C.M. Keck, Polyhydroxy surfactants for the formulation of lipid nanoparticles (SLN and NLC): Effects on size, physical stability and particle matrix structure, Int J Pharm. 406 (2011) 163–172. https://doi.org/10.1016/j.ijpharm.2010.12.036.
[283] M. Shah, Y.K. Agrawal, K. Garala, A. Ramkishan, Solid lipid nanoparticles of a water soluble drug, ciprofloxacin hydrochloride, Indian J Pharm Sci. 74 (2012) 434–442. https://doi.org/10.4103/0250-474X.108419.
[284] A. Kovačević, R.H. Müller, C.M. Keck, Formulation development of lipid nanoparticles: Improved lipid screening and development of tacrolimus loaded nanostructured lipid carriers (NLC), Int J Pharm. 576 (2020) 118918. https://doi.org/10.1016/j.ijpharm.2019.118918.
[285] E.B. Souto, W. Mehnert, R.H. Müller, Polymorphic behaviour of Compritol®888 ATO as bulk lipid and as SLN and NLC, J Microencapsul. 23 (2006) 417–433. https://doi.org/10.1080/02652040600612439.
[286] H. Salminen, T. Helgason, S. Aulbach, B. Kristinsson, K. Kristbergsson, J. Weiss, Influence of co-surfactants on crystallization and stability of solid lipid nanoparticles, J Colloid Interface Sci. 426 (2014) 256–263. https://doi.org/10.1016/j.jcis.2014.04.009.
[287] S. Martins, I. Tho, E. Souto, D. Ferreira, M. Brandl, Multivariate design for the evaluation of lipid and surfactant composition effect for optimisation of lipid nanoparticles, Eur J Pharm Sci. 45 (2012) 613–623. https://doi.org/10.1016/j.ejps.2011.12.015.
[288] T. Helgason, T.S. Awad, K. Kristbergsson, D.J. McClements, J. Weiss, Effect of surfactant surface coverage on formation of solid lipid nanoparticles (SLN), J Colloid Interface Sci. 334 (2009) 75–81. https://doi.org/10.1016/j.jcis.2009.03.012.
[289] H. Bunjes, M.H.J. Koch, K. Westesen, Effects of surfactants on the crystallization and polymorphism of lipid nanoparticles, in: Lagaly G. (Eds) Molecular Organisation on Interfaces. Progress in Colloid and Polymer Science, Springer, Berlin, Heidelberg, 2002. https://doi.org/10.1007/3-540-47822-1_2.
[290] K. Westesen, B. Siekmann, M.H.J. Koch, Investigations on the physical state of lipid nanoparticles by synchrotron radiation X-ray diffraction, Int J Pharm. 93 (1993) 189–199. https://doi.org/10.1016/s0378-5173(93)90177-h.
[291] W. Mehnert, K. Mäder, Solid lipid nanoparticles: Production, characterization and applications, Adv Drug Deliv Rev. 64 (2012) 83–101. https://doi.org/10.1016/j.addr.2012.09.021.
[292] M.N. Patil, A.B. Pandit, Cavitation--a novel technique for making stable nano-suspensions, Ultrason Sonochem. 14 (2007) 519–530. https://doi.org/10.1016/j.ultsonch.2006.10.007.
[293] T.S. Awad, T. Helgason, K. Kristbergsson, E.A. Decker, J. Weiss, D.J. McClements, Effect of cooling and heating rates on polymorphic transformations and gelation of tripalmitin Solid Lipid Nanoparticle (SLN) suspensions, Food Biophys. 3 (2008) 155–162. https://doi.org/10.1007/s11483-008-9057-8.

[294] C. Ban, S. Lim, P.S. Chang, Y.J. Choi, Enhancing the stability of lipid nanoparticle systems by sonication during the cooling step and controlling the liquid oil content, J Agric Food Chem. 62 (2014) 11557–11567. https://doi.org/10.1021/jf503489v.
[295] F. Tamjidi, M. Shahedi, J. Varshosaz, A. Nasirpour, Nanostructured lipid carriers (NLC): A potential delivery system for bioactive food molecules, Innovative Food Science and Emerging Technologies. 19 (2013) 29–43. https://doi.org/10.1016/j.ifset.2013.03.002.
[296] A. zur Mühlen, E. zur Mühlen, H. Niehus, W. Mehnert, Atomic force microscopy studies of solid lipid nanoparticles, Pharm Res. 13 (1996) 1411–1416. https://doi.org/10.1023/a:1016042504830.
[297] G. v. Lowry, R.J. Hill, S. Harper, A.F. Rawle, C.O. Hendren, F. Klaessig, U. Nobbmann, P. Sayre, J. Rumble, Guidance to improve the scientific value of zeta-potential measurements in nanoEHS, Environ Sci Nano. 3 (2016) 953–965. https://doi.org/10.1039/c6en00136j.
[298] K. Sato, L. Bayés-García, T. Calvet, M.À. Cuevas-Diarte, S. Ueno, External factors affecting polymorphic crystallization of lipids, European Journal of Lipid Science and Technology. 115 (2013) 1224–1238. https://doi.org/10.1002/ejlt.201300049.
[299] C. Freitas, R.H. Müller, Correlation between long-term stability of solid lipid nanoparticles (SLN(TM)) and crystallinity of the lipid phase, European Journal of Pharmaceutics and Biopharmaceutics. 47 (1999) 125–132. https://doi.org/10.1016/S0939-6411(98)00074-5.
[300] K. Westesen, H. Bunjes, M.H.J. Koch, Physicochemical characterization of lipid nanoparticles and evaluation of their drug loading capacity and sustained release potential, Journal of Controlled Release. 48 (1997) 223–236. https://doi.org/10.1016/s0168-3659(97)00046-1.
[301] K. Larsson, Tailoring lipid functionality in foods, Trends Food Sci Technol. 5 (1994) 311–315. https://doi.org/10.1016/0924-2244(94)90181-3.
[302] A.G. Marangoni, N. Acevedo, F. Maleky, E. Co, F. Peyronel, G. Mazzanti, B. Quinn, D. Pink, Structure and functionality of edible fats, Soft Matter. 8 (2012) 1275–1300. https://doi.org/10.1039/c1sm06234d.
[303] S. Metin, R.W. Hartel, Crystallization of Fats and Oils, Bailey's Industrial Oil and Fat Products. (2005). https://doi.org/10.1002/047167849x.bio021.
[304] M. Douaire, V. di Bari, J.E. Norton, A. Sullo, P. Lillford, I.T. Norton, Fat crystallisation at oil–water interfaces, Adv Colloid Interface Sci. 203 (2014) 1–10. https://doi.org/10.1016/j.jcis.2013.10.022.
[305] K. Sato, T. Kuroda, Kinetics of melt crystallization and transformation of tripalmitin polymorphs, Journal of the American Oil Chemists' Society 1987 64:1. 64 (1987) 124–127. https://doi.org/10.1007/bf02546266.
[306] M. Cirri, L. Maestrini, F. Maestrelli, N. Mennini, P. Mura, C. Ghelardini, L.D.C. Mannelli, Design, characterization and in vivo evaluation of nanostructured lipid carriers (NLC) as a new drug delivery system for hydrochlorothiazide oral administration in pediatric therapy, Drug Deliv. 25 (2018) 1910–1921. https://doi.org/10.1080/10717544.2018.1529209.
[307] R.H. Müller, M. Radtke, S.A. Wissing, Nanostructured lipid matrices for improved microencapsulation of drugs, Int J Pharm. 242 (2002) 121–128. https://doi.org/10.1016/s0378-5173(02)00180-1.
[308] M.A. Schubert, B.C. Schicke, C.C. Müller-Goymann, Thermal analysis of the crystallization and melting behavior of lipid matrices and lipid nanoparticles containing

high amounts of lecithin, Int J Pharm. 298 (2005) 242–254. https://doi.org/10.1016/j.ijpharm.2005.04.014.
[309] M.A. Rogers, D. Tang, L. Ahmadi, A.G. Marangoni, Fat crystal networks, Food Materials Science: Principles and Practice. (2008) 369–414. https://doi.org/10.1007/978-0-387-71947-4_17.
[310] A. Gordillo-Galeano, A. Ponce, C.E. Mora-Huertas, In vitro release behavior of SLN, NLC, and NE: An explanation based on the particle structure and carried molecule location, J Drug Deliv Sci Technol. 76 (2022) 103768. https://doi.org/10.1016/j.jddst.2022.103768.
[311] M.L. Bondì, M.R. Emma, C. Botto, G. Augello, A. Azzolina, F. di Gaudio, E.F. Craparo, G. Cavallaro, D. Bachvarov, M. Cervello, Biocompatible Lipid Nanoparticles as Carriers to Improve Curcumin Efficacy in Ovarian Cancer Treatment, J Agric Food Chem. 65 (2017) 1342–1352. https://doi.org/10.1021/acs.jafc.6b04409.
[312] W. Wang, T. Chen, H. Xu, B. Ren, X. Cheng, R. Qi, H. Liu, Y. Wang, L. Yan, S. Chen, Q. Yang, C. Chen, Curcumin-loaded solid lipid nanoparticles enhanced anticancer efficiency in breast cancer, Molecules. 23 (2018) 1578. https://doi.org/10.3390/molecules23071578.
[313] M. Shah, Y. Agrawal, Ciprofloxacin hydrochloride-loaded glyceryl monostearate nanoparticle: Factorial design of Lutrol F68 and Phospholipon 90G, J Microencapsul. 29 (2012) 331–343. https://doi.org/10.3109/02652048.2011.651498.
[314] S. Doktorovova, E.B. Souto, A.M. Silva, Hansen solubility parameters (HSP) for prescreening formulation of solid lipid nanoparticles (SLN): in vitro testing of curcumin-loaded SLN in MCF-7 and BT-474 cell lines, Pharm Dev Technol. 23 (2017) 96–105. https://doi.org/10.1080/10837450.2017.1384491.
[315] H. Bunjes, F. Steiniger, W. Richter, Visualizing the structure of triglyceride nanoparticles in different crystal modifications, Langmuir. 23 (2007) 4005–4011. https://doi.org/10.1021/la062904p.
[316] K. Jores, W. Mehnert, M. Drechsler, H. Bunjes, C. Johann, K. Mäder, Investigations on the structure of solid lipid nanoparticles (SLN) and oil-loaded solid lipid nanoparticles by photon correlation spectroscopy, field-flow fractionation and transmission electron microscopy, Journal of Controlled Release. 95 (2004) 217–227. https://doi.org/10.1016/j.jconrel.2003.11.012.
[317] M. Garcia-Fuentes, M.J. Alonso, D. Torres, Design and characterization of a new drug nanocarrier made from solid–liquid lipid mixtures, J Colloid Interface Sci. 285 (2005) 590–598. https://doi.org/10.1016/j.jcis.2004.10.012.
[318] K. Jores, W. Mehnert, K. Mäder, Physicochemical investigations on solid lipid nanoparticles and on oil-loaded solid lipid nanoparticles: A nuclear magnetic resonance and electron spin resonance study, Pharm Res. 20 (2003) 1274–1283. https://doi.org/10.1023/a:1025065418309.
[319] T. Chantaburanan, V. Teeranachaideekul, D. Chantasart, A. Jintapattanakit, V.B. Junyaprasert, Effect of binary solid lipid matrix of wax and triglyceride on lipid crystallinity, drug-lipid interaction and drug release of ibuprofen-loaded solid lipid nanoparticles (SLN) for dermal delivery, J Colloid Interface Sci. 504 (2017) 247–256. https://doi.org/10.1016/j.jcis.2017.05.038.
[320] K. Jores, A. Haberland, S. Wartewig, K. Mäder, W. Mehnert, Solid lipid nanoparticles (SLN) and oil-loaded SLN studied by spectrofluorometry and Raman spectroscopy, Pharm Res. 22 (2005) 1887–1897. https://doi.org/10.1007/s11095-005-7148-5.

[321] S. Weber, A. Zimmer, J. Pardeike, Solid Lipid Nanoparticles (SLN) and Nanostructured Lipid Carriers (NLC) for pulmonary application: A review of the state of the art, European Journal of Pharmaceutics and Biopharmaceutics. 86 (2014) 7–22. https://doi.org/10.1016/j.ejpb.2013.08.013.

[322] C.M. Keck, D. Specht, J. Brüßler, Influence of lipid matrix composition on biopharmaceutical properties of lipid nanoparticles, Journal of Controlled Release. 338 (2021) 149–163. https://doi.org/10.1016/j.jconrel.2021.08.016.

[323] R.M. Shah, F. Malherbe, D. Eldridge, E.A. Palombo, I.H. Harding, Physicochemical characterization of solid lipid nanoparticles (SLNs) prepared by a novel microemulsion technique, J Colloid Interface Sci. 428 (2014) 286–294. https://doi.org/10.1016/j.jcis.2014.04.057.

[324] J.Q. Zhang, J. Liu, X.L. Li, B.R. Jasti, Preparation and characterization of solid lipid nanoparticles containing silibinin, Drug Deliv. 14 (2007) 381–387. https://doi.org/10.1080/10717540701203034.

[325] S. Lombardi Borgia, M. Regehly, R. Sivaramakrishnan, W. Mehnert, H.C. Korting, K. Danker, B. Röder, K.D. Kramer, M. Schäfer-Korting, Lipid nanoparticles for skin penetration enhancement—correlation to drug localization within the particle matrix as determined by fluorescence and parelectric spectroscopy, Journal of Controlled Release. 110 (2005) 151–163. https://doi.org/10.1016/j.jconrel.2005.09.045.

[326] R. Sivaramakrishnan, C. Nakamura, W. Mehnert, H.C. Korting, K.D. Kramer, M. Schäfer-Korting, Glucocorticoid entrapment into lipid carriers — characterisation by parelectric spectroscopy and influence on dermal uptake, Journal of Controlled Release. 97 (2004) 493–502. https://doi.org/10.1016/j.jconrel.2004.04.001.

[327] R. Sivaramakrishnan, L. Kankate, H. Niehus, K.D. Kramer, Parelectric spectroscopy of drug-carrier-systems—distribution of carrier masses or activation energies, Biophys Chem. 114 (2005) 221–228. https://doi.org/10.1016/j.bpc.2004.12.007.

[328] H. Salminen, C. Gömmel, B.H. Leuenberger, J. Weiss, Influence of encapsulated functional lipids on crystal structure and chemical stability in solid lipid nanoparticles: Towards bioactive-based design of delivery systems, Food Chem. 190 (2016) 928–937. https://doi.org/10.1016/j.foodchem.2015.06.054.

[329] J. Mazuryk, T. Deptuła, A. Polchi, J. Gapiński, S. Giovagnoli, A. Magini, C. Emiliani, J. Kohlbrecher, A. Patkowski, Rapamycin-loaded solid lipid nanoparticles: Morphology and impact of the drug loading on the phase transition between lipid polymorphs, Colloids Surf A Physicochem Eng Asp. 502 (2016) 54–65. https://doi.org/10.1016/j.colsurfa.2016.05.017.

[330] J. Milsmann, K. Oehlke, R. Greiner, A. Steffen-Heins, Fate of edible solid lipid nanoparticles (SLN) in surfactant stabilized o/w emulsions. Part 2: Release and partitioning behavior of lipophilic probes from SLN into different phases of o/w emulsions, Colloids Surf A Physicochem Eng Asp. 558 (2018) 623–631. https://doi.org/10.1016/j.colsurfa.2017.05.050.

[331] C. Long, L. Zhang, Y. Qian, Mesoscale simulation of drug molecules distribution in the matrix of solid lipid microparticles (SLM), Chemical Engineering Journal. 119 (2006) 99–106. https://doi.org/10.1016/j.cej.2006.03.031.

[332] C.C. Berton-Carabin, J.N. Coupland, R.J. Elias, Effect of the lipophilicity of model ingredients on their location and reactivity in emulsions and solid lipid nanoparticles, Colloids Surf A Physicochem Eng Asp. 431 (2013) 9–17. https://doi.org/10.1016/j.colsurfa.2013.04.016.

[333] Y. Pan, R. v. Tikekar, N. Nitin, Distribution of a model bioactive within solid lipid nanoparticles and nanostructured lipid carriers influences its loading efficiency and oxidative stability, Int J Pharm. 511 (2016) 322–330. https://doi.org/10.1016/j.ijpharm.2016.07.019.

[334] S.F. Haag, M. Chen, D. Peters, C.M. Keck, B. Taskoparan, A. Fahr, C. Teutloff, R. Bittl, J. Lademann, M. Schäfer-Korting, M.C. Meinke, Nanostructured lipid carriers as nitroxide depot system measured by electron paramagnetic resonance spectroscopy, Int J Pharm. 421 (2011) 364–369. https://doi.org/10.1016/j.ijpharm.2011.10.009.

[335] S. Saeidpour, S.B. Lohan, A. Solik, V. Paul, R. Bodmeier, G. Zoubari, R. Bittl, M.C. Meinke, C. Teutloff, Drug distribution in nanostructured lipid particles, European Journal of Pharmaceutics and Biopharmaceutics. 110 (2017) 19–23. https://doi.org/10.1016/j.ejpb.2016.10.008.

[336] E. Kupetz, H. Bunjes, Lipid nanoparticles: Drug localization is substance-specific and achievable load depends on the size and physical state of the particles, Journal of Controlled Release. 189 (2014) 54–64. https://doi.org/10.1016/j.jconrel.2014.06.007.

[337] P.C. Christophersen, D. Birch, J. Saarinen, A. Isomäki, H.M. Nielsen, M. Yang, C.J. Strachan, H. Mu, Investigation of protein distribution in solid lipid particles and its impact on protein release using coherent anti-Stokes Raman scattering microscopy, Journal of Controlled Release. 197 (2015) 111–120. https://doi.org/10.1016/j.jconrel.2014.10.023.

[338] C. v. Garcia, G.H. Shin, J.T. Kim, Formulation of lipid nanocarriers for the food bioactive ingredients, Food Structure and Functionality. (2021) 133–156. https://doi.org/10.1016/b978-0-12-821453-4.00007-7.

[339] P. Ghasemiyeh, S. Mohammadi-Samani, Solid lipid nanoparticles and nanostructured lipid carriers as novel drug delivery systems: applications, advantages and disadvantages, Res Pharm Sci. 13 (2018) 288–303. https://doi.org/10.4103/1735-5362.235156.

[340] J. Miao, Y. Du, H. Yuan, X. Zhang, Q. Li, Y. Rao, M. Zhao, F. Hu, Improved cytotoxicity of paclitaxel loaded in nanosized lipid carriers by intracellular delivery, Journal of Nanoparticle Research. 17 (2015) 1–13. https://doi.org/10.1007/s11051-014-2852-x.

[341] T. Guo, Y. Zhang, J. Zhao, C. Zhu, N. Feng, Nanostructured lipid carriers for percutaneous administration of alkaloids isolated from Aconitum sinomontanum, J Nanobiotechnology. 13 (2015) 1–14. https://doi.org/10.1186/s12951-015-0107-3.

[342] A. Garg, S. Singh, Enhancement in antifungal activity of eugenol in immunosuppressed rats through lipid nanocarriers, Colloids Surf B Biointerfaces. 87 (2011) 280–288. https://doi.org/10.1016/j.colsurfb.2011.05.030.

[343] F.Q. Hu, S.P. Jiang, Y.Z. Du, H. Yuan, Y.Q. Ye, S. Zeng, Preparation and characteristics of monostearin nanostructured lipid carriers, Int J Pharm. 314 (2006) 83–89. https://doi.org/10.1016/j.ijpharm.2006.01.040.

[344] J. Shen, M. Sun, Q. Ping, Z. Ying, W. Liu, Incorporation of liquid lipid in lipid nanoparticles for ocular drug delivery enhancement, Nanotechnology. 21 (2009) 025101. https://doi.org/10.1088/0957-4484/21/2/025101.

[345] P.A. Makoni, K.W. Kasongo, R.B. Walker, Short Term Stability Testing of Efavirenz-Loaded Solid Lipid Nanoparticle (SLN) and Nanostructured Lipid Carrier (NLC) Dispersions, Pharmaceutics 2019, Vol. 11, Page 397. 11 (2019) 397. https://doi.org/10.3390/pharmaceutics11080397.

[346] L.M. Andrade, C. de Fátima Reis, L. Maione-Silva, J.L. v. Anjos, A. Alonso, R.C. Serpa, R.N. Marreto, E.M. Lima, S.F. Taveira, Impact of lipid dynamic behavior on physical stability, in vitro release and skin permeation of genistein-loaded lipid nanoparticles, European Journal of Pharmaceutics and Biopharmaceutics. 88 (2014) 40–47. https://doi.org/10.1016/j.ejpb.2014.04.015.

[347] W. Xu, M.K. Lee, Development and evaluation of lipid nanoparticles for paclitaxel delivery: a comparison between solid lipid nanoparticles and nanostructured lipid carriers, J Pharm Investig. 45 (2015) 675–680. https://doi.org/10.1007/s40005-015-0224-x.

[348] G.A. Islan, P.C. Tornello, G.A. Abraham, N. Duran, G.R. Castro, Smart lipid nanoparticles containing levofloxacin and DNase for lung delivery. Design and characterization, Colloids Surf B Biointerfaces. 143 (2016) 168–176. https://doi.org/10.1016/j.colsurfb.2016.03.040.

[349] S. Das, W.K. Ng, R.B.H. Tan, Are nanostructured lipid carriers (NLCs) better than solid lipid nanoparticles (SLNs): Development, characterizations and comparative evaluations of clotrimazole-loaded SLNs and NLCs?, European Journal of Pharmaceutical Sciences. 47 (2012) 139–151. https://doi.org/10.1016/j.ejps.2012.05.010.

[350] R.F.S. Gonçalves, A.A. Vicente, A.C. Pinheiro, Incorporation of curcumin-loaded lipid-based nano delivery systems into food: Release behavior in food simulants and a case study of application in a beverage, Food Chem. 405 (2023) 134740. https://doi.org/10.1016/j.foodchem.2022.134740.

[351] P. Mura, F. Maestrelli, M. D'Ambrosio, C. Luceri, M. Cirri, Evaluation and Comparison of Solid Lipid Nanoparticles (SLNs) and Nanostructured Lipid Carriers (NLCs) as Vectors to Develop Hydrochlorothiazide Effective and Safe Pediatric Oral Liquid Formulations, Pharmaceutics 2021, Vol. 13, Page 437. 13 (2021) 437. https://doi.org/10.3390/pharmaceutics13040437.

[352] G. Zoubari, S. Staufenbiel, P. Volz, U. Alexiev, R. Bodmeier, Effect of drug solubility and lipid carrier on drug release from lipid nanoparticles for dermal delivery, European Journal of Pharmaceutics and Biopharmaceutics. 110 (2017) 39–46. https://doi.org/10.1016/j.ejpb.2016.10.021.

[353] N. Dan, Nanostructured lipid carriers: Effect of solid phase fraction and distribution on the release of encapsulated materials, Langmuir. 30 (2014) 13809–13814. https://doi.org/10.1021/la5030197

[354] H. Jiang, D. Geng, H. Liu, Z. Li, J. Cao, Co-delivery of etoposide and curcumin by lipid nanoparticulate drug delivery system for the treatment of gastric tumors, Drug Deliv. 23 (2016) 3665–3673. https://doi.org/10.1080/10717544.2016.1217954.

[355] J.S.R. Viegas, F.G. Praça, A.L. Caron, I. Suzuki, A.V.P. Silvestrini, W.S.G. Medina, J.O. del Ciampo, M. Kravicz, M.V.L.B. Bentley, Nanostructured lipid carrier co-delivering tacrolimus and TNF-α siRNA as an innovate approach to psoriasis, Drug Deliv Transl Res. 10 (2020) 646–660. https://doi.org/10.1007/s13346-020-00723-6.

[356] D.M. Yu, W. Li, Y. Zhang, B. Zhang, Anti-tumor efficiency of paclitaxel and DNA when co-delivered by pH responsive ligand modified nanocarriers for breast cancer treatment, Biomedicine & Pharmacotherapy. 83 (2016) 1428–1435. https://doi.org/10.1016/j.biopha.2016.08.061.

[357] J.S. Baek, C.W. Cho, Controlled release and reversal of multidrug resistance by co-encapsulation of paclitaxel and verapamil in solid lipid nanoparticles, Int J Pharm. 478 (2015) 617–624. https://doi.org/10.1016/j.ijpharm.2014.12.018.

[358] O. Taratula, A. Kuzmov, M. Shah, O.B. Garbuzenko, T. Minko, Nanostructured lipid carriers as multifunctional nanomedicine platform for pulmonary co-delivery of anticancer drugs and siRNA, Journal of Controlled Release. 171 (2013) 349–357. https://doi.org/10.1016/j.jconrel.2013.04.018.

[359] H. Hajipour, M. Ghorbani, H. Kahroba, F. Mahmoodzadeh, R.Z. Emameh, R.A. Taheri, Arginyl-glycyl-aspartic acid (RGD) containing nanostructured lipid carrier co-loaded with doxorubicin and sildenafil citrate enhanced anti-cancer effects and overcomes drug resistance, Process Biochemistry. 84 (2019) 172–179. https://doi.org/10.1016/j.procbio.2019.06.013.

[360] A.A.A. Youssef, N. Dudhipala, S. Majumdar, Dual Drug Loaded Lipid Nanocarrier Formulations for Topical Ocular Applications, Int J Nanomedicine. 17 (2022) 2283. https://doi.org/10.2147/ijn.S360740.

[361] S. v. Mussi, R. Sawant, F. Perche, M.C. Oliveira, R.B. Azevedo, L.A.M. Ferreira, V.P. Torchilin, Novel nanostructured lipid carrier co-loaded with doxorubicin and docosahexaenoic acid demonstrates enhanced in vitro activity and overcomes drug resistance in MCF-7/Adr cells, Pharm Res. 31 (2014) 1882–1892. https://doi.org/10.1007/s11095-013-1290-2.

[362] C. Vitorino, J. Almeida, L.M. Gonçalves, A.J. Almeida, J.J. Sousa, A.A.C.C. Pais, Co-encapsulating nanostructured lipid carriers for transdermal application: From experimental design to the molecular detail, Journal of Controlled Release. 167 (2013) 301–314. https://doi.org/10.1016/j.jconrel.2013.02.011.

[363] L.M. Andrade, L.A.D. Silva, A.P. Krawczyk-Santos, I.C. de S.M. Amorim, P.B.R. da Rocha, E.M. Lima, J.L. v. Anjos, A. Alonso, R.N. Marreto, S.F. Taveira, Improved tacrolimus skin permeation by co-encapsulation with clobetasol in lipid nanoparticles: Study of drug effects in lipid matrix by electron paramagnetic resonance, European Journal of Pharmaceutics and Biopharmaceutics. 119 (2017) 142–149. https://doi.org/10.1016/j.ejpb.2017.06.014.

Chapter 3

Formulation design and development of lipid particles loaded with a hydrophobic active

Published as:

G.I. Sakellari, I. Zafeiri, H. Batchelor, F. Spyropoulos, Formulation design, production and characterisation of solid lipid nanoparticles (SLN) and nanostructured lipid carriers (NLC) for the encapsulation of a model hydrophobic active, Food Hydrocolloids for Health. (2021) 100024.

Synopsis

Lipid nanoparticles have been widely investigated for their use as either carriers for poorly water-soluble actives or as (Pickering) emulsion stabilisers. Recent studies have suggested that the fabrication of lipid nanostructures that can display both these performances concurrently, can enable the development of liquid formulations for multi-active encapsulation and release. Understanding the effects of different formulation variables on the microstructural attributes that underlie both these functionalities is crucial in developing such lipid nanostructures. In this study, two types of lipid-based nanoparticles, solid lipid nanoparticles and nanostructured lipid carriers, were fabricated using varying formulation parameters, namely type of solid lipid, concentration of liquid lipid and type/concentration of surface active species. The impact of these formulation parameters on the size, thermal properties, encapsulation efficiency, loading capacity and long-term storage stability of the developed lipid systems, was studied. Preliminary lipid screening and processing conditions studies, focused on creating a suitable lipid host matrix of appropriate dimensions that could enable the high loading of a model hydrophobic active (curcumin). Informed by this, selected lipid nanostructures were then produced. These were characterised by encapsulation efficiency and loading capacity values as high as 99% and 0.5%, respectively, and particle dimensions within the desirable size range (100–200 nm) required to enable Pickering functionality. Compatibility between the lipid matrix components, and liquid lipid/active addition were shown to greatly influence the polymorphism/crystallinity of the fabricated particles, with the latter demonstrating a liquid lipid concentration-dependent behaviour. Successful long-term storage stability of up to 28 weeks was confirmed for certain formulations.

3.1 Introduction

Lipid nanoparticles, namely solid lipid nanoparticles (SLNs) and nanostructured lipid carriers (NLCs) comprise a widely used platform of lipid-based colloidal vehicles, as they can accommodate solubility and bioavailability enhancement of poorly water-soluble actives [1–3], as well as improved stability and shielding of actives prone to degradation [4–11]. In the last decade, due to their auspicious usage in Pickering emulsion stabilisation [12–14], their applications portfolio has expanded to include the two-fold functionality of encapsulating/controlling the release of a hydrophobic active and stabilising o/w or w/o emulsion droplets, both achieved by tuning their surface properties [15]. However, there is still limited understanding on the correlation between the structural properties of lipid particles and the structures' capacity to afford effective Pickering stabilisation [16–17]. Nanoemulsion droplets with a volume-weighted mean particle diameter of 459 nm were stabilised by negatively charged glyceryl stearate citrate SLNs with a mean diameter of 152 nm for a period of 12 weeks [12]. Recently, Lim *et al*. [18] studied the interfacial characteristics of tristearin SLNs in respect to the interfacial and colloidal stability of the SLN-stabilised emulsions, demonstrating that increasing the concentration of surfactant used in the SLN preparation, can prolong the stability of the attained emulsions (up to 4 weeks under the studied conditions). In another study, tailoring of submicron-sized particles, in terms of their crystalline structure and morphology, was achieved by alternating the lipid phase composition between tripalmitin, palm stearin or combination of tripalmitin and the liquid lipid tricaprylin (4:1 w/w), that resulted in varying emulsion stabilisation efficiency due to wettability and inter-particle interaction changes [19].

The significance of the above properties and how they can be modulated to achieve desirable characteristics is not only limited to the development of lipid nanoparticle dispersions suitable for Pickering stabilisation. The tendency of SLNs to transform into highly ordered crystalline structures and lead to active expulsion during storage has been addressed by partial substitution with incompatible liquid lipids (NLCs), to create imperfections in the lipid crystal lattice, that will in turn also accommodate higher active incorporation [20,21]. The choice of the type and ratio between the solid and liquid lipids participating in such combinations can greatly affect the resulting lipid core organisation and active carrying/delivery performance, while this can be further modified by the encapsulated molecule and the surfactant contribution [22–32]. The structural organisation of SLNs and NLCs has been a subject of debate, with numerous reports in literature utilising a range of structural and imaging techniques to determine the positioning of the solid lipid, liquid lipid and active components [23,24,29,30,33–35]. Oehlke *et al*. [36] proposed the presence of the lipophilic tocopherol in the lipid matrix near the tail of the surfactant, as opposed to the location of the hydrophilic ferulic acid in the headgroup region, with the location of the former explaining the greater impact on halting prolonged melting behaviour changes. The effect of the relative affinity between the encapsulated active and the lipid used was demonstrated by the higher loading and slower release of the drug diclofenac from lipid particles containing high ratio of the solid lipid Gelucire® 50/13 compared to the drug dexamethasone, while faster release for both drugs was recorded when a partially miscible solid lipid (Witepsol® S55) and a liquid lipid (Capryol® 90) were added in the lipid matrix that was attributed to the creation of a less ordered crystalline state [37]. Thus, understanding how and to what extent certain composition factors, including the gradual addition of liquid lipid and/or active, influence the structure of the solid lipid matrix can potentially provide further

insight on how to form lipid particles with customised properties tailored to their intended functionalities and applications.

The present work aims to investigate the impact of formulation variables, including the incorporation of curcumin used as a model hydrophobic active, on specific physical characteristics of SLNs and NLCs. Curcumin is a lipophilic polyphenolic compound, widely studied by the pharmaceutical, cosmetic and food sectors due to its numerous attributes, including but not limited to anti-inflammatory, antimicrobial, anticancer and antioxidant properties [38]. Similarly to other hydrophobic actives, curcumin requires the use of a suitable carrier, among which are lipid-based systems, to enhance its bioavailability and harness its health benefits [39], and thus it has been previously employed as a model hydrophobic active during the development of delivery systems [9,40]. The selection of lipid components (solid and liquid lipids) with high compatibility towards one another, that also show affinity for curcumin, was one of the primary focuses of the early development stages, towards the creation of a lipid core that can achieve high active entrapment and long-term physical integrity. For this purpose, theoretical predictions using the Hansen solubility parameter and experimental lipid screening studies were performed for both solid and liquid lipids, along with miscibility studies. Thereafter, lipid dispersions of both SLNs and NLCs were fabricated via a melt-emulsification-ultrasonication method in the presence of surface active species. Two types of solid lipids (singly or as blends), varying concentration of the liquid lipid and type/concentration of the surface active species were evaluated. The effect of these parameters on physical markers linked to Pickering functionality, that herein was confined in terms of appropriate size, together with the thermal properties, loading capacity and long-term storage stability of the lipid nanoparticles were assessed. Lipid screening as a formulation development aspect, and alterations in the formulation variables of the lipid nanoparticles have been

previously studied individually towards the creation of systems with optimised properties. However, there has been a lack of cumulative investigation of the impact of these formulation aspects on the physical characteristics of particles fabricated under consistent processing parameters, where the novelty of the current study lies. Thus, it is envisaged that through this comprehensive study, gaining a better insight on the reliance between formulation composition and crystalline structure properties of the SLNs and NLCs will eventually allow for tuning of the release profiles of the encapsulated actives, without compromising the microstructural attributes that enable their Pickering functionality.

3.2 Materials and methods

3.2.1 Materials

Glyceryl behenate (Compritol® 888 ATO), glyceryl palmitostearate (Precirol® ATO 5), linoleoyl polyoxyl-6-glycerides (Labrafil® M 2125 CS), propylene glycol dicaprolate/dicaprate (Labrafac™ PG), cetyl palmitate and lauroyl polyoxyl-32 glycerides (Gelucire® 44/14) were kindly provided from Gattefossé (Saint-Priest, France). Glyceryl monostearate (Imwitor® 960K), glyceryl citrate/lactate/linoleate/oleate (Imwitor® 375) and medium chain triglycerides (MCTs) (Miglyol® 812), microcrystalline glyceryl tristearate (Dynasan® 118) were a kind gift from IOI Oleo (IOI Oleochemicals GmbH, Germany). Polyoxyethylene sorbitan monooleate (Tween® 80), Poloxamer 188 (Pluronic® F-68), poly(vinyl alcohol) (PVA, MW 89,000-98,000), castor oil and curcumin (≥65%, HPLC) were purchased from Sigma-Aldrich (Sigma-Aldrich, UK). All chemicals were used without further purification. Double distilled water from Milli-Q systems (Millipore, Watford, UK) was used for all experiments.

3.2.2 Lipid screening

Lipid screening was performed to evaluate the solubility of curcumin, the chosen model hydrophobic active, in a variety of solid and liquid lipids, a parameter of critical importance in the formulation development process. In this study, the solubilisation capacity of various lipids towards curcumin was assessed through both theoretical and experimental lipid screening.

3.2.2.1 Theoretical lipid screening

Theoretical predictions regarding the compatibility between the selected active and different solid and liquid lipids were based on calculations of the Hansen solubility parameter (HSP). For this purpose, the lipids were treated as the organic "solvents" and curcumin was the organic active under investigation. According to the theory proposed by Hansen [41], the total cohesion energy in an organic molecule is the sum of three individual energy sources arising from nonpolar, polar and hydrogen bonding interactions. Thus, the solubility parameter (δ) of a substance can be decomposed into three distinct components. The partial HSP parameters account for the aforementioned dispersion interactions (δ_D), permanent dipole-permanent dipole forces (δ_P) and hydrogen bonding (δ_H), measured in $MPa^{1/2}$.

HSPs for curcumin and a variety of solid and liquid lipids were calculated as follows:

$$\delta_D = \frac{\sum_i F_{di}}{V_m} \tag{3.1}$$

$$\delta_P = \frac{\sqrt{\sum_i F_{pi}^2}}{V_m} \tag{3.2}$$

$$\delta_H = \sqrt{\frac{\sum_i E_{hi}}{V_m}} \tag{3.3}$$

$$\delta = \sqrt{(\delta_D^2 + \delta_P^2 + \delta_H^2)} \tag{3.4}$$

where F_d, F_p, E_h denote the group contribution parameters associated with the dispersion and polar forces, and hydrogen bonding energy that characterise each functional group of the molecular structure, respectively, and V_m represents the molar volume. The group contribution values used for the calculations were in accordance with the work published by van Krevelen *et al*. [42]. Curcumin can exist in two tautomeric forms; a diketo and an enol conformation, which have relative ratios that vary depending on the temperature, solvent polarity, pH and aromatic ring substitution [43]. Therefore, the solubility screening was performed for both tautomeric forms. Depending on the chemical composition of each lipid (see Appendix A1, Table A1.1), the total and individual HSP for each constituent were estimated. An example of the calculations performed can be found in Appendix A. For lipids with clearly defined chemical composition and consistency, HSPs were calculated for each of their components and an overall parameter was then obtained based on molar weighted averages (Table 3.1). For the solid lipid Imwitor® 960K and the liquid lipids Labrafil® M 2125 CS and Imwitor® 375, where an exact composition was not provided by the manufacturer (see Appendix A1, Table A1.2), calculations were carried out using available information about the lipid component composition and making assumptions for the potential consistency combinations; in this case HSPs are displayed as averages (Table 3.1 & Fig. 3.1), rather than absolute values.

The miscibility between two substances can be visualised using the three partial solubility parameters, acting as coordinates in a three-dimensional space developed by Hansen (HSP 3D

space). The close proximity of two points, each corresponding to a different material, can be used as a measure of high interactions and miscibility occurrence. The modified difference between the HSP of the active (A) and a given lipid (B) (R_a), representing the distance between the two substances A and B in the HSP 3D space, was determined as follows:

$$R_a = \sqrt{4(\delta_{DA} - \delta_{DB})^2 + (\delta_{PA} - \delta_{PB})^2 + (\delta_{HA} - \delta_{HB})^2} \quad (3.5)$$

For a combination of miscible substances, the distance R_a should not exceed the radius of interaction (R_0), which gives the maximum difference allowed to define affinity between the active and a chosen solvent. The R_0 for the studied active can be found empirically using Equation 3.5 for a series of solvents with experimentally known HSPs [41]. More specifically, the solvents known to have good solubilisation capacity for curcumin and thus used in this study were propanone, ethyl ethanoate, n-butanol, methanol, ethanol and isopropanol (see Appendix A1, Table A1.2).

3.2.2.2 Experimental lipid screening

a. Selection of solid lipids

The maximum amount of curcumin that can be dissolved in 1 g of each solid lipid (Compritol® 888 ATO, Precirol® ATO 5, Dynasan® 118, cetyl palmitate, Imwitor® 960K) was determined by adding stepwise increasing amount of the active (1–2 mg) into the solid lipids. In order to mimic the experimental conditions followed for the lipid dispersions production (Section 3.2.3), each mixture was thermostatically maintained at 5–10°C above the melting point of each solid lipid, and let to stir for 1 h. The solubilisation of curcumin was evaluated by visual observation

of formation of transparent homogeneous solutions with no visible traces of active crystals [44]. The mixtures were left to cool down and stored in the dark at room temperature until further analysis.

b. Selection of liquid lipids

The choice of the liquid lipid used for the NLC dispersions was based on their ability to solubilise curcumin. A series of liquid lipids (Labrafil® M 2125 CS, Labrafac™ PG, Imwitor® 375, Miglyol® 812, castor oil) were tested, by adding increasing amount of the active (1–2 mg) in 1 g of each liquid lipid thermostated at 85°C and let to stir for 1 h, to simulate the process followed for the preparation of the lipid particle dispersions (Section 3.2.3). Similarly to the method described above for the selection of solid lipids, the solubilising power of each liquid lipid towards curcumin was assessed on their capacity to form transparent mixtures [45].

c. Miscibility of solid and liquid lipid systems

Blends of the solid and liquid lipids displaying the highest solubilising power towards curcumin were prepared in fractions, chosen based on the minimum and maximum amount of liquid lipid that was going to be used for the lipid dispersion fabrication, to examine their miscibility. The two solid lipids were mixed at a 50:50 w/w ratio, while 30% w/w of the solid lipid or solid lipid mixture was substituted by the liquid lipid for the blends containing both types of lipids. Curcumin was dissolved at 0.5% w/w of the total sample mass. The samples were agitated for 1 h at a temperature 5–10°C higher than the melting point of the solid lipids, to prepare the tempered solid lipids and blends of lipids, and then allowed to cool down at room temperature. The compatibility between the components was evaluated by both visual inspection for signs

of turbidity or phase separation, coupled with differential scanning calorimetry (DSC, Setaram μDSC3 evo microcalorimeter, Setaram Instrumentation, France) analysis [27]. Specifically, the thermograms of the physical mixtures between the solid and liquid lipids with or without curcumin were compared to the thermograms of the respective tempered solid lipid.

3.2.3 Preparation of SLN and NLC aqueous dispersions

Blank and curcumin-loaded solid lipid nanoparticles and nanostructured lipid carriers (denoted as B-SLN or B-NLC and SLN or NLC, respectively) were prepared by a melt-emulsification-ultrasonication method, that has been previously described elsewhere [14]. In brief, 2.5% of the lipid phase relating to the total mass (% w/w) was heated 5–10°C above the melting point of the lipid to ensure complete melting, and the heating state was maintained for approximately 1 h to avoid lipid thermal memory effects [46]. More specifically, Compritol® 888 ATO and Precirol® ATO 5 were heated up to 85 and 70°C, respectively, and their 1:1 mixture was melted to around 85°C. When curcumin-loaded lipid particles were prepared, curcumin (0.5% w/w of the lipid mass) was added to the lipid phase and kept under magnetic stirring, until the active was completely dissolved (~1 h). The concentration of curcumin used was based on preliminary lipid screening studies. The temperature was monitored using a digital thermometer throughout all processes. For the NLCs, the liquid lipid concentrations used were 10, 20, or 30% of the total lipid content. The surfactant, Tween® 80 or Pluronic® F-68 (1.2 or 0.5% w/w of the total mass), was dissolved in the aqueous phase, which was heated to the same temperature as the molten lipid phase. The two phases were mixed by adding the aqueous to the lipid phase, and the mixture was stirred with a magnetic stirring bar for 15 minutes. The pre-emulsion was then homogenised using a high intensity ultrasonic Vibra-cell™ VC 505 processor (Sonics & Materials, Inc., CT, USA), operating continuously at 750 Watt and 20 kHz, at a sonication

amplitude of 95% of the total power over a period of 5 minutes. To obtain the solid lipid particles, the o/w emulsion was subsequently cooled using an ice bath to a temperature below the crystallisation point of the lipid or mixture of lipids (1–4°C), with a cooling rate ranging between 0.5 and 2 °C/min. Samples were stored at 4°C protected from light (since curcumin is photodegradable) until further analysis.

3.2.4 Physicochemical characterisation

3.2.4.1 Particle size, polydispersity and zeta potential analyses

Particle size and size distribution profiles were assessed either by dynamic light scattering (DLS) using a Zetasizer Nano ZS (Malvern Instruments, UK), or laser diffraction (LD) using a Mastersizer 2000 (Malvern Instruments, UK). For DLS measurements, the mean particle size (*Z*-average) was determined at a backscattering angle of 173° at 25°C. Polydispersity index (PDI) and zeta potential (ζ-potential) were additionally measured. All samples were appropriately diluted to avoid multiple scattering phenomena. In the case of LD, the samples were diluted with distilled water and stirred at 1200 rpm until an obscuration rate of approximately 5% was obtained. The mean diameters $D_{3,2}$ and span values were acquired to confirm signs of particle aggregation suggested by DLS measurements. The refractive indices of the materials used throughout the experiments were 1.55 for Compritol® 888 ATO and Precirol® ATO 5, 1.52 for their mixtures with Miglyol® 812, 1.52 for their 1:1 w/w mixture, 1.50 for their ternary mixture with Miglyol® 812 and 1.33 for distilled water. The absorption index was set at 0.01. Results are presented as the average value of 6 measurements with standard deviation (±S.D.).

3.2.4.2 Thermal analysis

Thermal analysis of the bulk materials and dispersions of lipid particles was carried out using a Setaram μDSC3 evo microcalorimeter (Setaram Instrumentation, France). Samples were accurately weighted (approximately 6.5 mg of bulk lipids or lipid mixtures and 600 mg of the lipid dispersions) and scanned between 20 and 90°C at a heating rate of 1.2 °C/min, followed by a cooling cycle from 90 to 5°C. DSC data were used to investigate the compatibility of the lipid mixtures, the solid state of the cooled samples and the melting and crystallisation behaviour of the lipid dispersions. For bulk lipids, thermograms were obtained before and after tempering the lipids for 1 h at a temperature 5–10°C above their melting point. Information about the enthalpy, onset and peak temperatures was acquired through the Calisto Processing software. The DSC thermogram of pure curcumin was obtained using a DSC 25 (TA Instruments®, FR), where the sample was heated inside a Tzero® Hermetic Aluminum pan. The physical mixtures containing curcumin were additionally studied using the same equipment to investigate the presence or absence of crystalline curcumin by achieving higher temperature range. The temperature ramp used was 25 to 200°C at 5 °C/min. Bulk materials were assessed against an empty reference cell, while for the lipid particle dispersions, the reference cell was filled with equal amount of distilled water. All enthalpy values and thermograms reported, are normalised for the amount of crystallising material present in the samples.

The degree of crystallinity was determined using the enthalpy derived from DSC data for the lipid nanoparticle dispersions and the lipid physical mixtures, and expressed by means of the recrystallisation indices (RI) which were calculated following the equation [47]:

$$RI = \frac{\Delta H_{SLN,NLC}}{\Delta H_{b.l.} \times C_{l.p.}} \times 100\ (\%) \qquad (3.6)$$

where $\Delta H_{SLN,\ NLC}$ and $\Delta H_{b.l.}$ represent the molar melting enthalpy (J/g) of the SLN and NLC aqueous dispersions and the bulk lipid phase respectively, and $C_{l.p.}$ is the % w/w concentration of the lipid phase.

3.2.4.3 Encapsulation efficiency and loading capacity

The entrapment efficiency (EE) and loading capacity (LC) were determined by ultrafiltration using centrifugal ultrafiltration tubes (Amicon® Ultra-4 filter 10 kDa cut-off, Millipore, Billerica, MA, USA). 1 mL of the curcumin-loaded lipid dispersions was added to the upper chamber of the centrifugal tube and centrifuged at 2,400 rcf for 1 h at room temperature using a SIGMA 3K-30 centrifuge (SciQuip®, UK). The concentration of unentrapped curcumin in the filtrate was subsequently determined by measuring the UV absorbance (Orion AquaMate 8000, Thermo-Scientific®, UK) at 425 nm, using a calibration curve that has been previously generated with linearity studied for 0–6 μg/mL and linear regression value of $R^2 = 0.9995$. The EE and LC were calculated using the following equations:

$$EE = \frac{W_{i.\ CRM} - W_{u.\ CRM}}{W_{i.\ CRM}} \times 100\ (\%) \qquad (3.7)$$

$$LC = \frac{W_{i.\ CRM} - W_{u.\ CRM}}{W_{l.p.}} \times 100\ (\%) \qquad (3.8)$$

where $W_{i.\ CRM}$ is the amount of curcumin that was initially used during the preparation of the aqueous lipid dispersions, $W_{u.\ CRM}$ is the amount of curcumin measured in the filtrate and $W_{l.p.}$ is the total amount of the lipid components used in the dispersions.

3.2.4.4 Assessment of storage stability

Stability studies of the aqueous SLN and NLC dispersions were performed over a period of 28 weeks with interval measurements performed at 1, 4 and 16 weeks, for samples stored at 4°C by measuring *Z*-average, PDI and ζ-potential. Changes in the physical state of the samples indicating destabilisation were assessed by visual inspection. Thermal behaviour and encapsulation efficiency were also evaluated over the same period.

3.2.5 Statistical analysis

Samples were prepared in at least duplicates and measurements were performed in at least triplicate and averages are reported with standard deviation. Figures depict the calculated average with error bars showing the standard deviation above and below the average. Comparison of means was conducted by ANOVA analysis followed by an all pairwise multiple comparison test using the Student-Newman-Keuls Method (SigmaPlot 14.5). The differences were considered statistically significant when $p \leq 0.05$.

3.3 Results and discussion

3.3.1 Theoretical and experimental lipid screening

Using the Hansen solubility approach, theoretical predictions regarding the solubility of curcumin in different solid and liquid lipids, as well as their mixtures were performed. Based on that, materials with similar solubility parameters will be miscible and by extension, actives will have a high affinity for lipids that are characterised by closely matching HSPs, leading to improved dispersion. This approach has been previously employed for the prediction of the

miscibility between actives and different types of solid and liquid lipids [48], in combination with experimental screening in some instances [44,49–51], in order to identify the most suitable lipid-based solvent.

Comparing the intermolecular interactions between curcumin and the lipids under examination, shows that these mainly differ in their polar (δ_P) and hydrogen bonding (δ_H) forces, while the variation between the dispersion (δ_D) interactions was of smaller magnitude (Table 3.1). The smaller difference in the Hansen solubility parameter ($\Delta\delta$) between the active and the individual components of the lipids was observed for glyceryl mono-substituted esters (Table 3.1 & Appendix A1, Fig. A1.1). The presence of hydroxyl groups in the backbone of the glyceryl and polyethylenglycols (PEG) moieties could account for polar and hydrogen bonding interactions of higher strength with the hydroxyl groups of curcumin, explaining the aforementioned affinity. Exceptions to this observation were glyceryl monocitrate and glyceryl monolactate, components of Imwitor® 375, that were characterised by vastly different partial HSPs to those of curcumin, owing to the carboxylic acid and hydroxyl groups, respectively, present in their structure giving rise to significantly higher δ_P and δ_H values. The affinity of curcumin for di- and tri-substituted esters of glyceryl and polyethylenglycols was considerably lower. Similar results for curcumin have been reported previously by Doktorovova *et al*. [44], but also for other actives showing increased affinity for monoglycerides compared to di- and triglycerides [49,50]. Employing the calculated distance (R_a) in the Hansen 3D space, between curcumin and the various lipids, further confirmation about the greater solubilisation capacity of lipids containing higher percentage of monoglycerides (Compritol® 888 ATO, Precirol® ATO 5, Imwitor® 960K) was provided, on the basis that as the distance between them gets smaller, the miscibility increases (Fig. 3.1). Regarding the liquid lipids, Labrafac™ PG and castor oil

displayed the smallest R_a values for either tautomeric form. In their majority, liquid lipids were found to possess smaller R_a values than those of the solid lipids.

Due to the theoretical basis of the Hansen solubility parameter being restricted to liquid phase systems, and thus only providing indication about the solubilisation capacity of the melted state of the lipids, experimental lipid screening was also performed. This revealed that among all lipids, only Dynasan® 118, cetyl palmitate and Imwitor® 960K were not able to solubilise 0.5% w/w of the active (Table 3.1). Compritol® 888 ATO and Precirol® ATO 5 were the solid lipids that exhibited the highest curcumin solubility, approximately 0.6 and 0.7% w/w, respectively, which was in accordance with the theoretical predictions. For the liquid lipids Miglyol® 812 and Labrafil® M 2125 CS, this was close to 1% w/w. Overall, good agreement between theoretical and experimental results was observed, with a certain inconsistency for Imwitor® 960K. The percentage of monoglycerides in the specific lipid was the highest between the solid lipids, and thus it would be expected to show high affinity for curcumin. However, since the precise consistency of the lipids was unspecified and the theoretical predictions were based on average values resulting from different consistency combinations, the HSPs reported here could only be seen as approximations of the true values. Accordingly, data for Imwitor® 375 and Labrafil® M 2125 CS should be viewed in the same way. Another observation made regarding the HSP predictions was that correlation between the calculated R_a and R_0 (8.01 for the diketo and 7.41 for the enol form), suggests that most lipids (except cetyl palmitate) are expected to solubilise curcumin, since their R_a values were smaller than the radius of interaction, as suggested previously in literature [44]. A possible explanation could be given by the fact that the R_0 used here was deduced employing substances that are known to display relatively high curcumin affinity. Including solvents with a wider range of HSPs could have impacted the predictions, and therefore, while HSPs calculated here offer an adequate approach for

comparisons between the lipids, they should not be regarded as an actual measure of solvent solubility.

Finally, the theoretical solubility predictions, that were earlier performed to predict the compatibility of CRM with different lipids, were subsequently also applied to gain further insight into the miscibility between Compritol® 888 ATO and Precirol® ATO 5, and MCTs. The lipid used in the smaller proportion (Miglyol® 812) in the lipid matrix was treated as an "active", and glyceryl behenate and glyceryl palmitostearate as the "solvents" under investigation. Based on their Hansen solubility parameter difference, it was shown that MCTs have theoretically a higher compatibility with glyceryl behenate ($\Delta\delta$ = 0.42) compared to glyceryl palmitostearate ($\Delta\delta$ = 0.71). Kovacevic *et al*. [28] and Araujo *et al*. [22] briefly raised the importance of the lipid chemical nature, and solid-to-liquid lipid compatibility regarding their performance in relation to the location of the liquid fraction within the lipid matrix. The location of the liquid lipid in the crystalline matrix could also dictate the positioning of the hydrophobic active, as a result of the relatively higher affinity of hydrophobic actives for liquid lipids compared to solid lipids, and thus information about the former could provide performance prediction capabilities for the latter.

In view of both theoretical and experimental lipid screening, the solid lipids chosen to progress to the next steps of the investigation were Compritol® 888 ATO and Precirol® ATO 5, while Miglyol® 812 was used as the liquid lipid in further experiments. Among the liquid lipids that were evaluated, Miglyol® 812 showed the highest capacity to solubilise curcumin based on both theoretical and experimental screening data. Mixtures of these lipids, that contain fatty acids of vastly different alkyl chain lengths, could potentially accommodate higher active loading capacities, due to the presence of imperfections in the formed matrices [52]. The curcumin

concentration, for both the physical mixtures and the lipid nanoparticle dispersions preparation, was fixed at 0.5% w/w (mass of active over mass of lipid content), which was within the solubilisation capacity limits for all selected lipids.

Table 3.1. Theoretical and experimental solubility screening of curcumin (CRM) in different solid and liquid lipids.

	Compound name	δ_D	δ_P	δ_H	δ	*R*a (diketo form)	*R*a (enol form)	$\Delta\delta$ (diketo form)	$\Delta\delta$ (enol form)	*S**
	CRM Diketo form	17.17	5.47	12.33	21.83					
	CRM Enol form	16.80	5.54	14.16	22.66					
Solid lipids	Compritol® 888 ATO	16.87	1.75	7.31	18.47	6.27	7.83	3.36	4.19	+
	Precirol® ATO 5	16.89	2.18	7.87	18.76	5.57	7.14	3.07	3.90	+
	Dynasan® 118	16.70	1.53	5.96	17.80	7.54	9.13	7.50	9.13	−
	Cetyl palmitate	16.42	0.89	3.56	16.82	10.00	11.60	5.01	5.84	−
	Imwitor® 960K**	16.96±0.04	2.39±0.16	8.64±1.08	19.20±0.54	4.85±0.92	6.37±1.00	2.63±0.54	3.47±0.54	−
Liquid lipids	Labrafac™ PG	17.04	4.10	7.30	18.99	2.94	3.77	5.15	6.68	+
	Labrafil® M 2125 CS**	16.75±0.13	2.74±0.61	8.13±1.72	18.89±0.90	5.15±1.64	6.68±1.73	2.94±0.90	3.77±0.90	+
	Imwitor® 375**	16.11±6.68	6.42±4.73	13.80±8.24	22.42±11.11	14.34±8.43	14.11±8.52	−0.59±11.11	0.24±11.11	+
	Miglyol® 812	16.65	2.86	6.38	18.06	6.57	8.23	3.77	4.61	+
	Castor oil	16.94	2.23	9.03	19.32	4.65	6.11	2.51	3.34	+

***** *S* represents the solubility of 0.5% w/w curcumin. (+) indicates successful, while (−) indicates unsuccessful solubilisation after 1 h.

****** For lipids that the exact composition was unknown the average values are reported after accounting for all possible combinations, and each calculated value is presented with its respective standard deviation.

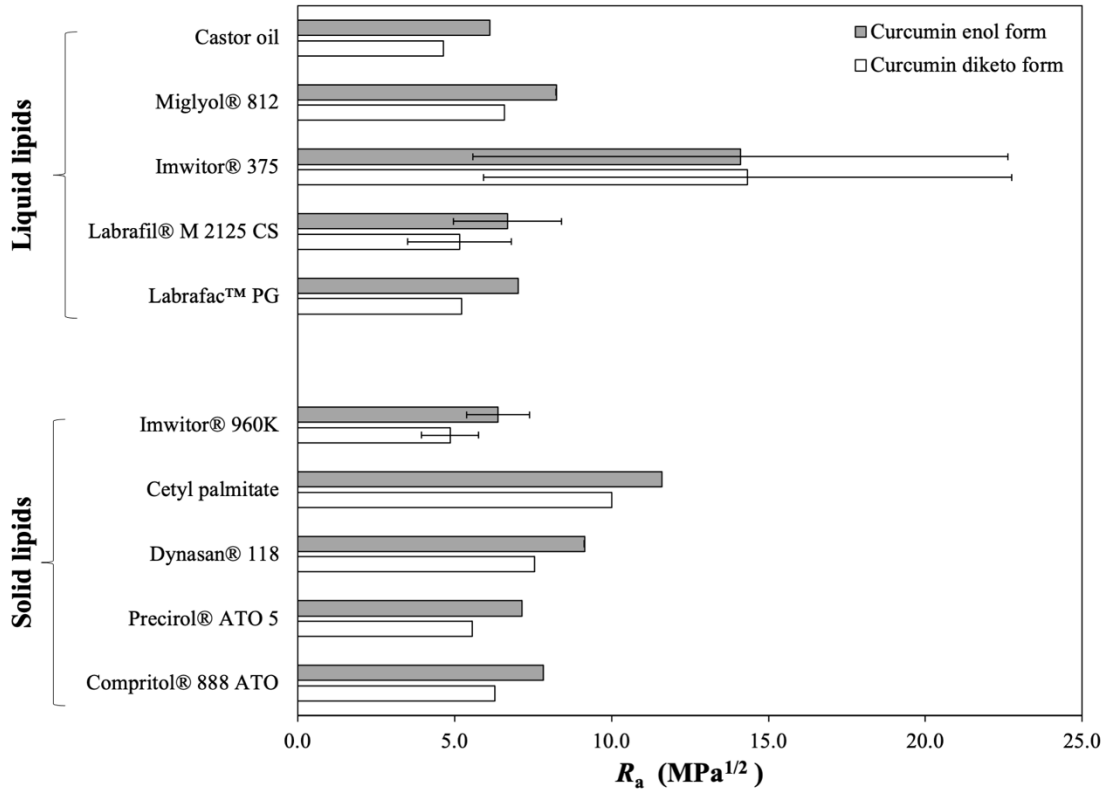

Fig. 3.1. Modified difference (R_a) between the two tautomeric forms of curcumin and various solid and liquid lipids. For lipids that the exact composition was unknown, the average R_a value is reported after accounting for all possible combinations, and the error bars represent the standard deviation.

3.3.2 Thermal analysis of bulk lipids and their mixtures

Initial assessment was performed by visual observation, that indicated good compatibility for both binary and ternary lipid mixtures, as there were no signs of separation or turbidity observed. For the samples containing curcumin, the mixtures appeared homogeneous and transparent while melting, forming limpid blends after solidification without any evidence of sedimented curcumin crystals. The heating thermogram of pure curcumin revealed a single endothermic peak at 180.1°C (see Appendix A1, Fig. A1.2). Absence of crystalline curcumin in the physical lipid mixtures was confirmed by their thermograms, with all identified thermal

events being ascribed to the lipid components (see Appendix A1, Fig. A1.3). DSC analysis provided further information about the thermal behaviour of the mixtures, in regard to changes in their lipid composition or addition of curcumin, and the melting and crystallisation thermograms are presented in Fig. 3.2.

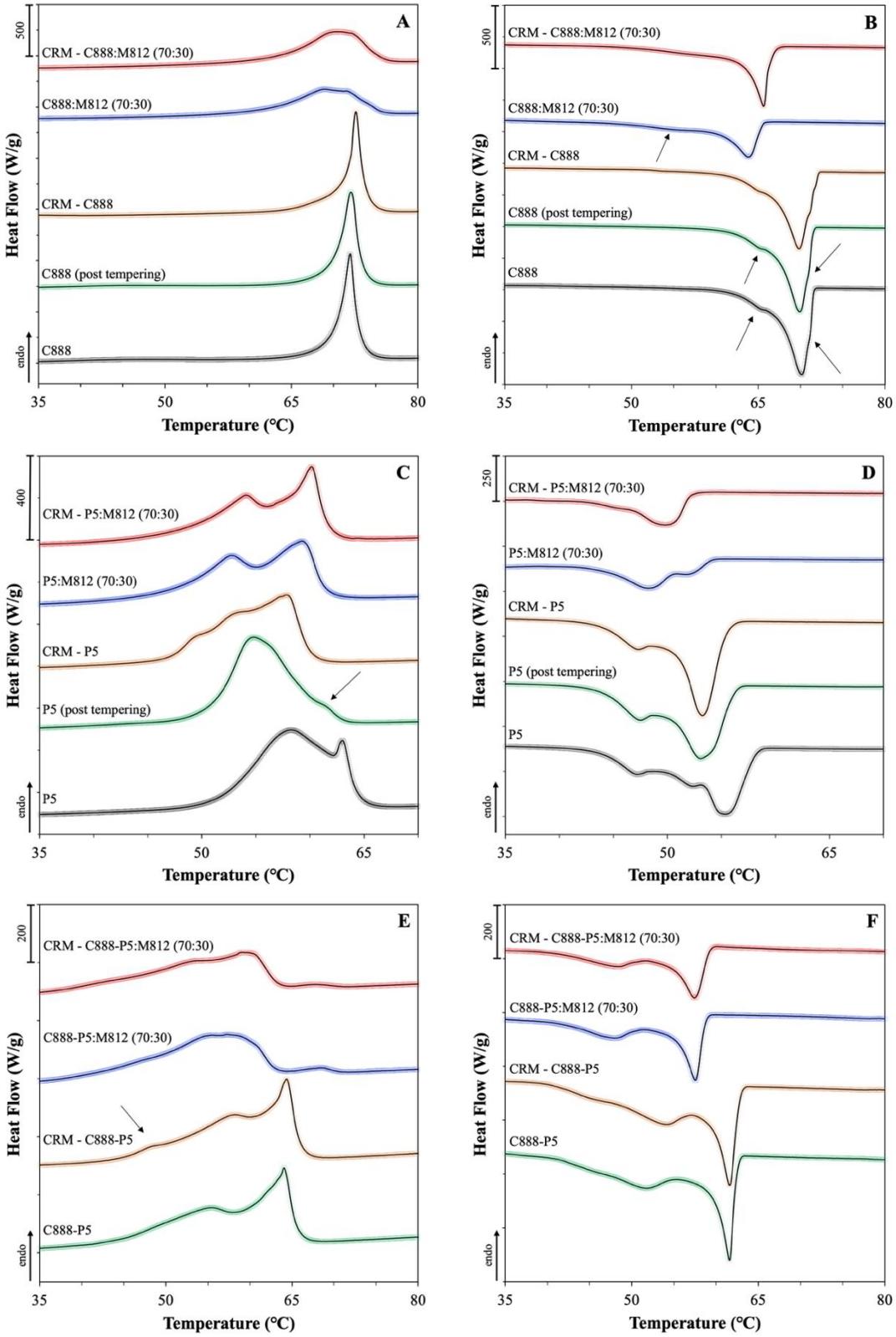

Fig. 3.2. DSC curves of binary and ternary solid and liquid lipid mixtures with or without curcumin (CRM, 0.5% w/w), consisting of Miglyol® 812 (M812) as the liquid lipid in combination with different solid lipids

or blends of them. The melting and crystallisation thermograms presented in pairs are (A) and (B) for Compritol® 888 ATO (C888), (C) and (D) for Precirol® ATO 5 (P5), and (E) and (F) for 50:50 w/w ratio blend of the two. Mixtures containing liquid lipid were prepared by substituting 30% w/w of the solid lipid content with Miglyol® 812. The normalised curves were shifted along the ordinate and presented in sets for better visualisation. Arrows are used to pinpoint certain thermal events.

The heating thermogram of bulk Compritol® 888 ATO shows a single endothermic peak at 71.9°C (Fig. 3.2A), which has been previously assigned to a mixture of metastable polymorphic forms [53]. Glyceryl behenate is a mixture of variable triacylglycerols (TAG), containing glyceryl mono-, di- and tribehenates, for which the transition rate from α to β via β' is known to be dependent on the degree of homogeneity [54]. Pivette *et al.* [55] demonstrated, after studying the polymorphism of the main components, separately and in proportions that correspond to the composition of glyceryl behenate, that this endothermic event can be attributed to α and sub-α or β' forms of mono-, di- and tribehenin. Regarding glyceryl behenate's re-crystallisation behaviour, the bulk and tempered lipids showed a single major exothermic peak at 70.2°C with a shoulder appearing at 71.1°C, both attributed to crystallisation of α forms, and a more pronounced at 66.1°C, relating to either a sub-α sub-cell or a β' transition (Fig. 3.2B) [56]. A level of reversibility of the thermal events occurring during melting can be detected during re-crystallisation. Overall, tempering or addition of curcumin did not cause any changes to the melting or re-crystallisation characteristics of glyceryl behenate. Addition of Miglyol® 812 resulted in broadening and shifting of the main peak for both thermograms, with a second very broad peak at 55°C appearing in the latter, attributed to a sub-α modification of the monoglyceride fraction of behenic acid [47]. The difference between the melting and onset temperature (ΔT) represents the range over which the melting event occurs, and therefore a greater difference can be taken as a measure of disorder of the lipid crystals and generation of

more amorphous structures [53,57], which was a feature recorded for the melting thermogram (see Appendix A1, Table A1.3). However, this observation is contradicted by the melting enthalpy increase. Both thermal events suggest increased crystallinity after the introduction of curcumin in the binary lipid mixture, denoted by the higher enthalpy values and shifting of the exothermic peak to higher temperature, possibly suggesting structural re-arrangement after the addition of curcumin. Similar data of increased enthalpy after active addition to the lipid melt have been reported for binary and ternary mixtures of Precirol® ATO 5 and Transcutol® HP with didanosine [27], and for mixtures of the solid lipid Imwitor® 900 with the poorly water-soluble drug RMZE98 [58]. Nnamani *et al.* [45] demonstrated that at a relatively low addition of the water-soluble drug artemether, same to the percentage used in the current study (0.5% w/w), the melting enthalpy was higher than the respective blank binary mixture of Gelucire® 43/01 and Transcutol® P, at a 70:30 w/w ratio.

The DSC thermograms of bulk glyceryl palmitostearate revealed that melting occurs between 56 and 63°C, with a main endothermic peak at 58.2°C bearing a shoulder at 63°C (Fig. 3.2C), while re-crystallisation showed a broad exothermic peak ranging between 42 and 59°C, with one main signal at 58.2°C and two lower intensity signals at 52.4 and 47.4°C (Fig. 3.2D). Tempering caused distinct changes in both profiles, with peak shifting and melting enthalpy reduction. The melting profile recorded in this study shows similarities with the curves obtained for temperatures in the higher spectrum, as reported by Reitz *et al.* [59], who showed that for glyceryl palmitostearate the obtained profile is tempering temperature-dependent. The main melting peak in the bulk lipid has been attributed to a stable β modification that transforms to a less stable α modification after tempering (peak at 54.8°C), based on wide-angle X-ray scattering (WAXS) measurements [60]. The decrease in the intensity of the peak at 63°C, could imply that this event occurs due to the presence of components in lower percentages (i.e.

triesters). Tempering is a process known to induce changes in the proportion between polymorphs, promoting the formation of the more stable one(s), which could explain the observed temperature and intensity shifting of the peaks [61]. As reported earlier, the presence of MCTs can promote the appearance of signals belonging to α polymorphs, in this case at 52.8°C in the melting and at 48.6°C in the cooling thermograms, the intensity of which can vary depending on the type and percentage of liquid lipid used [27,62]. In contrast to glyceryl behenate, CRM addition led to changes in the melting profile and enthalpy only for the single lipid mixture with glyceryl palmitostearate, while the melting and crystallisation characteristics of binary lipid mixture remained unaffected.

In the melting profile of the glyceryl palmitostearate and glyceryl behenate mixture (Fig. 3.2E), the discrete characteristic glyceride endothermic events can be clearly recognised at 55.5 and 64.0°C, respectively. A small suppression in the glyceryl behenate melting temperature was observed, compared to the thermogram of the singly tempered lipid, possibly caused by the presence of glyceryl palmitostearate. The profile obtained here is somewhat intermediate to the profiles reported by Hamdani *et al*. [63] that investigated 40:60 and 60:40 w/w ratios of the same solid lipids. Addition of MCTs caused a shift of the melting and crystallisation events to lower temperatures and a ΔT increase (see Appendix A1, Table A1.5). Even though a level of compatibility between the two solid lipids, due to inter-solubility of their monoacid triglyceride components [64], could be responsible for the identified melting temperature decrease, complete separation of the melting peaks when MCTs was added, indicates that potentially the lipids also co-exist as somewhat separate entities within the blend.

The curcumin-loaded binary and ternary lipid mixtures were almost identical to the blank samples, with the exception of the emergence of a small shoulder at 48.8°C at the binary

mixture; also identified in the curcumin-loaded glyceryl palmitostearate mixture (Fig. 3.2E). Reversibility of the endothermic events was detected in the re-crystallisation curves for all combinations (Fig. 3.2F). In all cases, the occurrence of distinct re-crystallisation of the two solid lipids is in support of the observations (based on the melting curves) that they co-exist in the blend, while the presence of a miscible blend could only be supported by lowering of the re-crystallisation temperature compared to their individual exothermic events [49].

Based on the data acquired from the DSC analysis, the thermal properties of both solid lipids seem to be influenced by the presence of additional components, as reflected by the altered thermal profiles and melting enthalpies. A certain discrepancy to the melting enthalpy trend after the addition of liquid lipid or active between the two solid lipids is recorded. In the literature, melting enthalpy reduction has been widely presented in support of incorporation of either the liquid lipid or active within the lipid matrix, and creation of defects in the crystalline structure [5,49], although it is not always clear whether the reported enthalpy reflects changes to the behaviour of the lipid phase in its entirety, or the crystallising material specifically. For the lipids examined in this study, a common occurrence in all combinations was the increased melting enthalpy values when the liquid lipid was added, as opposed to the active addition, that demonstrated a behaviour reliant on the relative solid-to-liquid lipid combination. The presence of liquid lipid can prompt acceleration of polymorphic transitions to more stable transformations in a concentration-dependent manner [65], that has also been described for dispersed active in the liquid state [23]. Therefore, it could be proposed that the observed thermal profile and enthalpy changes were the result of solubility between the solid and liquid lipids, rather than mixed crystal formation, as has been previously reported for tripalmitin or tristearin binary mixtures with triolein [66].

3.3.3 Characterisation of blank and curcumin-loaded SLNs and NLCs

3.3.3.1 Particle size, polydispersity and zeta potential

Part of the preliminary lipid dispersion preparation studies was focused on the reduction of the particle size to ensure that the developed systems would be within the desirable size range (sub-micron particles) to act as Pickering emulsion stabilisers [14,67]. Parameters associated with the processing stage were initially evaluated. More specifically, the duration of the homogenisation step, in this case sonication, was assessed for Precirol® ATO 5 and Compritol® 888 ATO SLNs (5% w/w total lipid content) and using 1.2% w/w PVA as the surfactant. For both lipids, it is quite evident that as the sonication time increases from 1 to 5 minutes (95% amplitude), the average particle size decreases (Fig. 3.3A), which could be explained by the fact that at longer sonication duration greater energy input can be conveyed to the pre-emulsion leading to more efficient droplet breakage, as it has been previously reported [68,69]. In a next step, formulation parameters were investigated; using both types of solid lipids and at the same lipid concentration, SLNs were fabricated with four types of surfactants at 1.2% w/w (Fig. 3.3B), with Tween® 80 and Pluronic® F-68 generating the smallest particle sizes for both lipids. Subsequently, the lipid concentration was decreased to 2.5% w/w that resulted in a significant particle size reduction (Fig. 3.3C), potentially due to a decrease in the droplet/particle collision events taking place at this lower lipid content and higher surfactant-to-lipid ratio [47]. Lastly, evaluating the effect of the concentration of Tween® 80 using 0.6, 1.2, 1.8 and 2.5% w/w, revealed that increasing the concentration from 0.6 to 1.2% w/w caused a significant decrease in the obtained particle size (Fig. 3.3D). However, further increase in surfactant content had a much smaller effect on the final average particle size, a phenomenon which has been previously described elsewhere [70]. The surface active agents have a dual role in the fabrication of lipid

particles; provide sufficient interfacial coverage/stabilisation to the droplets during the melt-emulsification stage, while hindering inter-droplet association during the cooling step (crystallisation). The presence of a higher number of surface active molecules in the system can lead to acceleration of interfacial coverage and smaller droplet sizes during the emulsification/droplet breakage step. Although, this event can be counterbalanced by the increased frequency of collisions occurring between droplets of smaller sizes, thus reaching a size reduction plateau at certain surfactant concentration. Hence, the sonication time used was fixed at 5 minutes, the lipid concentration was set at 2.5% w/w, and Tween® 80 and Pluronic® F-68 at 1.2% w/w were the chosen surfactants and concentration for subsequent experiments. Using these optimised formulation/processing parameters, aqueous dispersions of both SLNs and NLCs were prepared according to the compositions presented in Table 3.2. Concerning the formulation characteristics, the type of solid lipid, the concentration of the liquid lipid and the type and concentration of the employed surface active species were all explored, in terms of their effect on the size of the formed SLN and NLC particles.

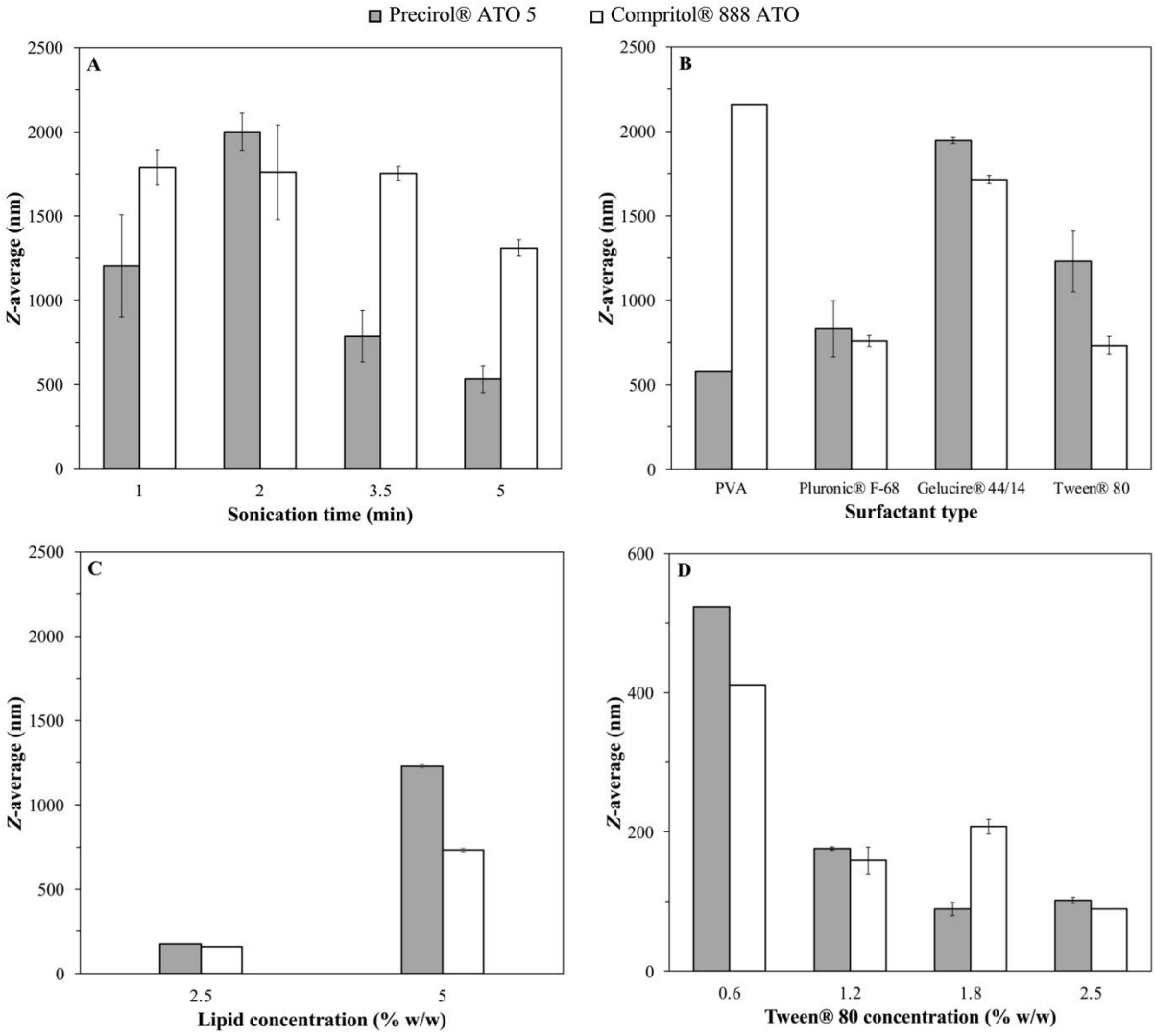

Fig. 3.3. Particle size of SLNs (*Z*-average) prepared with either Precirol® ATO 5 or Compritol® 888 ATO, when different processing and formulation parameters were used; (A) sonication time, (B) type of surfactant, (C) lipid concentration (% w/w) and (D) concentration of Tween® 80 (% w/w).

Table 3.2. Composition of SLN and NLC formulations prepared with Precirol® ATO5, Compritol® 888 ATO or 1:1 w/w ratio of the two as solid lipid matrix, Miglyol® 812 as the liquid lipid at various concentrations (10, 20 and 30% w/w of the lipid phase), and Tween® 80 or Pluronic® F-68 as surfactants, either blank or loaded with curcumin.

Formulation	Compound concentration (% w/w)						
	Compritol® 888 ATO	Precirol® ATO 5	Miglyol® 812	Tween® 80	Pluronic® F-68	Curcumin	Water
B-SLN$_1$	2.5	-	-	1.2	-	-	96.3
B-NLC$_1$	2.25	-	0.25	1.2	-	-	96.3
B-NLC$_2$	2.0	-	0.5	1.2	-	-	96.3
B-NLC$_3$	1.75	-	0.75	1.2	-	-	96.3
SLN$_1$	2.4875	-	-	1.2	-	0.0125	96.3
NLC$_1$	2.2388	-	0.2487	1.2	-	0.0125	96.3
NLC$_2$	1.99	-	0.4975	1.2	-	0.0125	96.3
NLC$_3$	1.7413	-	0.7462	1.2	-	0.0125	96.3
SLN$_2$	-	2.4875	-	1.2	-	0.0125	96.3
NLC$_4$	-	1.7413	0.7462	1.2	-	0.0125	96.3
SLN$_3$	1.2438	1.2437	-	1.2	-	0.0125	96.3
NLC$_5$	0.8707	0.8707	0.7461	1.2	-	0.0125	96.3
SLN$_4$	2.4875	-	-	0.5	-	0.0125	97
SLN$_5$	2.4875	-	-	-	1.2	0.0125	96.3

Initially, lipid particle dispersions were prepared with Compritol® 888 ATO in the absence of curcumin by progressively replacing 10, 20 and 30% w/w of the solid lipid mass with Miglyol® 812 (formulations B-SLN$_1$ and B-NLC$_1$–B-NLC$_3$). All formulations displayed monomodal size distributions, with sizes ranging between 140 and 160 nm. It was observed that addition of the liquid lipid did not result in particle size or distribution profile changes for 10% w/w, and it was only at 20% w/w that a statistically significant (p<0.05) decrease was recorded (Fig. 3.4A & Table 3.3). At 30% w/w liquid lipid, a plateau in terms of size was reached, with no further

particle size variations. Correspondingly, the PDI showed a distinctive trend of decreasing values for NLCs of increasing liquid lipid content. Incremental incorporation of MCTs (up to 20% w/w) causing changes in the viscosity of the glyceryl behenate melt droplets could be responsible for the gradual decrease in the particle size and PDI of the lipid particles obtained after crystallisation. Gokce *et al.* [71] reported that the incorporation of different percentages of MCTs in the solid matrix of glyceryl behenate overall resulted in reduced particle sizes of the NLCs compared to the respective SLNs, which was attributed to more effective homogenisation and improved energy transfer due to the liquid lipid presence. Similarly, in another study, Hu *et al.* [20] reported that incorporation of 30% w/w of the liquid lipid oleic acid in stearic acid reduced both the viscosity and surface tension in the lipid melt droplets, thus ultimately resulting in the formation of smaller NLC particles (164.6 nm compared to the 379.7 nm in the formulation without any oleic acid). Incorporation of curcumin to the blank lipid dispersions led to a slight increase in the particle sizes for all systems (SLN_1 and NLC_1–NLC_3), which amongst them however displayed almost identical sizes, irrespective of the solid-to-liquid lipid mass ratio. Comparison between the blank and curcumin-loaded dispersions, showed a significant size increase only for the 20 and 30% w/w NLC formulations (NLC_2, NLC_3). This behaviour has been reported previously, when the average sizes of blank and active-loaded SLNs and NLCs were compared and was attributed to a combination of swelling of the lipid core due to active encapsulation and increase of the interfacial tension and/or viscosity of the dispersed phase causing inefficient particle size reduction [20,72,73]. Both the size distribution profiles (Fig. 3.4B) and PDI values for the CRM-loaded SLNs/NLCs systems remained unaffected.

The size characteristics of the particles produced using Precirol® ATO 5 as the solid lipid were also evaluated. Glyceryl palmitostearate SLNs (SLN_2) displayed a slightly broader size

distribution (higher PDI value) and larger particle sizes in comparison to SLNs composed of glyceryl behenate (SLN_1). These findings, possibly outline the impact of the processing parameters, and more specifically the duration of the sonication step. The statistically significant increase to the *Z*-average due to the presence of an additional small peak identified at 5.5 μm in SLN_2 could have been caused by excess energy transfer to the system inducing extreme acoustic cavitation and temperature rise (starting at 70°C prior to sonication to 94°C after sonication), resulting in enhanced pre-emulsion droplet breakage and coalescence (Fig. 4.4C) [74,75]. By contrast, comparing formulations NLC_3 and NLC_4 (NLCs fabricated with glyceryl behenate and glyceryl palmitostearate, respectively), reveals that the latter were characterised by smaller *Z*-average values. The overall lower viscosity of the Precirol® ATO 5/Miglyol® 812 blend to the equivalent Compritol® 888 ATO NLCs could explain the lower particle sizes. The combination of the characteristics of the two solid lipids can be accounted for the somewhat intermediate behaviour that was observed for both the SLN and NLC formulations fabricated with 1:1 mass ratio mixture of the two (SLN_3–NLC_5).

In regard to the particles formed with different surfactant parameters, Compritol® 888 ATO SLNs were produced using 1.2% and 0.5% w/w Tween® 80 (SLN_1 and SLN_4, respectively), and 1.2% w/w Pluronic® F-68 (SLN_5) (Fig. 4.4D). Particles prepared with reduced surface active species concentration (SLN_4) (to study the relation between surfactant concentration/particle size with curcumin loading in a next step), showed bimodal size distribution profile, with higher *Z*-average and PDI compared to the respective formulation of higher surfactant concentration (SLN_1). The lack of sufficient number of surface active species to fully cover and stabilise the pre-emulsion droplets creates a system that is more prone to coalescence, particularly under relatively high sonication durations (5 min), when the chances of droplet collisions are increased due to the combination of high energy input and long period

of interaction. In contrast, Pluronic® F-68 (Poloxamer 188) appeared to drive the SLN size reduction a bit further than Tween® 80 (SLN_1), implying better coalescence hindrance, leading to smaller lipid particles after crystallisation. The effect of the characteristics and concentration of surfactant on the resultant particle size has been previously highlighted in a study by Zafeiri *et al.* [14].

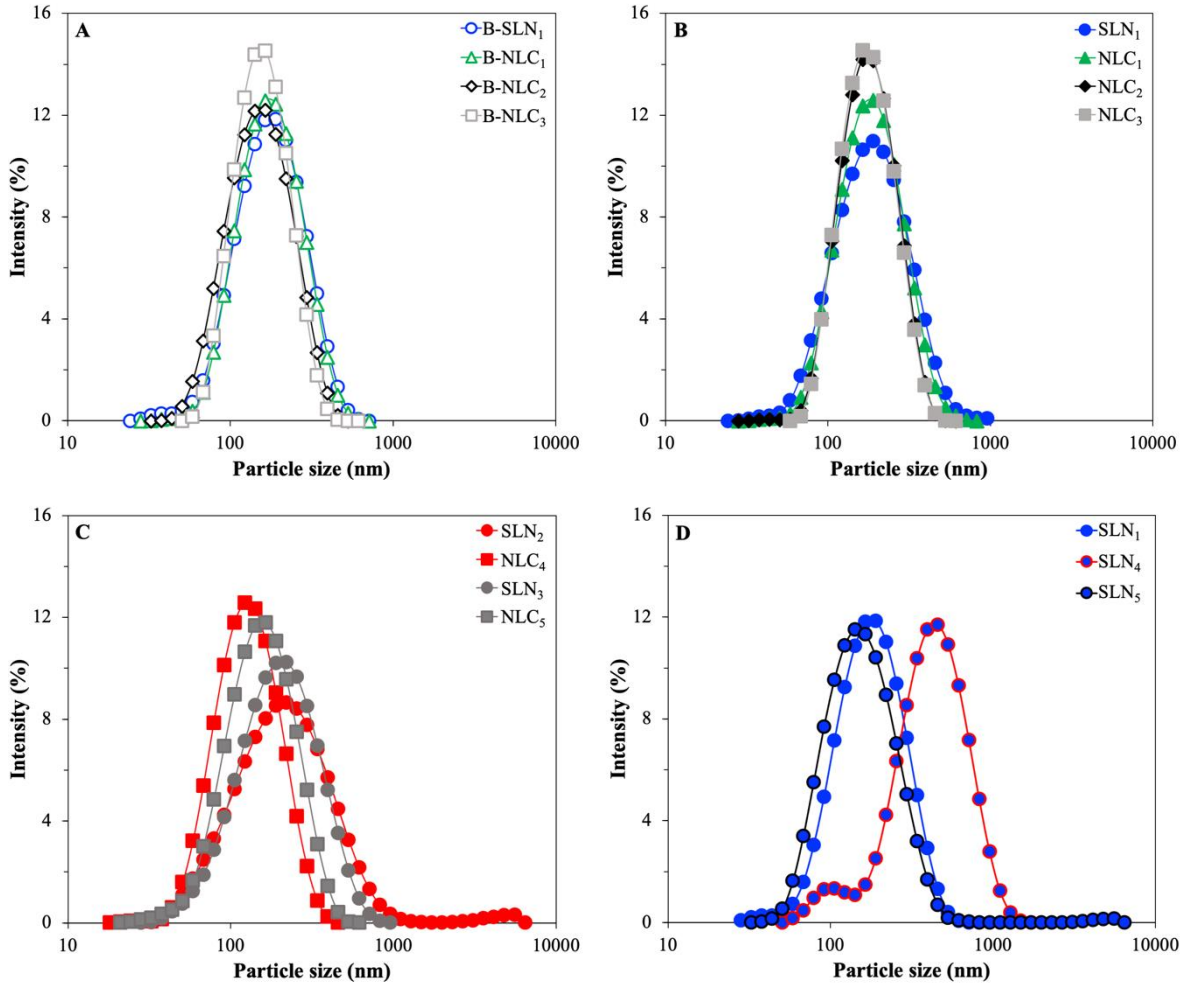

Fig. 3.4. Dynamic light scattering measurements showing the particle size distribution of SLN and NLC formulations after preparation. (A) Formulations B-SLN_1 and B-NLC_1–B-NLC_3, (B) SLN_1 and NLC_1–NLC_3, (C) SLN_2–SLN_3 and NLC_4–NLC_5, and (D) SLN_1 and SLN_4–SLN_5.

In terms of the zeta potential values acquired, all glyceryl behenate-containing lipid dispersions were characterised by values ranging between 19 and 25 mV (Table 3.3), without any major changes identified after the addition of curcumin. A slight decrease with increasing liquid lipid concentration for both blank and curcumin-loaded lipid dispersions, but also for all types of solid lipid compositions can be seen, suggesting a reduction to the particles' surface potential and further indicating changes at the surface of the NLCs; such as potential shifts in the shear plane [76–79]. SLNs prepared with Tween® 80 did not differ significantly from lipid dispersions fabricated with Poloxamer 188 in their zeta potential values (formulations SLN_1 and SLN_5, respectively), while the formulation with lower concentration of the former (Tween® 80) yielded particles with higher ζ-potential (SLN_4). The negative charge in all formulations is attributed to the presence of free fatty acids at the surface of the particles, as both types of surfactants are non-ionic, and hence their interfacial presence does not contribute to the surface charge [76].

Table 3.3. *Z*-average, polydispersity index (PDI) and zeta potential (ζ-potential) of different SLN and NLC formulations measured after preparation. Identical lowercase letters indicate no significant differences between samples (for p>0.05 and sample size equal to 3).

Formulation	*Z*-average (nm)	PDI	ζ-potential (mV)
B-SLN_1	158.9±10.6[a]	0.20±0.02[a]	−23.0±1.3[a]
B-NLC_1	160.5±3.8[a]	0.16±0.02[a]	−22.3±1.9[a]
B-NLC_2	140.4±20.1[b]	0.15±0.02[a]	−19.5±2.6[a]
B-NLC_3	145.8±3.4[b]	0.12±0.02[a]	−20.1±0.7[a]
SLN_1	165.1±2.7[a]	0.20±0.02[a]	−25.2±2.6[a]
NLC_1	165.4±5.3[a]	0.16±0.02[a]	−25.0±3.0[a]
NLC_2	162.5±6.5[a]	0.13±0.01[a]	−21.7±1.3[a]
NLC_3	163.2±3.8[a]	0.12±0.01[a]	−20.5±0.7[a]
SLN_2	176.0±9.6[c]	0.28±0.04[b]	−32.7±0.9[b]

NLC_4	114.4±7.1[d]	0.14±0.04[a]	−26.0±2.7[a]
SLN_3	170.9±15.2[c]	0.23±0.01[a]	−27.6±1.4[a]
NLC_5	136.2±2.5[b]	0.19±0.01[a]	−24.4±1.9[a]
SLN_4	343.9±26.5[e]	0.24±0.03[b]	−29.0±2.8[b]
SLN_5	139.7±1.9[b]	0.20±0.01[a]	−24.4±0.7[a]

3.3.3.2 Thermal analysis of aqueous lipid dispersions

DSC analysis was used to gain a better insight on the effect of the specific particle characteristics and varying formulation parameters on the thermal properties and crystallinity of the produced SLNs and NLCs (shown in Table 3.2). These are important factors when it comes to predicting the long-term physical stability of the lipid nanoparticles, but also their ability to maintain physical integrity both in terms of active expulsion phenomena and liquid lipid expulsion/separation (in the case of NLCs) [47,76]. The melting and crystallisation thermograms are presented in Fig. 3.5 and 3.6, respectively.

Comparison between the lipid nanoparticles prepared with glyceryl behenate and combination with MCTs at 70:30 w/w ratio (systems B-SLN_1 and B-NLC_3), and their respective physical mixtures reveals peak broadening and shifting towards lower temperatures (Fig. 3.5A & B). According to the Gibbs-Thompson effect, sub-micron sized solid lipid particles can reach thermodynamic equilibrium at lower temperatures compared to the larger crystals in their lipid physical mixtures [33,76,80]. In addition, polymorphic transitions and crystallisation process modulation can be further prompted by the adsorption of surfactant molecules on the lipid particle surface, explaining changes in the melting and crystallisation profiles [81]. A level of polymorphism can be identified in the SLN formulation, due to the presence of a split (at 68.9°C) on the main peak (70.7°C), that has also been shown in the data reported by Jenning *et al.* [33] and Freitas *et al.* [47], albeit the split appeared at higher temperatures (approximately

at 75 and 73°C, respectively). This discrepancy could be attributed to the varying surfactant to lipid ratio, with the proportion used in this study being higher (approximately 1:2) than the almost 1:8 used in the aforementioned studies, or differences in the fabrication/analysis conditions. As discussed earlier, Compritol® ATO 888 is a composite mixture of behenic acid esters, which could account for the complex polymorphic behaviour of the resulting lipid particle dispersions, particularly so in the presence of MCTs. In the work by Jenning *et al.* [33], both SLNs and NLCs with various solid-to-liquid lipid mass ratios exhibited the metastable β', while increasing amount of intermediate β_i polymorphs were also identified in the NLCs with increasing MCTs concentration, as suggested by wide-angle X-ray scattering (WAXS) measurements. Pronounced polymorphic transitions in the presence of MCTs were additionally suggested by the recrystallisation thermograms of the SLNs displaying a main thermal event bearing a shoulder peak at a lower temperature, that became progressively more intense with increasing liquid lipid concentration, ultimately being the main peak for the B-NLC_3 and NLC_3 formulations (Fig. 3.6A & B). Addition of the active in formulations B-SLN_1 and B-NLC_1–B-NLC_3 appears to have somewhat altered the polymorph ratios, as implied by the differences in the relative peak intensities in both the melting and re-crystallisation thermograms (Fig. 3.5B & 3.6B).

Variations in the thermal event characteristics could provide further information regarding the impact imposed by the oil (liquid lipid) and/or active incorporation to glyceryl behenate, which is the only component undergoing phase transition within the particle structure. As the liquid lipid concentration increases in both blank and curcumin-loaded lipid particles, the melting and onset temperatures display a negative slope, with the width of melting significantly increasing from the SLNs to the NLCs with 20% w/w liquid lipid (Table 3.4 & Fig. 3.7A). Accordingly, looking at the melting enthalpy trend, gradual increase of MCTs in formulations B-NLC_1–B-

NLC_3 shows that at 20% w/w mass and beyond, there was a pronounced reduction in the melting enthalpy of the crystalline matter compared to formulation B-SLN_1 (Table 3.4 & Fig. 3.7B). Lipid phase crystallinity loss was suggested by the recrystallisation indices (RI), which showed a linear decreasing trend with increasing MCTs concentration. RI values of over 100% could be attributed to the presence of a more stable polymorph in the lipid particles compared to the bulk lipid, in this case the β_i form distinguishable in all formulations (peaks indicated by arrows in Fig. 3.5A & B); a transformation that has been previously described for glyceryl behenate particles kept in storage [82]. A distinction between the information extracted from these two parameters needs to be made at this point; RI value comparison reflects changes to the lipid phase, as the total mass of the lipid phase used for calculations is not accounting for solid lipid mass reductions in NLCs, while enthalpy data signify variations in the crystallising matter behaviour. Bunjes *et al.* [83] attributed the melting point depression of glyceryl behenate/medium chain triglycerides nanoparticles on eutectic behaviour, although a slight solubility between the components was not excluded. Combining the ΔH and RI trends with the findings from the physical mixtures indicating partial solubility between the two lipids, a liquid lipid incorporation in the lattice created by the solid lipid, leading to a less ordered internal crystalline structure could be proposed. However, the pattern of non-linear relationship between the interval increases of MCTs and the thermal properties does not allow excluding the occurrence of oil phase separation within the lipid particles at higher liquid lipid concentrations. This is in accordance with previously reported data in literature indicating a liquid lipid concentration-dependent formation of distinct lipid structures [24,33]. An equivalent behaviour of the melting enthalpy was not however observed with the formulations containing curcumin (SLN_1 and NLC_1–NLC_3), for which no statistically significant deviations were recorded. Comparison of the ΔH and RI values between blank and CRM-loaded

formulations demonstrated, that systems NLC_2 and NLC_3 were characterised by a statistically significant crystallinity increase. These observations for both blank and CRM-loaded formulations are consistent with the particle size trends reported earlier (Section 3.3.3.1). Incorporation of curcumin in the particles conveys an effect on their thermal behaviour that appears to be reliant on the relative solid-to-liquid lipid ratio, and possibly on the extent to which the liquid lipid addition affects the physical properties of the crystalline lipid matrix, as demonstrated by both melting and crystallisation temperature, and enthalpy characteristics.

Following the investigations using glyceryl behenate, curcumin-loaded SLNs and NLCs with 30% w/w liquid lipid content were fabricated with glyceryl palmitostearate. As expected, Precirol® ATO 5 SLNs (SLN_2) and NLCs (NLC_4) demonstrated lower melting and crystallisation maxima as opposed to the respective CRM-containing physical mixtures (Fig. 3.5C & 3.6C). Incorporation of MCTs in the pre-emulsion blend (NLC_4) enhanced the polymorphism and led to reduction of the ΔH and melting temperature, and increase in the RI and ΔT values. Possible explanations could lie on the creation of a less crystalline with structural defects lipid matrix after incorporation of the liquid lipid, statistically significant particle size reduction compared to the SLNs, or combination of the two. The relative behaviour between formulations SLN_2 and NLC_4 is similar to the corresponding glyceryl behenate formulations (SLN_1 and NLC_3), albeit the decrease of the melting width of the former was lower comparatively. This is likely underlining the impact of the surfactant on the overall thermal behaviour of the particles, which appears to have been greater in the case of the glyceryl behenate formulations compared to glyceryl palmitostearate. Indeed, Fang *et al.* [78] did not detect any melting point shifts caused by the addition of Tween® 80 in the physical mixtures of glyceryl palmitostearate and squalene. The effect of the type and chemistry of the surfactant not only on the resulting particles size, but also on the interactions developed with the

crystalline matrix depending on its composition has been previously shown to be important parameters governing the particles' crystalline properties [14].

The co-existence of the individual solid lipids within a partially miscible blend of them, which was hypothesised based on the DSC data of their physical mixtures, cannot be ruled out also for their SLNs (SLN_3) and NLCs (NLC_5), based on the somewhat intermediate melting behaviour of their single SLN dispersions, and the peak separation observed in the melting and re-crystallisation profile, respectively (Fig. 3.5C & 3.6C). The high RI of formulation SLN_3 (104.0%), which is comparable to that of SLN_1, suggests the presence of high ratio of β_i forms attributed to glyceryl behenate, whereas the intermediate RI of NLC_5 to both NLCs composed of the individual components (NLC_3 and NLC_4) could be the result of the combined accelerated polymorphic transitions of both solid lipids due to the liquid lipid addition. Regarding the thermal profiles of the SLNs with lower surfactant concentration (SLN_4), melting and crystallisation events of reduced 'complexity' can be observed, that could be due to the different packing of the surfactant at the particles' interface as a function of its concentration, compared to formulation SLN_1 [70]. On the contrary, the crystallisation profile for the Poloxamer 188 particles appears to be more complex, but in line with data reported in literature [84] for the same combination of solid lipid and surfactant (Fig. 6D). In the melting profile of SLN_5 (Fig. 5D), the single endothermic peak at 71.0°C that could be attributed to a stable β_i polymorphic form and the higher RI value compared to formulation SLN_1 indicate the existence of a more highly ordered internal lattice. Thus, higher compatibility between glyceryl behenate and Tween® 80 can be postulated, as that would allow part of the surfactant's structure to participate in the crystalline network close to the surface region of the particles, and in a higher degree than Poloxamer 188 molecules, leading to decreased packing of the crystalline structure and transition to less stable polymorphs (β'), observed for Tween® 80 particles.

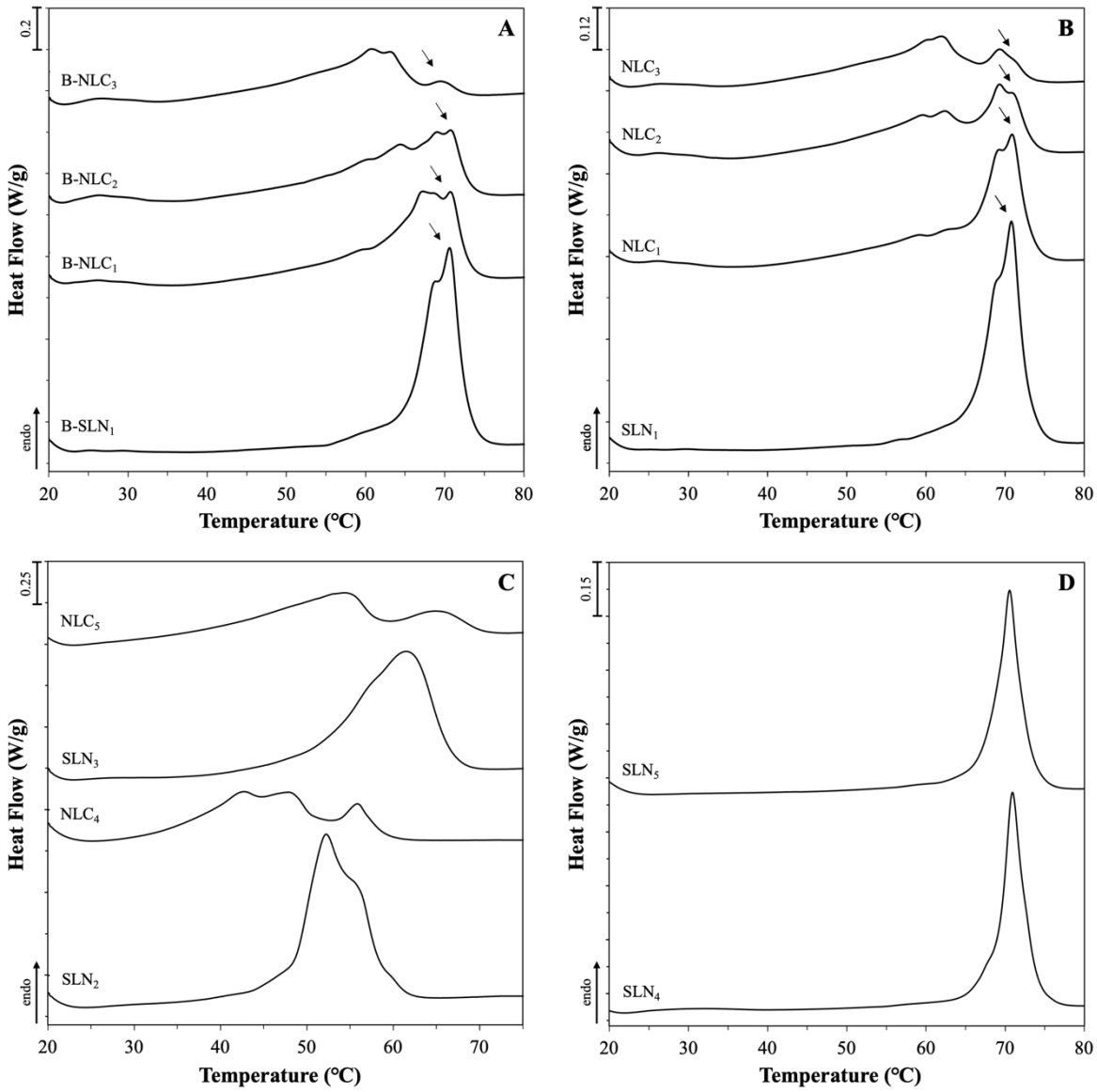

Fig. 3.5. DSC melting curves of SLN and NLC aqueous dispersions consisting of Miglyol® 812 as the liquid lipid in combination with different solid lipids or blends of them. Graphs (A), (B) and (D) show the melting behaviour of formulations prepared with Compritol® 888 ATO without curcumin, with 0.0125% w/w curcumin and with varying type or concentration of surfactants, respectively. Graph (C) displays the melting curves of formulations fabricated with either Precirol® ATO 5 or blend of the two solid lipids at 50:50 w/w ratio. The exact composition of the formulations can be found in Table 3.2. The normalised curves were shifted along the ordinate and presented in sets for better visualisation. Arrows are used to pinpoint certain thermal events.

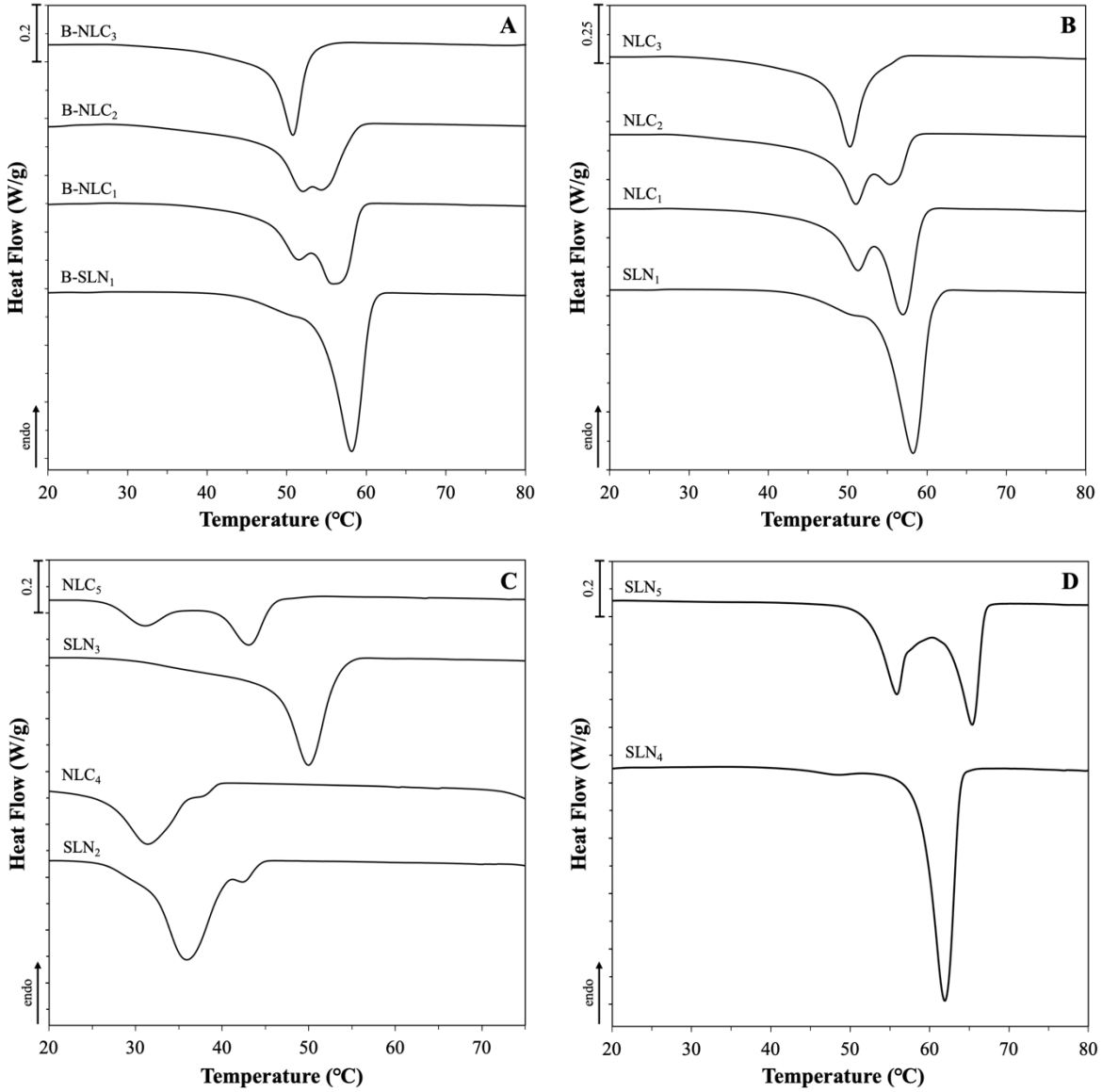

Fig. 3.6. DSC crystallisation curves of SLN and NLC aqueous dispersions consisting of Miglyol® 812 as the liquid lipid in combination with different solid lipids or blends of them. Graphs (A), (B) and (D) show the melting behaviour of formulations prepared with Compritol® 888 ATO without curcumin, with 0.0125% w/w curcumin and with varying type or concentration of surfactants, respectively. Graph (C) displays the crystallisation curves of formulations fabricated with either Precirol® ATO 5 or blend of the two solid lipids at 50:50 w/w ratio. The exact composition of the formulations can be found in Table 3.2. The normalised curves were shifted along the ordinate and presented in sets for better visualisation.

Table 3.4. DSC melting and crystallisation parameters of SLN and NLC aqueous dispersions. Enthalpy values (Δ*H*) reflect the total enthalpy measured after integration of all thermal events present. The maximum melting and crystallisation (T_{max}) and onset (T_{onset}) temperatures are given for the individual occurring thermal events, as well as the width between the two (Δ*T*) and the recrystallisation index (RI) for each formulation.

		Δ*H* (J/g)	T_{max} (°C)	T_{onset} (°C)	Δ*T* (°C)	RI (%)
B-SLN$_1$	**Melting**	140.1±3.2	70.7±0.2	65.6±0.2	5.1±0.4	106.8±3.2
	Crystallisation	−149.4±2.2	58.2±0.3	60.6±0.3	−2.4±0.2	
B-NLC$_1$	**Melting**	141.3±14.4	68.9±2.7	62.4±1.5	6.5±1.3	97.0±9.9
	Crystallisation	−120.6±25.7	55.9±1.0	59.1±0.8	−3.2±0.2	
B-NLC$_2$	**Melting**	115.1±2.9	64.0±0.3	50.9±1.8	13.1±1.1	79.0±2.0
	Crystallisation	−114.8±2.6	51.5±0.1	56.9±1.8	−5.4±1.7	
B-NLC$_3$	**Melting**	98.6±3.4	60.7±0.1	44.7±0.3	16.0±0.3	67.7±2.3
	Crystallisation	−97.0±3.3	50.8±0.1	53.2±0.6	−2.4±0.7	
SLN$_1$	**Melting**	146.8±2.2	70.8±0.1	65.4±0.8	5.4±0.8	101.9±1.8
	Crystallisation	−148.8±1.6	58.3±0.1	60.7±0.2	−2.4±0.1	
NLC$_1$	**Melting**	147.7±3.5	70.8±0.1	62.4±0.3	8.3±0.3	101.4±2.4
	Crystallisation	−146.7±4.2	57.0±0.2	59.4±0.1	−2.5±0.2	
NLC$_2$	**Melting**	148.7±11.3	69.3±0.1	47.4±0.5	21.9±0.5	90.6±6.7
	Crystallisation	−138.3±4.8	51.1±0.1	58.2±0.1	−7.1±0.1	
NLC$_3$	**Melting**	139.1±7.1	61.9±0.1	46.5±0.2	15.5±0.2	74.2±3.8
	Crystallisation	−130.6±5.5	50.3±0.2	53.4±0.2	−3.1±0.3	
SLN$_2$	**Melting**	157.4±5.2	52.3±0.1	47.7±0.1	4.5±0.1	89.1±2.9
	Crystallisation	−138.6±3.5	36.0±0.3	41.8±1.1	−5.9±1.2	
NLC$_4$	**Melting**	144.6±8.8	46.3±3.4	35.2±0.3	11.1±3.2	57.3±3.5
	Crystallisation	−121.0±3.6	31.4±0.3	36.4±0.1	−5.0±0.4	
SLN$_3$	**Melting**	162.3±21.0	61.5±0.6	49.5±1.3	11.9±1.0	104.0±9.7
	Crystallisation	−140.1±22.3	48.9±0.5	53.2±0.2	−3.4±0.2	
NLC$_5$	**Melting**	142.2±6.6	53.7±0.7	36.0±0.6	17.7±0.2	64.7±3.0
	Crystallisation	−114.5±2.4	43.1±0.2	46.0±0.3	−2.8±0.5	
SLN$_4$	**Melting**	152.2±3.9	71.3±0.1	69.0±0.3	2.3±0.3	115.3±3.0
	Crystallisation	−154.2±6.2	61.9±0.1	63.9±0.1	−2.0±0.1	

SLN_5	**Melting**	156.0±7.2	71.0±0.0	68.6±0.1	2.4±0.1	116.9±5.5
	Crystallisation	−156.6±7.9	65.4±0.1	66.9±0.1	−1.5±0.0	

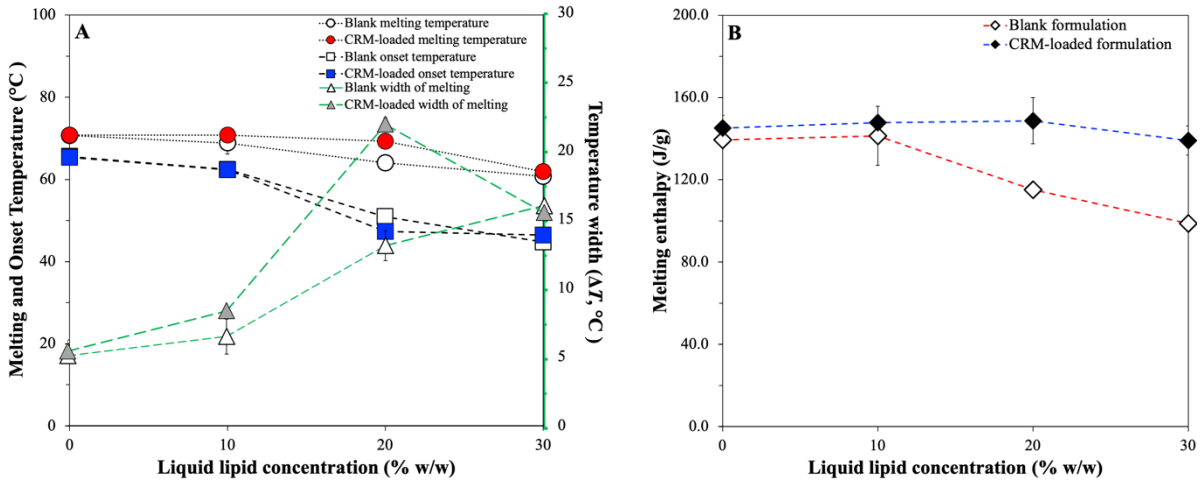

Fig. 3.7. (A) Melting and onset temperature, and width between these two temperatures trends, and (B) melting enthalpy trends at increasing liquid lipid concentration from 0% to 30% w/w for blank (B-SLN_1 and B-NLC_1–B-NLC_3) and CRM-loaded formulations (SLN_1 and NLC_1–NLC_3).

3.3.3.3 Encapsulation efficiency and loading capacity

To establish the amount of curcumin incorporated within the lipid particles and evaluate whether the chosen materials were able to achieve high active loadings, the encapsulation efficiency (EE) and loading capacity (LC) were determined. All formulations were characterised by EE and LC values of 99.9±0.0% and 0.5±0.0%, respectively. It appears that changes in the chemical and physical characteristics of the SLN/NLC particles, did not convey any changes to their ability to enclose curcumin. Even when the value of the *Z*-average almost doubled (SLN_4), or the RI was high (SLN_1, NLC_1, SLN_2, SLN_3, SLN_4 and SLN_5), characteristics that are generally considered to have a negative impact on active entrapment [21,85], the EE and LC values remained equally high. This is in agreement with other studies using the same materials and similar concentration of the active in relation to the lipid phase.

Araujo *et al.* [22] have recently demonstrated how the composition of NLCs influences curcumin loading, reporting that NLCs prepared with Compritol® 888 ATO and MCT at 0.75% w/w curcumin in the lipid phase had an EE of 88.34±2.84% and LC of 2.22±0.01%. In another study, NLCs prepared with either Compritol® 888 ATO or Precirol® ATO 5 as the solid lipids and Labrasol® as the liquid lipid showed EE ranging between 79.70 and 96.89% and LC between 2.63 and 3.26% for the 0.5% w/w curcumin to lipids concentration used; both EE and LC were found to depend on the type of surfactant used (Tween® 80 or Poloxamer 407) and with higher values attributed to Precirol® ATO 5 [86]. In both studies, the method followed for the preparation of curcumin-loaded lipid dispersions involved the simple solubilisation of curcumin in the lipid melts under stirring. The use of solvents, such as ethanol or chloroform, to increase the amount of solubilised curcumin in the lipid phase have been reported to give LC up to 23.38% and EE up to 54% w/w of curcumin in lipid content [87,88]. In an aforementioned work [44], that explored the selection of a suitable solid lipid for curcumin encapsulation, the authors attempted to increase the percentage of curcumin to 2 and 3% w/w, from the initial 1% w/w that was defined as the maximum soluble quantity, which led to precipitation. Therefore, it is not clear at this stage and following the described processing and formulation parameters, whether increasing the percentage of curcumin in regard to the lipid phase concentration would result in equally high EE and LC values. Since the solubility of the active in the lipid phase changes during crystallisation, maintaining the concentration of the active close to the solubility threshold defined during preliminary solubility studies could explain the high EE and LC achieved in this study.

3.3.3.4 Storage stability

Formulations fabricated with glyceryl behenate, both blank (B-SLN_1 and B-NLC_1–B-NLC_3) and curcumin-loaded (SLN_1 and NLC_1–NLC_3), showed good storage stability over the examined time, with no deviation in the particle size (see Appendix A1, Table A1.6), well-maintained thermal profiles (see Appendix A1, Table A1.7), and unchanged EE and LC values. On the contrary, formulations comprising of glyceryl palmitostearate (SLN_2–SLN_3 and NLC_4–NLC_5) did not preserve their size characteristics above the 4 weeks mark. Physical modifications taking place during ageing of Precirol® ATO 5 have been reported to cause destabilisation of their physical properties to a greater extent than in longer fatty acid chain lipids, such as Compritol® 888 ATO [63,89]. Additionally, the greater temperature difference between the melting and crystallisation temperatures of glyceryl palmitostearate (compared to glyceryl behenate), would mean that droplets maintain their molten state over a longer period (prior to crystallisation) and thus are potentially exposed to a high risk of emulsion instabilities (e.g. coalescence), which in turn ultimately result in the formation of larger particles post-crystallisation (peak at 5.5 μm). The ageing modifications and/or destabilisation caused by liquid lipid expulsion could be assigned to the oily film formation observed for formulation NLC_4 at four weeks of storage. Since no such observation was made for glyceryl behenate and MCTs formulation, the lower affinity of MCTs for glyceryl palmitostearate that was suggested by the theoretical lipid screening studies could be responsible for this outcome. For samples containing both solid lipids, it was proposed by Bose *et al.* [90] that the varying rates of crystallisation of the two lipids (period of several months of glyceryl behenate and rapid for glyceryl palmitostearate) resulted in overall faster lipid transformation, leaving limited number of surfactant molecules to cover new surfaces formed during storage-induced lipid transformations, consequently causing aggregation. Changes in the ζ-potential values recorded

for most formulations over time can be used as indicators of electrostatic properties variations [91,92], which in turn is a sign of destabilisation. However, Tween® 80 and Poloxamer 188 are known to provide stabilisation through superposition of electrostatic and steric factors acting synergistically, which explains the stability preservation despite the values lower than |30| mV and their variations [93,94]. Long-term aggregation of Poloxamer 188-stabilised SLNs (SLN_5) confirmed by LD measurements (data not shown) could be the result of electrostatic repulsion losses induced by the bridging effects or gelling properties of block co-polymers like Poloxamer 188, as discussed by Freitas *et al.* [94]. In addition, the pre-existence of larger particles, in this case, as shown in Fig. 3.4D could have further promoted this effect. In instances where insufficient number of surfactant molecules are present in the system (SLN_4), the lipid particle surfaces remain uncovered, allowing for lipid particles to approach each other and result in aggregation, due to the absence of either steric or electrostatic repulsion forces, which was supported by LD data.

3.4 Conclusions

The present work explores the impact of different formulation parameters on the physical properties of SLNs and NLCs used as carriers of a model hydrophobic active. Theoretical active-to-lipid miscibility predictions, employing the Hansen solubility parameter, aligned well with experimental data, and this lipid screening approach is demonstrated to be an effective tool for selecting lipid components that can achieve high solubilisation of a chosen active; in this case curcumin. Lipid nanoparticles, of dimensions compatible to those required for Pickering functionality, were fabricated with varying combinations of the selected lipid materials and exhibited equally high encapsulation efficiency and loading capacity values, irrespective of their exact composition. Incremental addition of liquid lipid was shown to have

a concentration-dependent effect on both the obtained size and thermal behaviour of the formed particles with glyceryl behenate as the solid lipid, while the impact of active incorporation in the same particles was reliant on the relative solid-to-liquid lipid mass ratio. The influence of the compatibility between the lipid matrix components on the size and polymorphism was highlighted. Specifically, this was denoted by investigating the compatibility between solid lipid(s) and liquid lipid, when solid lipids with varying melting and crystallisation temperatures were used, and the affinity of the surfactant to the lipid blend, when different type of surface active species were employed. The formulation approach adopted in this study, whereby pre-formulation compatibility evaluation is performed between the active under investigation and the lipid components, could lead to the generation of a range of diverse lipid structures in terms of their crystalline properties, that are ensured to retain high active loadings over prolonged periods. Future work using the developed systems will aim to investigate/confirm the ability of the lipid particles to act as Pickering emulsion stabilisers, while maintaining their stability and active-carrier functionalities. Additionally, the improved understanding on their crystalline structure properties could be utilised to design/achieve controlled and tailor-made release patterns.

References

[1] H. Bunjes, Lipid nanoparticles for the delivery of poorly water-soluble drugs, Journal of Pharmacy and Pharmacology. 62 (2010) 1637–1645. https://doi.org/10.1111/j.2042-7158.2010.01024.x.

[2] L. Hu, X. Tang, C. Correspondence, : X Tang, F. Cui, Solid lipid nanoparticles (SLNs) to improve oral bioavailability of poorly soluble drugs, Journal of Pharmacy and Pharmacology. 56 (2004) 1527–1535. https://doi.org/10.1211/0022357044959.

[3] C.W. Pouton, Formulation of poorly water-soluble drugs for oral administration: Physicochemical and physiological issues and the lipid formulation classification system, European Journal of Pharmaceutical Sciences. 29 (2006) 278–287. https://doi.org/10.1016/j.ejps.2006.04.016.

[4] S. Sapino, M.E. Carlotti, E. Pelizzetti, D. Vione, M. Trotta, L. Battaglia, Protective effect of SLNs encapsulation on the photodegradation and thermal degradation of retinyl palmitate introduced in hydroxyethylcellulose gel, J Drug Deliv Sci Technol. 15 (2005) 159–165. https://doi.org/10.1016/s1773-2247(05)50021-2.

[5] E.B. Souto, R.H. Müller, SLN and NLC for topical delivery of ketoconazole, J Microencapsul. 22 (2005) 501–510. https://doi.org/10.1080/02652040500162436.

[6] R.H. Müller, M. Radtke, S.A. Wissing, Nanostructured lipid matrices for improved microencapsulation of drugs, Int J Pharm. 242 (2002) 121–128. https://doi.org/10.1016/s0378-5173(02)00180-1.

[7] A. Borges, V. de Freitas, N. Mateus, I. Fernandes, J. Oliveira, Solid lipid nanoparticles as carriers of natural phenolic compounds, Antioxidants. 9 (2020) 998. https://doi.org/10.3390/antiox9100998.

[8] P. Jaiswal, B. Gidwani, A. Vyas, Nanostructured lipid carriers and their current application in targeted drug delivery, Artif Cells Nanomed Biotechnol. 44 (2016) 27–40. https://doi.org/10.3109/21691401.2014.909822.

[9] S. Khan, S. Baboota, J. Ali, S. Khan, R.S. Narang, J.K. Narang, Nanostructured lipid carriers: An emerging platform for improving oral bioavailability of lipophilic drugs, Int J Pharm Investig. 5 (2015) 182–191. https://doi.org/10.4103/2230-973x.167661.

[10] P. Severino, T. Andreani, A.S. Macedo, J.F. Fangueiro, M.H.A. Santana, A.M. Silva, E.B. Souto, Current State-of-Art and New Trends on Lipid Nanoparticles (SLN and NLC) for Oral Drug Delivery, J Drug Deliv. 2012 (2012) 750891. https://doi.org/10.1155/2012/750891.

[11] J. Weiss, E.A. Decker, D.J. McClements, K. Kristbergsson, T. Helgason, T. Awad, Solid lipid nanoparticles as delivery systems for bioactive food components, Food Biophys. 3 (2008) 146–154. https://doi.org/10.1007/s11483-008-9065-8.

[12] R. Gupta, D. Rousseau, Surface-active solid lipid nanoparticles as Pickering stabilizers for oil-in-water emulsions, Food Funct. 3 (2012) 302–311. https://doi.org/10.1039/c2fo10203j.

[13] A. Pawlik, D. Kurukji, I. Norton, F. Spyropoulos, Food-grade Pickering emulsions stabilised with solid lipid particles, Food Funct. 7 (2016) 2712–2721. https://doi.org/10.1039/c6fo00238b.

[14] I. Zafeiri, J.E. Norton, P. Smith, I.T. Norton, F. Spyropoulos, The role of surface active species in the fabrication and functionality of edible solid lipid particles, J Colloid Interface Sci. 500 (2017) 228–240. https://doi.org/10.1016/j.jcis.2017.03.085.

[15] G.I. Sakellari, I. Zafeiri, A. Pawlik, D. Kurukji, P. Taylor, I.T. Norton, F. Spyropoulos, Independent co-delivery of model actives with different degrees of hydrophilicity from oil-in-water and water-in-oil emulsions stabilised by solid lipid particles via a Pickering mechanism: a-proof-of-principle study, J Colloid Interface Sci. 587 (2021) 644–649. https://doi.org/10.1016/j.jcis.2020.11.021.

[16] A. Schröder, M. Laguerre, J. Sprakel, K. Schroën, C.C. Berton-Carabin, Pickering particles as interfacial reservoirs of antioxidants, J Colloid Interface Sci. 575 (2020) 489–498. https://doi.org/10.1016/j.jcis.2020.04.069.

[17] I. Zafeiri, P. Smith, I.T. Norton, F. Spyropoulos, Fabrication, characterisation and stability of oil-in-water emulsions stabilised by solid lipid particles: The role of particle characteristics and emulsion microstructure upon Pickering functionality, Food Funct. 8 (2017) 2583–2591. https://doi.org/10.1039/c7fo00559h.

[18] H. Lim, M. Jo, C. Ban, Y.J. Choi, Interfacial and colloidal characterization of oil-in-water emulsions stabilized by interface-tunable solid lipid nanoparticles, Food Chem. 306 (2020) 125619. https://doi.org/10.1016/j.foodchem.2019.125619.

[19] A. Schröder, J. Sprakel, K. Schroën, C.C. Berton-Carabin, Tailored microstructure of colloidal lipid particles for Pickering emulsions with tunable properties, Soft Matter. 13 (2017) 3190–3198. https://doi.org/10.1039/c6sm02432g.

[20] F.Q. Hu, S.P. Jiang, Y.Z. Du, H. Yuan, Y.Q. Ye, S. Zeng, Preparation and characterization of stearic acid nanostructured lipid carriers by solvent diffusion method in an aqueous system, Colloids Surf B Biointerfaces. 45 (2005) 167–173. https://doi.org/10.1016/j.colsurfb.2005.08.005.

[21] L.J. Jia, D.R. Zhang, Z.Y. Li, F.F. Feng, Y.C. Wang, W.T. Dai, C.X. Duan, Q. Zhang, Preparation and characterization of silybin-loaded nanostructured lipid carriers, Drug Deliv. 17 (2010) 11–18. https://doi.org/10.3109/10717540903431586.

[22] V.H.S. Araujo, P.B. da Silva, I.O. Szlachetka, S.W. da Silva, B. Fonseca-Santos, M. Chorilli, R. Ganassin, G.R.T. de Oliveira, M.C.O. da Rocha, R.P. Fernandes, M. de Carvalho Vieira Queiroz, R.B. Azevedo, L.A. Muehlmann, The influence of NLC composition on curcumin loading under a physicochemical perspective and in vitro evaluation, Colloids Surf A Physicochem Eng Asp. 602 (2020) 125070. https://doi.org/10.1016/j.colsurfa.2020.125070.

[23] H. Bunjes, M. Drechsler, M.H.J. Koch, K. Westesen, Incorporation of the model drug ubidecarenone into solid lipid nanoparticles, Pharm Res. 18 (2001) 287–293. https://doi.org/10.1023/a:1011042627714.

[24] K. Jores, W. Mehnert, K. Mäder, Physicochemical investigations on solid lipid nanoparticles and on oil-loaded solid lipid nanoparticles: A nuclear magnetic resonance and electron spin resonance study, Pharm Res. 20 (2003) 1274–1283. https://doi.org/10.1023/a:1025065418309.

[25] S. Anantachaisilp, S.M. Smith, A. Treetong, S. Pratontep, S. Puttipipatkhachorn, U.R. Ruktanonchai, Chemical and structural investigation of lipid nanoparticles: Drug-lipid interaction and molecular distribution, Nanotechnology. 21 (2010). https://doi.org/10.1088/0957-4484/21/12/125102.

[26] S. Das, A. Chaudhury, Recent advances in lipid nanoparticle formulations with solid matrix for oral drug delivery, AAPS PharmSciTech. 12 (2011) 62–76. https://doi.org/10.1208/s12249-010-9563-0.

[27] K.W. Kasongo, J. Pardeike, R.H. Müller, R.B. Walker, Selection and characterization of suitable lipid excipients for use in the manufacture of didanosine-loaded solid lipid

nanoparticles and nanostructured lipid carriers, J Pharm Sci. 100 (2011) 5185–5196. https://doi.org/10.1002/jps.22711.

[28] A. Kovačević, S. Savic, G. Vuleta, R.H. Müller, C.M. Keck, Polyhydroxy surfactants for the formulation of lipid nanoparticles (SLN and NLC): Effects on size, physical stability and particle matrix structure, Int J Pharm. 406 (2011) 163–172. https://doi.org/10.1016/j.ijpharm.2010.12.036.

[29] R.H. Müller, K. Mäder, S. Gohla, Solid lipid nanoparticles (SLN) for controlled drug delivery - A review of the state of the art, European Journal of Pharmaceutics and Biopharmaceutics. 50 (2000) 161–177. https://doi.org/10.1016/s0939-6411(00)00087-4.

[30] R.H. Müller, M. Radtke, S.A. Wissing, Solid lipid nanoparticles (SLN) and nanostructured lipid carriers (NLC) in cosmetic and dermatological preparations, Adv Drug Deliv Rev. 54 (2002). https://doi.org/10.1016/s0169-409x(02)00118-7.

[31] A. Obinu, E.P. Porcu, S. Piras, R. Ibba, A. Carta, P. Molicotti, R. Migheli, A. Dalpiaz, L. Ferraro, G. Rassu, E. Gavini, P. Giunchedi, Solid lipid nanoparticles as formulative strategy to increase oral permeation of a molecule active in multidrug-resistant tuberculosis management, Pharmaceutics. 12 (2020) 1132. https://doi.org/10.3390/pharmaceutics12121132.

[32] M. Shah, Y.K. Agrawal, K. Garala, A. Ramkishan, Solid lipid nanoparticles of a water soluble drug, ciprofloxacin hydrochloride, Indian J Pharm Sci. 74 (2012) 434–442. https://doi.org/10.4103/0250-474x.108419.

[33] V. Jenning, A.F. Thünemann, S.H. Gohla, Characterisation of a novel solid lipid nanoparticle carrier system based on binary mixtures of liquid and solid lipids, Int J Pharm. 199 (2000) 167–177. https://doi.org/10.1016/s0378-5173(00)00378-1.

[34] K. Jores, W. Mehnert, M. Drechsler, H. Bunjes, C. Johann, K. Mäder, Investigations on the structure of solid lipid nanoparticles (SLN) and oil-loaded solid lipid nanoparticles by photon correlation spectroscopy, field-flow fractionation and transmission electron microscopy, Journal of Controlled Release. 95 (2004) 217–227. https://doi.org/10.1016/j.jconrel.2003.11.012.

[35] E. Wolska, M. Sznitowska, K. Krzemińska, M.F. Monteiro, Analytical techniques for the assessment of drug-lipid interactions and the active substance distribution in liquid dispersions of solid lipid microparticles (SLM) produced de novo and reconstituted from spray-dried powders, Pharmaceutics. 12 (2020) 664. https://doi.org/10.3390/pharmaceutics12070664.

[36] K. Oehlke, D. Behsnilian, E. Mayer-Miebach, P.G. Weidler, R. Greiner, Edible solid lipid nanoparticles (SLN) as carrier system for antioxidants of different lipophilicity, PLoS One. 12 (2017) e0171662. https://doi.org/10.1371/journal.pone.0171662.

[37] G. Zoubari, S. Staufenbiel, P. Volz, U. Alexiev, R. Bodmeier, Effect of drug solubility and lipid carrier on drug release from lipid nanoparticles for dermal delivery, European Journal of Pharmaceutics and Biopharmaceutics. 110 (2017) 39–46. https://doi.org/10.1016/j.ejpb.2016.10.021.

[38] J. Sharifi-Rad, Y. el Rayess, A.A. Rizk, C. Sadaka, R. Zgheib, W. Zam, S. Sestito, S. Rapposelli, K. Neffe-Skocińska, D. Zielińska, B. Salehi, W.N. Setzer, N.S. Dosoky, Y. Taheri, M. el Beyrouthy, M. Martorell, E.A. Ostrander, H.A.R. Suleria, W.C. Cho, A. Maroyi, N. Martins, Turmeric and Its Major Compound Curcumin on Health: Bioactive Effects and Safety Profiles for Food, Pharmaceutical, Biotechnological and Medicinal Applications, Front Pharmacol. 11 (2020) 1021. https://doi.org/10.3389/fphar.2020.01021.

[39] P. Anand, A.B. Kunnumakkara, R.A. Newman, B.B. Aggarwal, Bioavailability of curcumin: Problems and promises, Mol Pharm. 4 (2007) 807–818. https://doi.org/10.1021/mp700113r.

[40] C. Scomoroscenco, M. Teodorescu, A. Raducan, M. Stan, S.N. Voicu, B. Trica, C.M. Ninciuleanu, C.L. Nistor, C.I. Mihaescu, C. Petcu, L.O. Cinteza, Novel gel microemulsion as topical drug delivery system for curcumin in dermatocosmetics, Pharmaceutics. 13 (2021) 505. https://doi.org/10.3390/pharmaceutics13040505.

[41] C.M. Hansen, Hansen solubility parameters: A user's handbook: Second edition (2nd ed.), CRC Press, 2007. https://doi.org/10.1201/9781420006834.

[42] D.W. van Krevelen, K. te Nijenhuis, Chapter 7 - Cohesive Properties and Solubility in Properties of Polymers, in: Properties of Polymers (Fourth Edition), Elsevier, Amsterdam, 2009: pp. 189–227. https://doi.org/10.1016/b978-0-08-054819-7.00007-8.

[43] W.-H. Lee, C.-Y. Loo, M. Bebawy, F. Luk, R. Mason, R. Rohanizadeh, Curcumin and its Derivatives: Their Application in Neuropharmacology and Neuroscience in the 21st Century, Curr Neuropharmacol. 11 (2013) 338–378. https://doi.org/10.2174/1570159x11311040002.

[44] S. Doktorovova, E.B. Souto, A.M. Silva, Hansen solubility parameters (HSP) for prescreening formulation of solid lipid nanoparticles (SLN): in vitro testing of curcumin-loaded SLN in MCF-7 and BT-474 cell lines, Pharm Dev Technol. 23 (2017) 96–105. https://doi.org/10.1080/10837450.2017.1384491.

[45] P.O. Nnamani, S. Hansen, M. Windbergs, C.M. Lehr, Development of artemether-loaded nanostructured lipid carrier (NLC) formulation for topical application, Int J Pharm. 477 (2014) 208–217. https://doi.org/10.1016/j.ijpharm.2014.10.004.

[46] K. van Malssen, R. Peschar, C. Brito, H. Schenk, Real-time X-ray powder diffraction investigations on cocoa butter. III. Direct β-crystallization of cocoa butter: Occurrence of a memory effect, JAOCS, Journal of the American Oil Chemists' Society. 73 (1996) 1225–1230. https://doi.org/10.1007/bf02525450.

[47] C. Freitas, R.H. Müller, Correlation between long-term stability of solid lipid nanoparticles (SLN(TM)) and crystallinity of the lipid phase, European Journal of Pharmaceutics and Biopharmaceutics. 47 (1999) 125–132. https://doi.org/10.1016/s0939-6411(98)00074-5.

[48] M. Shah, Y. Agrawal, Ciprofloxacin hydrochloride-loaded glyceryl monostearate nanoparticle: Factorial design of Lutrol F68 and Phospholipon 90G, J Microencapsul. 29 (2012) 331–343. https://doi.org/10.3109/02652048.2011.651498.

[49] A. Kovačević, R.H. Müller, C.M. Keck, Formulation development of lipid nanoparticles: Improved lipid screening and development of tacrolimus loaded nanostructured lipid carriers (NLC), Int J Pharm. 576 (2020) 118918. https://doi.org/10.1016/j.ijpharm.2019.118918.

[50] P.A. Makoni, J. Ranchhod, K. WaKasongo, S.M. Khamanga, R.B. Walker, The use of quantitative analysis and Hansen solubility parameter predictions for the selection of excipients for lipid nanocarriers to be loaded with water soluble and insoluble compounds, Saudi Pharmaceutical Journal. 28 (2020) 308–315. https://doi.org/10.1016/j.jsps.2020.01.010.

[51] M. Shah, Y. Agrawal, High throughput screening: an in silico solubility parameter approach for lipids and solvents in SLN preparations., Pharm Dev Technol. 18 (2013) 582–590. https://doi.org/10.3109/10837450.2011.635150.

[52] R.H. Müller, M. Radtke, S.A. Wissing, Nanostructured lipid matrices for improved microencapsulation of drugs, Int J Pharm. 242 (2002) 121–128. https://doi.org/10.1016/s0378-5173(02)00180-1.

[53] E.B. Souto, W. Mehnert, R.H. Müller, Polymorphic behaviour of Compritol®888 ATO as bulk lipid and as SLN and NLC, J Microencapsul. 23 (2006) 417–433. https://doi.org/10.1080/02652040600612439.

[54] L. Bayés-García, K. Sato, S. Ueno, Polymorphism of Triacylglycerols and Natural Fats, Bailey's Industrial Oil and Fat Products. (2020) 1–49. https://doi.org/10.1002/047167849x.bio020.pub2.

[55] P. Pivette, V. Faivre, J.B. Brubach, G. Daste, M. Ollivon, S. Lesieur, Polymorphism of glyceryl behenates: From the individual compounds to the pharmaceutical excipient, Chem Phys Lipids. 183 (2014) 191–203. https://doi.org/10.1016/j.chemphyslip.2014.07.005.

[56] J.B. Brubach, V. Jannin, B. Mahler, C. Bourgaux, P. Lessieur, P. Roy, M. Ollivon, Structural and thermal characterization of glyceryl behenate by X-ray diffraction coupled to differential calorimetry and infrared spectroscopy, Int J Pharm. 336 (2007) 248–256. https://doi.org/10.1016/j.ijpharm.2006.11.057.

[57] P. Severino, S.C. Pinho, E.B. Souto, M.H.A. Santana, Crystallinity of Dynasan ®114 and Dynasan ®118 matrices for the production of stable Miglyol ®-loaded nanoparticles, J Therm Anal Calorim. 108 (2011) 101–108. https://doi.org/10.1007/s10973-011-1613-7.

[58] E. Zimmermann, E.B. Souto, R.H. Müller, Physicochemical investigations on the structure of drug-free and drug-loaded solid lipid nanoparticles (SLN^{TM}) by means of DSC and 1H NMR, Pharmazie. 60 (2005) 508–513.

[59] C. Reitz, P. Kleinebudde, Influence of thermal and thermo-mechanical treatment : CCComparison of two lipids with respect to their suitability for solid lipid extrusion, J Therm Anal Calorim. 89 (2007) 669–673. https://doi.org/10.1007/s10973-006-7953-z.

[60] K.W. Kasongo, R. Shegokar, R.H. Müller, R.B. Walker, Formulation development and in vitro evaluation of didanosine-loaded nanostructured lipid carriers for the potential treatment of AIDS dementia complex, Drug Dev Ind Pharm. 37 (2011) 396–407. https://doi.org/10.3109/03639045.2010.516264.

[61] K. Sato, Crystallization behaviour of fats and lipids - A review, Chem Eng Sci. 56 (2001) 2255–2265. https://doi.org/10.1016/s0009-2509(00)00458-9.

[62] M. Cirri, L. Maestrini, F. Maestrelli, N. Mennini, P. Mura, C. Ghelardini, L.D.C. Mannelli, Design, characterization and in vivo evaluation of nanostructured lipid carriers (NLC) as a new drug delivery system for hydrochlorothiazide oral administration in pediatric therapy, Drug Deliv. 25 (2018) 1910–1921. https://doi.org/10.1080/10717544.2018.1529209.

[63] J. Hamdani, A.J. Moës, K. Amighi, Physical and thermal characterisation of Precirol® and Compritol® as lipophilic glycerides used for the preparation of controlled-release matrix pellets, Int J Pharm. 260 (2003) 47–57. https://doi.org/10.1016/S0378-5173(03)00229-1.

[64] H. Bunjes, K. Westesen, M.H.J. Koch, Crystallization tendency and polymorphic transitions in triglyceride nanoparticles, Int J Pharm. 129 (1996) 159–173. https://doi.org/10.1016/0378-5173(95)04286-5.

[65] H. Yoshino, M. Kobayashi, M. Samejima, Influence of the Liquid Phase Coexisting in Fatty Suppository Bases on the Polymorphic Transition Rate, Chem Pharm Bull (Tokyo). 30 (1982) 2941–2950. https://doi.org/10.1248/cpb.30.2941.

[66] I.T. Norton, C.D. Lee-Tuffnell, S. Ablett, S.M. Bociek, A calorimetric, NMR and X-ray diffraction study of the melting behavior of tripalmitin and tristearin and their mixing behavior with triolein, J Am Oil Chem Soc. 62 (1985) 1237–1244. https://doi.org/10.1007/bf02541834.

[67] D. Rousseau, Fat crystals and emulsion stability - A review, Food Research International. 33 (2000) 3–14. https://doi.org/10.1016/s0963-9969(00)00017-x.

[68] R. Kumar, A. Singh, N. Garg, P.F. Siril, Solid lipid nanoparticles for the controlled delivery of poorly water soluble non-steroidal anti-inflammatory drugs, Ultrason Sonochem. 40(Pt A) (2018) 686–696. https://doi.org/10.1016/j.ultsonch.2017.08.018.

[69] S. Das, W.K. Ng, P. Kanaujia, S. Kim, R.B.H. Tan, Formulation design, preparation and physicochemical characterizations of solid lipid nanoparticles containing a hydrophobic drug: Effects of process variables, Colloids Surf B Biointerfaces. 88 (2011) 483–489. https://doi.org/10.1016/j.colsurfb.2011.07.036.

[70] T. Helgason, T.S. Awad, K. Kristbergsson, D.J. McClements, J. Weiss, Effect of surfactant surface coverage on formation of solid lipid nanoparticles (SLN), J Colloid Interface Sci. 334 (2009) 75–81. https://doi.org/10.1016/j.jcis.2009.03.012.

[71] E.H. Gokce, E. Korkmaz, E. Dellera, G. Sandri, M. Cristina Bonferoni, O. Ozer, Resveratrol-loaded solid lipid nanoparticles versus nanostructured lipid carriers: Evaluation of antioxidant potential for dermal applications, Int J Nanomedicine. 7 (2012) 1841–1850. https://doi.org/10.2147/ijn.s29710.

[72] F. Tamjidi, M. Shahedi, J. Varshosaz, A. Nasirpour, Design and characterization of astaxanthin-loaded nanostructured lipid carriers, Innovative Food Science and Emerging Technologies. 26 (2014) 366–374. https://doi.org/10.1016/j.ifset.2014.06.012.

[73] A. Akhoond Zardini, M. Mohebbi, R. Farhoosh, S. Bolurian, Production and characterization of nanostructured lipid carriers and solid lipid nanoparticles containing lycopene for food fortification, J Food Sci Technol. 55 (2018) 287–298. https://doi.org/10.1007/s13197-017-2937-5.

[74] J.P. Canselier, H. Delmas, A.M. Wilhelm, B. Abismaïl, Ultrasound emulsification - An overview, J Dispers Sci Technol. 23 (2001) 333–349. https://doi.org/10.1080/01932690208984209.

[75] S. Kentish, T.J. Wooster, M. Ashokkumar, S. Balachandran, R. Mawson, L. Simons, The use of ultrasonics for nanoemulsion preparation, Innovative Food Science and Emerging Technologies. 9 (2008) 170–175. https://doi.org/10.1016/j.ifset.2007.07.005.

[76] A. Kovačević, S. Savic, G. Vuleta, R.H. Müller, C.M. Keck, Polyhydroxy surfactants for the formulation of lipid nanoparticles (SLN and NLC): Effects on size, physical stability and particle matrix structure, Int J Pharm. 406 (2011) 163–172. https://doi.org/10.1016/j.ijpharm.2010.12.036.

[77] P.A. Makoni, K.W. Kasongo, R.B. Walker, Short term stability testing of efavirenz-loaded solid lipid nanoparticle (SLN) and nanostructured lipid carrier (NLC) dispersions, Pharmaceutics. 11 (2019) 397. https://doi.org/10.3390/pharmaceutics11080397.

[78] J.Y. Fang, C.L. Fang, C.H. Liu, Y.H. Su, Lipid nanoparticles as vehicles for topical psoralen delivery: Solid lipid nanoparticles (SLN) versus nanostructured lipid carriers (NLC), European Journal of Pharmaceutics and Biopharmaceutics. 70 (2008) 633–640. https://doi.org/10.1016/j.ejpb.2008.05.008.

[79] R.H. Müller, K. Mäder, S. Gohla, Solid lipid nanoparticles (SLN) for controlled drug delivery - A review of the state of the art, European Journal of Pharmaceutics and Biopharmaceutics. 50 (2000) 161–177. https://doi.org/10.1016/s0939-6411(00)00087-4.

[80] M. Perez, Gibbs-Thomson effects in phase transformations, Scr Mater. 52 (2005) 709–712. https://doi.org/10.1016/j.scriptamat.2004.12.026.

[81] H. Bunjes, M.H.J. Koch, K. Westesen, Effects of surfactants on the crystallization and polymorphism of lipid nanoparticles, in: Lagaly G. (Eds) Molecular Organisation on Interfaces. Progress in Colloid and Polymer Science, Springer, Berlin, Heidelberg, 2002. https://doi.org/10.1007/3-540-47822-1_2.

[82] V. Jenning, M. Schäfer-Korting, S. Gohla, Vitamin A-loaded solid lipid nanoparticles for topical use: Drug release properties, Journal of Controlled Release. 66 (2000) 115–126. https://doi.org/10.1016/S0168-3659(99)00223-0.

[83] H. Bunjes, T. Unruh, Characterization of lipid nanoparticles by differential scanning calorimetry, X-ray and neutron scattering, Adv Drug Deliv Rev. 59 (2007) 379–402. https://doi.org/10.1016/j.addr.2007.04.013.

[84] A. zur Mühlen, C. Schwarz, W. Mehnert, Solid lipid nanoparticles (SLN) for controlled drug delivery - Drug release and release mechanism, European Journal of Pharmaceutics and Biopharmaceutics. 45 (1998) 149–155. https://doi.org/10.1016/s0939-6411(97)00150-1.

[85] E.B. Souto, S.A. Wissing, C.M. Barbosa, R.H. Müller, Development of a controlled release formulation based on SLN and NLC for topical clotrimazole delivery, Int J Pharm. 278 (2004) 71–77. https://doi.org/10.1016/j.ijpharm.2004.02.032.

[86] M.A. Espinosa-Olivares, N.L. Delgado-Buenrostro, Y.I. Chirino, M.A. Trejo-Márquez, S. Pascual-Bustamante, A. Ganem-Rondero, Nanostructured lipid carriers loaded with curcuminoids: Physicochemical characterization, in vitro release, ex vivo skin penetration, stability and antioxidant activity, European Journal of Pharmaceutical Sciences. 155 (2020) 105533. https://doi.org/10.1016/j.ejps.2020.105533.

[87] M.L. Bondì, M.R. Emma, C. Botto, G. Augello, A. Azzolina, F. di Gaudio, E.F. Craparo, G. Cavallaro, D. Bachvarov, M. Cervello, Biocompatible Lipid Nanoparticles as Carriers to Improve Curcumin Efficacy in Ovarian Cancer Treatment, J Agric Food Chem. 65 (2017) 1342–1352. https://doi.org/10.1021/acs.jafc.6b04409.

[88] W. Wang, T. Chen, H. Xu, B. Ren, X. Cheng, R. Qi, H. Liu, Y. Wang, L. Yan, S. Chen, Q. Yang, C. Chen, Curcumin-loaded solid lipid nanoparticles enhanced anticancer efficiency in breast cancer, Molecules. 23 (2018) 1578. https://doi.org/10.3390/molecules23071578.

[89] W. Sutananta, D.Q.M. Craig, J.M. Newton, The effects of ageing on the thermal behaviour and mechanical properties of pharmaceutical glycerides, Int J Pharm. 111 (1994) 51–62. https://doi.org/10.1016/0378-5173(94)90401-4.

[90] S. Bose, Y. Du, P. Takhistov, B. Michniak-Kohn, Formulation optimization and topical delivery of quercetin from solid lipid based nanosystems, Int J Pharm. 441 (2013) 56–66. https://doi.org/10.1016/j.ijpharm.2012.12.013.

[91] E.B. Souto, S.A. Wissing, C.M. Barbosa, R.H. Müller, Evaluation of the physical stability of SLN and NLC before and after incorporation into hydrogel formulations, European Journal of Pharmaceutics and Biopharmaceutics. 58 (2004) 83–90. https://doi.org/10.1016/j.ejpb.2004.02.015.

[92] T.M. Riddick, Control of colloid stability through zeta potential: with a closing chapter on Its Relationship to Cardiovascular Disease, Zeta-Meter, Inc., 1968.

[93] T.B. Tan, W.C. Chu, N.S. Yussof, F. Abas, H. Mirhosseini, Y.K. Cheah, I.A. Nehdi, C.P. Tan, Physicochemical, morphological and cellular uptake properties of lutein nanodispersions prepared by using surfactants with different stabilizing mechanisms, Food Funct. 7 (2016) 2043–2051. https://doi.org/10.1039/c5fo01621e.

[94] C. Freitas, R.H. Müller, Effect of light and temperature on zeta potential and physical stability in solid lipid nanoparticle (SLN®) dispersions, Int J Pharm. 168 (1998) 221–229. https://doi.org/10.1016/S0378-5173(98)00092-1.

Appendix A1

Theoretical lipid screening – Calculations example

An example of the calculations performed to determine the solubility parameter for Compritol® 888 ATO (glyceryl behenate) is given below. According to the composition provided by the manufacturer, glyceryl behenate comprises of glyceryl tribehenate, dibehenate and monobehenate at 30.1, 50.1 and 17.8% (w/w) concentrations, respectively. For each constituent, the individual Hansen solubility parameters were calculated based on their chemical structure and using the group contribution tables by van Krevelen *et al*. [1].

The individual parameters (molar volume, dispersion and polar forces, and hydrogen bonding energy contributions) used in the HSPs were calculated as follows:

		F_{di} ($J^{1/2}$ $cm^{3/2}$ mol^{-1})	F_{pi}^2 ($J^{1/2}$ $cm^{3/2}$ mol^{-1})	E_{hi} (J/mol)	V_m (cm^3/mol)
Glyceryl tribehenate	3×(-CH_3-)	1260	0	0	100.5
	62×(-CH_2-)	17010	0	0	998.2
	3×(-COO-)	1170	1470	21000	54
	1×(-CH-)	80	0	0	−1
Glyceryl dibehenate	2×(-CH_3-)	840	0	0	67
	42×(-CH_2-)	11340	0	0	676.2
	2×(-COO-)	780	980	14000	36
	1×(-CH-)	80	0	0	−1
	1×(-OH-)	210	500	20000	10
Glyceryl monobehenate	1×(-CH_3-)	420	0	0	33.5
	22×(-CH_2-)	5940	0	0	354.2
	1×(-COO-)	390	490	7000	18
	1×(-CH-)	80	0	0	−1
	2×(-OH-)	420	1000	40000	20

The individual Hansen parameters for each component are given below:

Glyceryl tribehenate: $\delta_D = \frac{\sum_i F_{di}}{V_m} = 16.71\ MPa^{1/2},\ \delta_P = \frac{\sqrt{\sum_i F_{pi}^2}}{V_m} = 1.28\ MPa^{1/2},\ \delta_H = \sqrt{\frac{\sum_i E_{hi}}{V_m}} =$ $4.27\ MPa^{1/2}$

Glyceryl dibehenate: $\delta_D = \frac{\sum_i F_{di}}{V_m} = 16.81\ MPa^{1/2},\ \delta_P = \frac{\sqrt{\sum_i F_{pi}^2}}{V_m} = 1.40\ MPa^{1/2},\ \delta_H = \sqrt{\frac{\sum_i E_{hi}}{V_m}} =$ $6.57\ MPa^{1/2}$

Glyceryl monobehenate: $\delta_D = \frac{\sum_i F_{di}}{V_m} = 17.07\ MPa^{1/2},\ \delta_P = \frac{\sqrt{\sum_i F_{pi}^2}}{V_m} = 2.62\ MPa^{1/2},\ \delta_H = \sqrt{\frac{\sum_i E_{hi}}{V_m}} =$ $10.52\ MPa^{1/2}$

For lipids, like the example presented here, that consist of more than one component, the molar ratio contribution of each was calculated using the molecular weight and % (w/w) concentration, and the final Hansen parameters are given as the normalised value. For Compritol® 888 ATO the normalised Hansen solubility parameters were the following:

$$\delta_D = \frac{\sum_i F_{di}}{V_m} = 16.87\ MPa^{1/2}, \qquad \delta_P = \frac{\sqrt{\sum_i F_{pi}^2}}{V_m} = 1.75\ MPa^{1/2}, \qquad \delta_H = \sqrt{\frac{\sum_i E_{hi}}{V_m}} = 7.31\ MPa^{1/2}$$

The same method was followed to calculate the parameters for the remaining lipids and the results are presented in Table A1.1.

Table A1.1. Trade name, chemical composition and consistency of the solid and liquid lipids used for the lipid screening.

Lipid (Trade name)	Chemical composition	Consistency
Compritol® 888 ATO	Glyceryl tribehenate Glyceryl dibehenate Glyceryl monobehenate	30.1% (w/w) 50.1% (w/w) 17.8% (w/w)
Precirol® ATO 5	Glyceryl tristearate Glyceryl distearate Glyceryl monostearate Glyceryl tripalmitate Glyceryl dipalmitate Glyceryl monopalmitate	51.2% (w/w) Diesters 29.9% (w/w) Triesters 18% (w/w) Monoesters
Dynasan® 118	Glyceryl tristearate	100% (w/w)
Cetyl palmitate	Cetyl palmitate	100% (w/w)
Imwitor® 960K	Glyceryl distearate Glyceryl monostearate Glyceryl dipalmitate Glyceryl monopalmitate	30.7% (w/w) Monoesters
Labrafac™ PG	Propylene glycol dicaprylate Propylene glycol dicaprate	55.4% (w/w) 43.4% (w/w)
Labrafil® M 2125 CS	Glyceyl trilinoleate Glyceryl dilinoleate Glyceryl monolinoleate Glyceryl tripalmitate Glyceryl dipalmitate Glyceryl palmitate Glyceryl trioleate Glyceryl dioleate Glyceryl oleate Propylene dilinoleate Propylene linoleate Propylene dipalmitate Propylene palmitate	51.8% (w/w) Linoleic acid 32.2% (w/w) Oleic acid 11.5% (w/w) Palmitic acid

	Propylene dioleate Propylene oleate	
Imwitor® 375	Glyceryl dicitrate Glyceryl monocitrate Glyceryl dilactate Glyceryl monolactate Glyceryl dilinoleate Glyceryl monolinoleate Glyceryl dioleate Glyceryl monooleate	21% (w/w) Monoglycerides
Miglyol® 812	Glyceryl tricaprylate Glyceryl tricaprate	57.1% (w/w) 42.6% (w/w)
Castor oil	Glyceryl triricinoleate Glyceryl trioleate Glyceryl trilinoleate	90% (w/w) 3% (w/w) 4.2% (w/w)

Table A1.2. Solubility screening of curcumin in the solid and liquid lipid components and organic solvents.

Compound name	Composition	δ_D	δ_P	δ_H	δ	*Ra* (diketo form)	*Ra* (enol form)	$\Delta\delta$ (diketo form)	$\Delta\delta$ (enol form)
Curcumin	Diketo form	17.17	5.47	12.33	21.83				
	Enol form	16.80	5.54	14.16	22.66				
Compritol® 888 ATO	Glyceryl tribehenate	16.71	1.28	4.27	17.30	9.13	10.77	4.53	5.36
	Glyceryl dibehenate	16.81	1.40	6.57	18.10	7.09	8.65	3.73	4.56
	Glyceryl monobehenate	17.07	2.62	10.52	20.22	3.37	4.69	1.61	2.44
Precirol® ATO 5	Glyceryl tristearate	16.70	1.53	5.96	17.80	7.54	9.13	4.03	4.86
	Glyceryl distearate	16.82	1.67	7.18	18.36	6.43	7.98	3.47	4.30
	Glyceryl monostearate	17.12	3.09	11.42	20.81	2.54	3.69	1.02	1.85
	Glyceryl tripalmitate	16.70	1.71	4.94	17.49	8.35	9.99	4.34	5.17
	Glyceryl dipalmitate	16.82	1.85	5.94	17.94	7.37	9.01	3.89	4.72
	Glyceryl monopalmitate	17.16	3.39	11.97	21.19	2.10	3.15	0.64	1.47
Dynasan® 118	Glyceryl tristearate	16.70	1.53	5.96	17.80	7.54	9.13	7.50	9.13
Cetyl palmitate	Cetyl palmitate	16.42	0.89	3.56	16.82	10.00	11.60	5.01	5.84
Imwitor® 960K	Glyceryl distearate	16.82	1.67	7.18	18.36	6.43	7.98	3.47	4.30
	Glyceryl monostearate	17.12	3.09	11.42	20.81	2.54	3.73	1.02	1.85
	Glyceryl dipalmitate	16.82	1.85	5.94	17.94	7.37	9.01	3.89	4.72
	Glyceryl monopalmitate	17.16	3.39	11.97	21.19	2.10	3.15	0.64	1.47
Labrafac™ PG	Propylene glycol dicaprylate	18.46	4.25	7.44	20.35	5.66	7.60	1.48	2.32
	Propylene glycol dicaprate	15.01	3.89	7.12	17.06	6.94	8.07	4.77	5.60
Labrafil® M 2125 CS	Glyceyl trilinoleate	16.36	1.59	4.76	17.11	8.66	10.24	4.72	5.55
	Glyceryl dilinoleate	16.49	1.72	7.30	18.11	6.41	7.88	3.72	4.55
	Glyceryl monolinoleate	16.83	3.18	11.59	20.68	2.49	3.49	1.15	1.98
	Glyceryl tripalmitate	16.82	1.85	5.94	17.94	8.35	9.99	3.89	4.72
	Glyceryl dipalmitate	16.70	1.71	4.94	17.49	7.37	9.01	4.34	5.17
	Glyceryl palmitate	17.16	3.39	11.97	21.19	2.10	3.15	0.64	1.47
	Glyceryl trioleate	16.53	1.56	4.72	17.26	8.65	10.26	4.57	5.40
	Glyceryl dioleate	16.66	1.70	7.24	18.24	6.42	7.92	3.59	4.42
	Glyceryl monooleate	16.98	3.14	11.50	20.75	2.50	3.60	1.08	1.91
	Propylene dilinoleate	16.60	2.75	5.98	17.86	6.99	8.65	3.97	4.80
	Propylene monolinoleate	16.89	4.07	8.98	19.56	3.67	5.39	2.27	3.10
	Propylene dipalmitate	16.87	2.91	6.15	18.19	6.71	8.43	3.64	4.47
	Propylene monopalmitate	17.11	4.25	9.17	19.87	3.38	5.19	1.96	2.79
	Propylene dioleate	16.74	2.35	5.53	17.78	7.53	9.20	4.05	4.88
	Propylene monooleate	16.69	4.03	8.93	19.62	3.70	5.45	2.21	3.04
Imwitor® 375	Glyceryl tricitrate	21.56	3.38	10.23	24.10	9.26	10.51	−2.27	−1.44
	Glyceryl trilactate	23.67	6.78	14.48	28.57	13.26	13.80	−6.74	−5.91
	Glyceryl trilinoleate	16.36	1.59	4.76	17.11	8.66	10.24	4.72	5.55
	Glyceryl trioleate	16.53	1.56	4.72	17.26	8.65	10.26	4.57	5.40
	Glyceryl dicitrate	21.46	10.35	21.24	31.92	13.30	12.65	−10.09	−9.26
	Glyceryl monocitrate	21.25	11.98	24.15	34.32	15.77	14.84	−12.49	−11.66
	Glyceryl dilactate	18.68	11.05	21.36	30.45	11.04	9.81	−8.62	−7.79
	Glyceryl monolactate	19.16	14.13	24.49	34.15	15.45	14.24	−12.32	−11.49
	Glyceryl dilinoleate	16.49	1.72	7.30	18.11	6.41	7.88	3.72	4.55
	Glyceryl monolinoleate	16.83	3.18	11.59	20.68	2.49	3.49	1.15	1.98
	Glyceryl dioleate	16.66	1.70	7.24	18.24	6.42	7.92	3.59	4.42
	Glyceryl monooleate	16.98	3.14	11.50	20.75	2.50	3.60	1.08	1.91
Miglyol® 812	Glyceryl tricaprylate	16.64	2.99	6.54	18.13	6.39	8.04	3.70	4.54
	Glyceryl tricaprate	16.65	2.64	6.15	17.95	6.87	8.53	3.88	4.71
Castor oil	Glyceryl triricinoleate	16.98	2.28	9.38	19.53	4.36	5.80	2.30	3.13
	Glyceryl trioleate	16.53	1.56	4.72	17.26	8.65	10.26	4.57	5.40
	Glyceryl trilinoleate	16.36	1.59	4.76	17.11	8.66	10.24	4.72	5.55
Propanone		14.52	9.90	5.07	18.29	10.01	11.06	8.90	10.33
Ethyl ethanoate		14.84	4.85	8.32	17.69	6.18	7.07	4.68	6.20
n-Butanol		15.69	5.45	14.76	22.22	3.84	2.32	2.85	1.27
Methanol		14.48	11.49	21.44	28.31	12.18	10.49	11.25	9.69
Ethanol		15.10	8.39	18.32	25.18	7.85	6.09	6.98	5.32
Isopopanol		14.18	5.37	14.66	21.09	6.42	5.28	3.79	2.68

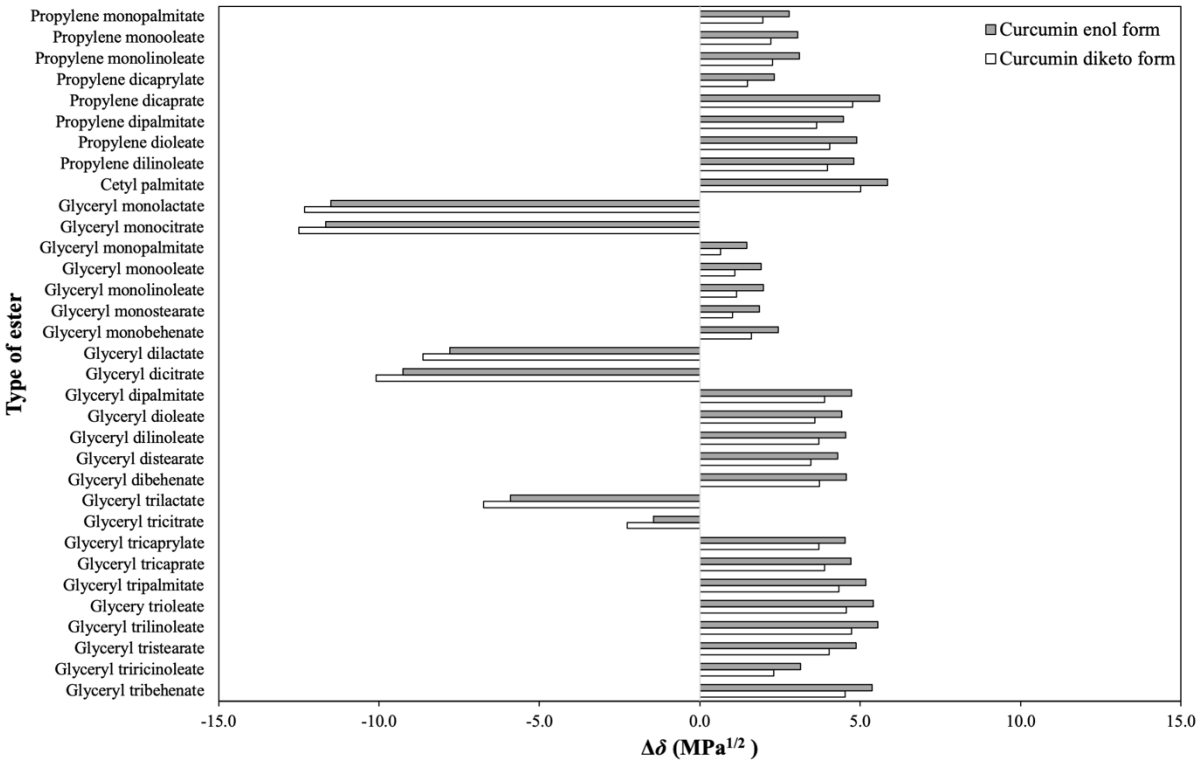

Fig. A1.1. Difference of the Hansen solubility parameter (Δδ) between the two tautomeric forms of curcumin and lipid components.

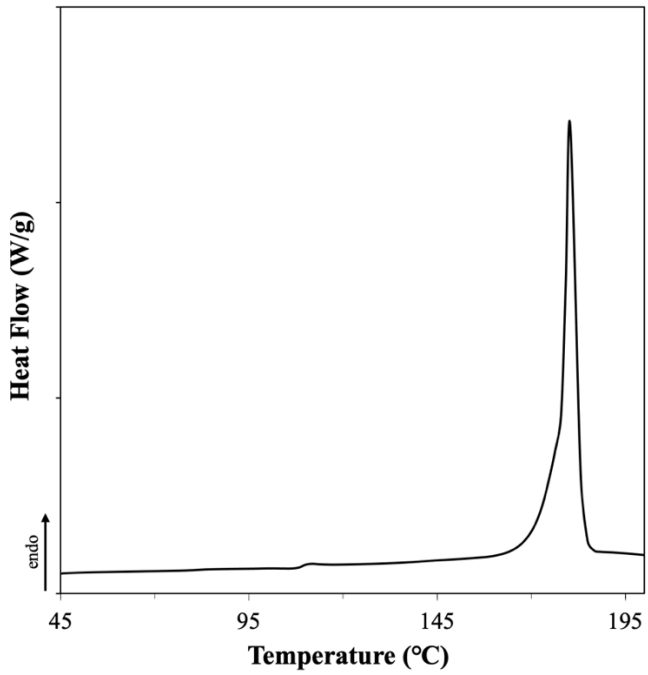

Fig. A1.2. DSC melting curve of pure curcumin.

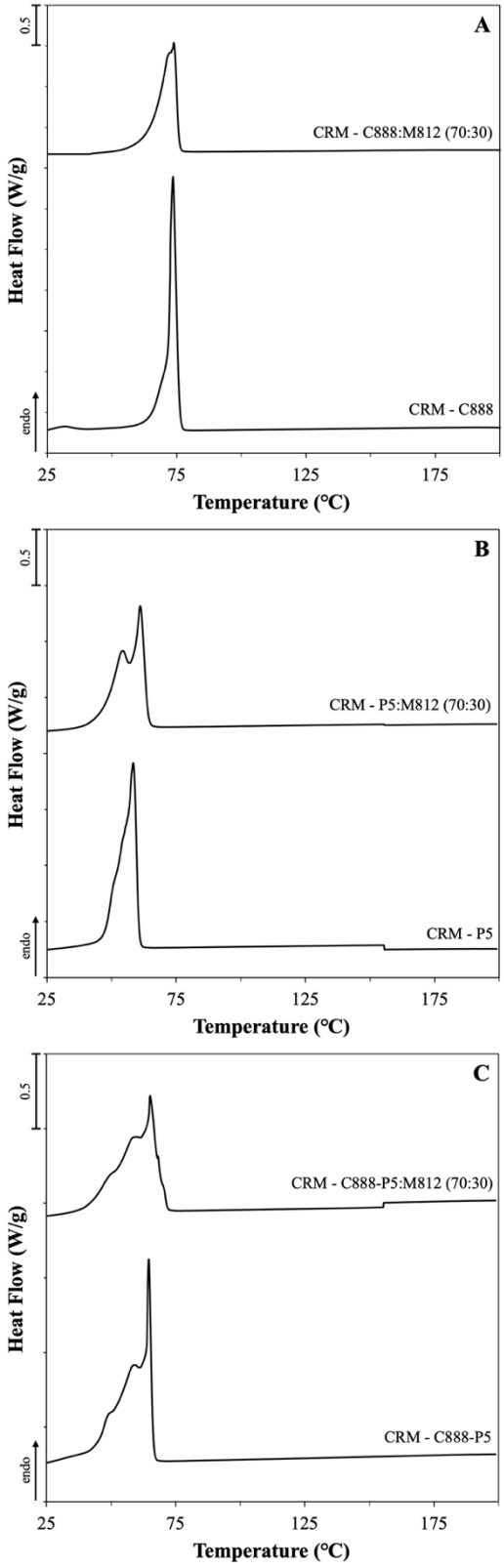

Fig. A1.3. DSC melting curves of binary and ternary solid and liquid lipid mixtures with curcumin (CRM, 0.5% w/w) showing the absence of any thermal events caused by curcumin. The mixtures contain Miglyol®

812 (M812) as the liquid lipid in combination with different solid lipids or blends of them, (A) Compritol® 888 ATO (C888), (B) Precirol® ATO 5 (P5) or (C) blend of the two solid lipids at 50:50 w/w ratio.

Table A1.3. DSC melting and crystallisation parameters of bulk Compritol® 888 ATO (C888) and its physical mixtures with Miglyol® 812 (M812) and curcumin (CRM).

		ΔH (J/g)	T_{max} (°C)	T_{onset} (°C)	ΔT (°C)
C888	**Melting**	131.2±0.0	71.9±0.1	70.2±0.1	1.8±0.1
	Crystallisation	−142.3±0.2	70.2±0.1	71.9±0.0	−1.8±0.0
C888 (after tempering)	**Melting**	125.9±5.6	72.1±0.0	70.2±0.0	1.8±0.0
	Crystallisation	−140.0±2.9	70.0±0.1	71.5±0.1	−1.5±0.0
CRM-C888	**Melting**	133.0±1.5	72.6±0.1	71.4±0.2	1.2±0.1
	Crystallisation	−139.3±2.9	69.9±0.3	71.5±0.5	−1.6±0.2
70:30 C888:M812	**Melting**	169.2±4.7	70.0±2.1	61.6±1.9	8.4±0.2
	Crystallisation	−135.8±3.8	63.9±0.0	65.5±0.3	−1.6±0.2
CRM-70:30 C888:M812	**Melting**	197.9±4.9	70.7±1.9	64.8±0.5	5.9±1.4
	Crystallisation	−143.3±14.3	65.6±0.5	66.7±0.2	−1.1±0.7

Table A1.4. DSC melting and crystallisation parameters of bulk Precirol® ATO 5 (P5) and its physical mixtures with Miglyol® 812 (M812) and curcumin (CRM).

		ΔH (J/g)	T_{max} (°C)	T_{onset} (°C)	ΔT (°C)
P5	**Melting**	176.6±2.2	58.2±0.2	51.5±0.7	6.7±0.9
	Crystallisation	−137.6±6.3	55.6±1.1	58.0±0.5	−2.4±0.6
P5 (after tempering)	**Melting**	155.2±1.4	54.8±0.3	50.8±0.2	4.0±0.6
	Crystallisation	−134.0±2.2	53.7±0.9	56.0±0.7	−2.3±0.2
CRM-P5	**Melting**	142.2±2.4	57.6±0.5	50.2±2.4	7.5±2.9
	Crystallisation	−134.0±1.1	53.4±0.5	55.5±0.8	−2.1±0.3
70:30 P5:M812	**Melting**	188.8±0.1	59.0±0.7	48.2±0.9	10.8±1.4
	Crystallisation	−131.9±1.8	48.6±2.4	52.4±2.2	−2.3±0.2
CRM-70:30 P5:M812	**Melting**	183.1±15.6	59.6±0.8	49.2±1.6	10.4±2.4
	Crystallisation	−128.2±7.0	49.7±0.1	52.6±0.2	−2.9±0.3

Table A1.5. DSC melting and crystallisation parameters of Compritol® 888 ATO (C888) and Precirol® ATO 5 (P5) (50:50 w/w) and its physical mixtures with Miglyol® 812 (M812) and curcumin (CRM). Melting and crystallisation enthalpies in some cases correspond to more than one polymorphic forms present in the samples.

		ΔH (J/g)	T_{max} (°C)	T_{onset} (°C)	ΔT (°C)
C888-P5	**Melting**	132.9±7.0	64.0±0.1	61.5±1.6	2.5±1.5
	Crystallisation	−131.3±6.7	61.6±0.1	62.4±0.1	−0.8±0.2
CRM-C888-P5	**Melting**	130.7±3.0	64.2±0.3	60.5±0.1	3.7±0.2
	Crystallisation	−129.0±2.0	61.6±0.1	62.8±0.2	−1.2±0.1
70:30 C888-P5:M812	**Melting**	157.6±4.3	55.6±2.0	42.7±3.6	12.9±1.6
	Crystallisation	−130.2±4.2	57.7±5.6	58.6±5.9	−1.1±0.3
CRM-70:30 C888-P5:M812	**Melting**	145.0±12.6	59.4±1.6	49.0±5.3	10.5±3.7
	Crystallisation	−126.9±8.9	57.5±0.3	59.2±0.3	−1.7±0.1

Table A1.6. *Z*-average, polydispersity index (PDI) and ζ-potential of different SLN and NLC formulations measured at various time intervals over a storage period of 28 weeks for blank (B-SLN_1 and B-NLC_1–B-NLC_3) and CRM-loaded (SLN_1 and NLC_1–NLC_3) formulations, and 4 weeks for formulations SLN_2–SLN_5 and NLC_4–NLC_5 at 4°C.

Formulation	Storage period (weeks)	*Z*-average (nm)	PDI	ζ-potential (mV)
B-SLN_1	0	158.9±10.6	0.20±0.02	−23.0±1.3
	1	162.0±12.4	0.18±0.03	−23.0±1.4
	4	161.7±10.7	0.20±0.04	−21.9±2.0
	28	165.7±13.5	0.20±0.03	−19.2±1.6
B-NLC_1	0	160.5±3.8	0.16±0.02	−22.3±1.9
	1	164.8±4.4	0.17±0.03	−23.1±2.5
	4	167.9±2.8	0.15±0.03	−21.0±0.3
	28	177.0±11.7	0.19±0.07	−20.6±0.6
B-NLC_2	0	140.4±20.1	0.15±0.02	−19.5±2.6
	1	142.0±20.5	0.15±0.02	−21.8±0.6
	4	144.2±19.1	0.15±0.02	−21.3±2.3
	28	149.3±21.5	0.16±0.03	−18.7±1.7
B-NLC_3	0	145.8±3.4	0.12±0.02	−20.1±0.7
	1	148.1±3.5	0.12±0.02	−19.3±0.9

	4	148.7±3.6	0.12±0.02	−19.5±1.2
	28	153.5±4.0	0.12±0.01	−17.6±0.7
SLN_1	0	165.1±2.7	0.20±0.02	−25.2±2.6
	1	167.4±4.1	0.20±0.02	−22.5±1.4
	4	168.8±3.3	0.20±0.02	−24.5±0.7
	28	173.9±3.6	0.21±0.01	−20.7±1.2
NLC_1	0	165.4±5.3	0.16±0.02	−25.0±3.0
	1	168.3±5.6	0.17±0.02	−21.6±1.2
	4	172.9±6.5	0.16±0.03	−23.6±1.6
	28	179.9±4.4	0.19±0.01	−20.0±0.7
NLC_2	0	162.5±6.5	0.13±0.01	−21.7±1.3
	1	167.6±9.4	0.14±0.01	−21.5±0.5
	4	170.2±7.0	0.14±0.00	−21.9±1.0
	28	176.3±8.2	0.15±0.01	−18.3±0.7
NLC_3	0	163.2±3.8	0.12±0.01	−20.5±0.7
	1	167.1±1.7	0.12±0.01	−20.7±0.1
	4	176.4±8.5	0.16±0.05	−20.5±0.8
	28	173.9±4.3	0.13±0.01	−21.0±0.7
SLN_2	0	176.0±9.6	0.28±0.04	−32.7±0.9
	1	162.6±3.4	0.23±0.01	−29.8±1.5
	4	160.0±2.8	0.22±0.01	−30.3±0.4
NLC_4	0	114.4±7.1	0.14±0.04	−26.0±2.7
	1	114.6±7.6	0.17±0.01	−25.3±1.9
	4	115.3±7.0	0.16±0.01	−26.2±0.9
SLN_3	0	170.9±15.2	0.23±0.01	−27.6±1.4
	1	174.5±14.1	0.22±0.02	−26.8±2.3
	4	180.7±15.7	0.24±0.01	−27.1±0.5
NLC_5	0	136.2±2.5	0.19±0.01	−24.4±1.9
	1	137.5±2.7	0.18±0.01	−24.9±1.5
	4	141.0±2.1	0.18±0.01	−22.4±1.4
SLN_4	0	343.9±26.5	0.24±0.03	−29.0±2.8
	1	353.5±12.6	0.28±0.03	−26.9±0.7
	4	256.0±19.3	0.26±0.01	−23.2±3.9
SLN_5	0	139.7±1.9	0.20±0.01	−24.4±0.7
	1	139.9±2.2	0.20±0.01	−26.2±1.7
	4	142.9±2.8	0.21±0.01	−25.1±2.6

Table A1.7. DSC melting and crystallisation parameters of SLN an NLC aqueous dispersions after prolonged storage at 4°C. The measurements were performed 28 weeks for blank (B-SLN_1 and B-NLC_1–B-NLC_3) and CRM-loaded (SLN_1 and NLC_1–NLC_3) formulations, and 4 weeks for formulations SLN_2–SLN_5 and NLC_4–NLC_5 after production. Enthalpy values (ΔH) reflect the total enthalpy measured after integration of all thermal events present.

		ΔH (J/g)	T_{max} (°C)	T_{onset} (°C)	ΔT (°C)	RI
B-SLN_1	**Melting**	145.4±6.8	70.6±0.1	65.5±0.5	5.1±0.4	110.9±5.2
	Crystallisation	−146.5±6.4	58.4±0.3	60.7±0.3	−2.3±0.1	
B-NLC_1	**Melting**	137.1±10.0	68.8±0.8	61.5±3.0	7.3±3.8	89.4±6.5
	Crystallisation	−133.4±8.9	53.4±3.1	58.7±0.6	−4.8±2.4	
B-NLC_2	**Melting**	121.0±0.7	66.6±4.0	49.1±1.9	17.5±1.5	78.9±0.5
	Crystallisation	−114.9±3.6	51.8±0.1	57.6±0.5	−5.8±0.6	
B-NLC_3	**Melting**	98.0±0.7	61.3±0.2	45.3±0.2	16.0±0.4	63.9±0.5
	Crystallisation	−99.8±2.8	51.3±0.2	53.3±0.5	−2.0±0.7	
SLN_1	**Melting**	138.6±5.0	70.8±0.2	65.7±0.1	5.1±0.1	105.6±3.8
	Crystallisation	−142.7±0.6	58.3±0.1	60.5±0.3	−2.2±0.4	
NLC_1	**Melting**	143.1±6.8	70.7±0.1	61.7±0.0	9.1±0.1	98.2±4.6
	Crystallisation	−140.1±3.1	56.9±0.1	59.5±0.0	−2.7±0.1	
NLC_2	**Melting**	147.0±8.4	69.4±0.0	46.9±1.0	22.5±0.0	89.7±5.1
	Crystallisation	−138.0±5.4	51.2±0.0	58.3±0.1	−7.1±0.2	
NLC_3	**Melting**	129.1±3.1	61.1±2.0	46.2±0.2	14.9±2.2	68.9±1.6
	Crystallisation	−129.7±6.2	50.6±0.1	53.7±0.5	−3.1±0.4	
SLN_2	**Melting**	158.9±4.6	52.3±0.1	47.5±0.5	4.8±0.4	101.2±1.3
	Crystallisation	−139.4±6.5	36.0±0.4	42.4±0.3	−6.4±0.7	
NLC_4	**Melting**	155.7±0.6	45.4±4.6	34.0±0.8	11.5±3.8	61.0±0.2
	Crystallisation	−121.3±7.4	31.6±0.5	36.5±0.3	−5.0±0.8	
SLN_3	**Melting**	148.8±0.1	61.5±0.4	50.5±0.4	11.0±0.8	104.8±11.7
	Crystallisation	−123.7±1.9	49.8±0.9	52.9±0.9	−3.3±0.1	
NLC_5	**Melting**	145.1±11.1	53.0±0.1	37.0±1.1	16.0±1.2	65.7±5.0
	Crystallisation	−109.5±0.6	43.4±0.0	46.1±0.3	−2.7±0.4	
SLN_4	**Melting**	149.6±4.0	71.3±0.1	69.2±0.1	2.1±0.1	108.4±2.9
	Crystallisation	−148.0±3.6	62.0±0.1	64.2±0.1	−2.2±0.0	
SLN_5	**Melting**	153.0±6.4	71.1±0.0	68.7±0.2	2.4±0.2	110.9±4.6
	Crystallisation	−156.1±8.1	65.4±0.1	67.0±0.0	−1.7±0.0	

Chapter 4

Lipid particles of dual functionality at emulsion interfaces. Part I: Pickering functionality

Published as:

G.I. Sakellari, I. Zafeiri, H. Batchelor, F. Spyropoulos, Solid lipid nanoparticles and nanostructured lipid carriers of dual functionality at emulsion interfaces. Part I: Pickering stabilisation functionality, Colloids Surf A Physicochem Eng Asp. (2022) 130135.

Synopsis

Solid lipid nanoparticles and nanostructured lipid carriers are two types of lipid nanoparticulate systems, that have been primarily studied for their capability to function as active carriers, and only more recently utilised in Pickering emulsion stabilisation. Unveiling the factors that impact upon the lipid particle characteristics related to their Pickering functionality could enable the development of a liquid formulation with tailored microstructure and potentially the capacity to display a two-fold performance. In part I, this work investigates how certain formulation characteristics, namely solid-to-liquid lipid mass ratio and presence of unadsorbed surfactant in the aqueous carrier phase, affect the structural properties of the lipid particles, and in turn how these influence their Pickering stabilisation capacity. The effect of the formulation parameters was assessed in terms of the wettability and physicochemical properties of the lipid particles, including particle size, crystallinity and interfacial behaviour. Lipid particles fabricated with higher liquid lipid content (70% w/w) were shown to be more hydrophilic and have lower surfactant decoration at their surface compared to particles containing lower or no liquid lipid in their crystalline matrix. The emulsion stabilisation ability through a Pickering mechanism was confirmed for all types of lipid particles using polarised microscopy. Increasing liquid lipid content and removal of excess surfactant did not compromise the particle stabilisation capacity, though emulsion droplets of larger sizes were initially acquired in the latter case. The particle-stabilised emulsions maintained their physical integrity, with particles retaining close association with the emulsion interface over a storage period of 12 weeks.

4.1 Introduction

Emulsions stabilised by colloidal particles offer the versatility required by multi-delivery formulations, not only due to the superior Pickering stabilisation [1,2], but also for their potential to enable the segregated co-encapsulation of actives within discrete 'compartments' of their microstructure [3–5]. Within this scope, the aptitude of solid lipid nanoparticles (SLNs) and nanostructured lipid carriers (NLCs) to function as active carriers [6–9] and Pickering emulsion stabilisers [10–13] in tandem within a single formulation has only been recently explored [3,14]. Therefore, there is a dearth of research on the effect of the particles' formulation characteristics and structural properties influence on this dual functionality, and how these both can be controlled/manipulated (without compromising one another). Within the limited number of particle characteristics already identified, the composition of the lipid matrix and the type and concentration of surfactant used have been shown to greatly impact the long-term stability of the SLNs within the emulsion systems, with the occurrence of solid matter loss phenomena and weakening of their structural integrity, that could in turn impinge upon their Pickering functionality. For SLNs fabricated with either cetyl palmitate or tristearin, it was shown that over time particle desorption from the interface of the emulsions stabilised with the latter was recorded [11]. Schröder *et al*. [15] showed that lath-like SLNs, formed jammed interfacial layers and three-dimensional networks in the continuous phase of the emulsions, whereas thin interfacial layers were observed when NLCs with platelet-like morphology were employed. Other studies have discussed the importance of particle wettability [10,13,16,17], and more specifically how changes in the surfactant type and concentration can cause variations in the resulting interfacial layer morphology and SLN hydrophilicity/hydrophobicity [12,18], with improved emulsion stability induced by increased surfactant usage [18]. The presence of excess surfactant in a continuous phase that also contains lipid particles can impact the affinity

that the latter have for the emulsion interface. This has been shown for different particulate systems [19–20], suggesting that the use of surfactants with higher HLB value and concentration can lead to further interfacial tension reduction and improved stability. In lipid particle-stabilised emulsions, regardless of whether the SLNs are added in a pre-formulated emulsion [21] or if the emulsion is fabricated with the continuous phase comprising of the lipid particles prior or post-removal of excess unadsorbed surfactant [18,22], a fraction of the surface active species used to form the SLNs has been proposed [22] to migrate to the droplets' interfaces, ultimately creating a mixed emulsifier system (stabilised by both colloidal solid structures and surface active molecules).

The aim of part I of this study is to enhance understanding regarding the formulation characteristics of lipid (both SLN and NLC) particles that affect their interfacial properties and consequently their functionality as Pickering emulsion stabilisers. Hence, part of the work presented here focuses on the investigation of the extent to which the removal of excess unbound surfactant from the aqueous phase carrying the lipid particles affects their physicochemical characteristics, that have been known to impact on their Pickering functionality. The effect of the lipid composition and remnant surfactant removal on the particle wettability were also assessed. Thereafter, SLNs and NLCs with varying solid-to-liquid lipid mass ratios used as produced and after removal of unbound surfactant, were studied for their ability to stabilise o/w emulsions. Lipid particle-stabilised emulsions were characterised for their size distribution, zeta potential and long-term storage stability. Consequently, the insight gained from the findings of this study could contribute to extending the approaches that can be devised to intervene at a lipid particle level and manipulate the properties that enable the successful realisation of a Pickering functionality. As a lot of these characteristics have also

been shown to impact on the capacity of lipid particles to carry and deliver actives, this work would also pave the way to successfully realise the dual functionality envisaged.

4.2 Materials and methods

4.2.1 Materials

Glyceryl behenate (Compritol® 888 ATO) was kindly provided from Gattefossé (Saint-Priest, France). Medium chain triglycerides (MCTs) (Miglyol® 812) was a kind gift from IOI Oleo (IOI Oleochemicals GmbH, Germany). Polyoxyethylene sorbitan monooleate (Tween® 80), perylene and Nile Red were purchased from Sigma-Aldrich (Sigma-Aldrich, UK). Sunflower oil was purchased from a local supermarket and stored in a closed container at ambient temperature in the dark. The consistency of the oil used in this work was monitored through interfacial tension measurements between distilled water and the used commercial oil (at least on a weekly basis). No significant deviation in the equilibrium value of the interfacial tension was observed (21.8 ± 0.3 mN/m). All chemicals were used without further purification. Double distilled water from Milli-Q systems (Millipore, Watford, UK) was used during all sample preparation processes and characterisation measurements.

4.2.2 Preparation of lipid particles

The lipid nanoparticle dispersions were fabricated following a protocol that is fully described elsewhere [6]. Briefly, solid and different solid-to-liquid lipid mass ratio (9:1, 8:2 and 7:3) lipid melts were processed with a melt-emulsification-ultrasonication method followed by quench cooling to obtain the crystalline lipid particles. All systems were composed of 2.5% w/w total

lipid phase, and 1.2% w/w surfactant concentration in distilled water. Removal of excess unbound surfactant from the lipid dispersions was achieved through dialysis. A known amount of each dispersion was added in a cellulose dialysis membrane (43 mm width, 14 kDa M.W. cut-off, Sigma-Aldrich Company Ltd., Dorset, UK,), that was pre-hydrated overnight, and immersed in distilled water under constant stirring at room temperature. The dialysis medium was changed every 24 hours, and the process was continued until an equilibrium surface tension value similar to that of distilled water was obtained (~ 21 days). Surface tension measurements were performed with a profile analysis tensiometer (PAT-1M, Sinterface Technologies, Berlin, Germany). Further information about the instrument setup is given in a later section (Section 4.2.5). Following that, the lipid dispersions were retrieved from the tubing and diluted to their initial mass with distilled water, to maintain the initial lipid phase concentration. All samples were stored at 4°C until further analysis.

4.2.3 Particle size and ζ-potential measurements

Dynamic light scattering (DLS) was employed to determine the lipid particle size characteristics of dialysed and undialysed dispersions, and zeta potential (ζ-potential) of both lipid particles and their respective o/w emulsion systems using a Zetasizer Nano ZS (Malvern Instruments, UK). *Z*-average, polydispersity index (PDI) and ζ-potential values were acquired to assess the stability of the lipid particles dispersions after dialysis. All measurements were performed at a backscattering angle of 173° at 25°C, and samples were appropriately diluted with distilled water to avoid multiple scattering phenomena. The refractive indices for the materials used were determined by a refractometer (J357 series, Rudolph Research Analytical, USA) at 20°C, and used accordingly [6]. For distilled water, the refractive index used was 1.33 and the absorption index was set at 0.01. Measurements were performed immediately after

preparation and over time in triplicate, and the average values with standard deviation (±S.D.) are presented. Representative size distributions of lipid particles used as produced and after dialysis were also acquired with laser diffraction (LD) using a Mastersizer 2000 (Malvern Instruments, UK) for comparison purposes. A more detailed description of the technique is provided below (Section 4.2.8).

4.2.4 Thermal analysis

The thermal behaviour of the lipid particle dispersions used as produced and after dialysis was determined by Differential Scanning Calorimetry (DSC) using a Setaram μDSC3 evo microcalorimeter (Setaram Instrumentation, France). The temperature was cycled between 20 and 80°C at a heating rate of 1.2 °C/min. Information about peak temperatures and melting enthalpies was obtained using the Calisto Processing software. All enthalpy values and thermograms reported, are normalised for the amount of crystallising material present in the samples. The thermograms of the lipid particle dispersions were obtained with the reference cell being filled with equal amount of distilled water. All measurements were performed in at least triplicate on three individually prepared samples.

4.2.5 Surface and interfacial tension measurements

Interfacial properties at the oil/water interface were obtained with the pendant drop method utilising a profile analysis tensiometer (PAT-1M, Sinterface Technologies, Berlin, German), at 20°C. A drop of the lipid particle dispersions (prior and after dialysis) was suspended via a straight stainless-steel capillary (3 mm outer diameter) in the sunflower oil phase contained in a quartz cuvette, with the cross-sectioned surface area remaining constant at 27 mm^2. When

surface tension measurements were performed, the quartz cuvette was used empty. Data were collected until equilibrium was reached (standard deviation of the last twenty measurements was smaller than 0.05 mN/m). Density values of the samples were determined using a densitometer (Densito, Mettler Toledo, US), at 20°C. All measurements were conducted in at least triplicate on three individually prepared samples.

4.2.6 Contact angle measurements

The effect of the lipid composition on wettability was assessed by melting (approximately at 80°C) glyceryl behenate singly or in blends with medium chain triglycerides at different solid-to-liquid lipid mass ratios (9:1, 8:2, 7:3) and let to cool down at room temperature on a hydrophobic surface provided by a polydimethylosiloxane (PDMS) film to obtain a smoothly solidified lipid layer. The crystallised lipid was used to determine the contact angle (θ) of an oil droplet on the lipid surface following a previously proposed method with slight modifications [10]. Briefly, flat discs of solidified lipid or lipid blends were placed on top of a water-containing quartz cuvette, and a small volume (~ 10 μl) of sunflower oil was injected through a very small slit created during the crystallisation of the lipids using a micropipette, to create a pendant oil droplet. Images were acquired once equilibrium was reached, using a profile analysis tensiometer (PAT-1M, Sinterface Technologies, Berlin, German) and the contact angles were determined with the angle-measuring tool of ImageJ. Similarly, to investigate the effect of the presence of excess surfactant on the hydrophilicity of the lipid particles, lipid particle dispersions used as produced and after dialysis were freeze dried and the powders obtained were compressed to obtain flat pellets of ~2 mm thickness using a universal material testing machine (Z030, Zwick Roell, Germany). A sessile drop (~ 10 μl) of distilled water was deposited on the surface of the pellet and the contact angle was measured

according to the method described above. All measurements were performed in at least triplicate, the contact angle on both the left and right side were measured and the average θ values were calculated.

The free energy of displacement (ΔG_d) for a particle at the oil-water interface was calculated using the following equation [10]:

$$\Delta G_{\mathrm{d}} = \pi r^2 \gamma_{ow} (1 - |cos\theta|)^2 \quad (4.1)$$

where r is the particle radius calculated from the *Z*-average values, and θ is the contact angle as determined above. The sunflower oil/water interfacial tension γ_{ow} was determined using the method described in the previous section (15.2 mN/m). In addition, the solid lipid-water γ_{sw} and solid lipid-oil γ_{so} interfacial tensions were calculated as follows [10,23]:

$$\cos\theta = \frac{(0.015\gamma_{ow} - 2)(\gamma_{ow}\gamma_{sw})^{1/2} + \gamma_{ow}}{\gamma_{ow}[0.015(\gamma_{ow}\gamma_{sw})^{1/2} - 1]} \quad (4.2)$$

$$\gamma_{ow}\cos\theta = \gamma_{sw} - \gamma_{so} \quad (4.3)$$

4.2.7 Preparation of oil-in-water emulsions

Oil-in-water (o/w) emulsions were prepared with 90% (w/w) aqueous phase containing any of the different lipid nanoparticle systems and 10% (w/w) sunflower oil phase. Emulsification was realised using a high intensity ultrasonic Vibra-cell™ VC 505 processor (Sonics & Materials, Inc., CT, USA), operating continuously at 750 Watt and 20 kHz, at a sonication amplitude of 95% of the total power over a period of 30 seconds. When different emulsification methods were assessed for their effect on the obtained droplet size, the parameters are summarised in

Fig. 4.6. Samples were immersed in an ice bath during processing, to avoid shear-induced heating. The produced systems were stored at 4°C until further analysis.

4.2.8 Droplet size measurements

The droplet size of the o/w emulsion droplets and their stability over time was assessed by laser diffraction (LD) using a Mastersizer 2000 (Malvern Instruments, UK) equipped with a Hydro SM manual small volume sample dispersion unit. Measurement parameters including RI values and absorption index were kept the same as for the particle size measurements described above. The stirrer speed was set at 1300 rpm during all measurements, and all samples were mixed by hand before analysis. The refractive index of sunflower oil was set at 1.47. Samples were analysed immediately after production and after 1, 4, 8 and 12 weeks. All measurements were performed in triplicate on three individually prepared samples.

4.2.9 Imaging

The microstructure of the prepared o/w emulsions was visualised through polarised light microscopy and confocal laser scanning microscopy (CLSM), to confirm the Pickering performance of the lipid particles. The confocal microscopy images were obtained using a confocal laser light microscope (Leica TCS SPE, Heidelberg, Germany), equipped with a laser operating at a wavelength of 532 nm. For the visualisation of the different components of the emulsion systems, dyes with different excitation wavelengths were employed. Perylene (0.005% w/w) was used to stain the lipid particle dispersions, by addition to the lipid melt phase prior to ultrasonication, and Nile Red (0.005% w/w) was added to the sunflower oil phase, prior to emulsification. The excitation wavelength for Nile Red was set at 488 nm and 405 nm for perylene. The polarised light microscopy images were acquired with an optical microscope

(DM 2500 LED, Leica®, CH). When larger emulsion droplets were visualised using both analyses, the emulsions were prepared using a low level of shear provided by a high-shear mixer (Silverson L5 M, Silverson Machines Ltd, UK), operating at 9000 rpm for 2 min, and the images were acquired with a 100x oil immersion lens using a coverslip to cover the sample.

4.2.10 Statistical analysis

Samples were analysed in at least triplicate and averages are reported with standard deviation. Figures depict the calculated average value with error bars showing the standard deviation above and below the average. Comparison of means was conducted by ANOVA analysis followed by an all pairwise multiple comparison test using the Student-Newman-Keuls Method (SigmaPlot 14.5). The differences were considered statistically significant when $p \leq 0.05$.

4.3 Results and discussion

4.3.1 The effect of excess surfactant on the physicochemical characteristics of lipid particles

Among the parameters that can affect the physicochemical properties of the lipid particles while in an aqueous dispersion environment, and subsequently their effectiveness to act as Pickering emulsion stabilisers, is the presence of excess unadsorbed surfactant in their continuous phase. A sufficient excess concentration of surfactant in the aqueous phase carrying the lipid particles is required during their fabrication, to ensure rapid adsorption of the surfactant molecules on the particle surfaces, which is a crucial parameter in preventing particle-particle collisions and particle destabilisation phenomena [24]. Therefore, previously studied and characterised SLNs and NLCs of different solid-to-liquid lipid mass ratios (9:1, 8:2 and 7:3) were dialysed to

remove any excess surface active species. The process of the unadsorbed surfactant removal was monitored with surface tension measurements of the dissolution medium (Fig. 4.1), and the effect that this had on the size, ζ-potential, thermal behaviour and interfacial tension reduction ability of the particles was investigated (Fig. 4.2–4.4).

The amount of surface active species associated with the surface of the lipid particles is an important parameter that can dictate not only their functionalities, but also their long-term physical stability. In this study, investigation of the surface load (Γ_s) can provide information regarding the relative association of the surfactant with the lipid matrix composition, as well as the effect that this has on the interfacial properties of the aqueous lipid particles. As presented in Fig. 4.1A–D, there is progressive flattening of the surface tension curvature for all formulations, with the curves being similar to that of distilled water at 21 days. More specifically, the rate of surfactant loss appeared to be similar for the SLN and 9:1 NLC formulations, and also for the 8:2 and 7:3 NLC systems (inset graphs, Fig. 4.1). The first pair shows an initial fast diffusion rate that only decelerates at day 10, whereas the removal of surfactant for the latter group (8:2 and 7:3 NLCs) seems to occur at a steadier rate. Although based on the available data it is not possible to determine the degree of contribution of each possible mechanism to the observed difference, two factors could be pointed out, according to variations identified in the used systems. The first stems from disparities in the total surface area available, with smaller particle sizes (Fig. 4.2) in the latter pair (particles with the highest liquid lipid content), allowing for a larger surface area to entrap the available surfactant, and hence a lower concentration of Tween® 80 discharging to the acceptor phase. The second could be attributed to differences in the lipid mixtures composition affecting the dynamics of surfactant exchange between the particle surface and the continuous phase, that further impacts the diffusion rate.

In order to compare with literature data, the surface load was calculated using the equation described by Dickinson [25] (see Appendix A2, Equation A2.1). This was done by presuming that the particles are spherical in shape, and following the assumption that the entirety of the available surfactant molecules ($C_{a,max}$) is adsorbed and/or associated with the surface of the particles, based on which the calculated values would correspond to the maximum achievable Γ_s (see Appendix A2). In a study investigating the impact of sonication during crystallisation and liquid lipid content, Ban *et al*. [26] reported that the surface load varied from 6.34 mg/m^2 for the SLN, to 7.50 mg/m^2 belonging to the 7:3 NLC formulation, while there was a proportional relationship between liquid lipid content and surface load. In another work by the same authors [27], increased Γ_s was observed with increasing surfactant concentration until saturation was reached at lower values for surfactants with saturated chains (34 mM) compared to unsaturated (65 mM) on the tristearin (5% w/w) SLN surface. Analogous results of Γ_s increase with increasing surfactant concentration were obtained for tristearin particles (2.5% w/w lipid phase), with values starting at 9 mg/m^2 for 10 mmol/kg concentration of Tween® 60 and Brij® S20, reaching 15 and 19 mg/m^2 for 24 mmol/kg, respectively, and 25 mg/m^2 for 8 mmol/kg Brij® S100 concentration [18]. The Γ_s values calculated here were 9.6 mg/m^2 for the SLN and 9:1 NLC formulations, 8.4 mg/m^2 for the 8:2 NLC and 8.7 mg/m^2 for the 7:3 NLC systems. These values, that correspond to 1.2% w/w (or 10.1 mmol/kg) concentration of Tween® 80 and 2.5% w/w lipid phase, are within the value range reported in literature for similar particle size and lipid phase-to-surfactant mass ratio [24,28]. The fact that they are slightly closer to the higher end of the value spectrum could be attributed to the longer unsaturated hydrophobic tail of Tween® 80, and also the different lipid/surfactant combination used in this study, allowing for greater participation of surfactant molecules in the crystalline lattice of the lipid particles, thus resulting in higher Γ_s [6,27]. Additionally, the presence of lipid

particles that are non-spherical, as suggested by the presence of different polymorphs in the DSC thermograms of the lipid dispersions, could explain the requirement for a higher surfactant concentration to saturate the lipid particle surfaces compared to only spherical structures [24,28–30]. Variations in the surfactant molecule orientation and packing at the particle surface could be the cause of the surface load deviations between the different types of lipid particles [18]. However, it should be highlighted here, that for the Γ_s calculations, several assumptions were made, including sphericity of the particles and considering that the entirety of the available surfactant was associated with the particles. This is not necessarily a realistic representation of the particle state, but rather an attempt to set the scene for the surface coverage of the examined particles using a marginal scenario, as a small but detectable proportion of the initially added surfactant was removed, according to the surface tension measurements. Therefore, to improve the theoretical picture drawn for the quantity of surfactant associated with the particles, the minimum concentration of Tween® 80 ($C_{a,min}$) required to form a monolayer at the interface of the particles was also calculated (see Appendix A2). According to the theoretical calculations, the minimum concentration required to fully cover the particle surface would be 0.5% w/w for the SLN and 9:1 NLC formulations, and 0.6% w/w for the 8:2 and 7:3 NLCs, suggesting that there was an excess of approximately 50% of Tween® 80 concentration used to prepare the particle dispersions (1.2% w/w used during fabrication). Based on both the assumptions for the maximum surface load and the theoretical calculations for the minimum concentration of adsorbed surfactant, it could be hypothesised that the true value of surfactant concentration associated with the particles lies between these two predictions. Due to the hypotheses adopted and the overall theoretical nature of these calculations, the results presented above should only be perceived as a qualitative characterisation, rather than an attempt to quantitively describe the systems.

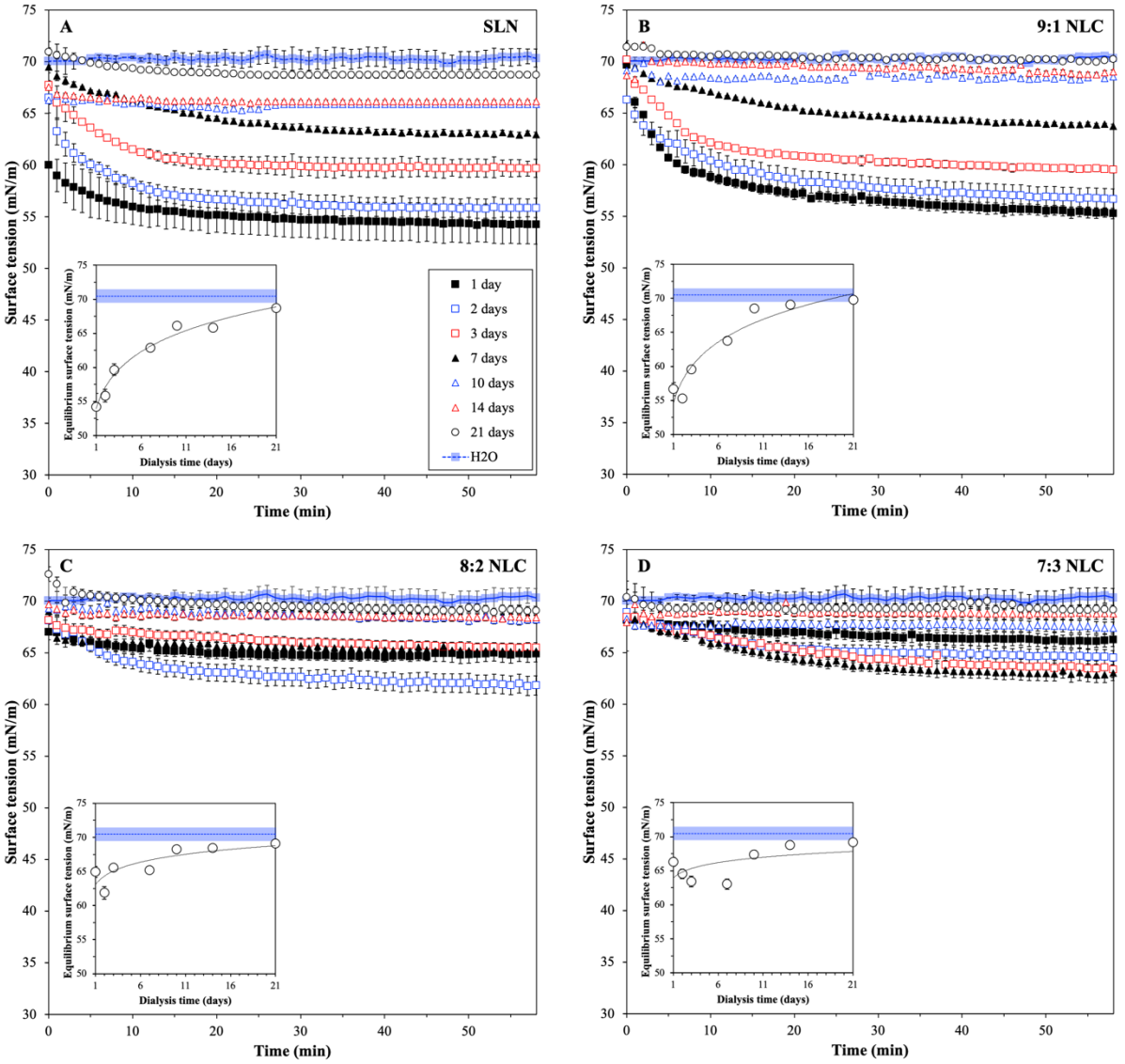

Fig. 4.1. Surface tension of aqueous lipid particle dispersions of SLN (A), 9:1 NLC (B), 8:2 NLC (C) and 7:3 NLC (D) at various time points during dialysis. The inset graphs for each type of lipid particle dispersion depict the time evolution of the equilibrium surface tension values over the dialysis period. The surface tension of distilled water is also presented as a comparison. When not visible, error bars are smaller than symbols.

4.3.1.1 Particle size and zeta potential

Regarding the effect of excess surfactant removal on the size of the lipid particles, it is evident from Fig. 4.2A, that the *Z*-average slightly increased immediately after dialysis for all types of NLCs, while the increase was not statistically significant for the SLNs. Changes in the steric hindrance-induced stability due to the removal of free surfactant molecules, and the osmotic stress applied to the dispersions during the diffusion of the molecules through the dialysis membrane could have promoted flocculation and/or aggregation, as further supported by increase in the PDI values (see Appendix A2, Fig. A2.1). On the other hand, the ζ-potential decreased for all formulations (Fig. 4.2B), with the exception of 8:2 NLC. This could be due to small but considerable for their effect on the ζ-potential, variations in the viscosity of the formulations after removal of excess surfactant, and more prominently, aggregation of the particles after dialysis, as Tween® 80 is a non-ionic surfactant, and thus does not contribute to the charge of the electric double layer. Both the possibility of decrease in the dynamic viscosity values from 1.1 to 1 mPa·s (according to literature data for similar concentrations of surfactant) [31], causing changes in the mobility of the particles [32,33], and the presence of particle aggregation [34,35] could have ultimately resulted in the observed statistically significant decrease of the absolute ζ-potential values. Small but statistically significant differences in both the *Z*-average and ζ-potential values recorded between the different types of particles could have been caused by discrepancies in the arrangement of the hydrophilic heads of the surfactant at the surface of the particles and/or the depth of association with the surface [18,27,36]. The surface of the lipid particles is not fully covered by the surfactant molecules [6], and this is further supported by the negative ζ-potential arising from the free fatty acids at the surface of the particles [37].

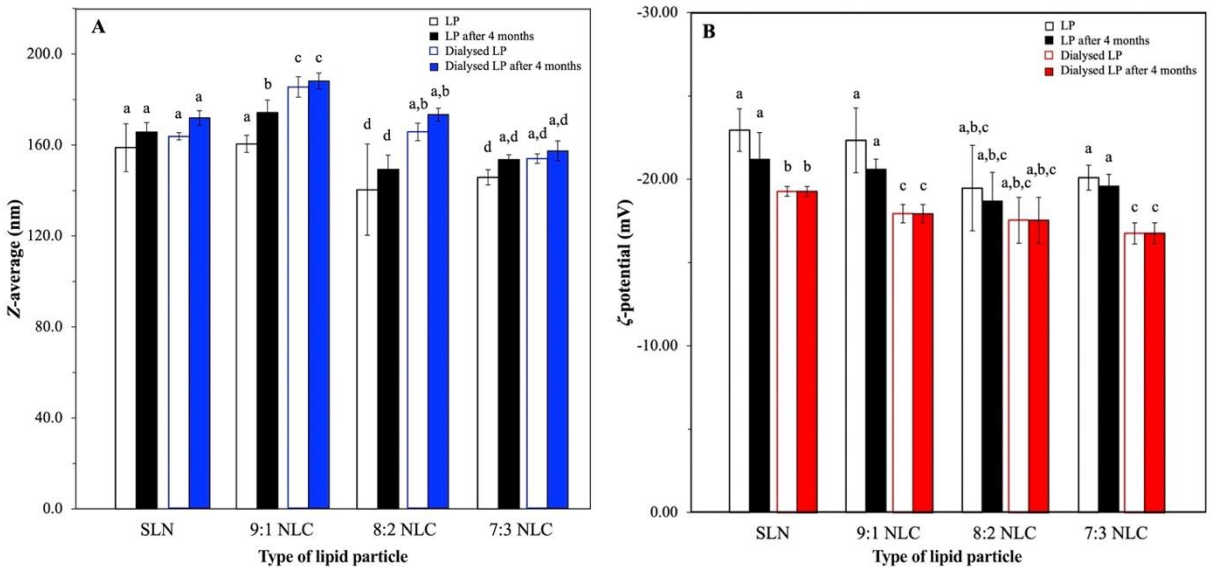

Fig. 4.2. Particle size (*Z*-average) (A) and zeta potential (ζ-potential) (B) of lipid particle dispersions (LP) before and after dialysis measured immediately after production and after 4 months of storage. Identical lowercase letters indicate no significant differences between samples (for p>0.05 and sample size equal to 3).

4.3.1.2 Crystallinity

The crystallinity of the lipid particles was assessed after dialysis to determine changes in the properties of the crystalline matter after surfactant removal (Fig. 4.3). Previous work regarding the SLN and NLC formulations revealed that increase in the liquid lipid concentration leads to increasing loss of lipid phase crystallinity and more pronounced polymorphic transitions, as suggested by the melting enthalpy (Δ*H*), recrystallisation indices (RI) and both the melting and crystallisation thermograms (Fig. 4.3A & B) [6]. Comparing the thermograms of the lipid particle dispersions after preparation and after 4 months of storage following dialysis, no major differences can be identified in their melting and crystallisation profiles, with only very slight shifts of the peaks in some instances. Their ability to maintain their crystallinity is further confirmed by their melting enthalpies for which no statistically significant deviations were

recorded (see Appendix A2, Fig. A2.2). Overall, it appears that removal of excess surfactant from their aqueous phase did not affect their crystalline structure.

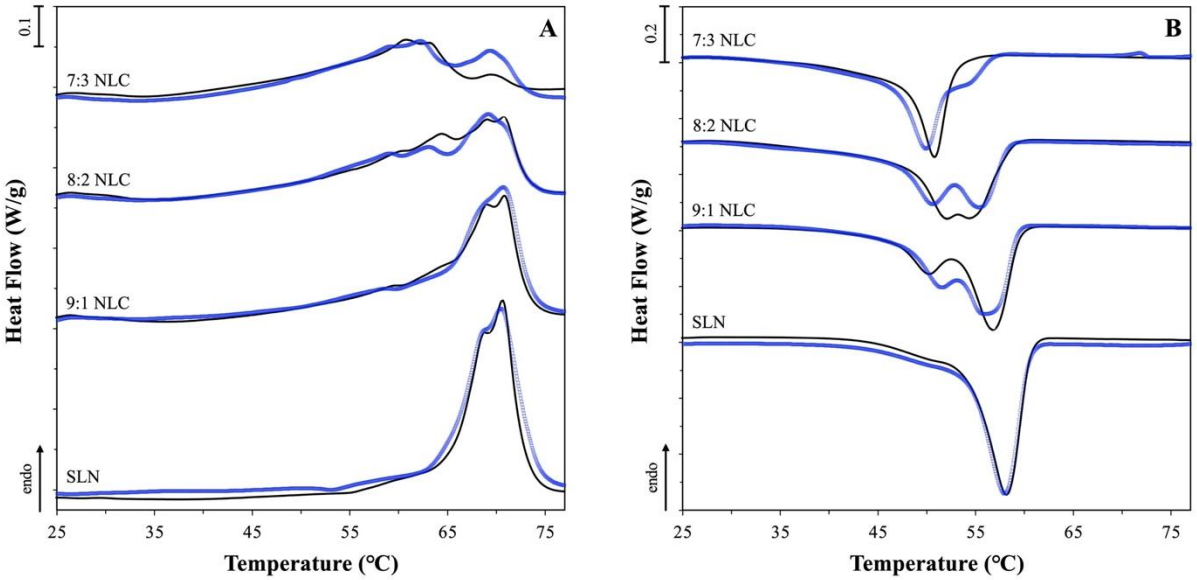

Fig. 4.3. Melting (A) and crystallisation (B) curves of SLN and NLC aqueous dispersions before dialysis (black curve) and after 4 months of storage following removal of excess surfactant (blue curve).

4.3.1.3 Interfacial tension

As part of gaining further insight regarding the capability of the SLN and NLC formulations to exhibit a Pickering functionality, the sunflower oil/water dynamic interfacial tension was assessed using the different lipid particle dispersions as the aqueous phase. In addition, the presence of unadsorbed surfactant in the aqueous continuous phase of the lipid particle dispersions, and its effect on the dynamic interfacial tension reduction was further investigated by comparing the behaviour of the lipid particle systems before and after dialysis (Fig. 4.4).

For particles used as prepared, the interfacial tension reduction ability appears to be not as effective as that of equal concentration of surface active species in aqueous phase (1.2% w/w)

(Fig. 4.4A). Similar data have been previously reported for solid lipid nanoparticles with varying particle sizes, fabricated with different types of lipid materials and with surface active species having a range of distinct characteristics (i.e. molecular weight and/or HLB value) [17,22,38]. The comparison between lipid particles with different solid-to-liquid lipid mass ratio reveals that as the liquid lipid increases, the ability of the system to lower the interfacial tension decreases, with particles containing 20 and 30% w/w liquid lipid having almost identical dynamic interfacial tension curves. More specifically, the SLN formulation reached an equilibrium value of 5 mN/m, 6.6 mN/m was the value for the 9:1 NLC, and 7.2 and 7.3 mN/m were the equilibrium interfacial tension values for the 8:2 and 7:3 NLCs, respectively. The efficiency of the surfactant to alter the interfacial curvature is highly influenced both by the distribution of the surfactant molecules in the dispersion, and also by their packing characteristics [19]. The latter is not only relevant to the molecular packing density at the oil/water interface, but it also relates to potential lipid crystalline network participation [17,38]. In this instance, the interfacial affinity of the lipid particles for the oil/water interface, possibly conferred by their surfactant-decorated surfaces, could be influenced by the level of surfactant decoration. Considering that the only variation between the aqueous lipid particle dispersions is the composition of the lipid matrix, it could be proposed that the higher interfacial tension values for the systems containing higher liquid lipid percentages (9:1, 8:2 and 7:3 NLCs) is the result of the preferential trapping of surfactant molecules in the solid crystal/liquid oil crystal network interfaces. This is in accordance with what was previously hypothesised for the formulations presented here, regarding the relatively high compatibility between the lipid core components, particularly in the presence of increased MCT content and Tween® 80, and the involvement of the latter in the crystalline network, based on DSC data [6]. In terms of the effect of particle size, the results reported are somewhat contradictory to what would be

expected for the larger particle sizes of the SLN and 9:1 NLC formulations. However, the seemingly unsubstantial impact of particle size on the interfacial tension reduction ability of the particles could be due to the much greater effect of the previously discussed parameters.

A more comprehensive understanding of the mechanism via which these systems lower the interfacial tension of the sunflower oil/water interface can be gained through investigation of the behaviour of the dispersions after removal of excess surfactant from the continuous phase. Comparing the obtained curves and equilibrium values, it was observed that only the SLN formulation (dSLN) presents a small but statistically significant increase in interfacial tension after dialysis (Fig. 4.4B). Taking into consideration that only marginal changes were recorded in the particle characteristics after processing, it could be postulated that this is the effect of presence of free surfactant molecules in the continuous phase of the SLN dispersion, possibly due to the high internal crystalline arrangement of the SLN lipid core. On the contrary, the lack of variation in the behaviour of the dialysed NLC formulations compared to the undialysed (9:1 dNLC, 8:2 dNLC and 7:3 dNLC) most likely suggests that the vast majority of surface active species present in the samples are associated with the surface of the lipid particles, which are therefore not available to interact with the oil/water interface. Exchange of surfactant molecules between the lipid particles and the o/w interface has been proposed as a possible phenomenon in such dynamic systems, though it would entail that the surfactant molecules are easily displaced from the particle surface, due to their unfavourable trapping in the lipid core [21,22,39]. There is very limited literature discussing the interfacial tension alteration mechanism in the presence of lipid particles. Zaferi *et* al.[38] and Li *et* al.[17] showed that in the presence of SLNs, the interfacial tension reduction potential of the surfactant is lower than that of the pure surface active species solution in the absence of SLNs. Dieng *et al*.[22] suggested that once the SLNs arrive at the oil/water interface, part of the adsorbed surfactant

(in which case was Kolliphor® HS15) is released, resulting in a conjugated particle/surfactant molecules adsorption mechanism. Linking the contradictory observations made here, regarding the greater interfacial tension reduction ability of the SLNs and the higher surface load values reported previously (Section 4.3.1), it is suggested that the level of decoration of the surfactant molecules on the surface of the particles is the interfacial tension reduction limiting factor, rather than the concentration of free molecules. Although no final conclusions can be drawn about the exact mechanism of participation of the lipid particles in the interfacial tension (e.g. occurrence of inter-particle or particle/free surfactant molecule interactions), it is clear that changes in the composition of the lipid particles and therefore in the adsorbed surfactant arrangement, and co-adsorption of particles and surfactant play an important role in the final interfacial curvature.

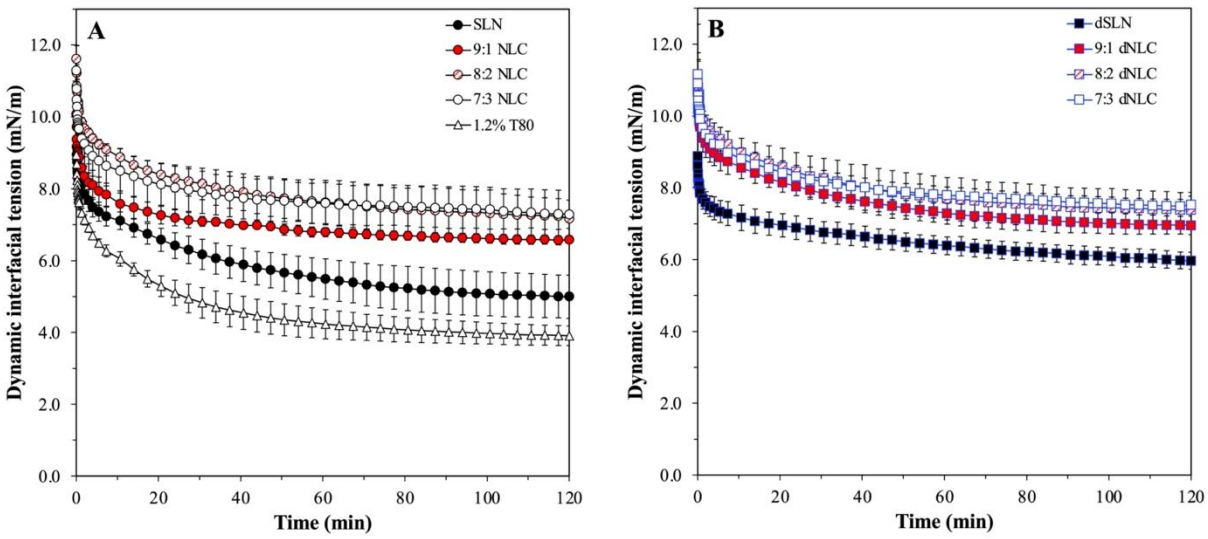

Fig. 4.4. Dynamic interfacial tension of aqueous dispersions of SLN and NLC formulations before (A) and after dialysis (B). The curve of pure Tween® 80 (T80) solution with similar concentration (1.2% w/w) as the one used for the formulation of the dispersions is also presented for comparison. Data points are the average of three measurements and error bars represent the standard deviation.

4.3.2 Wettability

Another parameter that was evaluated regarding the ability of the particles to stabilise emulsion droplets and their positioning at the sunflower oil/water interface was their wettability [40–42]. Following the method described by Gupta *et al.*[10], the effect of increasing liquid lipid content (0 to 30% w/w) on the contact angle of a sunflower oil droplet at the lipid mixture/water interface was initially evaluated (Fig. 4.5A). The contact angle values ranged from 130.6° for the pure glyceryl behenate (SLN) surface to 147.6° for the 30% w/w MCTs concentration (7:3 NLC). Homogeneous distribution of MCTs in the mixtures with glyceryl behenate led to progressively increased hydrophilicity of the blend, resulting in higher contact angles and thus lower wettability by the hydrophobic sunflower oil droplet. Using the experimental contact angle and γ_{ow} values and *Equations 2 & 3*, the γ_{sw} and γ_{so} were calculated for each system. In every case, the condition $\gamma_{ow} > \gamma_{so} - \gamma_{sw}$ was satisfied, indicating efficient wetting by both phases, and positioning of the particles at the oil/water interface. Furthermore, the free energy of displacement ΔG_d was found to be an order of magnitude lower than that for similar systems reported in literature [10], ranging between $3.7 \times 10^4 \times k_B T$ for glyceryl behenate to $0.62 \times 10^4 \times k_B T$ for the 30% w/w liquid lipid content blend. Though not vastly lower, the ΔG_d values show a decline with increasing MCTs content (Fig. 4.5A). Since ΔG_d depends on the square of the particle radius and the $\cos\theta$, it is expected to have lower values for smaller particle radii and larger contact angles, which explains the trend observed for increasing liquid lipid content.

Besides the nature of the lipid used itself, the level of surfactant decoration on the particle and any excess surfactant within the aqueous carrier system could also contribute to the affinity between a lipid particle and an interface. It has been shown that incorporation of surfactant within the lipid particles in the first place can lower the water/lipid particle contact angle by

reducing the hydrophobicity of the bulk lipid [43]. Delving further into the effect of the degree of surfactant decoration on a lipid particle, it has been proposed that surface load can be used as a means of controlling the obtained ΔG_d and particle wettability, by altering their hydrophilicity [18]. Therefore, it would be expected that as the proportion of surfactant associated with the particles increases with increasing liquid lipid content, based on previous indications provided by interfacial tension measurements, so would their hydrophilicity. Indeed, this was confirmed by the decreasing contact angle values obtained for increasing MCTs content (Fig. 4.5B). Notably, the difference in the hydrophilicity of the surface was statistically significant only for the SLN and 9:1 NLC formulations, when freeze dried powders were used after removal of excess surfactant, further reinforcing the evidence provided above regarding the influence of the lipid composition on the favourable surfactant entrapment. Overall, based on the contact angle data and the high energy of desorption obtained for all systems, it could be postulated that the particles fabricated with these lipid combinations will be preferentially wetted by the aqueous phase and therefore will be able to effectively stabilise o/w emulsion droplets [40,44].

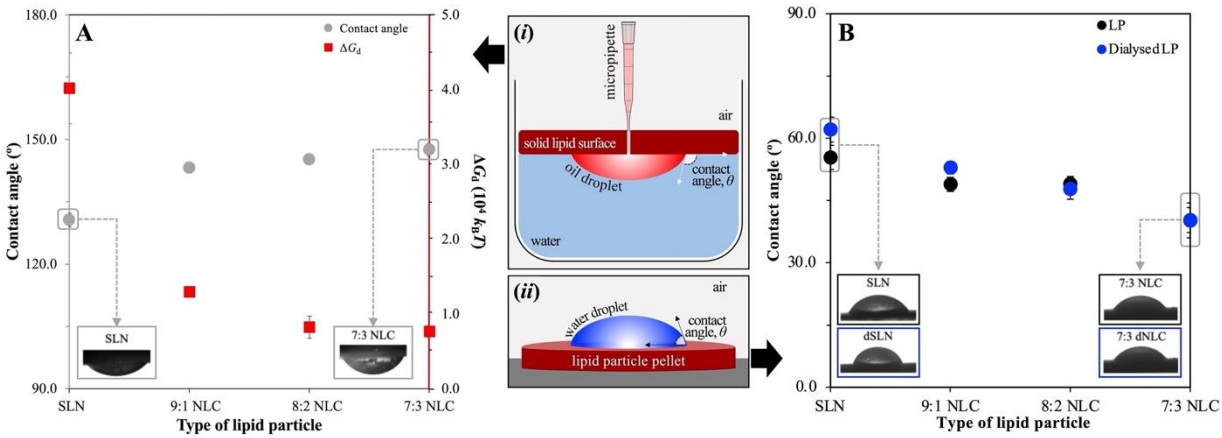

Fig. 4.5. Contact angle for a sunflower oil droplet at the water/solid interface, and displacement energy (ΔG_d) of the lipid particles at increasing liquid lipid concentration (0 to 30% w/w) (A). The lipid content

used to prepare the solid interfaces employed for the contact angle measurements represent the lipid matrix composition of the respective lipid particles. Contact angle for a water droplet at the air/particle interface formed by freeze dried powder of lipid particles used as produced and after dialysis (B). The experimental setup is also provided in a schematic representation. When not visible, error bars are smaller than symbols.

4.3.3 Production and characterisation of particle stabilised emulsions

4.3.3.1 Processing of emulsions

The ability of lipid particles to stabilise o/w emulsions through a Pickering mechanism was investigated using SLNs as the continuous phase and sunflower oil as the dispersed phase. During preliminary studies, emulsions in the presence of SLNs were prepared employing a range of processing conditions of varying energy input. Fig. 4.6A depicts the average droplet size ($D_{4,3}$) of all emulsions produced, with the processing parameters employed also given. Sonication led to smaller droplet sizes (<1 μm) compared to methods that provide a lower level of shear, such as high-shear homogenisation. In addition, emulsions prepared with high-shear homogenisation, exhibited an oil layer formation and increased droplet sizes over storage, that indicate the occurrence of coalescence. Among the various sonication parameters that were examined, pulsed processes are known to alleviate the risk of heat-induced destabilisation phenomena, in this instance relevant to the lipid particles. However, it was shown that sonication for 30 s (method 5) without the use of pulser produced the most physically stable systems (no oil layer formed) over an observation period of 30 days, possibly due to the continuous delivery of high level of energy. Thus, that was the processing method chosen in later steps.

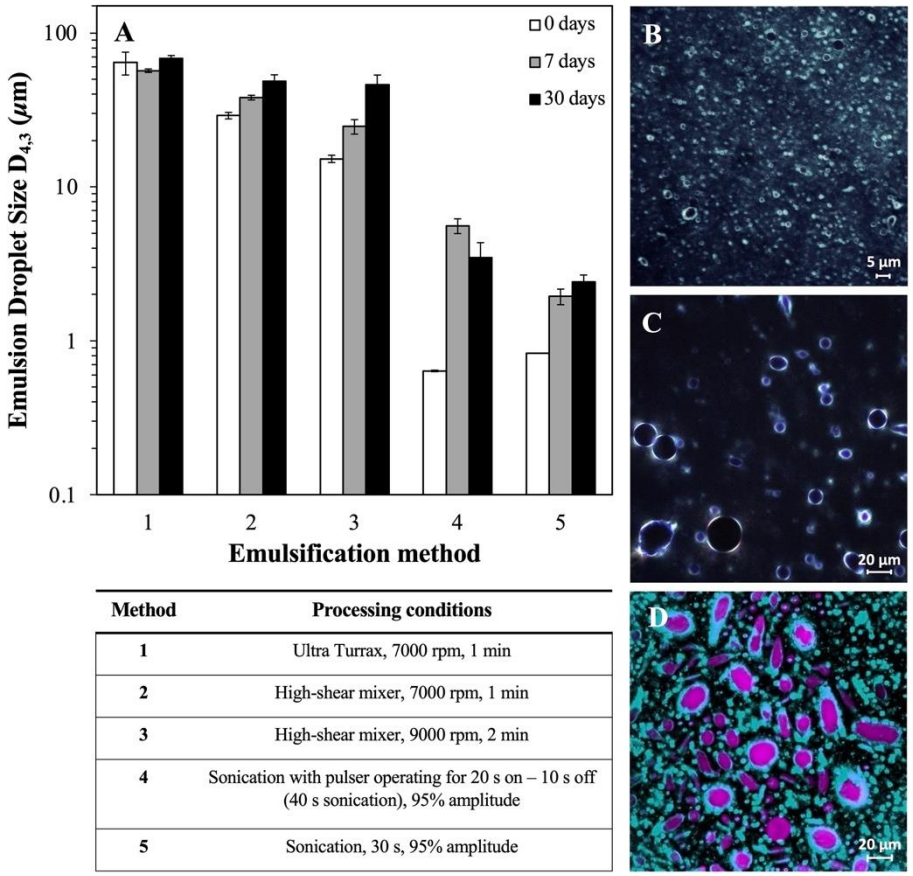

Method	Processing conditions
1	Ultra Turrax, 7000 rpm, 1 min
2	High-shear mixer, 7000 rpm, 1 min
3	High-shear mixer, 9000 rpm, 2 min
4	Sonication with pulser operating for 20 s on – 10 s off (40 s sonication), 95% amplitude
5	Sonication, 30 s, 95% amplitude

Fig. 4.6. Average droplet size of o/w emulsions with solid lipid nanoparticles prepared with different processing conditions at 0, 7 and 30 days (A). Representative images of SLN-stabilised o/w emulsions fabricated following methods 5 and 3 and acquired within 3 hours after production using polarised light microscopy (B and C, respectively), and CLSM of system prepared with method 3 (D).

In order to assess whether the SLNs present in the system contributed to the stability of the produced emulsions, the microstructure of the emulsions was visualised using light microscopy, polarised light microscopy and confocal laser scanning microscopy CLSM (Fig. 4.6B–D). o/w emulsions with SLN were prepared following method 5 to confirm the Pickering stabilisation when using the preferred processing route (Fig. 4.6B), but also with method 3 to better visualise the microstructure of the emulsions (Fig. 4.6C & D). Images were acquired within 1–2 hours after their fabrication. The Maltese cross birefringence pattern at the emulsion droplet surface

(Fig. 4.6C) provides confirmation of the close association between the crystalline lipid particles (possibly containing a lamellar phase [45]) and the emulsion surface [15]. Similarly, the presence of particles adsorbed at the droplet interface was further supported by CLSM micrographs of particles loaded with perylene and emulsion droplets containing Nile Red (Fig. 4.6D) [11]. It was also observed that non-spherical, elongated droplets were also present in the samples, that could be attributed to the strong adsorption of the lipid particles, creating a jammed interface, hence preventing droplet shape relaxation, that has been previously reported for lipid particle stabilised o/w emulsions [15,18,46].

4.3.3.2 Droplet size and zeta potential

Following the processing method described above, 10% o/w emulsions were prepared using the dispersions as the aqueous continuous phase. Lipid particles with varying liquid lipid content used as produced and after dialysis were employed, at a constant concentration of 2.5% w/w of the aqueous phase. The size distribution graphs of the emulsions prepared in the presence of lipid particles used as produced (Fig. 4.7A) showed a bimodal distribution, with a peak at ~0.150 μm which is suggested to correspond to excess lipid particles (non interfacially adsorbed), and a second population at ~1 μm belonging to the produced emulsion droplets. Emulsions prepared with dialysed particle dispersions (Fig. 4.7B), displayed an additional (but much smaller) peak at larger droplet sizes, that appeared consistently in all formulations. In fact, in either case, the size distribution of emulsions prepared with different types of lipid particle dispersions showed an almost identical behaviour, with excess amount of unadsorbed lipid particles remaining in the continuous phase, possibly suggesting that the droplet formation is a process dominated by the process type rather than the properties of the lipid particles (e.g. hydrophilicity). The interfacial adsorption of particles in all cases was corroborated by optical

microscopy (inset graphs, Fig. 4.7). The presence of larger emulsion droplets in the systems with dialysed lipid particles could be ascribed to various factors, among which is the limited availability of surfactant molecules during emulsification. In contrast to lipid particles, surfactant molecules can move promptly at the interface of the droplets and reduce the interfacial tension, subsequently preventing the droplet size increase [47,48]. This is particularly noticeable for the SLN formulation, as the interfacial tension measurement for the as produced dispersion suggested statistically significant higher levels of interfacial tension reduction compared to that used after dialysis (Fig. 4.4). This could have led to formation of smaller emulsion droplets in the former during emulsification. Although the interfacial tension between undialysed and dialysed NLCs did not show any statistically significant changes, the same droplet size trend as for the SLNs was observed. Another contributing factor could be the presence of excess surfactant in the continuous phase, that was previously demonstrated to increase the particle wettability by the aqueous phase based on contact angle data on one hand, and on the other hand increase the continuous phase viscosity (Section 4.3.1.1). Similar data were reported for MCT o/w emulsion droplets stabilised by cyclodextrins in the presence of Tween® 80, where increased surfactant concentration resulted in crystal movement towards the continuous phase, either due to replacement or faster adsorption of surfactant molecules to the interface [49]. Correspondingly, it could be suggested here, that the presence of excess surfactant in the aqueous phase of the lipid particle dispersions moved the particles away from the interface and closer to the water phase, which could in turn potentially provide improved steric hindrance against droplet collisions. What is more, even small differences in the viscosity of the continuous phase, due to the presence of additional surfactant, could have impacted the droplet size reduction aptitude [33,49]. Lastly, droplet aggregation, and additionally lower number of lipid particles for the same initial solid lipid phase concentration in the dialysed

dispersions, due to the previously discussed particle size increase could have also contributed to the enlargement of the emulsion droplets [22].

In terms of the ζ-potential, when the lipid particles were used as produced, the resulting emulsions had a negative charge of ∼−29 mV, while for particles after dialysis the charge had a higher absolute value of ∼−34 mV (Fig. 4.8A). Consistently with the size distribution data, there were almost no differences in the ζ-potential values recorded among the different types of lipid particle dispersions. Comparing the surface charge of the particles alone to that of the respective particle-stabilised emulsions (in the range of −20 mV and −30 mV, respectively), it is observed that the emulsions displayed a higher charge that was statistically significant. More specifically, the difference between the lipid particle and the lipid particle-stabilised emulsion ζ-potential values was greater for the dialysed particles than that of the particles used as prepared, although the dialysed particles (alone) exhibited a lower surface charge (expressed as absolute values). In order to further explore why this was instigated, the theoretical number of lipid nanoparticles required to form a packed monolayer at the emulsion interface and the number of particles introduced during emulsification were calculated. These were correlated and expressed as percentage of particle excess (Fig. 4.8B). For this, the particle *Z*-average and the droplet $D_{3,2}$ values, as measured immediately after preparation (see Appendix A2, Table A2.1), were used to estimate the total number of lipid particles and emulsion droplets present in each system, assuming spherical shape in both cases, while the hexagonal packing correction was applied for the calculation of the maximum number of particles per emulsion droplet (see Appendix A2). As depicted in Fig. 4.8B, for particles with only slight variations in their average sizes when used as produced and after dialysis, the quantity required to fully cover the emulsion droplets decreases with increasing droplet diameter. However, in both instances there was an abundance of particles available in the continuous phase of the emulsions, the percentage of

which was dictated mainly by the droplet surface. Based on the higher emulsion surface charge values obtained for the emulsions stabilised by dialysed lipid particles and the negative charge contribution of sunflower oil [50], it could be hypothesised that there are more exposed uncovered areas on these oil droplets compared to the droplets stabilised by particles before removal of excess surfactant. The inability of the lipid particles to form a densely packed monolayer at the interface and fully cover the droplet surface could be explained by their negative charge causing electrostatic repulsions [13,51,52]. Furthermore, the lack of available surfactant molecules in the dialysed dispersions, available to provide coverage on the droplets surface or fill in the gaps between particles adsorbed at the surface (as further supported by droplet size data) could have resulted in negatively charged chains of sunflower oil protruding towards the continuous phase. Similar trends of lower ζ-potential were described for canola oil emulsion droplets stabilised by tristearin lipid particles (ranging approximately between −30 and −45 mV) compared to the particles alone when prepared with similar concentration, as the one used in this study, of the surfactants Tween® 60 (−19 mV), Brij® S20 (−3 mV) or Brij® S100 (−24 mV) [18]. On the other hand, in a study by Schröder *et al*. [14], the ζ-potential values recorded for tripalmitin particles of an average diameter of 145 nm fabricated with sodium caseinate were identical (∼−36 mV) to the particle-stabilised sunflower oil emulsion droplets with average diameter of 1 μm. The difference in the reported surface charge data could be explained by the pre-treatment of sunflower oil to remove impurities, in combination with the use of a bulkier surface active species in the aforementioned study, that could have potentially resulted in more sparse surface coverage of the emulsion droplets.

The long-term storage behaviour of the particle-stabilised emulsions showed slight peak shifts for that of the unadsorbed particles and of the emulsion droplets to larger sizes over the first week (see Appendix A2, Fig. A2.3, Table A2.2). However, no further size distribution changes,

and more importantly no loss of emulsion integrity with oil layer formation were recorded for up to 12 weeks (see Appendix A2, Table A2.2). Appearance of a thin cream layer in all formulations around the first week due to droplet aggregation could account for the initial size shift. As indicated above, the interfacial layer of the emulsion droplets for all systems is characterised by uncovered spots, that could be prone to coalescence [13,53,54]. Gautier *et al*. [55] described two limiting situations for when coalescence phenomena halt in silica- or latex-stabilised emulsions; either after a dense monolayer has been formed, or when emulsions flocculate due to attractive interactions or bridge formation between particles. The latter explanation could apply in the systems reported here, as on one hand particle network formation has been previously described for lipid particles fabricated with Tween® 60 [18] and on the other, droplets in close proximity can be identified in the microscopy images, confirming droplet flocculation (see Appendix A2, Fig. A2.3). Despite that, polarised light microscopy images at 12 weeks suggest that lipid particles still remain adsorbed at the oil-water interface, which could be due to the high ΔG_d of the particles resulting in irreversible adsorption [56].

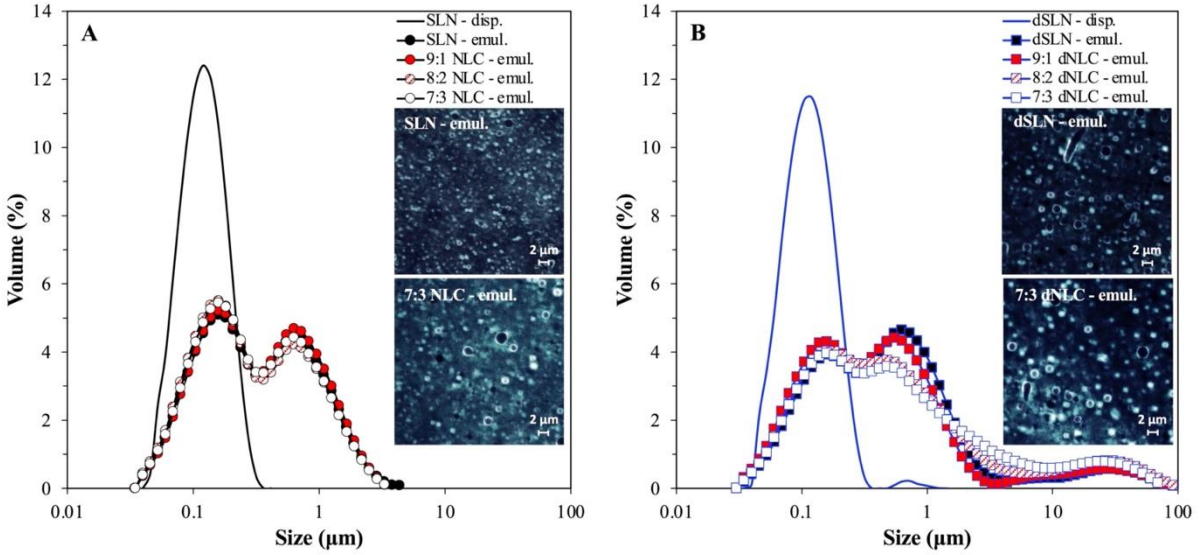

Fig. 4.7. Droplet size distribution of 10% o/w emulsions containing lipid particles with varying liquid lipid mass ratios (SLN, 9:1, 8:2 or 7:3 NLCs) used as produced (A) and after dialysis (B). The size distribution of the SLN formulation used as prepared and after removal of excess surfactant acquired using LD is also presented as a representative particle size example for comparison purposes in each graph, respectively. Representative polarised light microscopy images of SLN and 7:3 NLC-stabilised emulsions are provided in both graphs (inset graphs).

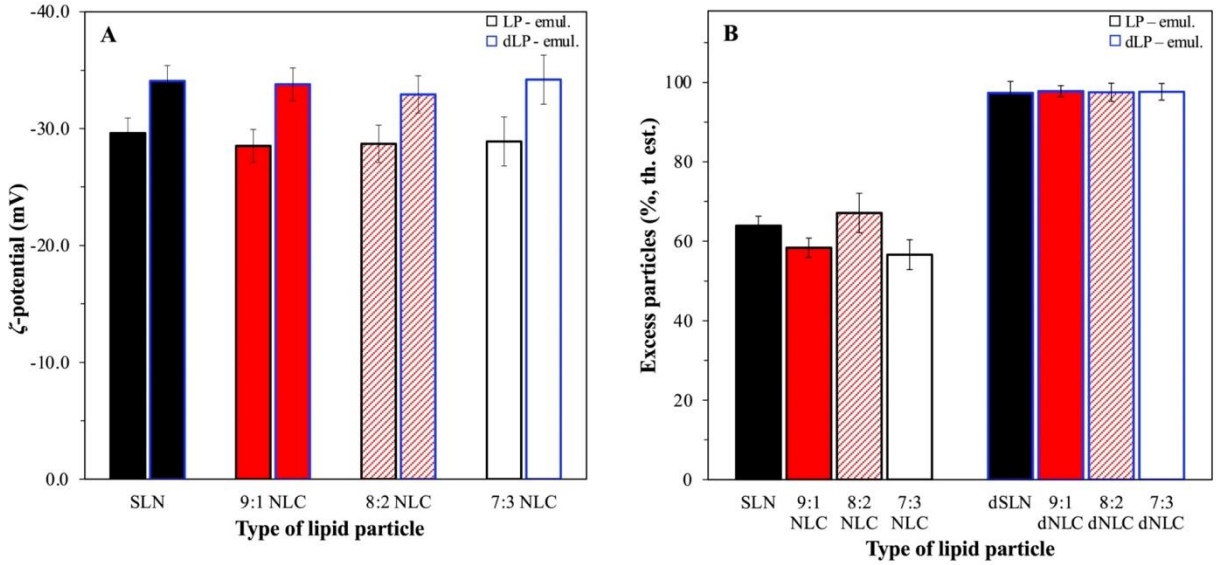

Fig. 4.8. (A) ζ-potential of emulsions stabilised with different types of lipid particles used as produced (LP) and after dialysis (dLP), and (B) percentage of excess particles still available in the continuous phase of the

emulsions after emulsification, for different types of lipid particles used as produced before and after dialysis, based on theoretical estimations (th.est.).

4.4 Conclusions

This study explores the impact of formulation parameters, namely the lipid matrix composition and the presence of excess/remnant unadsorbed surfactant in the aqueous carrier phase, on the potential of lipid particles to act as Pickering stabilisers of o/w emulsion droplets. In regard to the effect of excess surfactant removal from the lipid particle dispersions, it was demonstrated that although some changes in the particle sizes and ζ-potential values were observed initially, possibly imposed by the dialysis process, all types of particles maintained their crystallinity and relative stability over time. The role of the lipid matrix composition, and more specifically the affinity between the lipids and the surfactant used in relation to the interfacial decoration and relative hydrophilicity of the particles was highlighted. Lipid particles containing higher liquid lipid content were shown to be more hydrophilic not only due to the introduction of the relatively more hydrophilic liquid lipid, but also owing to the entrapment of higher proportion of the available surfactant within their crystalline structure, as supported by both interfacial tension and wettability data. Despite variations in their interfacial architecture, the Pickering functionality was confirmed for both SLNs and NLCs. Lastly, although the absence of remnant surfactant from the aqueous carrier phase of the dispersions led to larger emulsion droplet sizes, the affinity of the particles for the emulsion interface was not compromised. Investigations as to how these lipid particle formulation aspects, and consequently the obtained emulsion microstructures affect the concurrent particle functionality as active carriers are the focus of the second part of this study.

References

[1] E. Dickinson, Food emulsions and foams: Stabilization by particles, Curr Opin Colloid Interface Sci. 15 (2010) 40–49. https://doi.org/10.1016/j.cocis.2009.11.001.

[2] H. Jiang, Y. Sheng, T. Ngai, Pickering emulsions: Versatility of colloidal particles and recent applications, Curr Opin Colloid Interface Sci. 49 (2020) 1–15. https://doi.org/10.1016/j.cocis.2020.04.010.

[3] G.I. Sakellari, I. Zafeiri, A. Pawlik, D. Kurukji, P. Taylor, I.T. Norton, F. Spyropoulos, Independent co-delivery of model actives with different degrees of hydrophilicity from oil-in-water and water-in-oil emulsions stabilised by solid lipid particles via a Pickering mechanism: a-proof-of-principle study, J Colloid Interface Sci. 587 (2021) 644–649. https://doi.org/10.1016/j.jcis.2020.11.021.

[4] Y. Wei, C. Wang, X. Liu, A. Mackie, M. Zhang, L. Dai, J. Liu, L. Mao, F. Yuan, Y. Gao, Co-encapsulation of curcumin and β-carotene in Pickering emulsions stabilized by complex nanoparticles: Effects of microfluidization and thermal treatment, Food Hydrocoll. 122 (2022) 107064. https://doi.org/10.1016/j.foodhyd.2021.107064.

[5] F. Spyropoulos, D. Kurukji, P. Taylor, I.T. Norton, Fabrication and Utilization of Bifunctional Protein/Polysaccharide Coprecipitates for the Independent Codelivery of Two Model Actives from Simple Oil-in-Water Emulsions, Langmuir. 34 (2018) 3934–3948. https://doi.org/10.1021/acs.langmuir.7b04315.

[6] G.I. Sakellari, I. Zafeiri, H. Batchelor, F. Spyropoulos, Formulation design, production and characterisation of solid lipid nanoparticles (SLN) and nanostructured lipid carriers (NLC) for the encapsulation of a model hydrophobic active, Food Hydrocolloids for Health. (2021) 100024. https://doi.org/10.1016/j.fhfh.2021.100024.

[7] A. Borges, V. de Freitas, N. Mateus, I. Fernandes, J. Oliveira, Solid lipid nanoparticles as carriers of natural phenolic compounds, Antioxidants. 9 (2020) 998. https://doi.org/10.3390/antiox9100998.

[8] P. Jaiswal, B. Gidwani, A. Vyas, Nanostructured lipid carriers and their current application in targeted drug delivery, Artif Cells Nanomed Biotechnol. 44 (2016) 27–40. https://doi.org/10.3109/21691401.2014.909822.

[9] J. Weiss, E.A. Decker, D.J. McClements, K. Kristbergsson, T. Helgason, T. Awad, Solid lipid nanoparticles as delivery systems for bioactive food components, Food Biophys. 3 (2008) 146–154. https://doi.org/10.1007/s11483-008-9065-8.

[10] R. Gupta, D. Rousseau, Surface-active solid lipid nanoparticles as Pickering stabilizers for oil-in-water emulsions, Food Funct. 3 (2012) 302–311. https://doi.org/10.1039/c2fo10203j.

[11] I. Zafeiri, P. Smith, I.T. Norton, F. Spyropoulos, Fabrication, characterisation and stability of oil-in-water emulsions stabilised by solid lipid particles: The role of particle characteristics and emulsion microstructure upon Pickering functionality, Food Funct. 8 (2017) 2583–2591. https://doi.org/10.1039/c7fo00559h.

[12] A. Pawlik, D. Kurukji, I. Norton, F. Spyropoulos, Food-grade Pickering emulsions stabilised with solid lipid particles, Food Funct. 7 (2016) 2712–2721. https://doi.org/10.1039/c6fo00238b.

[13] A. Schröder, J. Sprakel, K. Schroën, J.N. Spaen, C.C. Berton-Carabin, Coalescence stability of Pickering emulsions produced with lipid particles: A microfluidic study, J Food Eng. 234 (2018) 63–72. https://doi.org/10.1016/j.jfoodeng.2018.04.007.

[14] A. Schröder, M. Laguerre, J. Sprakel, K. Schroën, C.C. Berton-Carabin, Pickering particles as interfacial reservoirs of antioxidants, J Colloid Interface Sci. 575 (2020) 489–498. https://doi.org/10.1016/J.JCIS.2020.04.069.

[15] A. Schröder, J. Sprakel, K. Schroën, C.C. Berton-Carabin, Tailored microstructure of colloidal lipid particles for Pickering emulsions with tunable properties, Soft Matter. 13 (2017) 3190–3198. https://doi.org/10.1039/c6sm02432g.

[16] D. Johansson, B. Bergenståhl, Sintering of fat crystal networks in oil during post-crystallization processes, J Am Oil Chem Soc. 72 (1995) 911–920. https://doi.org/10.1007/BF02542069.

[17] G. Li, W.J. Lee, C.P. Tan, O.M. Lai, Y. Wang, C. Qiu, Tailored rigidity of W/O Pickering emulsions using diacylglycerol-based surface-active solid lipid nanoparticles, Food Funct. 12 (2021) 11732–11746. https://doi.org/10.1039/d1fo01883c.

[18] H. Lim, M. Jo, C. Ban, Y.J. Choi, Interfacial and colloidal characterization of oil-in-water emulsions stabilized by interface-tunable solid lipid nanoparticles, Food Chem. 306 (2020) 125619. https://doi.org/10.1016/j.foodchem.2019.125619.

[19] I. Zafeiri, C. Horridge, E. Tripodi, F. Spyropoulos, Emulsions Co-Stabilised by Edible Pickering Particles and Surfactants: The Effect of HLB Value, Colloid Interface Sci Commun. 17 (2017) 5–9. https://doi.org/10.1016/j.colcom.2017.02.001.

[20] R. Pichot, F. Spyropoulos, I.T. Norton, Competitive adsorption of surfactants and hydrophilic silica particles at the oil–water interface: Interfacial tension and contact angle studies, J Colloid Interface Sci. 377 (2012) 396–405. https://doi.org/10.1016/j.jcis.2012.01.065.

[21] J. Milsmann, K. Oehlke, K. Schrader, R. Greiner, A. Steffen-Heins, Fate of edible solid lipid nanoparticles (SLN) in surfactant stabilized o/w emulsions. Part 1: Interplay of SLN and oil droplets, Colloids Surf A Physicochem Eng Asp. 558 (2018) 615–622. https://doi.org/10.1016/j.colsurfa.2017.05.073.

[22] S.M. Dieng, N. Anton, P. Bouriat, O. Thioune, P.M. Sy, N. Massaddeq, S. Enharrar, M. Diarra, T. Vandamme, Pickering nano-emulsions stabilized by solid lipid nanoparticles as a temperature sensitive drug delivery system, Soft Matter. 15 (2019) 8164–8174. https://doi.org/10.1039/c9sm01283d.

[23] B.P. Binks, T.S. Horozov, Colloidal particles at liquid interfaces, Cambridge University Press, 2006. https://doi.org/10.1017/cbO9780511536670.

[24] T. Helgason, T.S. Awad, K. Kristbergsson, D.J. McClements, J. Weiss, Effect of surfactant surface coverage on formation of solid lipid nanoparticles (SLN), J Colloid Interface Sci. 334 (2009) 75–81. https://doi.org/10.1016/j.jcis.2009.03.012.

[25] E. Dickinson, An Introduction to Food Colloids, Oxford University Press, 1992.

[26] C. Ban, S. Lim, P.S. Chang, Y.J. Choi, Enhancing the stability of lipid nanoparticle systems by sonication during the cooling step and controlling the liquid oil content, J Agric Food Chem. 62 (2014) 11557–11567. https://doi.org/10.1021/jf503489v.

[27] C. Ban, M. Jo, S. Lim, Y.J. Choi, Control of the gastrointestinal digestion of solid lipid nanoparticles using PEGylated emulsifiers, Food Chem. 239 (2018) 442–452. https://doi.org/10.1016/j.foodchem.2017.06.137.

[28] A.M. Nik, S. Langmaid, A.J. Wright, Nonionic surfactant and interfacial structure impact crystallinity and stability of β-carotene loaded lipid nanodispersions, J Agric Food Chem. 60 (2012) 4126–4135. https://doi.org/10.1021/jf204810m.

[29] K. Westesen, B. Siekmann, Investigation of the gel formation of phospholipid-stabilized solid lipid nanoparticles, Int J Pharm. 151 (1997) 35–45. https://doi.org/10.1016/S0378-5173(97)04890-4.

[30] H. Bunjes, F. Steiniger, W. Richter, Visualizing the structure of triglyceride nanoparticles in different crystal modifications, Langmuir. 23 (2007) 4005–4011. https://doi.org/10.1021/la062904p.

[31] K. Szymczyk, A. Taraba, Aggregation behavior of Triton X-114 and Tween 80 at various temperatures and concentrations studied by density and viscosity measurements, J Therm Anal Calorim. 126 (2016) 315–326. https://doi.org/10.1007/S10973-016-5631-3.

[32] G. v. Lowry, R.J. Hill, S. Harper, A.F. Rawle, C.O. Hendren, F. Klaessig, U. Nobbmann, P. Sayre, J. Rumble, Guidance to improve the scientific value of zeta-potential measurements in nanoEHS, Environ Sci Nano. 3 (2016) 953–965. https://doi.org/10.1039/c6eN00136j.

[33] Q. Yuan, R.A. Williams, Co-stabilisation mechanisms of nanoparticles and surfactants in Pickering Emulsions produced by membrane emulsification, J Memb Sci. 497 (2016) 221–228. https://doi.org/10.1016/j.memsci.2015.09.028.

[34] P. Prombutara, Y. Kulwatthanasal, N. Supaka, I. Sramala, S. Chareonpornwattana, Production of nisin-loaded solid lipid nanoparticles for sustained antimicrobial activity, Food Control. 24 (2012) 184–190. https://doi.org/10.1016/j.foodcont.2011.09.025.

[35] E.B. Souto, S.A. Wissing, C.M. Barbosa, R.H. Müller, Evaluation of the physical stability of SLN and NLC before and after incorporation into hydrogel formulations, European Journal of Pharmaceutics and Biopharmaceutics. 58 (2004) 83–90. https://doi.org/10.1016/j.ejpb.2004.02.015.

[36] H. Salminen, T. Helgason, S. Aulbach, B. Kristinsson, K. Kristbergsson, J. Weiss, Influence of co-surfactants on crystallization and stability of solid lipid nanoparticles, J Colloid Interface Sci. 426 (2014) 256–263. https://doi.org/10.1016/j.jcis.2014.04.009.

[37] D.J. McClements, H. Xiao, Potential biological fate of ingested nanoemulsions: Influence of particle characteristics, in: Food Funct, The Royal Society of Chemistry, 2012: pp. 202–220. https://doi.org/10.1039/c1fo10193e.

[38] I. Zafeiri, J.E. Norton, P. Smith, I.T. Norton, F. Spyropoulos, The role of surface active species in the fabrication and functionality of edible solid lipid particles, J Colloid Interface Sci. 500 (2017) 228–240. https://doi.org/10.1016/j.jcis.2017.03.085.

[39] J. Milsmann, K. Oehlke, R. Greiner, A. Steffen-Heins, Fate of edible solid lipid nanoparticles (SLN) in surfactant stabilized o/w emulsions. Part 2: Release and partitioning behavior of lipophilic probes from SLN into different phases of o/w emulsions, Colloids Surf A Physicochem Eng Asp. 558 (2018) 623–631. https://doi.org/10.1016/j.colsurfa.2017.05.050.

[40] B.P. Binks, Particles as surfactants - Similarities and differences, Curr Opin Colloid Interface Sci. 7 (2002) 21–41. https://doi.org/10.1016/S1359-0294(02)00008-0.

[41] S.U. Pickering, CXCVI. - Emulsions, Journal of the Chemical Society, Transactions. 91 (1907) 2001–2021. https://doi.org/10.1039/ct9079102001.

[42] B.P. Binks, J.H. Clint, Solid wettability from surface energy components: Relevance to pickering emulsions, Langmuir. 18 (2002) 1270–1273. https://doi.org/10.1021/la011420k.

[43] A. Shirvani, S.A.H. Goli, J. Varshosaz, L. Salvia-Trujillo, O. Martín-Belloso, Fabrication of edible solid lipid nanoparticle from beeswax/propolis wax by spontaneous emulsification: Optimization, characterization and stability, Food Chem. 387 (2022) 132934. https://doi.org/10.1016/j.foodchem.2022.132934.

[44] R. Aveyard, J.H. Clint, T.S. Horozov, Aspects of the stabilisation of emulsions by solid particles: Effects of line tension and monolayer curvature energy, Physical Chemistry Chemical Physics. 5 (2003) 2398–2409. https://doi.org/10.1039/b210687f.

[45] J.B. Brubach, V. Jannin, B. Mahler, C. Bourgaux, P. Lessieur, P. Roy, M. Ollivon, Structural and thermal characterization of glyceryl behenate by X-ray diffraction coupled to differential calorimetry and infrared spectroscopy, Int J Pharm. 336 (2007) 248–256. https://doi.org/10.1016/j.ijpharm.2006.11.057.

[46] J. Tan, M. Zhang, J. Wang, J. Xu, D. Sun, Temperature induced formation of particle coated non-spherical droplets, J Colloid Interface Sci. 359 (2011) 171–178. https://doi.org/10.1016/j.jcis.2011.03.065.

[47] P.Y. Liu, R.Y. Yang, A.B. Yu, Self-diffusion of wet particles in rotating drums, Physics of Fluids. 25 (2013) 063301. https://doi.org/10.1063/1.4807596.

[48] I.T. Norton, F. Spyropoulos, P.W. Cox, Effect of emulsifiers and fat crystals on shear induced droplet break-up, coalescence and phase inversion, Food Hydrocoll. 23 (2009) 1521–1526. https://doi.org/10.1016/j.foodhyd.2008.09.014.

[49] X. Li, H. Li, Q. Xiao, L. Wang, M. Wang, X. Lu, P. York, S. Shi, J. Zhang, Two-way effects of surfactants on Pickering emulsions stabilized by the self-assembled microcrystals of a-cyclodextrin and oil, Phys. Chem. Chem. Phys. 16 (2014) 14059. https://doi.org/10.1039/c4cp00807c.

[50] A.T. Florence, J.A. Rogers, Emulsion stabilization by non-ionic surfactants: experiment and theory, Journal of Pharmacy and Pharmacology. 23 (1971) 153–169. https://doi.org/10.1111/j.2042-7158.1971.tb08637.x.

[51] O.S. Deshmukh, D. van den Ende, M.C. Stuart, F. Mugele, M.H.G. Duits, Hard and soft colloids at fluid interfaces: Adsorption, interactions, assembly & rheology, Adv Colloid Interface Sci. 222 (2015) 215–227. https://doi.org/10.1016/j.cis.2014.09.003.

[52] M. Destribats, S. Gineste, E. Laurichesse, H. Tanner, F. Leal-Calderon, V. Héroguez, V. Schmitt, Pickering emulsions: What are the main parameters determining the emulsion type and interfacial properties?, Langmuir. 30 (2014) 9313–9326. https://doi.org/10.1021/la501299u.

[53] T.S. Horozov, B.P. Binks, Particle-Stabilized Emulsions: A Bilayer or a Bridging Monolayer?, Angewandte Chemie International Edition. 45 (2006) 773–776. https://doi.org/10.1002/anie.200503131.

[54] S.P. Nagarkar, S.S. Velankar, Morphology and rheology of ternary fluid–fluid–solid systems, Soft Matter. 8 (2012) 8464–8477. https://doi.org/10.1039/c2sm25758k.

[55] F. Gautier, M. Destribats, R. Perrier-Cornet, J.F. Dechézelles, J. Giermanska, V. Héroguez, S. Ravaine, F. Leal-Calderon, V. Schmitt, Pickering emulsions with stimulable particles: from highly- to weakly-covered interfaces, Physical Chemistry Chemical Physics. 9 (2007) 6455–6462. https://doi.org/10.1039/b710226g.

[56] R. Aveyard, B.P. Binks, J.H. Clint, Emulsions stabilised solely by colloidal particles, Adv Colloid Interface Sci. 100 (2003) 503–546. https://doi.org/https://doi.org/10.1016/S0001-8686(02)00069-6.

Appendix A2

Surface load calculation

The amount of surfactant covering a unit area of particle surface denoted as surface load (Γ_s) and measured in mg/m^2 was calculated as follows [2]:

$$\Gamma_s = \frac{C_{a,max} D_{SLN,\ NLC}}{6\Phi_{SLN,\ NLC}} \quad \text{(A2.1)}$$

where $C_{a,max}$ is the maximum mass of surfactant adsorbed to the surface of the lipid particles, $D_{SLN,\ NLC}$ is the *Z*-average of the lipid particles, and $\Phi_{SLN,\ NLC}$ is the dispersed phase volume fraction (i.e. ~0.027). The volume fraction for the different lipid phase compositions was estimated based on the mass fraction of the lipid phase used for the preparation of the aqueous dispersion and estimations of the density of each mixture, based on the individual densities and the mass ratio of each lipid component in the mixture (i.e. Compritol® 888 ATO d=0.94 g/ml^3, Miglyol® 812 d=0.92 g/ml^3). All types of particles were considered to have a spherical shape. For the calculations of Γ_s, it was assumed that the entirety of available surfactant was associated with the particles, and therefore the calculated Γ_s would correspond to the maximum achievable Γ_s.

Minimum adsorbed surfactant calculation

To estimate the minimum concentration ($C_{a,min}$) of surfactant required to form a monolayer at the surface of the particles, the surface area occupied by the lipid particles in each system was calculated based on their *Z*-average values. The surface area occupied by a Tween® 80 molecule at the water/air interface was considered to be 42.14 Å^2 [3], and the hexagonal packing

consideration that provides the highest packing density (0.9069), was used to correct the required amount of surfactant to form a monolayer at the surface of the particles. Additionally, it was assumed that all types of particles had a spherical shape. The result was expressed as % w/w concentration of Tween® 80 required to fully cover the surface of the particles.

The effect of excess surfactant on the physicochemical characteristics of lipid particles

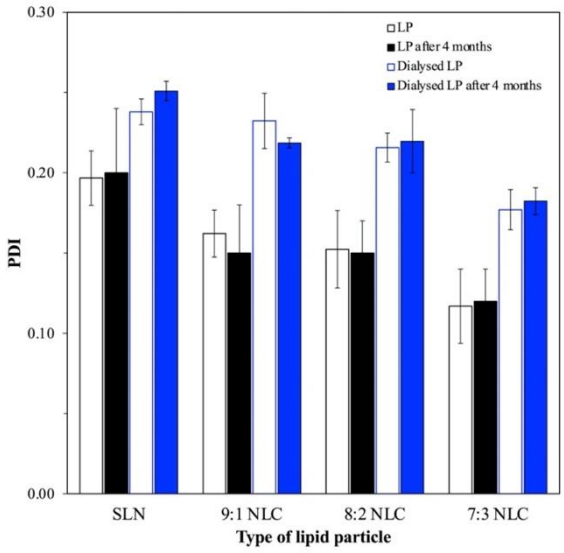

Fig. A2.1. Polydispersity index (PDI) of lipid particle (LP) dispersions after preparation and after 4 months of storage following removal of excess surfactant (dLP).

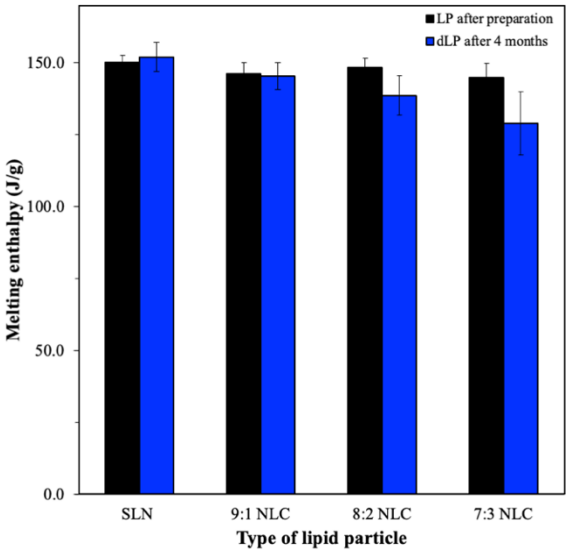

Fig. A2.2. Melting enthalpy of lipid particle (LP) dispersions after preparation and after 4 months of storage following removal of excess surfactant (dLP). The DSC melting curves for each sample are shown in Fig. 4.3.

Particle interfacial coverage calculation

The number of particles theoretically required to cover the emulsion droplet interface was calculated based on the particle and droplet average diameters. The assumption that all particles have the same diameter, and that both species are spherical in shape were used throughout the following estimations. For the particle average diameter, the *Z*-average values acquired by DLS measurements were employed. For the emulsion droplets the LD data obtained immediately after preparation, were used to calculate the $D_{3,2}$ values for the peak(s) presumed to describe emulsion droplets. More specifically, using the size distribution data, overlapping peaks were separated by fitting the Weibull model (model that gave the best fit), in order to manually calculate both the $D_{4,3}$ and $D_{3,2}$ values for each peak. When more than one peaks corresponded to the emulsion droplets the contribution of each peak to the total surface was factored in by calculating the area under each peak using SigmaPlot 14.5 (SYSTAT Software, USA). An

example of the peak separation and fitting is provided below, along with the data used for the calculation of the percentage of excess particles still available in the continuous phase of the emulsions after emulsification, for different types of lipid particles used as produced before and after dialysis (Table A2.1).

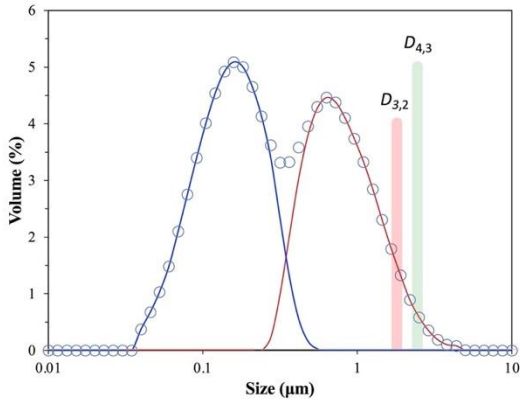

Example of peak separation and fitting on size distribution data as acquired by LD measurements, used for the calculation of the particle interfacial coverage.

Table A2.1. *Z*-average values for lipid particles, $D_{3,2}$ values for emulsion droplets and percentage of peak distribution for emulsion droplets used for the calculation of the percentage of excess particles available in the continuous phase of the emulsions after emulsification, as provided in Fig. 4.8B.

Particle-stabilised emulsions	*Z*-average (nm) for particles	$D_{3,2}$ (μm) for emulsion droplets		Percentages of peak contribution for emulsion droplets (%)	
		Peak 1	Peak 2	Peak 1	Peak 2
SLN	158.9±10.6	1.8±0.0	-	100	-
9:1 NLC	160.5±3.8	1.6±0.0	-	100	-
8:2 NLC	140.4±20.1	1.8±0.0	-	100	-
7:3 NLC	145.8±3.4	1.4±0.0	-	100	-
dSLN	238.0±8.0	3.2±0.9	39.6±1.5	18	82
9:1 dNLC	232.2±17.2	1.4±0.2	49.5±1.2	16	84

8:2 dNLC	216.9±9.0	2.6±0.5	52.1±2.3	12	88
7:3 dNLC	177.9±12.5	5.3±1.6	42.9±1.9	8	92

The total number of lipid particles and emulsion droplets was calculated for each system as follows:

$$n_{p,d} = \frac{V_t}{V_{p,d}} \quad \text{(A2.2)}$$

where $n_{p,d}$ is the total number of particles or droplets present in each system, V_t is the total volume of the lipid or oil phase (considering that the density for Compritol® 888 ATO is 0.94 g/ml^3, for Miglyol® 812 is 0.92 g/ml^3 and for sunflower oil is 0.92 g/ml^3) and $V_{p,d}$ is the volume of a single lipid particle or a single emulsion droplet.

The number of particles per emulsion droplet was then calculated as follows:

$$N_p = \frac{S_d}{S_p} \quad \text{(A2.3)}$$

where N_p is the number of lipid particles per emulsion droplet, S_d is surface area of an emulsion droplet and S_p is the surface area of a lipid particle.

The amount of lipid nanoparticles required to fully cover all emulsion droplets was estimated as follows:

$$N_t = 0.9069 \times N_p \times n_d \quad \text{(A2.4)}$$

where N_t is the total number of lipid particles required to cover all emulsion droplets in a system, N_p is the number of lipid particles per emulsion droplet, and n_d is the total number of droplets present in the system. At this stage, the hexagonal packing consideration was used, that provides the highest packing density (0.9069), considering that the surface coverage provided by a lipid particle corresponds to that of the surface area of a circle and that the particles form a packed monolayer. Lastly, the percentage of particles excess was calculated based on the N_t and n_p number of particles present in each system.

Droplet size and zeta potential over storage

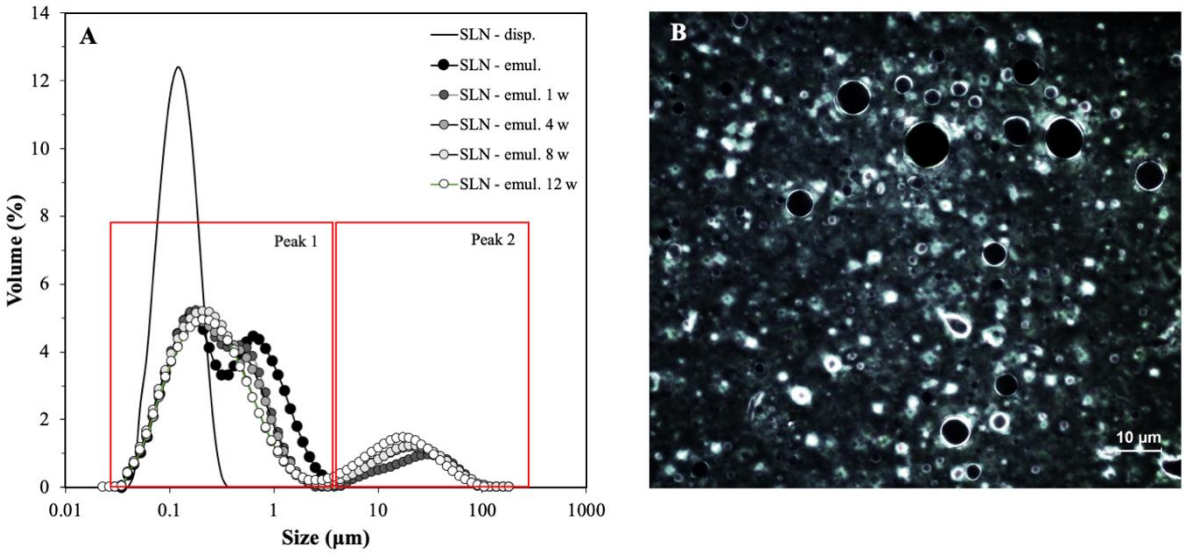

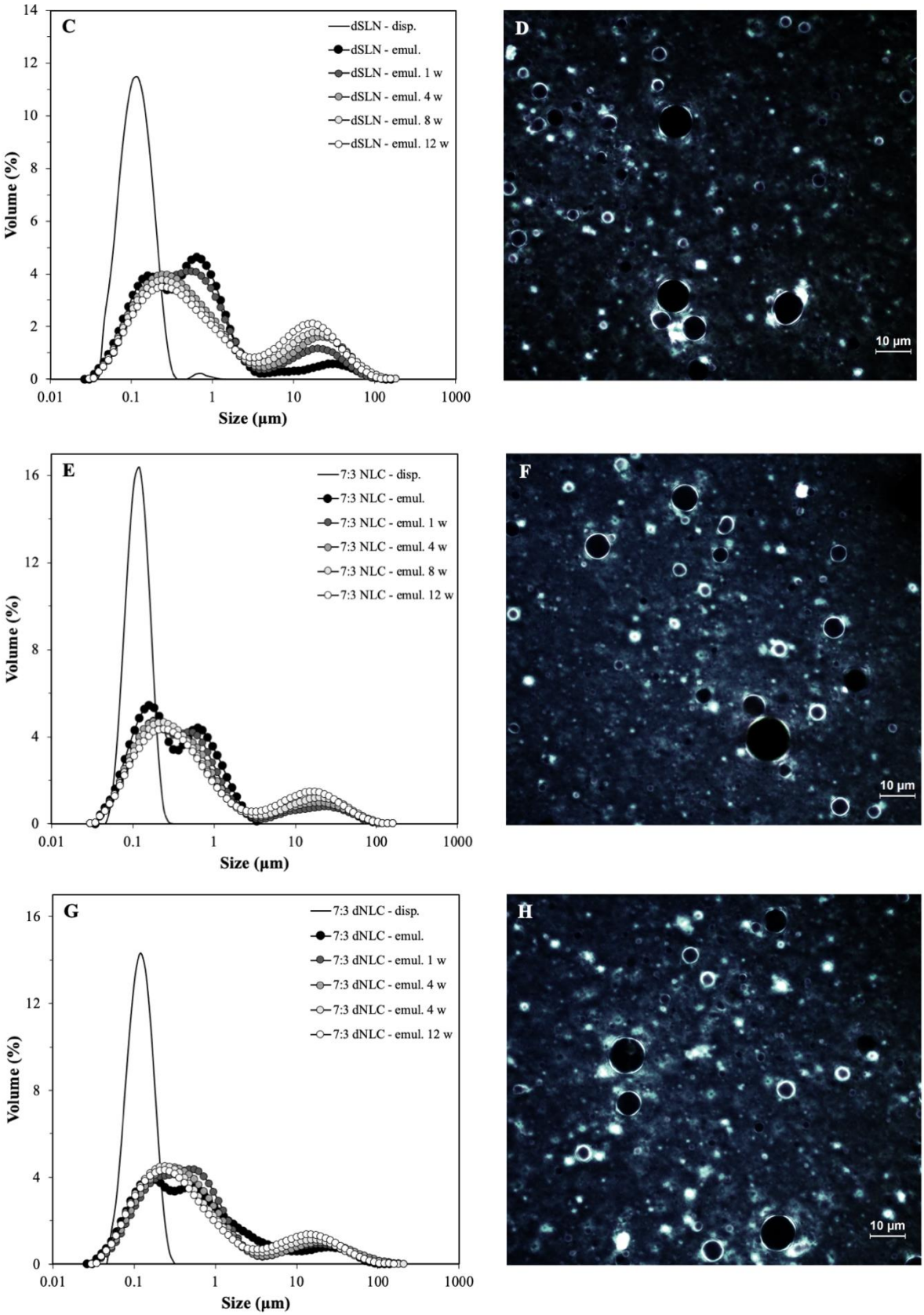

Fig. A2.3. Time evolution of characteristic examples of size distribution of particle-stabilised emulsions at 0, 1, 4, 8 and 12 weeks, and representative polarised light microscopy images at 12 weeks for SLN (A, B),

dSLN (C, D), 7:3 NLC (E, F) and 7:3 dNLC (G, H) containing systems. The size distribution of the respective lipid particle dispersions is also presented in each graph for comparison purposes.

Table A2.2. $D_{4,3}$, $D_{3,2}$, and ζ-potential of o/w emulsions stabilised by different SLN and NLC (9:1, 8:2 and 7:3) dispersions used as produced and after dialysis and measured at various time intervals over a storage period of 12 weeks at 4°C. For the size distribution parameters calculation, the peak separation was performed according to the schematic presented in Fig. A2.3A.

Particle-stabilised emulsions	Storage period (weeks)	$D_{4,3}$ (μm)		$D_{3,2}$ (μm)		ζ-potential (mV)
		Peak 1	Peak 2	Peak 1	Peak 2	
SLN	0	2.2±0.5	-	1.8±0.0	-	−29.6±1.6
	1	1.2±0.8	54.6±1.9	0.2±0.0	35.5±0.7	−29.9±1.3
	4	2.2±1.8	78.6±3.2	0.3±0.0	34.3±0.9	−30.0±1.5
	8	1.7±0.6	62.5±1.4	0.4±0.1	36.1±0.6	−32.1±2.9
	12	1.3±0.5	63.5±1.7	0.5±0.1	34.0±0.7	−29.0±1.1
9:1 NLC	0	1.9±0.3	-	1.6±0.0	-	−28.5±2.9
	1	2.5±0.4	61.4±2.3	0.3±0.0	30.2±2.7	−29.3±2.1
	4	3.7±1.1	76.9±3.4	0.3±0.1	29.4±3.2	−30.7±2.6
	8	2.6±0.9	58.5±4.5	0.4±0.1	33.9±2.9	−33.3±3.3
	12	5.5±1.3	54.7±3.4	0.5±0.1	31.5±2.3	−29.8±1.9
8:2 NLC	0	1.9±0.4	-	1.8±0.0	-	−28.3±2.1
	1	3.8±0.7	68.7±3.5	0.4±0.0	30.3±2.5	−29.3±1.1
	4	2.6±0.8	62.1±3.1	0.3±0.1	29.6±3.1	−28.8±1.3
	8	2.4±0.6	68.2±2.9	0.4±0.1	35.4±3.4	−31.9±2.7
	12	4.9±1.1	64.0±3.0	0.5±0.2	32.8±2.9	−29.2±0.9
7:3 NLC	0	1.9±0.2	-	1.4±0.0	-	−27.3±2.4
	1	3.6±0.9	57.6±2.8	0.3±0.0	27.3±1.8	−27.5±1.5
	4	2.5±0.9	60.0±2.6	0.3±0.0	30.2±1.6	−30.0±1.7
	8	2.6±0.4	67.0±1.9	0.4±0.1	34.5±1.9	−33.9±3.7
	12	2.8±0.2	65.4±2.3	0.5±0.0	32.8±2.3	−29.1±4.1

dSLN	0	7.7±1.5	69.0±2.5	0.2±0.0	49.1±1.5	−32.8±3.3
	1	2.8±1.0	65.7±3.1	0.2±0.0	38.7±1.3	−32.3±2.9
	4	2.6±0.8	80.7±4.5	0.3±0.0	37.4±1.7	−28.7±2.1
	8	2.7±0.4	75.4±3.8	0.4±0.1	37.0±1.9	−29.1±1.5
	12	5.0±1.9	61.9±3.4	0.5±0.0	33.3±1.6	−31.5±2.9
9:1 dNLC	0	9.0±1.1	61.2±2.9	0.3±0.0	49.5±1.2	−33.1±1.7
	1	3.3±0.4	57.1±3.1	0.4±0.1	37.9±1.9	−32.9±1.2
	4	2.9±0.6	90.2±4.8	0.4±0.1	38.6±2.4	−32.0±2.0
	8	2.2±1.1	85.1±4.3	0.4±0.1	33.0±2.3	−28.8±2.0
	12	6.0±2.1	93.5±5.1	0.5±0.0	31.4±2.8	−31.2±2.0
8:2 dNLC	0	4.8±2.3	64.2±2.6	0.3±0.0	53.1±2.3	−31.9±2.8
	1	3.3±1.0	68.7±2.3	0.4±0.0	42.3±3.1	−31.5±0.5
	4	3.1±1.1	62.1±3.6	0.5±0.1	38.1±2.9	−31.8±3.2
	8	2.7±0.6	93.7±6.7	0.4±0.1	38.3±3.0	−29.1±2.0
	12	5.0±1.6	87.7±4.2	0.5±0.1	35.6±2.8	−31.1±1.7
7:3 dNLC	0	7.6±2.3	56.5±2.1	0.3±0.0	42.9±1.9	−32.7±3.3
	1	1.7±0.9	76.8±4.3	0.5±0.1	33.8±2.0	−32.5±1.1
	4	2.9±1.4	78.3±4.8	0.8±0.2	37.8±2.4	−32.7±4.6
	8	2.7±0.7	75.8±4.1	0.4±0.1	31.4±2.9	−30.8±3.1
	12	5.1±1.9	62.6±5.3	05±0.1	28.5±3.3	−33.6±3.6

Chapter 5

Lipid particles of dual functionality at emulsion interfaces. Part II: active carrying/delivery functionality

Published as:

G.I. Sakellari, I. Zafeiri, H. Batchelor, F. Spyropoulos, Solid lipid nanoparticles and nanostructured lipid carriers of dual functionality at emulsion interfaces. Part II: active carrying/delivery functionality, Colloids and Surfaces A: Physicochemical Engineering Aspects. (2023) 130787.

Synopsis

The utilisation of lipid nanostructures that can in tandem act as Pickering emulsion stabilisers and as active carrier/delivery systems, could potentially enable the development of liquid (emulsion-based) formulations with the capacity for multi-active encapsulation and delivery. Part I of this work focused on the first aspect of this two-fold functionality by investigating the capacity of both solid lipid nanoparticles (SLNs) and nanostructured lipid carriers (NLCs) to act as effective Pickering particles in o/w emulsions. Herein, attention shifts to the secondary functionality, with part II of this study assessing both SLNs and NLCs in terms of their capacity to act as carriers and release regulators for curcumin, a model hydrophobic active. The previously established Pickering functionality and physical properties in terms of particle size, zeta potential and interfacial tension of the lipid particles remained unaffected after encapsulation of curcumin. In emulsions, loss of crystalline (solid lipid) matter and particle interfacial presence were specifically investigated, as these aspects can impact upon the particles' active carrying and delivery performance. Low solid matter losses were recorded for all emulsions (ranging between 0% and 15%), with increasing liquid lipid fraction in the particles (SLNs to NLCs) resulting in relatively higher depletion of crystallinity. Removal of unadsorbed surfactant (remnant from the particle formation processing step) prior to emulsification led to higher particle interfacial occupancy. Despite said changes, the lipid particles' curcumin carrying capacity, expressed as encapsulation efficiency and loading capacity, did not differ between an emulsion and dispersion setting. Although the active carrying capacity was retained, it was shown that the presence of the particles at the emulsion interfaces affects the curcumin release rate. Partial migration of curcumin to the oil droplet and creation of an additional release-inducing potential to the

particles in close proximity to the droplet interface are proposed to be responsible for the overall faster active expulsion. What is more, the curcumin release profile from either SLNs or NLCs (also) stabilising an emulsion microstructure, was shown to persist after storage; either storage of the particles (up to 4 months) prior to emulsification, or storage of emulsions (up to 3 months) stabilised by 'freshly' formed lipid particles. Overall, the present study provides evidence that the two-fold functionality of the lipid particles can be indeed realised, markedly demonstrating that their concurrency does not compromise one another.

5.1 Introduction

Among the most desirable characteristics of a multi-active carrying/delivery system is the ability to simultaneously and independently regulate the release of its encapsulated species, along with other physicochemical (e.g. surface properties, loading capacity) properties, tailoring of which can enable the development of targeted delivery systems (e.g. suitable for oral ingestion) [1–3]. The development of formulations that allow the segregated/individual encapsulation of multiple actives has shown potential in addressing these challenges, through the employment of hierarchical multicompartmental triple emulsions [4], o/w emulsion droplets stabilised by sodium caseinate/chitosan co-precipitated complexes [5], and multicompartment polymeric hydrogels [6], among others. More recently, Pickering emulsions stabilised by solid lipid nanoparticles (SLNs) demonstrated promising capacity to facilitate individually-tailored multi-active delivery [7], though NLCs have not been utilised yet in a similar formulation approach despite their carrying/delivery advantages [8–18]. Therefore, understanding how (and to what extent) formulation parameters of both types of lipid particles (parameters which in part I of this study [19] were investigated for their effect on the Pickering stabilisation capacity of these lipid microstructures), affect their active carrying/delivery functionality, could eventually enable the attainment of a truly dual-functional system.

In emulsions, the regulation of mass transfer from the dispersed phase carrying the active to the external phase is typically achieved by modifying the interfacial layer architecture via the presence of a colloidal (or otherwise) load, which is what systems such as Pickering particles have been studied for in the past. Adjusting the interfacial layer permeability and thickness of emulsions stabilised by emulsifiers with Pickering-like characteristics [20], resulted in hindered active release rate. Frasch-Melnik *et al*. [21] and Garrec *et al*. [22] demonstrated that melting

of the sintered fat shell formed at the surface of w/o droplets led to complete release of the salt incorporated within the water droplets, with similar behaviour observed by SLNs [23]. Encapsulation of an active within such lipid particles, which themselves are then positioned at an emulsion interface, can pose a challenge to the particles' ability to maintain both functionalities intact, due to solid lipid particle matter [24–26] and loaded active migration into the dispersed oil phase [27–28]. However, the exact mechanism by which active migration into the droplets takes place, as well as how formulation aspects of both SLNs and NLCs can be exploited to control such phenomena, have yet to be studied.

Part II of this work investigates whether adopting an active carrying and delivery functionality compromises the previously defined capacity of the lipid particles to act as Pickering emulsion stabilisers (part I), but also explores the parameters that affect this secondary (but concurrent) functionality, and the mechanisms involved in its manifestation. An issue known to impact on the Pickering functionality of lipid particles, but in the present scenario potentially also their additional role as active carriers, is their capacity to preserve their solid matter once exposed to an emulsion setting [24–26]. Therefore, this study initially assesses how lipid particle type/composition (SLNs and NLCs of increasing solid-to-liquid lipid mass ratio) and interfacial occupancy can promote solid (fat) matter losses, as destabilisation promoter. Subsequently, the influence of curcumin (CRM, used as a model active) incorporation on the properties (including size, zeta potential and interfacial behaviour) of lipid particles "used-as-produced" (i.e., those containing excess surfactant, remnant from the particle formation stage) or "dialysed" (i.e., those essentially deprived of any such excess surfactant load), were explored. The ability of the now loaded-lipid particles to retain their Pickering stabilisation functionality was then studied, and the droplet size and ζ-potential of the resulting systems were measured. Lastly, the release

performance of (prior- and post-dialysis) lipid particles in an emulsion setting was investigated and compared to that observed in simple aqueous dispersions.

5.2 Materials and methods

5.2.1 Materials

Glyceryl behenate (Compritol® 888 ATO) was a kind gift from Gattefossé (Saint-Priest, France). Medium chain triglycerides (MCTs) (Miglyol® 812) were kindly provided from IOI Oleo (IOI Oleochemicals GmbH, Germany). Polyoxyethylene sorbitan monooleate (Tween® 80) and curcumin (≥65%, HPLC) were purchased from Sigma-Aldrich (Sigma-Aldrich, UK). Oxoid™ phosphate buffered saline (PBS) pH 7.4 tablets were obtained from Thermo Scientific (Sheffield, UK). Sunflower oil was purchased from a local supermarket, stored in a closed container at ambient temperature in the dark and used without any further purification. Double distilled water from Milli-Q systems (Millipore, Watford, UK) was employed throughout this study.

5.2.2 Lipid particle preparation

Lipid nanoparticle dispersions were fabricated using a melt-emulsification-ultrasonication method followed by cooling of solid and different solid-to-liquid lipid mass ratio (9:1, 8:2 and 7:3) lipid melts in an ice bath. When curcumin was loaded within the lipid particles, 0.5% w/w curcumin, in relation to the total lipid mass, was added to the lipid melt and kept under magnetic stirring until fully dissolved. All samples were stored at 4°C until further analysis. A detailed preparation protocol is given elsewhere [29]. The removal of excess unbound surfactant from

the lipid dispersions was realised by immersing a known amount of each dispersion contained within cellulose dialysis membrane (43 mm width, 14 kDa M.W. cut-off, Sigma-Aldrich Company Ltd., Dorset, UK,) in distilled water under constant stirring at room temperature. The dialysis membranes were pre-hydrated in distilled water overnight. The dialysis medium was changed every 24 h and the process was continued until an equilibrium surface tension value (standard deviation of the last twenty measurements was smaller than 0.05 mN/m) similar to that of distilled water was obtained. Surface tension measurements were performed with a profile analysis tensiometer (PAT-1M, Sinterface Technologies, Berlin, Germany). Briefly, a drop of the dissolution medium was suspended via a straight stainless-steel capillary (3 mm outer diameter) in air, with the cross-sectioned surface area remaining constant at 27 mm^2. Density values of the samples were determined using a densitometer (Densito, Mettler Toledo, US), at 20°C. Dialysed samples were retrieved from the tubing and diluted to their initial mass with distilled water, to maintain the initial lipid phase concentration at 2.5% w/w.

5.2.3 Emulsion preparation

The oil-in-water (o/w) emulsions were prepared with 90% (w/w) aqueous phase containing any of the different lipid nanoparticle systems (SLNs, NLCs) and 10% (w/w) sunflower oil phase. Emulsification was performed using a high intensity ultrasonic Vibra-cell™ VC 505 processor (Sonics & Materials, Inc., CT, USA), operating continuously at 750 Watt and 20 kHz, at a sonication amplitude of 95% of the total power over a period of 30 s. All samples were kept in an ice bath during processing, to avoid shear-induced heating. The produced systems were stored at 4°C until further analysis.

5.2.4 Particle/droplet size and ζ-potential measurements

The particle size expressed as *Z*-average and zeta potential (ζ-potential) of curcumin-loaded lipid nanoparticles used as produced and after dialysis were measured with dynamic light scattering (DLS) employing a Zetasizer Nano ZS (Malvern Instruments, UK). All measurements were performed at a backscattering angle of 173° at 25°C, and samples were appropriately diluted to avoid multiple scattering phenomena. The refractive indices for the materials used were determined using a refractometer (J 357 series, Rudolph Research Analytical, USA) at 20°C, and used accordingly [29]. For distilled water, the refractive index used was 1.33 and the absorption index was set at 0.01. Measurements were performed in triplicate and the average values with standard deviation (±S.D.) are presented. Laser diffraction (LD) was employed to determine the droplet size of the curcumin-loaded lipid particle-stabilised o/w emulsions after incorporation of curcumin in the lipid particles, using a Mastersizer 2000 (Malvern Instruments, UK) equipped with a Hydro SM manual small volume sample dispersion unit. The refractive index of sunflower oil was set at 1.47. All measurements were performed in triplicate. Zeta potential measurements of the o/w emulsion systems were performed following the method described above.

5.2.5 Interfacial tension measurements

Interfacial properties at the oil/water interface of the curcumin-loaded lipid nanoparticles used as produced and after removal of excess surfactant were determined with the pendant drop method utilising a profile analysis tensiometer (PAT-1M, Sinterface Technologies, Berlin, German), at 20°C. A drop of the samples was suspended via a straight stainless-steel capillary (3 mm outer diameter) in the sunflower oil phase contained in a quartz cuvette, with the cross-

sectioned surface area remaining constant at 27 mm^2. Data were collected until equilibrium was reached (standard deviation of the last twenty measurements was smaller than 0.05 mN/m). Density values of the samples were determined using a densitometer (Densito, Mettler Toledo, US), at 20°C. All measurements were conducted in at least triplicate.

5.2.6 Thermal analysis

The thermal behaviour of the lipid particles both in the dispersions and within the emulsion systems was assessed via Differential Scanning Calorimetry (DSC) using a Setaram μDSC3 evo microcalorimeter (Setaram Instrumentation, France). The temperature was cycled between 20 and 80°C at a heating rate of 1.2 °C/min. The thermograms were obtained with the reference cell being filled with equal amount of distilled water. Data processing, including information about peak temperatures, melting enthalpies and deconvolution of peaks, was carried out using the Calisto Processing software (Setaram Instrumentation, France). Information from the thermal profiles of the lipid particles within this temperature range was used to study the behaviour of the particles within an emulsion setting and assess their stability over time (immediately and at 4, 8 and 12 weeks after emulsification). More specifically, the loss of crystalline matter was determined using information from the total melting enthalpies of the particles within an emulsion environment (ΔH^T_{em}) and those in an aqueous dispersion setting (ΔH_{dis}), and was expressed as a $\Delta H^T_{em}/\Delta H_{dis}$ ratio. The ΔH_{dis} and ΔH^T_{em} values were obtained from peak integration of the particle dispersion and particle-stabilised emulsion melting thermograms, respectively. The proportion of lost particles was calculated as a fraction of the particles initially present in the aqueous dispersions ($(\Delta H_{dis} - \Delta H^T_{em})/\Delta H_{dis}$). Information regarding the relative positioning of the lipid particles remaining within the emulsion systems was gained through deconvolution of the two melting events (ΔH^i_{em}, i =1 or 2) occurring in

each system. Particles were distinguished into two categories; particles present in the continuous phase (denoted as ΔH^1_{em} and peak 1) or at the emulsion interface (denoted as ΔH^2_{em} and peak 2). The proportion of each population was calculated as a fraction and expressed as unadsorbed ($\Delta H^1_{em}/(\Delta H^1_{em} + \Delta H^2_{em})$) and adsorbed ($\Delta H^2_{em}/(\Delta H^1_{em} + \Delta H^2_{em})$) particles. Examples of the peak integration/deconvolution of representative lipid particle dispersion samples and their respective emulsion systems are provided in Appendix A3 (Fig. A3.1). All enthalpy values and thermograms reported, are normalised for the amount of crystallising material present in each sample. Specifically for the emulsion systems, each thermogram was normalised using the information of the respective SLN or NLC dispersion (see Appendix A3, Fig. A3.2) that was used for the emulsification. All measurements were performed at least in triplicate and on three independently prepared samples.

5.2.7 Imaging

Representative images of the microstructure of o/w emulsion droplets stabilised with curcumin-loaded lipid particles were obtained using confocal laser scanning microscopy (CLSM) (Leica TCS SPE, Heidelberg, Germany), equipped with a laser operating at a wavelength of 532 nm. The excitation wavelength for curcumin was set at 488 nm and the images were acquired with a 63x oil immersion lens using a coverslip to cover the sample. Emulsion systems with larger droplet sizes were visualised by preparing the samples with a low level of shear, employing a high-shear mixer (Silverson L5 M, Silverson Machines Ltd, UK), operating at 9000 rpm for 2 min.

5.2.8 Encapsulation efficiency and loading capacity

The encapsulation efficiency (EE) and loading capacity (LC) of the curcumin-loaded lipid dispersions and curcumin-loaded particle-stabilised emulsions was determined by ultrafiltration using centrifugal ultrafiltration tubes (Amicon® Ultra-4 filter 10 kDa cut-off, Millipore, Billerica, MA, USA). 1 mL of the samples was added to the upper chamber of the centrifugal tube and centrifuged at 2,400 rcf for 1 h at room temperature using a SIGMA 3K-30 centrifuge (SciQuip®, UK). The concentration of unentrapped curcumin in the filtrate was subsequently determined by measuring the UV absorbance (Genova Bio Life Science Spectrophotometer, Jenway®, Cole-Palmer, UK) at 425 nm, using a calibration curve that has been previously generated with linearity studied for 0–6 μg/mL and linear regression value of $R^2 = 0.9995$. The EE and LC were calculated using the following equation:

$$EE = \frac{W_{i.\ CRM} - W_{u.\ CRM}}{W_{i.\ CRM}} \times 100\ (\%) \quad (5.1)$$

$$LC = \frac{W_{i.\ CRM} - W_{u.\ CRM}}{W_{l.p.}} \times 100\ (\%) \quad (5.2)$$

where $W_{i.\ CRM}$ is the amount of curcumin that was initially used during the preparation of the aqueous lipid dispersions, $W_{u.\ CRM}$ is the amount of curcumin measured in the filtrate, and $W_{l.p.}$ is the total amount of the lipid components used in the dispersions.

5.2.9 *In vitro* release

In vitro release of curcumin, used as a model hydrophobic active, from curcumin-loaded lipid particle dispersions alone and particle-stabilised (Pickering) o/w emulsions was performed by

diffusion through a dialysis membrane. A known amount of the particle dispersions or the Pickering emulsions was enclosed in a cellulose dialysis membrane (43 mm width, 14 kDa M.W. cut-off, Sigma-Aldrich Company Ltd., Dorset, UK), and the tubing was introduced in the *in vitro* release medium (130 g) consisting of phosphate buffer saline (PBS, pH 7.4) and 1.0% w/w Tween® 80. For the emulsion systems' release assessment, the effect of the water volume reduction (compared to the dispersions) within the dialysis membranes on the overall release rate was considered negligible, considering the subsequent decrease in CRM concentration and perpetuation of sink conditions. The specific type and mass of dissolution medium were chosen to enable sufficient curcumin solubilisation and ensure sink conditions (the active concentration was approximately eight times less than its saturation solubility in the dissolution medium). A pure curcumin solution was prepared by dissolving equal amount of curcumin to that in the lipid particle dispersions (0.0125% w/w) in a solution that consisted of the dissolution medium. Dialysis membranes were soaked in the dissolution medium overnight, prior to usage. At predetermined time intervals, 1 mL aliquots of the dissolution medium were collected and analysed by UV-Vis spectrophotometry (Genova Bio Life Science Spectrophotometer, Jenway®, Cole-Palmer, UK), at 425 nm using a calibration curve that has been previously generated with linearity studied for 0–6 μg/mL and linear regression value of $R^2 = 0.9995$. To maintain sink conditions, the sampled dissolution medium was each time replaced by an equal volume of fresh media. The volume correction has been accounted for in the reported cumulative release plots. The release profiles were studied using an Incu-Shake MIDI shaker incubator (Sciquip, UK) operating at 25°C under constant shaking (180 rpm). For stability assessments, the lipid particle dispersions were used/studied immediately after preparation and after 4 months of storage, and their respective particle-stabilised emulsions were assessed

immediately after emulsification and after 3 months of storage at 4°C. Each test was conducted in triplicate using independently prepared samples.

5.2.10 Modelling of release data

The release data from the lipid particles and the particle-stabilised emulsions were fitted into the mechanistic model described by Crank [30], to gain further insight regarding the underlying release mechanism. The diffusion coefficient (*D*) was determined as follows:

$$\frac{Q_t}{Q_\infty} = 1 - \frac{6}{\pi^2}\sum_{n=1}^{\infty}\frac{1}{n^2}\exp\left(-\frac{Dn^2\pi^2 t}{r^2}\right) \tag{5.3}$$

where Q_t is the mass of active released at time *t*, Q_∞ is the total mass of active released when the formulation is exhausted, *n* is the number of the term in the series, *r* is the particle radius, and *D* is the apparent diffusion coefficient of the active within the system. The diffusion coefficients (*D*) and the coefficient of determination (R^2) used as a model fitness indicator are given in Table 5.2.

5.2.11 Statistical analysis

Samples were analysed in at least triplicate and averages are reported with standard deviation (±S.D.). Figures depict the calculated average with error bars showing the standard deviation above and below the average. Comparison of means was conducted by ANOVA analysis followed by an all pairwise multiple comparison test using the Student-Newman-Keuls Method (SigmaPlot 14.5). The differences were considered statistically significant when $p \leq 0.05$.

5.3 Results and discussion

5.3.1 The role of particle integrity and positioning in an emulsion setting

Literature suggests that in an emulsion setting, the presence of an oil phase can provoke the dissolution of solid matter from lipid particles positioned at the interface; e.g. dissolution into the dispersed phase oil droplets in the case of o/w emulsions [24–26]. The mechanism is driven by the presence of micellar-forming surfactants and the relative hydrophilicity of the used oil/fat. The latter determines the ability of either the oil or fat molecules to solubilise in the micelles and diffuse to the fat surface or oil droplets, respectively. This phenomenon can occur in both directions, and can overall promote a decline in solid/crystalline matter, that could thus lead to loss of the lipid particles' Pickering functionality and jeopardise the particles' active carrying capacity. Parameters that could affect the occurrence and/or kinetics of such phenomena, include the lipid particles' formulation characteristics and the presence of additional (unadsorbed) surfactant in the continuous phase of the Pickering emulsions. Therefore, SLNs and NLCs with increasing liquid lipid content (10, 20 and 30% w/w) used as produced and after removal of excess surfactant from their aqueous dispersion phase, were used as Pickering stabilisers and investigated for their water/oil interfacial presence, a parameter that could also potentially affect their active carrying/delivery capacity.

5.3.1.1 Loss of particle crystalline matter within emulsion systems

In this study, information regarding the loss of crystalline matter was gained through the melting thermograms of the emulsions, and specifically the ratio between the total melting enthalpies of the particles within an emulsion environment (ΔH^{T}_{em}) and those in a lipid particle aqueous dispersion setting (ΔH_{dis}) [24]. These ratios were calculated according to the melting

events occurring in each system immediately after preparation (Fig. 5.1), and the resulting enthalpy ratios themselves are presented in Fig. 5.2. Enthalpy data for all systems (particle-stabilised o/w emulsions or particle aqueous dispersions) were normalised against the mass of solid/crystalline matter present in each system, as in both cases the solid lipid is the only component undergoing phase transition. Herein, the impact of the oil addition was explicitly studied, as any effects arising from the liquid lipid incorporation in the solid matrix have already been investigated [29] and accounted for during enthalpy normalisation. Based on the calculated ratios, it is evident that the loss of solid lipid matter was minimal for all systems used as produced and after dialysis, with the percentage of original crystalline matter (generated at the particle manufacture stage) remaining in the systems following oil introduction (emulsification) ranging between 85 and 100%. Zafeiri *et al*. [24] investigated the dissolution of solid material from SLNs in increasing fractions of sunflower o/w emulsions, using cetyl palmitate and tristearin particles (2.5% w/w) fabricated in the presence of Tween® 80 or sodium caseinate (0.8% w/w). It was shown that sodium caseinate provided improved shielding over mass transfer phenomena compared to Tween® 80 (95 versus 68% of solid lipid matter was found to persist after emulsification for the 10% oil phase o/w emulsions, respectively), and cetyl palmitate exhibited greater loss of crystalline content (in the range of 55 and 75%) compared to tristearin (between 5 and 10%). Overall, it was suggested that dissolution mainly occurs shortly after emulsification, and the importance of the type and concentration of surfactant, and the type of lipid source used, relative to the rate of oil exchange was underlined. These observations have also been highlighted in a number of studies exploring the rate of oil exchange between o/w emulsion droplets and an aqueous phase, with surfactant molecules/micelles facilitating the transfer [26,31–34]. Notably, Samtlebe *et al*. [26] proposed that emulsion-originating oil molecules solubilised in micelles, diffuse and dissolve in the

crystalline fat of SLNs, particularly if the solid fat is of relatively high water solubility. In turn, the now dissolved fat can diffuse back to the oil phase through micelles, thus promoting increased lipid mass transfer. Herein, the presence of medium chain triglyceride molecules (Miglyol® 812) in the NLCs appears to have induced solid lipid mass transfer, particularly in the case of the 8:2 and 7:3 NLCs, compared to the SLN- and 9:1 NLC-containing formulations; suggested by the statistically significant changes in the $\Delta H^{T}_{em}/\Delta H_{dis}$ ratios (Fig. 5.2). Part I of this study [19] demonstrated, that increasing the liquid lipid content of the NLCs renders them more hydrophilic. Hence, it could be postulated here, that the increased hydrophilicity of the 8:2 and 7:2 NLC lipid matrix, further provoked oil dissolution and diffusion phenomena. When it comes to emulsions fabricated with lipid particles used after dialysis, the absence of excess surfactant (possibly in the form of micelles) from the continuous phase led to a decrease in the loss of crystalline matter. This is more evident for the highest liquid lipid content particles (8:2 and 7:3 NLCs), possibly due to their already lower $\Delta H^{T}_{em}/\Delta H_{dis}$ ratios.

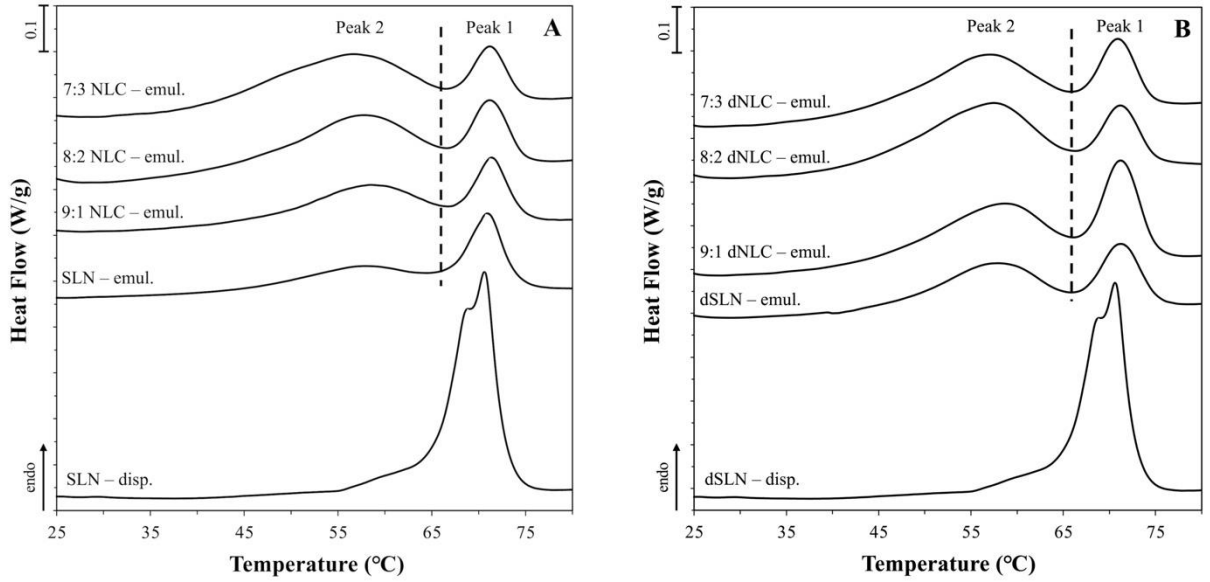

Fig. 5.1. DSC melting thermograms of particle-stabilised o/w emulsion prepared with different types of lipid particles (SLN, 9:1 NLC, 8:2 NLC and 7:3 NLC) before (A) and after removal of excess surfactant (B) from the aqueous lipid particle dispersions. The thermograms of the SLN formulation before and after dialysis are included in the corresponding graphs for comparison purposes. The curves were normalised for the amount of solid matter present in each sample and shifted along the ordinate for better visualisation. The dashed lines are used to distinguish between different thermal events.

It was previously shown [19], based on the melting and crystallisation thermograms of the lipid particle dispersions, that removal of excess surfactant via dialysis did not alter their thermal behaviour. Glyceryl behenate SLNs displayed a level of polymorphism with a minor shoulder (at 69.2°C) appearing on the main melting event at 70.7°C (also visible here in Fig. 5.1), that was shown to progressively intensify as the MCT (liquid lipid) content (9:1, 8:2 and 7:3 solid-to-liquid lipid mass ratios) in the NLCs increases (see Appendix A3, Fig. A3.2) [29]. Introduction of sunflower oil (emulsification) led to broadening of the main peak and appearance of a secondary peak at lower temperatures (~57°C), the intensity of which increased with increasing liquid lipid concentration in the lipid particle composition (Fig. 5.1A & B). This phenomenon has also been described in other studies employing lipid particles as Pickering

emulsion stabilisers, and it was proposed that the partition in the melting profile of the solid lipid was caused by the relative location of the particles in the system; either particles remaining unadsorbed in the continuous phase (peak at higher temperature, herein denoted as peak 1), or particles adsorbed at the interface of the emulsion droplets (peak at lower temperature, denoted as peak 2 in this study) [27,35,36]. More specifically, it has been shown that the type of lipid [35], the emulsion fabrication process (addition of particles prior- or post-homogenisation) [27], and the addition and type of surfactant [36], are among the factors affecting the relative intensity of the two peaks. Although a clear explanation regarding the difference in the melting temperatures of the adsorbed and unadsorbed particles has not been proposed, it could be assumed that the diversity in the specific heat capacities between the surrounding phases (sunflower oil and water, respectively) contributes to the way that heat transfers to the solid lipid matter during melting, with the oil phase heating up faster due to the lower specific heat capacity [37]. Overall, all types of particles retained a high proportion of their original solid lipid content, a parameter that could potentially alter their ability to preserve their active carrying capacity and delivery in a sustainable manner.

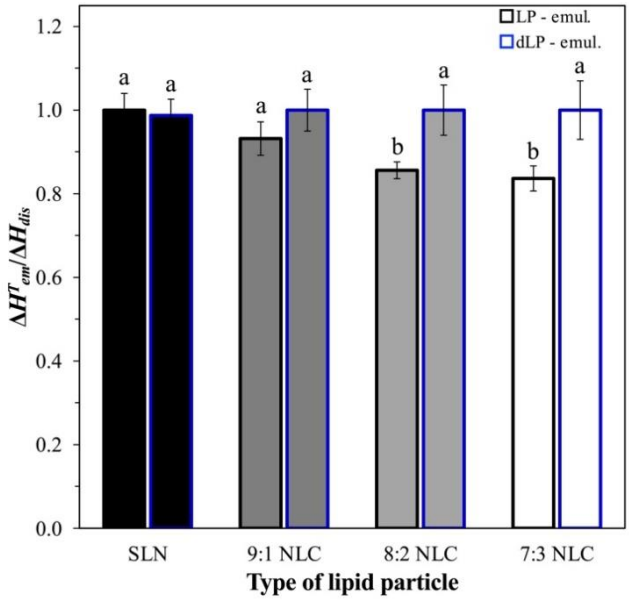

Fig. 5.2. Ratio of total melting enthalpies of the particles within an emulsion environment and those in a lipid particle dispersion setting ($\Delta H^T_{em}/\Delta H_{dis}$), representing the amount of crystalline material remaining within the emulsions stabilised by different types of lipid particles. The particles were either used as produced (LP), or after removal of excess surfactant (dLP). Identical lowercase letters indicate no significant differences between samples (for p>0.05 and sample size equal to 3).

5.3.1.2 Lipid particle type and its effect on the SLN/NLC interfacial presence

Another facet of the lipid particles' capacity to maintain their active carrying/delivery functionality is their relative positioning within the emulsion microstructure. Although it has been already established that the largest proportion of crystalline matter is maintained after emulsification, in such dynamic systems, the close proximity of the particles with the droplet interface could potentially affect their capacity to regulate the delivery of the enclosed active. Information about the proportion of lipid particles either present at the emulsion interface (i.e. exposed to the oil content in the droplets) or in the continuous phase (i.e. only largely exposed to an aqueous environment), could assist in discerning any such contributions on the overall active carrying/delivery performance of these systems.

To gain further insight regarding the distribution of lipid particles remaining in the emulsion systems, the melting curves of all lipid particle-stabilised emulsions were deconvolved into two individual peaks; see Fig. 5.1A & B. This was performed for both different types of lipid particles (SLNs and NLCs), and for particles used before and after dialysis, as removal of excess surfactant could potentially affect their interfacial residency. The corresponding melting enthalpy for each peak was then calculated and the resulting ratios were determined (see Section 5.2.6) to distinguish between the fraction of adsorbed and unadsorbed particles within the emulsion systems. As depicted in Fig. 5.3 (top), the proportion of lipid particles residing at the emulsion interface is approximately 60% (of the total population of remnant particles) and remains similar for both SLNs and NLCs. For lipid particles used after removal of excess surfactant, although the values were similar for different solid-to-liquid lipid mass ratios, they appear to be slightly higher than that of particles used as produced. Absence of free surfactant from the continuous phase could potentially allow a higher proportion of particles to reside at the interface of the droplets compared to the emulsions fabricated with the 'as produced' particle dispersions, where it could be assumed that part of the droplet interface is occupied by surfactant molecules. On the contrary, the ratio of unadsorbed particles (in the range of 30%) decreases with increasing amount of MCTs (Fig. 5.3, bottom) in both cases. This is particularly obvious for the two particle formulations with the highest liquid lipid content (8:2 and 7:3 NLCs). To begin with, this observation needs to be approached cautiously, as the peaks ascribed to adsorbed particles (peak 2) for these two systems could also encompass the melting of polymorphic forms present in both adsorbed and unadsorbed particles (see Appendix A3, Fig. A3.2). The presence of non-spherical particles as suggested by the different polymorphs, particularly in the DSC thermograms of the 8:2 and 7:3 NLC dispersions [19,29], could suggest different packing/arrangement at the emulsion interface [38,39]. Additionally, the smaller

particle size and differences in the zeta potential values of the aforementioned formulations (even though at marginal level) [29] could further support the requirement for higher interfacial residency. Such phenomena, not only explain the trends observed for the unadsorbed particles, but also for the respective adsorbed particles in the same formulations (Fig. 5.3, top). Another possible explanation when it comes to the decreasing percentage of unadsorbed particles in the systems with used as produced particles could be found in the occurrence of particle replacement at the emulsion interface. As more crystalline matter is lost at the emulsion interface, which is also reflected in the concurrent increase of lost particles (Table 5.1), the proportion of 'free particles' moving from the continuous phase to substitute the matter lost and maintain the same surface coverage increases (Fig. 5.4). This is in agreement with findings previously reported in literature [40], where it is shown that particles are reversibly adsorbed onto the emulsion droplets, and exchanges can occur between the continuous phase and the droplet interface. The data acquired from the DSC spectra shown here appear to give lower particle interfacial occupancy values when compared to the theoretical values of the (maximum) proportion of unadsorbed particles reported in part I of this work [19]. This suggests an overestimation in the latter theoretical values that could be attributed to 'adsorbed particle'-'free particle' bridging, that has previously been reported for particles covered by thin surfactant layers [41,42], or simply by the formation of multilayers of particles around the emulsion droplets (rather than the single layer assumed in the theoretical calculation). Information gained here does not only contribute to understanding regarding the effect of certain formulation parameters on the water/oil interfacial presence of the particles, but it could also assist in elucidating the active regulation mechanism of the particles in relation to their relative interfacial location within the emulsion systems in a later step.

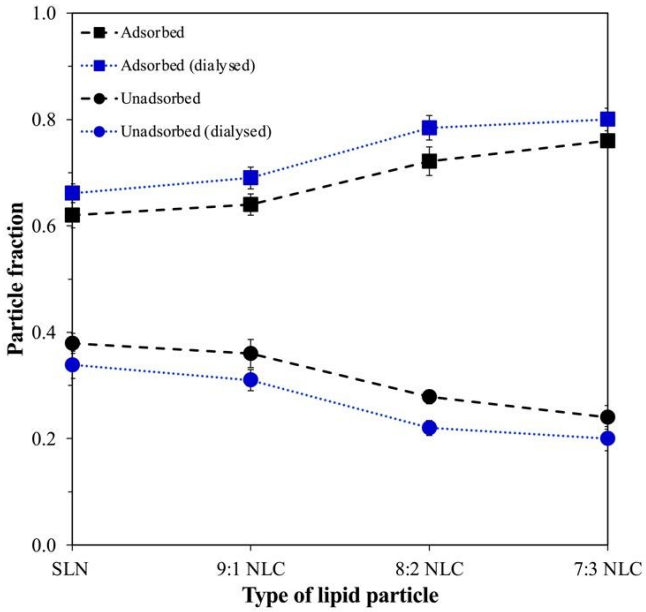

Fig. 5.3. Fraction of lipid particles unadsorbed and adsorbed for the different types of lipid particles used before and after dialysis, within an emulsion setting. For the ΔH^{i}_{em} calculations, the peaks were defined following deconvolution of the peaks presented in Fig. 5.1. When not visible, error bars are smaller than symbols.

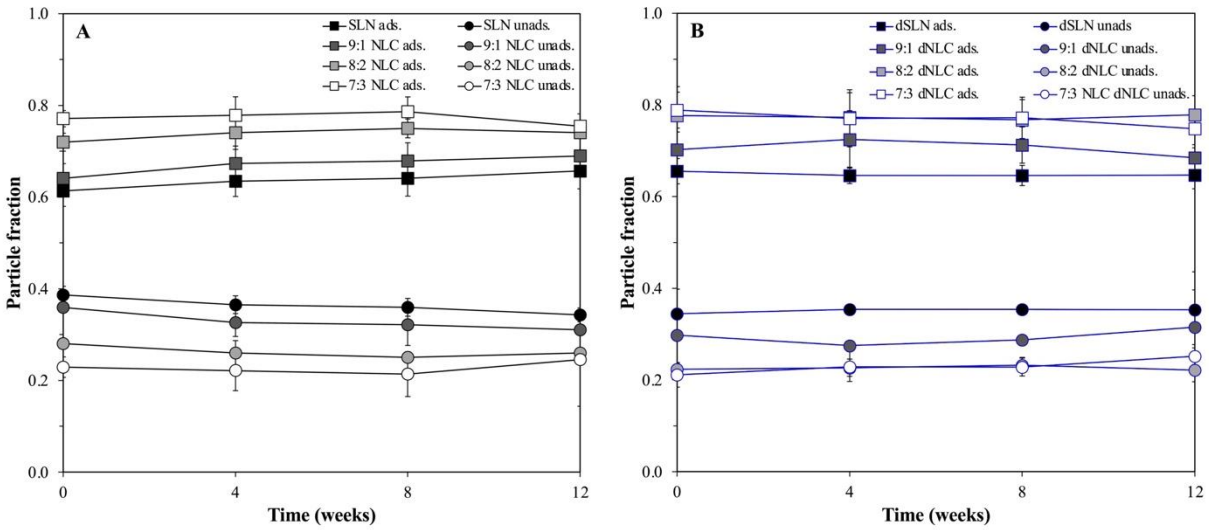

Fig. 5.4. Time evolution of the proportion of lipid particles adsorbed and unadsorbed for the different types of lipid particles used as produced (A) and after dialysis (B), within emulsion systems.

Table 5.1. ΔH_{dis}, ΔH^{T}_{em}, ΔH^{i}_{em}, and T^{i}_{melt} of o/w emulsions stabilised by different SLN and NLC (9:1, 8:2 and 7:3) dispersions used as produced and after dialysis and measured at various time intervals over a storage period of 12 weeks at 4°C. For the ΔH^{i}_{em} calculation, the peak separation was performed according to the peaks presented in Fig. 5.1, with peak 1 corresponding to unadsorbed and peak 2 to adsorbed particles. The fraction of particles lost overtime is also included for comparison purposes.

Type of lipid particle	Storage period (weeks)	ΔH_{dis} (J/g)	ΔH^{T}_{em} (J/g)	ΔH^{i}_{em} (J/g)		T^{i}_{melt} (°C)		Lost particles fraction
				ΔH^{1}_{em}	ΔH^{2}_{em}	T^{1}_{melt}	T^{2}_{melt}	
SLN	0	150.2±2.3	148.0±4.2	88.3±4.0	55.6±7.2	57.9±1.1	71.0±0.2	0.0±0.0
	4	146.8±2.2	145.8±8.4	92.4±3.8	53.2±8.4	59.4±0.9	71.7±0.3	0.0±0.0
	8	145.6±6.7	144.7±8.2	94.6±4.7	53.1±9.1	58.4±0.7	71.0±0.5	0.0±0.0
	12	140.9±5.4	140.8±6.2	90.6±5.8	47.3±6.3	58.9±0.5	71.1±0.3	0.1±0.0
9:1 NLC	0	146.1±4.1	136.2±4.4	85.3±5.7	47.8±7.7	58.5±0.8	71.3±0.2	0.1±0.0
	4	141.7±2.7	137.8±3.1	91.5±7.5	44.4±4.3	59.5±0.6	71.4±0.1	0.1±0.0
	8	143.1±6.5	142.8±9.9	94.5±5.4	44.7±6.7	58.9±0.3	71.4±0.1	0.1±0.0
	12	147.7±3.8	143.3±4.7	95.9±1.9	43.2±6.0	59.1±0.4	71.3±0.2	0.1±0.0
8:2 NLC	0	148.4±3.2	128.0±2.7	93.6±2.5	36.4±1.0	58.0±0.3	71.2±0.1	0.1±0.0
	4	145.9±6.3	136.5±8.1	101.0±10.5	35.5±3.7	58.0±0.3	71.5±0.2	0.1±0.0
	8	138.2±2.9	135.9±3.6	101.9±2.8	34.0±1.6	58.2±0.2	71.4±0.3	0.1±0.0
	12	134.0±4.7	127.1±6.9	92.6±1.0	32.5±1.5	58.4±0.1	71.5±0.2	0.1±0.0
7:3 NLC	0	144.9±5.0	121.2±3.7	93.4±7.1	27.8±2.7	55.9±3.4	71.4±0.5	0.1±0.0
	4	142.7±2.6	133.6±10.3	102.5±5.4	29.2±5.9	57.7±1.5	71.2±0.3	0.1±0.0
	8	141.2±3.4	134.7±14.5	105.9±8.4	28.8±6.6	56.9±0.9	71.3±0.2	0.1±0.0
	12	135.4±5.3	130.8±13.2	98.7±6.1	32.1±9.2	57.1±1.1	71.4±0.1	0.1±0.0
dSLN	0	145.0±5.1	143.9±5.8	95.6±4.2	50.2±5.7	57.9±1.1	71.0±0.2	0.0±0.0
	4	148.9±3.5	148.2±7.6	94.5±2.7	51.7±8.9	58.2±0.8	71.8±0.2	0.0±0.0
	8	147.5±6.1	146.3±10.5	93.2±3.2	51.1±7.4	58.1±0.6	71.4±0.1	0.0±0.0
	12	148.9±3.8	146.6±8.9	99.4±6.1	54.2±13.2	58.0±0.7	71.2±0.3	0.0±0.0
9:1 dNLC	0	149.9±4.7	149.5±14.3	106.7±5.9	45.2±6.9	58.5±0.8	71.3±0.2	0.0±0.0
	4	144.9±2.6	141.0±12.6	108.0±8.8	41.0±12.8	57.9±0.5	71.3±0.1	0.0±0.0
	8	148.1±4.6	146.1±10.4	107.3±5.9	43.3±12.5	57.8±0.4	71.2±0.2	0.0±0.0
	12	150.9±5.1	147.5±12.4	104.6±4.5	48.2±12.4	58.1±0.2	71.4±0.1	0.0±0.0
8:2 dNLC	0	138.7±4.1	137.3±9.4	108.2±5.4	31.1±2.7	58.4±1.8	71.2±0.4	0.0±0.0
	4	140.9±3.4	140.2±11.3	115.6±7.6	33.9±0.7	58.3±0.9	71.2±0.1	0.1±0.0
	8	141.7±3.3	140.3±10.6	109.1±6.3	33.0±5.2	58.1±0.4	71.0±0.2	0.0±0.0
	12	137.7±4.7	135.4±9.3	113.2±4.1	32.2±8.6	58.1±0.3	71.3±0.2	0.0±0.0

	0	139.0±11.1	138.8±3.5	109.3±5.4	29.3±3.7	55.9±3.4	71.4±0.5	0.0±0.0
7:3	4	135.6±5.9	132.2±4.4	108.7±8.9	32.3±4.7	57.2±2.9	71.5±0.3	0.1±0.0
dNLC	8	136.2±5.1	131.6±3.8	107.6±6.4	31.8±2.8	56.9±1.1	71.1±0.3	0.0±0.0
	12	140.6±4.3	139.4±7.9	106.3±5.6	35.8±3.4	57.1±1.5	71.2±0.2	0.0±0.0

5.3.2 Effect of active incorporation on the lipid particle Pickering functionality

5.3.2.1 Size, zeta potential and interfacial properties of lipid particles

Prior to studying the active carrying/delivery capacity of curcumin-loaded particles within an emulsion setting, the effect of curcumin encapsulation on the size, ζ-potential and dynamic interfacial tension reduction ability of the SLN and 7:3 NLC formulations (used as produced or after dialysis) was studied. The choice of these two formulations was based on the fact that they represent the two extremes in terms of liquid lipid particle composition investigated here. Regarding the particle size, a slight *Z*-average increase was observed after the addition of curcumin in the two types of lipid particles (Fig. 5.5A), that has also been previously identified and attributed to lipid core swelling due to the presence of the active [29]. The effect that the removal of excess surfactant (via dialysis) has on (CRM-loaded) particle size was the same as that previously observed for 'blank' lipid particles [19], with a statistically significant increase only shown for the 7:3 NLCs. Similarly, no further changes after curcumin entrapment were recorded for the ζ-potential values and interfacial tension reduction capacity of both lipid particle dispersion types (either used as produced or after dialysis), apart from those already described for the respective blank formulations (Fig. 5.5B & 5.6, respectively). A more in-depth discussion of said differences can be found in part I of this work [19].

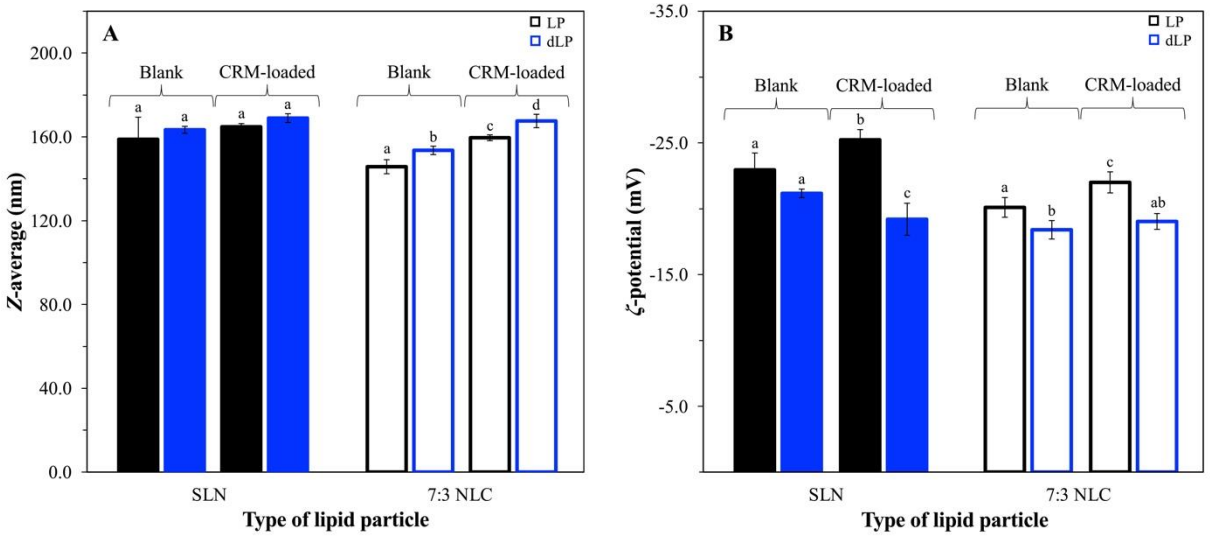

Fig. 5.5. Particle size (*Z*-average) (A) and *ζ*-potential (B) of curcumin-loaded lipid particle dispersions before (CRM-loaded LP) and after dialysis (CRM-loaded dLP). The respective data for blank lipid particles are also presented for comparison purposes. Identical lowercase letters indicate no significant differences between samples (for p>0.05 and sample size equal to 3).

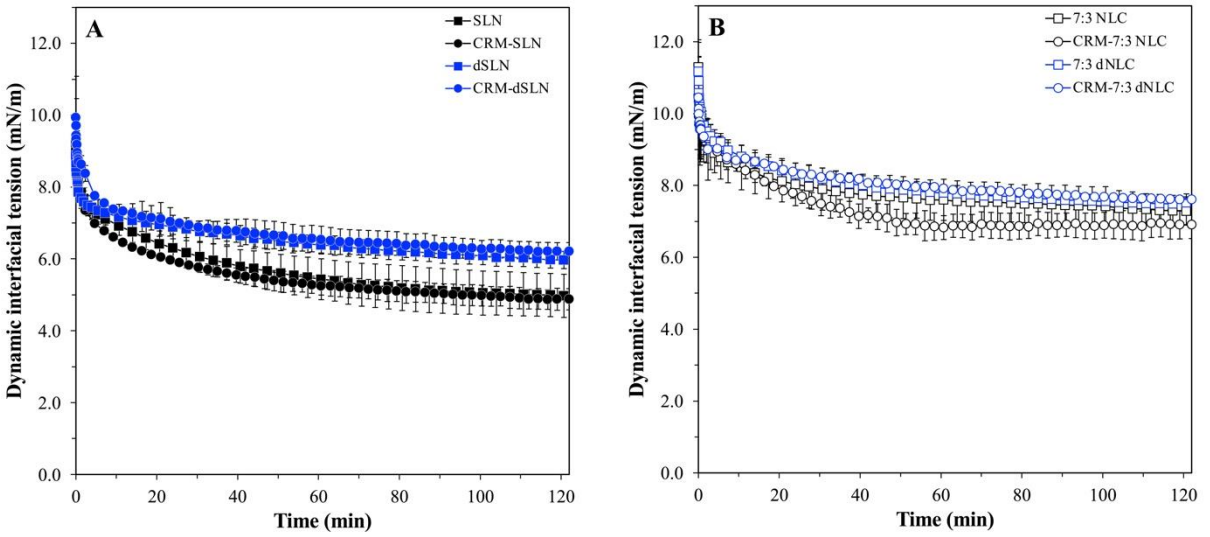

Fig. 5.6. Dynamic interfacial tension of aqueous dispersions of blank and CRM-loaded SLN (A) and 7:3 NLC formulations (B) used as produced and after dialysis. Data points are the average of three measurements and error bars represent the standard deviation.

.

5.3.2.2 Emulsion stabilisation behaviour

Having established that the encapsulation of curcumin does not alter characteristics of the lipid particles that were previously shown to contribute to effective Pickering emulsion functionality, the curcumin-loaded SLN and 7:3 NLC formulations were indeed used to stabilise o/w emulsions and the droplet size and ζ-potential of the resulting systems were measured (Fig. 5.7A & B). As depicted in Fig. 5.7A, both (SLN- or NLC-stabilised) Pickering o/w emulsions fabricated using lipid particle dispersions where excess surfactant had been removed (dialysed), showed an additional droplet size population at larger sizes compared to the ones prepared with dispersions before dialysis. This is in agreement with what was observed for blank lipid particle-stabilised emulsions (inset graph, Fig. 5.7Ai) [19]. Possible explanations could lie in the interfacial tension reduction capacity differences between the dispersions (with dialysed particles having higher interfacial tension equilibrium values), lack of excess surfactant in the continuous phase and/or reduced wettability by the aqueous phase for the dialysed particles [43,44]. Correspondingly, the ζ-potential values demonstrated the same trends as for the blank systems, with no further changes caused due to the presence of the active (Fig. 5.7B). Finally, the Pickering stabilisation in the presence of curcumin for a representative system (CRM-dSLN-stabilised emulsion) was confirmed using CLSM (inset, Fig. 5.7Aii). The work presented here suggests that lipid particle microstructural design for Pickering performance can precede the development of active encapsulation strategies. Thus, as long as the latter do not impact on key indicators of Pickering behaviour (e.g. particle dimensions), adopting an active carrying/delivery functionality will not impede the particles' emulsion stabilisation performance.

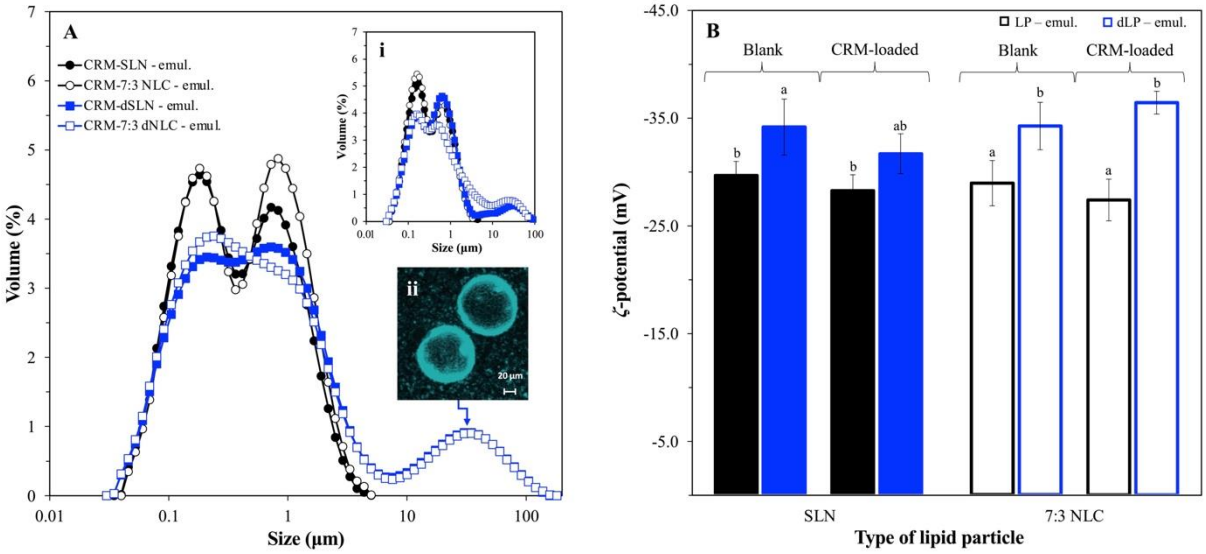

Fig. 5.7. Droplet size distribution (A) and ζ-potential (B) of o/w emulsion droplets stabilised with curcumin-loaded lipid particles used as produced (CRM-loaded LP) and after dialysis (CRM-loaded dLP). A CLSM image of selectively captured droplets of one of the systems is also depicted to illustrate the particle-covered interface (inset graph A, ii). The respective data for droplet size (inset graph A, i) and ζ-potential (B) for blank lipid particle-stabilised emulsions are also presented for comparison. Identical lowercase letters indicate no significant differences between samples (for p>0.05 and sample size equal to 3).

5.3.3.3 Encapsulation efficiency and loading capacity of lipid particles

Previous work by the present authors on the characterisation of the particles' active carrying capability, revealed that changes to their chemical/physical properties do not alter their encapsulation efficiency (EE) or loading capacity (LC); with values of 99.9±0.0% and 0.5±0.0% for each of these, respectively [29]. Values within this range have been previously reported for similar systems, where the incorporation of curcumin was achieved by simple solubilisation in lipid melts under stirring [45,46], whereas higher LC values were attained when organic solvents were employed [47,48]. Overall, the affinity of curcumin for the lipid matrix components (lipid and/or surfactant type and concentration) used was shown to greatly affect the obtained values. In the current study, the amount of curcumin persisting within the

(as produced) SLNs and 7:3 NLCs following dialysis, after incorporation within an emulsion microstructure, but also over storage, was evaluated by measuring both the corresponding EE and LC values. Herein, the values determined for both parameters were the same as for the aqueous lipid particle dispersions. Notably, neither exposure of the particles to the dialysis conditions, nor introduction of a second phase (oil droplets) during emulsification, compromised their active carrying capacity. Thus, curcumin appears to maintain a close association with the microstructure, with no evidence of migration to the continuous phase. This could be possibly the result of the good solubilisation capacity/affinity of the used lipid matrix components for the active, as has been previously shown [29], but also a consequence of the relatively low quantity of active used/entrapped, allowing for an improved detainment within the colloidal microstructures. However, it should also be noted here, that within an emulsion setting, the absence of the active from the continuous aqueous phase does not necessarily confirm that the high encapsulation efficiencies are maintained due to the presence of the active solely within the particle structure. The prospect of a level of active migration to the oil used as the dispersed phase (i.e. the oil droplets that the particles are stabilising and thus are in partial contact with) is also possible. This is discussed in more detail in the following section.

5.3.3.4 *In vitro* release performance of lipid particles

The initial parts of this work have demonstrated the ability of the lipid particles (studied here) to successfully exhibit a Pickering functionality while also acting as active carriers. The present section investigates the parameters affecting the capacity of these lipid structures to deliver their encapsulated load. What is more, it also assesses how lipid particle placement within an emulsion setting (interface or continuous phase) impacts on the release performance

demonstrated by the same colloidal species when present within a simple aqueous environment; i.e. release exhibited by the lipid particles in an aqueous dispersion. In both cases, the functionality of the lipid particles as delivery systems, was investigated prior and post dialysis. The SLN (Fig. 5.8A) and 7:3 NLC (Fig. 5.8B) lipid formulations, that were previously confirmed to be able to retain both functionalities of Pickering stabilisation and active carrying, were here employed to study the release of curcumin, selected as a model hydrophobic active [29].

It appears that both types of particles (in an aqueous dispersion) can function as release regulators for curcumin, with the obtained release rates showing drastic decrease compared to that from a pure curcumin aqueous solution; the latter having a curcumin concentration equivalent to that present in the continuous phase of both particles and emulsion systems, if none was contained within the dispersed phase. More specifically, the 7:3 NLCs demonstrated even more sustained release than the SLNs (both as undialysed lipid particles in dispersion), with 12.2% and 21.2% of curcumin released after 7 days, respectively. The differences in the curcumin release profiles cannot be explained in terms of particles size changes between the SLN (165 nm) and NLC (163 nm) lipid structures [29]. Instead, it could be that the incorporation of liquid lipid in the NLCs gives rise to structural re-organisation of the lipid particle matrix by the creation of a less ordered crystalline state, which could also be seen in their DSC profiles [29]. Such an effect could ultimately alter the active distribution/localisation within the particle structure, that could sequentially lead to acceleration [49,50] or hindering of the release profile [51]. Increase in the particles' liquid lipid content could also impact the relative compatibility between the active and the lipid matrix components, which (in this case) results in a hindrance of the release of the former [10,52]. Conversely, the dialysed particles (dSLNs and dNLCs) demonstrated an increased release rate compared to their undialysed

equivalents. This could have been instigated by the exposure of particles (dSLNs and 7:3 dNLCs) to the dialysis conditions (e.g. high osmotic stress) and bulk aqueous environment (of equivalent capacity/volume to that used during the release experiments themselves) for longer periods of time than the undialysed ones.

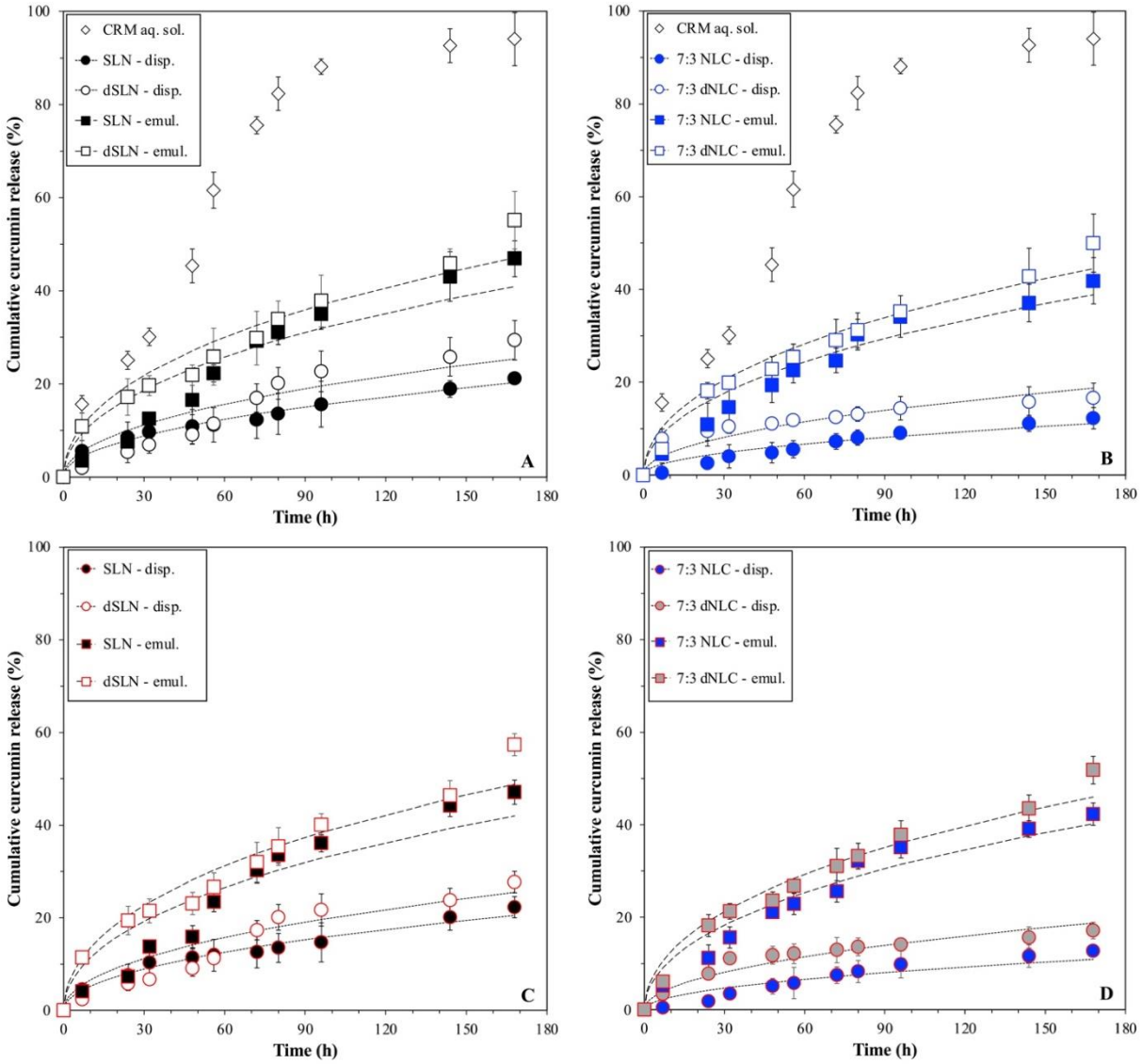

Fig. 5.8. *In vitro* release profile of a model hydrophobic active (curcumin) from SLN (A) and 7:3 NLC (B) dispersions used as produced and after dialysis, and also after emulsion incorporation. The release profile from a curcumin solution obtained under the same conditions is also depicted. The long-term stability of the release performance after 3 months of storage is depicted for all systems in (C) and (D), respectively.

The *in vitro* release kinetic Crank model fitting of curcumin for each dispersion (dotted line) and emulsion system (dashed line) is also presented.

In contrast, curcumin release from lipid particles within an emulsion setting (particles also acting as Pickering stabilisers for the emulsion droplets) was faster than that exhibited by equivalent particles in an aqueous dispersion (Fig. 5.8A & B). Similarly to what was observed earlier for the aqueous particle dispersions, emulsions fabricated with either dSLNs or 7:3 dNLCs (dialysed particles), showed a slightly higher release rate compared to their undialysed counterparts. Furthermore, when comparing the release profiles of the 7:3 NLC-stabilised emulsions to that of the respective SLN-stabilised systems, it is shown that the release rate of the former was marginally slower. As such, these observations suggest that the presence on an oil phase (in the emulsion scenario) plays a crucial role in the discharge of curcumin. At the same time, the perpetuation of the particles' release performance (to a certain degree) indicates that the active regulation ability of each particle type persists even within an emulsion setting.

Fitting the curcumin release data to the Crank model [30] gave diffusion coefficient (D) values for the particles within the dispersion environment ranging between 10.0 and 71.9×10^{-20} $cm^2\ s^{-1}$, while for those present in the emulsions the respective values were (in most instances) an order of magnitude higher (Table 5.2). The diffusion coefficients determined here for all systems are lower than the values reported in literature for curcumin-loaded SLNs fabricated with stearic acid as the lipid phase and Poloxamer 188 as surfactant [7,53]. The type of lipid source and surfactant used and their affinity for the enclosed active have been previously shown to influence the active loading capacity [29,46], which in turn can impact on the delivery performance. The lower D values reported here are in line with the high encapsulation efficiency/loading capacity values reported for all formulations, regardless of dialysis and/or

emulsion presence. This is indicative of not only the close association of curcumin with the particles' crystalline matrix leading to slow diffusion, but also corroborative of the relatively low percentage of curcumin being released. Considering the above, along with the persistence of the EE values after addition of the particles within the emulsion setting, it could be proposed that the release of curcumin could only be ascribed to diffusion either from the free particles and/or from within the microstructure provided by the Pickering emulsions.

According to the data reported above, it is clear that the exposure of the particles to the oil phase creates circumstances that accelerate the release of curcumin into the aqueous acceptor phase. Delving further into the behaviour of the particles within the emulsion systems, a condition that could explain the effect of the emulsion addition, is the differentiation between the particles adsorbed at the oil-water interface and those remaining in the continuous phase. It is therefore suggested that the relative location/setting renders the particles to experience different surroundings, as shown in the schematic representation (Fig. 5.9). One surrounding resembles that of a dispersion setting (Fig. 5.9B.2(i)), where the particles are only exposed to the aqueous environment of the continuous phase, and the other consisting of a hybrid setting (Fig. 5.9B.2(ii)), where part of the particle structure is exposed to the oil phase and the other experiencing the continuous phase environment. In terms of the discharge from the latter, the underlying mechanism could be the outcome of a number of different contributions. Among these, introduction of the oil phase could cause migration of curcumin molecules adsorbed near the oil/particle contact points to the oil phase, which following that are more easily released to the continuous phase through surfactant micelles. Although, this could only constitute a small contribution, as the release behaviour appears to remain unchanged overtime (Fig. 5.8C & D), but also due to the minimal solubilisation capacity of sunflower oil for curcumin [54]. Thereby, the obtained release profiles appear to be the composite of the release from free particles that

follow the release seen in simple dispersions, oil droplets that release curcumin a lot faster compared to the solid structure of the lipid particles, and lastly interfacially-adsorbed particles that would be expected to feed into both previous two patterns. Overall, the particle positioning at the oil/water interface results in a heterogeneous release pattern for curcumin and an utterly accelerated discharge in the emulsion's continuous phase (Fig. 5.9B.3), compared to the homogeneous release pattern of curcumin in the aqueous environment of the lipid particle dispersion (Fig. 5.9A.2).

Further to the curcumin migration presented above, other explanations could also lie in the creation of an added change-inducing potential to the particles themselves and around them, that leads to faster expulsion of curcumin. This could be stemming either from possible movement of the adsorbed surfactant molecules from the particle surface being in immediate exposure to the oil droplets [23,28,55], or even alterations to the arrangement of their hydrophilic chains, owing to changes in their surrounding environment [56,57]. Any of these explanations could lead to stripping of any loosely adsorbed curcumin near the particles' surface. Such phenomena appear to have further intensified in the dialysed particle-stabilised emulsions, causing slightly higher release rates and *D* values (Fig. 5.8A & B, Table 5.2). It was earlier shown (Fig. 5.3) that dialysed particles (dSLNs or dNLCs) have a higher interfacial presence, thus the faster release exhibited by their emulsions aligns well with the hypothesis presented here; i.e. that the presence of lipid particles at the emulsion interface facilitates further active discharge. The interaction and subsequent faster transfer of a fluorescent probe (25-NBD cholesterol) from adsorbed loaded-lipid particles to the oil phase compared to free loaded-particles in the continuous phase (and thus not directly associated with the emulsion droplets) could also be endorsed by the work of Schröder *et al*. [27]. Although minimal (as indicated by the DSC data presented earlier), the contribution of crystalline matter loss to the migration of

the active from the particles to the oil phase (droplets) of the emulsion, should also be considered.

Table 5.2. Diffusion coefficient (D) and coefficient of determination (R^2) describing the fitting into the Crank model of the release data from lipid particles used as produced and after dialysis, and from particle-stabilised emulsions. For the emulsions, data fitting is performed on systems prepared with freshly produced and stored lipid particle dispersions (4 months), and for stored emulsion systems (3 months) prepared with fresh particle dispersions.

Formulation	Storage period (months)	$D \times 10^{-20}$ (cm^2 s^{-1})	R^2
SLN – disp.	0	45.1±7.9	0.98
dSLN – disp.	0	71.9±6.3	0.92
7:3 NLC – disp.	0	10.0±1.2	0.97
7:3 dNLC – disp.	0	11.9±2.3	0.93
SLN – emul.	0	212±23.2	0.94
	0 (stored particles)	216±34.2	0.91
	3	227±25.8	0.93
dSLN – emul.	0	311±45.6	0.96
	3	340±52.5	0.96
7:3 NLC – emul.	0	177±25.4	0.97
	0 (stored particles)	194±28.9	0.94
	3	192±31.2	0.97
7:3 dNLC – emul.	0	268±49.8	0.98
	3	290±47.2	0.99

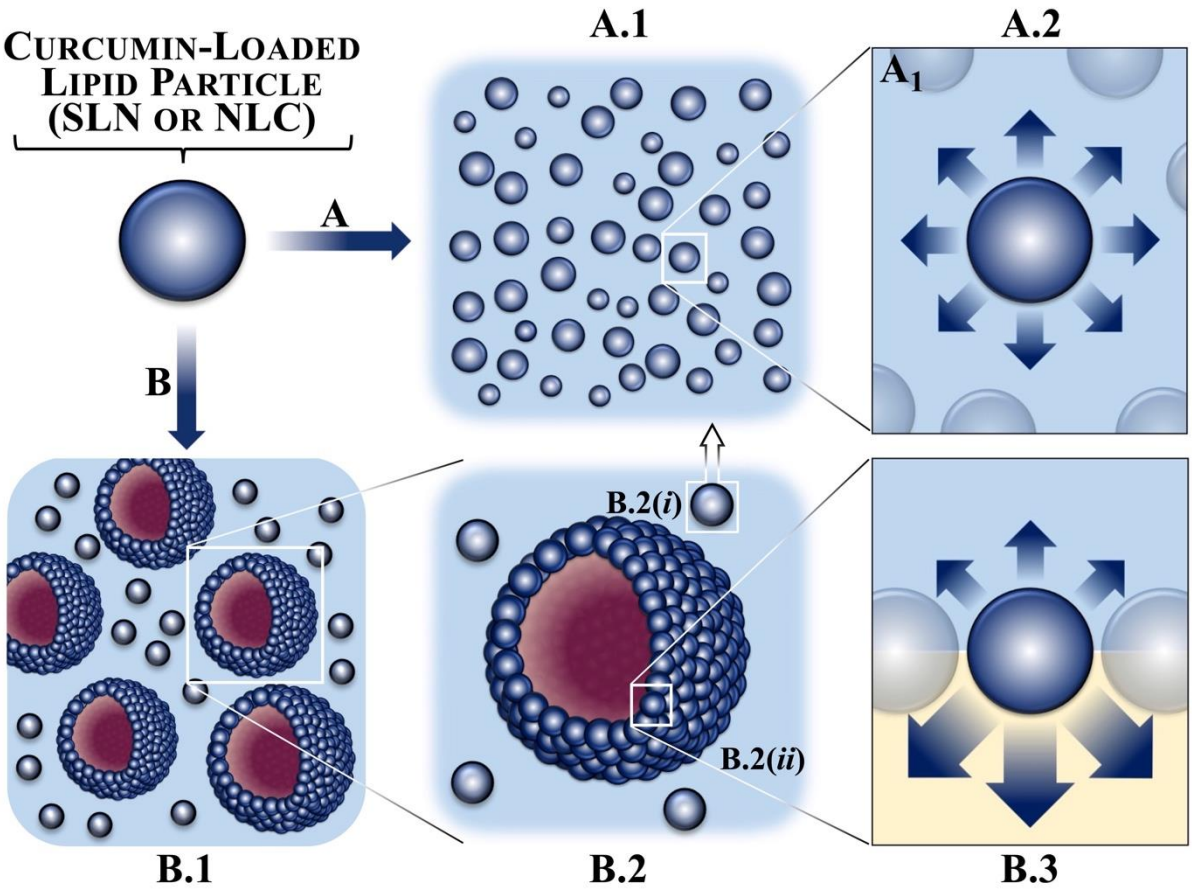

Fig. 5.9. Schematic diagram of the proposed release mechanism from lipid particles within aqueous dispersion (A) and emulsion (B) settings.

In an attempt to visualise the location of curcumin within the emulsion systems, the emulsion droplets were made larger (see Section 5.2.7) and CLSM was employed. Curcumin fluorescence [58] was primarily detected at the droplet interface and at particles remaining free in the continuous phase, of a representative emulsion system after 1 hour of production (Fig. 5.10A). This implies the association of curcumin with the particles (in this case SLNs), whereas after 1 day of storage curcumin could be also identified within the oil droplets or in closer proximity to them by migrating closer to the particles surface (Fig. 5.10B). However, this only stands as supportive evidence of the migration of a small proportion of curcumin in the oil phase (also owing to the low solubility in sunflower oil [54]), rather than a quantification

approach, as due to the nature of the visualisation, any occurring events can appear exaggerated. A similar approach was taken in a study by Milsmann *et al*. [28], where CLSM was used to visualise the transfer of coumarin 6 from tristearin SLNs to the oil phase of MCT o/w emulsions (pre-stabilised with different surfactants). This phenomenon is proposed to take place within a short period of time after preparation, as already after 1 day a level of migration from the adsorbed particles to the droplets can be distinguished, although the quantity is expected to be small in comparison to the total amount that came into the emulsion system through the particles. The latter is further suggested by the lack of substantial loss of crystalline matter and the consistent release profiles obtained following long-term storage of both the lipid particle containing dispersions and emulsions (Fig. 5.8C & D). Further investigations in the previously reported work [28] using a separated model emulsion system (containing pseudo-phases) and electron paramagnetic resonance (EPR) spectroscopy revealed the role of surfactant micelles as facilitators of the lipophilic spin probe TEMPOL-benzoate (2,2,6,6-tetramethyl-4-piperidinol-1-oxyl benzoate, TB) transfer between the two phases. Additionally, it was proposed that the probe was primarily expelled from the surface of the particles, rather than the crystalline matrix. Herein, the presence of surfactant micelles both in the continuous phase (only in undialysed particle dispersions) and within the dissolution medium accommodated the curcumin transport towards the acceptor phase. The particle structural properties, particularly the composition of their surface layer, is an aspect that could greatly impact the release kinetics of actives either encapsulated within lipid particles in a dispersion environment, or particle-stabilised emulsion droplets. Formation of thick layers due to the presence of bulkier proteins around the particles which in turn occupy the interface [7], or capsule-like layers created by the partial melting of the lipid particles at the interface of the oil droplets [23], can result in hindered release rates. Thus, the role of the particles as either facilitators or inhibitors of the active

passage from the crystalline structure that can halt the release rate, to the oil phase that can on the other hand accelerate it, could be manipulated by altering the interfacial properties of the former.

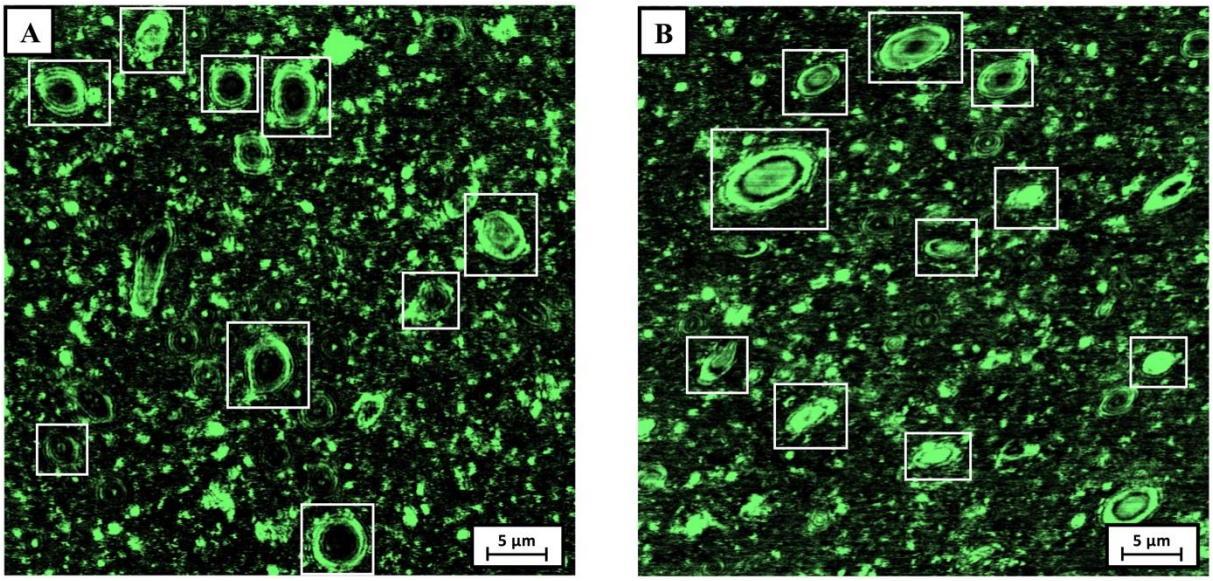

Fig. 5.10. Representative images of CRM-loaded SLN-stabilised o/w emulsions acquired using CLSM within 1 h after production (A) and after 1 d of storage (B), indicating the possibility of CRM migration from SLN to the oil droplets. White borders around droplets are used to indicate where the described phenomenon is more pronounced.

Lastly, the ability of the (curcumin-loaded) SLNs and NLCs to retain their release performance following prolonged storage was assessed. Curcumin release data were collected from either lipid particle-stabilised emulsions that were stored for up to 3 months (Fig. 5.8C & D), or from 'fresh' emulsions produced using particles that had been stored (as aqueous dispersions) for up to 4 months (see Appendix A3, Fig. A3.3). In both cases (and for both SLNs and NLCs), an almost identical release behaviour to that of 'freshly' produced emulsions stabilised by 'freshly' produced lipid particles, was exhibited (Fig. 5.11). The persistence of the particles' release behaviour even after 4 months of storage further highlights the catalytic effect of the oil phase

(droplet) addition on the release rate observed from the emulsion systems. Curcumin appears to stay entrapped within the microstructure even in the case of the emulsion systems, and only eventually release under the favourable dissolution conditions (presence of excess surfactant micelles facilitating the diffusion). Similar data regarding prolonged storage release have been previously reported for bovine serum albumin (BSA) release from double-layer chitosan-based particles [59,60] and for telmisartan (hydrophobic drug) release from liquisolid compacts [59,60], although literature appears to be quite limited. For microstructures intended to be used as active carriers and delivery systems, this is a particularly important attribute, as it contributes to broadening their application prospect.

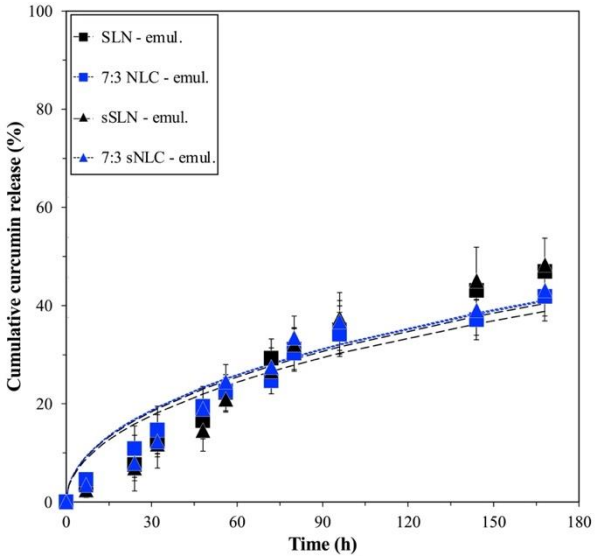

Fig. 5.11. Comparison of the *in vitro* release profile of curcumin from SLN and 7:3 NLC-stabilised emulsions fabricated with particles immediately after their preparation (SLN and 7:3 NLC), and after 4 months of storage (sSLN and 7:3 sNLC). *In vitro* release kinetic Crank model fitting of curcumin is presented with a dotted line for the former and a dashed line for the latter.

5.4 Conclusions

Having already established the Pickering functionality of both SLNs and NLCs used as produced and after removal of remnant surfactant from their aqueous carrier phase (in part I), this study demonstrated their concurrent capacity to act as active carriers/delivery systems of an encapsulated model hydrophobic active, thus rendering them dual-functional. In addition to investigating the active holding/delivery performance of these lipid structures prior- and post-emulsification, and the effect of certain formulation parameters on these characteristics, part of the focus was also placed on exploring whether this secondary functionality would compromise their previously established properties. Monitoring of crystalline matter loss from the lipid particles, a parameter that has thus far been closely associated with their Pickering functionality, but also consequently their active delivery regulation ability, revealed that the particles maintained their structural integrity within emulsions up to 12 weeks in storage conditions. Regarding their fate within the emulsion environment, it is suggested that the proportion of lipid particles residing at the emulsion interface can be influenced by the presence of excess surfactant in the aqueous phase. However, the percentage of adsorbed particles was shown to remain unaffected throughout the storage period, irrespectively of the presence/absence of excess surfactant. In terms of the effect of active incorporation on the interfacial properties and Pickering stabilisation capacity of the lipid particles, it was shown that encapsulation of curcumin within the SLN and 7:3 NLC formulations did not invoke any changes on either. Further to confirming the Pickering stabilisation capacity of the curcumin-loaded lipid particles, the concurrent functionality of acting as active carriers and release regulators was studied. More specifically, employing both SLNs and NLCs, the ability to regulate the release of curcumin was exhibited both in a dispersion system and within an emulsion setting; with the differentiation in the release mechanisms between the two systems being attributed to the

diversity in the surroundings that the interfacially-adsorbed and unadsorbed particles are experiencing. Future work using these dual-functional colloidal species could explore the use of simple o/w emulsions for the co-release of multiple actives, while devising further approaches to tailor their release performance, such as altering formulation parameters of the lipid particles.

References

[1] P. Vega-Vásquez, N.S. Mosier, J. Irudayaraj, Nanoscale Drug Delivery Systems: From Medicine to Agriculture, Front Bioeng Biotechnol. 8 (2020) 79. https://doi.org/https://doi.org/10.3389/fbioe.2020.00079.

[2] S.A.A. Rizvi, A.M. Saleh, Applications of nanoparticle systems in drug delivery technology, Saudi Pharmaceutical Journal. 26 (2018) 64–70. https://doi.org/10.1016/j.jsps.2017.10.012.

[3] H.K. Batchelor, J.F. Marriott, Formulations for children: problems and solutions, Br J Clin Pharmacol. 79 (2015) 405–418. https://doi.org/10.1111/bcp.12268.

[4] X.W. Chen, X.Y. Ning, X.Q. Yang, Fabrication of Novel Hierarchical Multicompartment Highly Stable Triple Emulsions for the Segregation and Protection of Multiple Cargos by Spatial Co-encapsulation, J Agric Food Chem. 67 (2019) 10904–10912. https://doi.org/10.1021/acs.jafc.9b03509.

[5] F. Spyropoulos, D. Kurukji, P. Taylor, I.T. Norton, Fabrication and Utilization of Bifunctional Protein/Polysaccharide Coprecipitates for the Independent Codelivery of Two Model Actives from Simple Oil-in-Water Emulsions, Langmuir. 34 (2018) 3934–3948. https://doi.org/10.1021/acs.langmuir.7b04315.

[6] W. Wang, H. Song, J. Zhang, P. Li, C. Li, C. Wang, D. Kong, Q. Zhao, An injectable, thermosensitive and multicompartment hydrogel for simultaneous encapsulation and independent release of a drug cocktail as an effective combination therapy platform, Journal of Controlled Release. 203 (2015) 57–66. https://doi.org/10.1016/j.jconrel.2015.02.015.

[7] G.I. Sakellari, I. Zafeiri, A. Pawlik, D. Kurukji, P. Taylor, I.T. Norton, F. Spyropoulos, Independent co-delivery of model actives with different degrees of hydrophilicity from oil-in-water and water-in-oil emulsions stabilised by solid lipid particles via a Pickering mechanism: a-proof-of-principle study, J Colloid Interface Sci. 587 (2021) 644–649. https://doi.org/10.1016/j.jcis.2020.11.021.

[8] F.Q. Hu, S.P. Jiang, Y.Z. Du, H. Yuan, Y.Q. Ye, S. Zeng, Preparation and characterization of stearic acid nanostructured lipid carriers by solvent diffusion method in an aqueous system, Colloids Surf B Biointerfaces. 45 (2005) 167–173. https://doi.org/10.1016/j.colsurfb.2005.08.005.

[9] L.J. Jia, D.R. Zhang, Z.Y. Li, F.F. Feng, Y.C. Wang, W.T. Dai, C.X. Duan, Q. Zhang, Preparation and characterization of silybin-loaded nanostructured lipid carriers, Drug Deliv. 17 (2010) 11–18. https://doi.org/10.3109/10717540903431586.

[10] K. Oehlke, D. Behsnilian, E. Mayer-Miebach, P.G. Weidler, R. Greiner, Edible solid lipid nanoparticles (SLN) as carrier system for antioxidants of different lipophilicity, PLoS One. 12 (2017) e0171662. https://doi.org/10.1371/journal.pone.0171662.

[11] L. Becker Peres, L. Becker Peres, P.H.H. de Araújo, C. Sayer, Solid lipid nanoparticles for encapsulation of hydrophilic drugs by an organic solvent free double emulsion technique, Colloids Surf B Biointerfaces. 140 (2016) 317–323. https://doi.org/10.1016/j.colsurfb.2015.12.033.

[12] J. Weiss, E.A. Decker, D.J. McClements, K. Kristbergsson, T. Helgason, T. Awad, Solid lipid nanoparticles as delivery systems for bioactive food components, Food Biophys. 3 (2008) 146–154. https://doi.org/10.1007/s11483-008-9065-8.

[13] P. Jaiswal, B. Gidwani, A. Vyas, Nanostructured lipid carriers and their current application in targeted drug delivery, Artif Cells Nanomed Biotechnol. 44 (2016) 27–40. https://doi.org/10.3109/21691401.2014.909822.

[14] A. Borges, V. de Freitas, N. Mateus, I. Fernandes, J. Oliveira, Solid lipid nanoparticles as carriers of natural phenolic compounds, Antioxidants. 9 (2020) 998. https://doi.org/10.3390/antiox9100998.

[15] E.B. Souto, S.A. Wissing, C.M. Barbosa, R.H. Müller, Development of a controlled release formulation based on SLN and NLC for topical clotrimazole delivery, Int J Pharm. 278 (2004) 71–77. https://doi.org/10.1016/j.ijpharm.2004.02.032.

[16] W. Mehnert, K. Mäder, Solid lipid nanoparticles: Production, characterization and applications, Adv Drug Deliv Rev. 64 (2012) 83–101. https://doi.org/10.1016/j.addr.2012.09.021.

[17] S. Sapino, M.E. Carlotti, E. Pelizzetti, D. Vione, M. Trotta, L. Battaglia, Protective effect of SLNs encapsulation on the photodegradation and thermal degradation of retinyl palmitate introduced in hydroxyethylcellulose gel, J Drug Deliv Sci Technol. 15 (2005) 159–165. https://doi.org/10.1016/s1773-2247(05)50021-2.

[18] E.B. Souto, R.H. Müller, SLN and NLC for topical delivery of ketoconazole, J Microencapsul. 22 (2005) 501–510. https://doi.org/10.1080/02652040500162436.

[19] G.I. Sakellari, I. Zafeiri, H. Batchelor, F. Spyropoulos, Solid lipid nanoparticles and nanostructured lipid carriers of dual functionality at emulsion interfaces. Part I: Pickering stabilisation functionality, Colloids Surf A Physicochem Eng Asp. (2022) 130135. https://doi.org/10.1016/j.colsurfa.2022.130135.

[20] F. Spyropoulos, C. Clarke, D. Kurukji, I.T. Norton, P. Taylor, Emulsifiers of Pickering-like characteristics at fluid interfaces: Impact on oil-in-water emulsion stability and interfacial transfer rate kinetics for the release of a hydrophobic model active, Colloids Surf A Physicochem Eng Asp. 607 (2020) 125413. https://doi.org/10.1016/j.colsurfa.2020.125413.

[21] S. Frasch-Melnik, I.T. Norton, F. Spyropoulos, Fat-crystal stabilised w/o emulsions for controlled salt release, J Food Eng. 98 (2010) 437–442. https://doi.org/10.1016/j.jfoodeng.2010.01.025.

[22] D.A. Garrec, S. Frasch-Melnik, J.V.L. Henry, F. Spyropoulos, I.T. Norton, Designing colloidal structures for micro and macro nutrient content and release in foods, Faraday Discuss. 158 (2012) 37–49. https://doi.org/10.1039/c2fd20024d.

[23] S.M. Dieng, N. Anton, P. Bouriat, O. Thioune, P.M. Sy, N. Massaddeq, S. Enharrar, M. Diarra, T. Vandamme, Pickering nano-emulsions stabilized by solid lipid nanoparticles as a temperature sensitive drug delivery system, Soft Matter. 15 (2019) 8164–8174. https://doi.org/10.1039/c9sm01283d.

[24] I. Zafeiri, P. Smith, I.T. Norton, F. Spyropoulos, Fabrication, characterisation and stability of oil-in-water emulsions stabilised by solid lipid particles: The role of particle characteristics and emulsion microstructure upon Pickering functionality, Food Funct. 8 (2017) 2583–2591. https://doi.org/10.1039/c7fo00559h.

[25] I.T. Norton, C.D. Lee-Tuffnell, S. Ablett, S.M. Bociek, A calorimetric, NMR and X-ray diffraction study of the melting behavior of tripalmitin and tristearin and their mixing behavior with triolein, J Am Oil Chem Soc. 62 (1985) 1237–1244. https://doi.org/10.1007/bf02541834.

[26] M. Samtlebe, U. Yucel, J. Weiss, J.N. Coupland, Stability of Solid Lipid Nanoparticles in the Presence of Liquid Oil Emulsions, J Am Oil Chem Soc. 89 (2012) 609–617. https://doi.org/10.1007/s11746-011-1944-3.

[27] A. Schröder, M. Laguerre, J. Sprakel, K. Schroën, C.C. Berton-Carabin, Pickering particles as interfacial reservoirs of antioxidants, J Colloid Interface Sci. 575 (2020) 489–498. https://doi.org/10.1016/j.jcis.2020.04.069.

[28] J. Milsmann, K. Oehlke, R. Greiner, A. Steffen-Heins, Fate of edible solid lipid nanoparticles (SLN) in surfactant stabilized o/w emulsions. Part 2: Release and partitioning behavior of lipophilic probes from SLN into different phases of o/w emulsions, Colloids Surf A Physicochem Eng Asp. 558 (2018) 623–631. https://doi.org/10.1016/j.colsurfa.2017.05.050.

[29] G.I. Sakellari, I. Zafeiri, H. Batchelor, F. Spyropoulos, Formulation design, production and characterisation of solid lipid nanoparticles (SLN) and nanostructured lipid carriers (NLC) for the encapsulation of a model hydrophobic active, Food Hydrocolloids for Health. (2021) 100024. https://doi.org/10.1016/j.fhfh.2021.100024.

[30] J. Crank, The Mathematics of Diffusion, 2nd Edition, Oxford University Press, London, 1975.

[31] J. Weiss, D.J. McClements, Mass Transport Phenomena in Oil-in-Water Emulsions Containing Surfactant Micelles: Solubilization, Langmuir. 16 (2000) 5879–5883. https://doi.org/10.1021/la9914763.

[32] D.J. McClements, S.R. Dungan, J.B. German, J.E. Kinsella, Evidence of oil exchange between oil-in-water emulsion droplets stabilized by milk proteins, J Colloid Interface Sci. 156 (1993) 425–429. https://doi.org/10.1006/jcis.1993.1133.

[33] D.J. McClements, S.R. Dungan, J.B. German, J.E. Kinsella, Factors which affect oil exchange between oil-in-water emulsion droplets stabilized by whey protein isolate: Protein concentration, droplet size and ethanol, Colloids Surf A Physicochem Eng Asp. 81 (1993) 203–210. https://doi.org/10.1016/0927-7757(93)80247-c.

[34] D.J. McClements, S.R. Dungan, Factors that affect the rate of oil exchange between oil-in-water emulsion droplets stabilized by a nonionic surfactant: droplet size, surfactant concentration, and ionic strength, Journal of Physical Chemistry. 97 (2002) 7304–7308. https://doi.org/10.1021/j100130A030.

[35] A. Schröder, J. Sprakel, W. Boerkamp, K. Schroën, C.C. Berton-Carabin, Can we prevent lipid oxidation in emulsions by using fat-based Pickering particles?, Food Research International. 120 (2019) 352–363. https://doi.org/10.1016/j.foodres.2019.03.004.

[36] A. Pawlik, D. Kurukji, I. Norton, F. Spyropoulos, Food-grade Pickering emulsions stabilised with solid lipid particles, Food Funct. 7 (2016) 2712–2721. https://doi.org/10.1039/c6fo00238b.

[37] O.O. Fasina, Z. Colley, Viscosity and Specific Heat of Vegetable Oils as a Function of Temperature: 35°C to 180°C, Int J Food Prop. 11 (2008) 738–746. https://doi.org/10.1080/10942910701586273.

[38] J.W.J. de Folter, E.M. Hutter, S.I.R. Castillo, K.E. Klop, A.P. Philipse, W.K. Kegel, Particle shape anisotropy in pickering emulsions: Cubes and peanuts, Langmuir. 30 (2014) 955–964. https://doi.org/10.1021/la402427q.

[39] W. Li, T. Suzuki, H. Minami, The interface adsorption behavior in a Pickering emulsion stabilized by cylindrical polystyrene particles, J Colloid Interface Sci. 552 (2019) 230–235. https://doi.org/10.1016/j.jcis.2019.05.058.

[40] D.J. French, A.T. Brown, A.B. Schofield, J. Fowler, P. Taylor, P.S. Clegg, The secret life of Pickering emulsions: particle exchange revealed using two colours of particle, Scientific Reports 2016 6:1. 6 (2016) 1–9. https://doi.org/10.1038/srep31401.

[41] A. Schröder, J. Sprakel, K. Schroën, C.C. Berton-Carabin, Tailored microstructure of colloidal lipid particles for Pickering emulsions with tunable properties, Soft Matter. 13 (2017) 3190–3198. https://doi.org/10.1039/c6sm02432g.

[42] M. Graca, J.H.H. Bongaerts, J.R. Stokes, S. Granick, Friction and adsorption of aqueous polyoxyethylene (Tween) surfactants at hydrophobic surfaces, J Colloid Interface Sci. 315 (2007) 662–670. https://doi.org/10.1016/j.jcis.2007.06.057.

[43] X. Li, H. Li, Q. Xiao, L. Wang, M. Wang, X. Lu, P. York, S. Shi, J. Zhang, Two-way effects of surfactants on Pickering emulsions stabilized by the self-assembled microcrystals of a-cyclodextrin and oil, Phys. Chem. Chem. Phys. 16 (2014) 14059. https://doi.org/10.1039/c4cp00807c.

[44] P.Y. Liu, R.Y. Yang, A.B. Yu, Self-diffusion of wet particles in rotating drums, Physics of Fluids. 25 (2013) 063301. https://doi.org/10.1063/1.4807596.

[45] V.H.S. Araujo, P.B. da Silva, I.O. Szlachetka, S.W. da Silva, B. Fonseca-Santos, M. Chorilli, R. Ganassin, G.R.T. de Oliveira, M.C.O. da Rocha, R.P. Fernandes, M. de Carvalho Vieira Queiroz, R.B. Azevedo, L.A. Muehlmann, The influence of NLC composition on curcumin loading under a physicochemical perspective and in vitro evaluation, Colloids Surf A Physicochem Eng Asp. 602 (2020) 125070. https://doi.org/10.1016/j.colsurfa.2020.125070.

[46] M.A. Espinosa-Olivares, N.L. Delgado-Buenrostro, Y.I. Chirino, M.A. Trejo-Márquez, S. Pascual-Bustamante, A. Ganem-Rondero, Nanostructured lipid carriers loaded with curcuminoids: Physicochemical characterization, in vitro release, ex vivo skin penetration, stability and antioxidant activity, European Journal of Pharmaceutical Sciences. 155 (2020) 105533. https://doi.org/10.1016/j.ejps.2020.105533.

[47] M.L. Bondì, M.R. Emma, C. Botto, G. Augello, A. Azzolina, F. di Gaudio, E.F. Craparo, G. Cavallaro, D. Bachvarov, M. Cervello, Biocompatible Lipid Nanoparticles as Carriers to Improve Curcumin Efficacy in Ovarian Cancer Treatment, J Agric Food Chem. 65 (2017) 1342–1352. https://doi.org/10.1021/acs.jafc.6b04409.

[48] W. Wang, T. Chen, H. Xu, B. Ren, X. Cheng, R. Qi, H. Liu, Y. Wang, L. Yan, S. Chen, Q. Yang, C. Chen, Curcumin-loaded solid lipid nanoparticles enhanced anticancer efficiency in breast cancer, Molecules. 23 (2018) 1578. https://doi.org/10.3390/molecules23071578.

[49] A. zur Mühlen, C. Schwarz, W. Mehnert, Solid lipid nanoparticles (SLN) for controlled drug delivery - Drug release and release mechanism, European Journal of Pharmaceutics and Biopharmaceutics. 45 (1998) 149–155. https://doi.org/10.1016/s0939-6411(97)00150-1.

[50] J. Liu, J. Zhu, Z. Du, B. Qin, Preparation and pharmacokinetic evaluation of Tashinone IIA solid lipid nanoparticles, Drug Dev Ind Pharm. 31 (2005) 551–556. https://doi.org/10.1080/03639040500214761.

[51] P.R. Ravi, N. Aditya, H. Kathuria, S. Malekar, R. Vats, Lipid nanoparticles for oral delivery of raloxifene: Optimization, stability, in vivo evaluation and uptake mechanism, European Journal of Pharmaceutics and Biopharmaceutics. 87 (2014) 114–124. https://doi.org/10.1016/j.ejpb.2013.12.015.

[52] G. Zoubari, S. Staufenbiel, P. Volz, U. Alexiev, R. Bodmeier, Effect of drug solubility and lipid carrier on drug release from lipid nanoparticles for dermal delivery, European Journal of Pharmaceutics and Biopharmaceutics. 110 (2017) 39–46. https://doi.org/10.1016/j.ejpb.2016.10.021.

[53] W. Tiyaboonchai, W. Tungpradit, P. Plianbangchang, Formulation and characterization of curcuminoids loaded solid lipid nanoparticles, Int J Pharm. 337 (2007) 299–306. https://doi.org/10.1016/j.ijpharm.2006.12.043.

[54] P. Ma, Q. Zeng, K. Tai, X. He, Y. Yao, X. Hong, F. Yuan, Development of stable curcumin nanoemulsions: effects of emulsifier type and surfactant-to-oil ratios, J Food Sci Technol. 55 (2018) 3485–3497. https://doi.org/10.1007/s13197-018-3273-0.

[55] J. Milsmann, K. Oehlke, K. Schrader, R. Greiner, A. Steffen-Heins, Fate of edible solid lipid nanoparticles (SLN) in surfactant stabilized o/w emulsions. Part 1: Interplay of SLN and oil droplets, Colloids Surf A Physicochem Eng Asp. 558 (2018) 615–622. https://doi.org/10.1016/j.colsurfa.2017.05.073.

[56] K. Szymczyk, A. Zdziennicka, B. Jańczuk, Effect of Polysorbates on Solids Wettability and Their Adsorption Properties, Colloids and Interfaces. 2 (2018) 26. https://doi.org/10.3390/colloids2030026.

[57] A. Amani, P. York, H. de Waard, J. Anwar, Molecular dynamics simulation of a polysorbate 80 micelle in water, Soft Matter. 7 (2011) 2900–2908. https://doi.org/10.1039/c0sm00965b.

[58] M.A. Gogoleva, B.P. Yakimov, S.A. Rodionov, T.N. Tikhonova, Y.I. Gurfinkel, V. v. Fadeev, J. Lademann, M.E. Darvin, E.A. Shirshin, Solid Lipid Curcumin-loaded Particles for in vivo Fluorescent Imaging in Humans: A Proof of Concept, Opt Spectrosc. 126 (2019) 730–735. https://doi.org/10.1134/s0030400x19060067.

[59] T. Xiang, J. Yang, S. Li, J. Li, W. Situ, Improvement in bioactive protein storage stability and colon-targeted release: a simple double-layer chitosan-based particle, 36 (2019) 474–484. https://doi.org/10.1080/02652048.2019.1646336.

[60] N. Chella, N. Narra, T.R. Rao, Preparation and Characterization of Liquisolid Compacts for Improved Dissolution of Telmisartan, J Drug Deliv. 2014 (2014) 1–10. https://doi.org/10.1155/2014/692793.

Appendix A3

Thermal analysis

Examples of peak integration of the melting thermograms of lipid particle dispersion samples (SLNs and 7:3 NLCs) performed to acquire the ΔH_{dis} data, and their respective emulsion systems to attain the ΔH^{T}_{em} information are presented below (Fig. A3.1). The peak deconvolution of the emulsion systems is also depicted, showing how the ΔH^{1}_{em} and ΔH^{2}_{em} values were acquired.

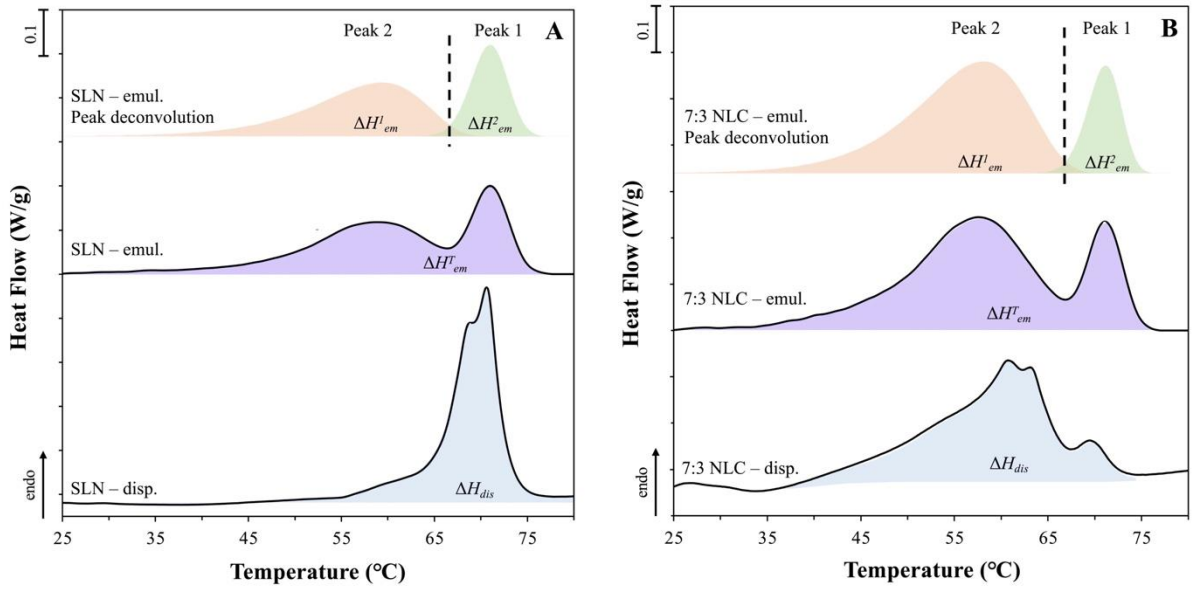

Fig. A3.1. Melting thermograms of representative SLN and 7:3 NLC dispersions and their respective emulsion systems showing the peak integration to acquire the ΔH_{dis} and ΔH^{T}_{em} data. Examples of peak deconvolution of the emulsion systems to obtain the ΔH^{1}_{em} and ΔH^{2}_{em} values, are also depicted.

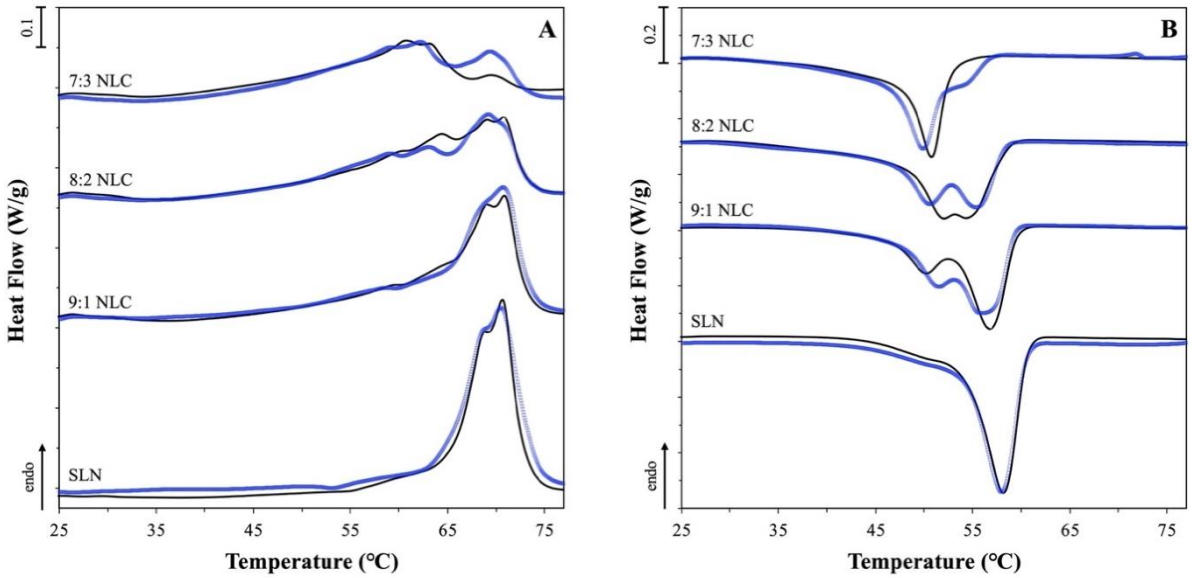

Fig. A3.2. Melting (A) and crystallisation (B) curves of SLN and NLC aqueous dispersions before dialysis (black curve) and after removal of excess surfactant (blue curve).

Stability of *in vitro* release from lipid particle dispersions

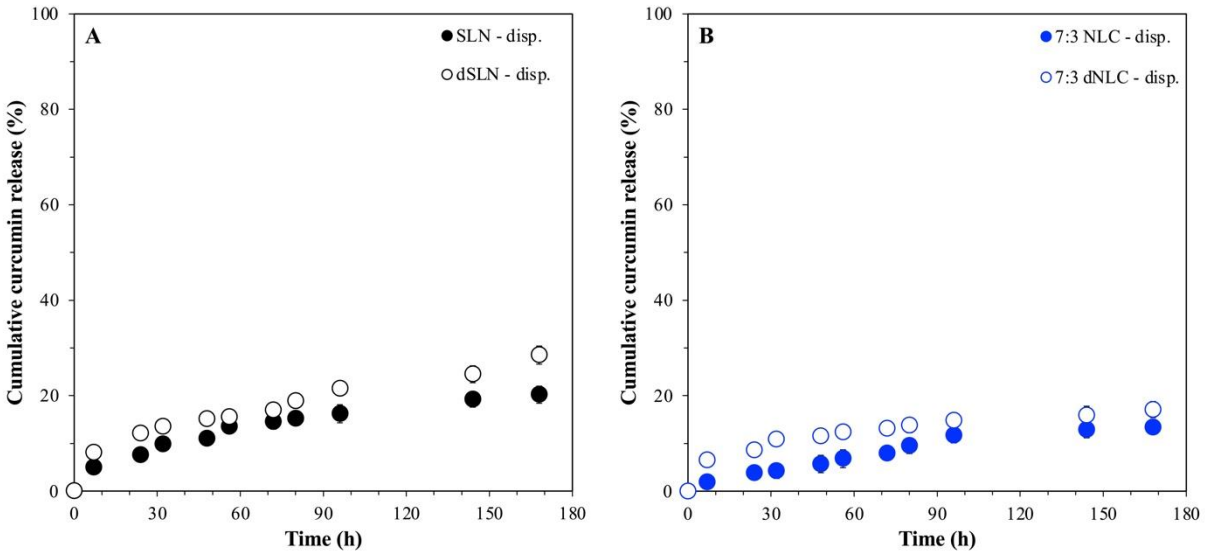

Fig. A3.3. *In vitro* release profile of a model hydrophobic active (curcumin) from SLN (A) and 7:3 NLC (B) dispersions used as produced and after dialysis after 4 months of storage.

References

[1] D.W. Van Krevelen, K. Te Nijenhuis, Chapter 7 - Cohesive Properties and Solubility in Properties of Polymers, in: Properties of Polymers (Fourth Edition), Elsevier, Amsterdam, 2009: pp. 189–227. https://doi.org/10.1016/b978-0-08-054819-7.00007-8.

[2] Eric. Dickinson, An Introduction to Food Colloids, Oxford University Press, 1992.

[3] K. Szymczyk, A. Zdziennicka, B. Jańczuk, Effect of Polysorbates on Solids Wettability and Their Adsorption Properties, Colloids and Interfaces. 2 (2018) 26. https://doi.org/10.3390/colloids2030026.

Chapter 6

The impact of the interfacial architecture on the release and co-release from lipid particle-stabilised emulsions

Synopsis

The effect of lipid particle formulation parameters on the release and co-release regulation of two hydrophobic actives separately encapsulated within the particles themselves and within lipid particle-stabilised (Pickering) emulsion droplets is explored. Having previously demonstrated the dual functionality of solid lipid nanoparticles (SLNs) and nanostructured lipid carriers (NLCs), with regard to their concurrent Pickering stabilisation and active carrying/delivery, the present work aims to provide further understanding on how the delivery of the actives can be regulated by tuning microstructural characteristics. Active-containing SLNs and NLCs were fabricated with different solid lipid and surfactant types, and their release profiles within dispersion and emulsion settings were attained. Disparities between the active release profiles from the particles in aqueous dispersions or at an emulsion interface, were related to the specific lipid matrix composition. Particles composed of lipids with higher compatibility with the oil phase of the emulsion droplets were shown to hold less control over their release regulation ability, as were particles in the presence of surfactant micelles. Irrespective of their formulation characteristics, all particles were able to provide a level of control of the release of the active encapsulated within the emulsion droplets. In particular, changes in the permeability of the interfacial layer due to particle sintering at the droplet interface resulted in more sustained droplet release rates. Compared to the sole release, the co-release performance was suggested to remain unaffected by the co-existence of the two hydrophobic actives (within the lipid particles and emulsion droplets), with the (co-release) behaviour persisting over a storage period of 1 month.

6.1 Introduction

Within the research area of multi-active encapsulation and delivery across different sectors [1–9], incorporating more than one active ingredients within the same vehicle has been shown to enhance efficacy and bioactivity through synergistic or additive effects between the encased species [10,11]. To this end, in pharmaceutical applications, solid-phase formulations have been primarily investigated [12–14], with less focus on liquid-based systems, despite numerous advantages [15–17]. Among the liquid-phase approaches, Pickering emulsions stabilised with particulates of varying physicochemical characteristics have been explored, with most studies primarily focusing on confirming the concurrent stabilisation and co-encapsulation aptitude of the systems, and less so on how the interfacial presence of the particles affects the co-release performance. The impact of the microstructural components' composition on the obtained co-encapsulation efficiency [18], the effect of co-encapsulation on the system's properties (i.e. droplet size) [19], and the influence of the particles' characteristics on attaining independent and triggered co-delivery [20] have been highlighted in relevant literature. Exploring further the impact of the active co-encapsulation and interfacial particle presence on the co-release performance, it has been suggested that the creation of less permeable interfacial layers, either due to encapsulation of an active in the Pickering particles [21], or particle sintering at the droplet interface [22] can overall hinder the release of the active encapsulated with the emulsion droplets. In fact, the potential of controlling the active release from w/o emulsions by manipulating the architecture of their lipid-decorated interfaces via sintering, has been previously revealed as a promising approach for attaining triggered release, through temperature control [23,24]. Thus, it appears that manipulating the interfacial layer characteristics could be a promising tool for simultaneously regulating the co-release behaviour of the separately encapsulated actives.

The current work aims to build upon previous research on the capacity of lipid particle-stabilised emulsions to act as a co-encapsulation and co-delivery system [25,26]. The effect of formulation characteristics of the lipid particles, both solid lipid nanoparticles (SLNs) and nanostructured lipid carriers (NLCs), on their concurrent emulsion stabilisation and active carrying/release regulation capability was explored. Herein, focus was also placed on the particles' ability to provide control over the encasing and release of an active encapsulated within the emulsion droplets. Therefore, the release profiles of a model hydrophobic active (curcumin) from SLNs and NLCs with varying formulations aspects, namely the types of solid lipid and surfactant used, were assessed both within aqueous dispersions and emulsion systems. Following that, the capacity and extent to which the same, in this case blank, lipid particles can serve as effective interfacial barriers for the controlled release of a different model hydrophobic active (cinnamaldehyde) encapsulated within the o/w emulsion droplets was examined. Their behaviour was compared to simple (surfactant-stabilised) emulsions, while also interfacial sintering was devised as a means to manipulate the interfacial barrier provided by the lipid particles and scrutinise how and to what degree further control could be achieved. Finally, the co-release performance of the two model hydrophobic actives from the lipid particle-stabilised emulsion was studied to confirm the co-encapsulation and co-delivery potential of the developed formulation.

6.2 Materials and methods

6.2.1 Materials

Compritol® 888 ATO (C888, glyceryl behenate) and Precirol® ATO 5 (P5, glyceryl palmitostearate) were kindly provided from Gattefossé (Saint-Priest, France). Miglyol® 812

(medium chain triglycerides, MCTs) was a kind gift from IOI Oleo (IOI Oleochemicals GmbH, Germany). Tween® 80 (T80, polyoxyethylene sorbitan monooleate), Pluronic® F-68 (Poloxamer 188, P188), curcumin (≥65%, HPLC, CRM), pentane (HPLC grade) and cinnamaldehyde (CA) were purchased from Sigma-Aldrich (Sigma-Aldrich, UK). Oxoid™ phosphate buffered saline (PBS) pH 7.4 tablets were obtained from Thermo Scientific (Sheffield, UK). Sunflower oil was purchased from a local supermarket, stored in a closed container at ambient temperature in the dark and used without any further purification. Double distilled water from Milli-Q systems (Millipore, Watford, UK) was used during all sample preparation processes and characterisation measurements.

6.2.2 Preparation of lipid particles

The aqueous dispersions of blank or curcumin-loaded SLNs and NLCs were prepared following a melt-emulsification-ultrasonication method that is fully described elsewhere [27]. The lipid melts (2.5% w/w) without or with curcumin (0.5% w/w of the lipid mass) were heated 5-10°C above the melting point of the solid lipid used (85°C for C888 and 70°C for P5) for 1 hour and were then combined with the aqueous surfactant solution (1.2% w/w T80 or P188). For the NLCs, 30% of the total lipid phase was substituted by MCTs. The formed pre-emulsion was homogenised for 5 min using ultrasonication (Vibra-cell™ VC 505 processor, Sonics & Materials, Inc., CT, USA), operating continuously at 750 Watt and 20 kHz, at a sonication amplitude of 95% of the total power. The crystalline particles were obtained by cooling the o/w emulsion using an ice bath to a temperature below the crystallisation point of the lipid melts. Samples were stored at 4°C in the dark (since curcumin is photodegradable) until further analysis.

6.2.3 Particle size

Information about the particle size (*Z*-average) and polydispersity index (PDI) was acquired with dynamic light scattering (DLS), using Zetasizer Nano ZS (Malvern Instruments, UK). All measurements were performed at a backscattering angle of 173° at 25°C, and samples were appropriately diluted with distilled water to avoid multiple scattering phenomena. The refractive indices were determined according to Sakellari *et al*. [25,27]. All measurements were performed in triplicate, immediately after preparation and over time, and the average values with standard deviation (±S.D.) are presented. Representative size distributions of lipid particles were also obtained with laser diffraction (LD) using a Mastersizer 2000 (Malvern Instruments, UK), following a method that is described in detail below.

6.2.4 Interfacial tension

Dynamic interfacial oil/water tensions at 20°C were measured with a profile analysis tensiometer, using the pendant drop method (PAT-1M, Sinterface Technologies, Berlin, German). A drop of the SLN or NLC dispersions was suspended via a straight stainless-steel capillary (3 mm outer diameter) in the sunflower oil phase contained in a quartz cuvette, with the cross-sectioned surface area remaining constant at 27 mm^2. The measurements were performed until equilibrium was reached (standard deviation of the last twenty measurements was smaller than 0.05 mN/m). Density information was acquired using a densitometer (Densito, Mettler Toledo, US), at 20°C. All measurements were conducted in at least triplicate on three individually prepared samples.

6.2.5 Preparation of oil-in-water emulsions

Simple or Pickering o/w emulsions were prepared with 90% (w/w) aqueous phase containing either of the two surfactants at 1% w/w concentration, or any of the different (blank or curcumin-loaded) lipid nanoparticle systems, respectively, and 10% (w/w) sunflower oil phase. When cinnamaldehyde (0.3% w/w of the oil phase mass) was encapsulated within the oil droplets, the active and sunflower oil were stirred together for 1 h prior to the aqueous phase addition. During emulsification, which was performed employing ultrasonication under the same conditions as described above for a period of 30 s, the samples were immersed in an ice bath to avoid shear-inducing heating, and were later stored at 4°C until further analysis.

Emulsions that were thermally processed post-fabrication were heated at either 64 or 78°C for 5, 20 or 60 min (after the desired temperature was reached) using a hotplate under stirring, and were then cooled in an ice bath.

6.2.6 Droplet size measurements

Laser diffraction (LD) was utilised to obtain droplet size information, employing a Mastersizer 2000 (Malvern Instruments, UK) equipped with a Hydro SM manual small volume sample dispersion unit. The stirrer speed was set at 1300 rpm, and all samples were hand-mixed before analysis. The refractive index for sunflower oil was set at 1.47. All measurements were performed in triplicate on three individually prepared samples.

6.2.7 Thermal analysis

The thermal behaviour of the SLNs and NLCs within the dispersion and emulsion systems was evaluated via Differential Scanning Calorimetry (DSC) using a Setaram μDSC3 evo microcalorimeter (Setaram Instrumentation, France). The temperature cycle used ranged between 20 and 80°C at a heating rate of 1.2 °C/min. The thermograms were obtained with the reference cell being filled with equal amount of distilled water. Data processing was carried out using the Calisto Processing software (Setaram Instrumentation, France), to obtain information regarding peak temperatures and melting enthalpies. The loss of crystalline matter for the emulsion systems was determined using information from the total melting enthalpies of the particles within an emulsion environment (ΔH^{T}_{em}) and those in an aqueous dispersion setting (ΔH_{dis}), and was expressed as a $\Delta H^{T}_{em}/\Delta H_{dis}$ ratio. The ΔH_{dis} and ΔH^{T}_{em} values were obtained from peak integration of the particle dispersion and particle-stabilised emulsion melting thermograms, respectively. All enthalpy values and thermograms reported, are normalised for the crystallising material amount present in each sample. Specifically for the emulsion systems, each thermogram was normalised using the information of the respective SLN or NLC dispersion that was used for the emulsification. All measurements were performed in at least duplicate.

6.2.8 Electron microscopy

The surface morphology of the emulsion droplets was visualised with cryogenic scanning electron microscopy (cryo-SEM), using a FEI Helios G4 CX DualBeam - high resolution monochromated field emission gun, scanning electron microscope (FEG-SEM) with precise focused ion beam (FIB) (FEI company, Hillsboro, OR, USA) coupled to a PP3010 cryo-SEM

preparation system (Quorum Technologies, Lewes, UK). The cryo-system was pre-pumped and cooled to −140°C on the stage with an anti-contaminator which was cooled to −175°C. During imaging the SEM was using 2 kV and 0.10 nA probe current.

6.2.9 Encapsulation efficiency and loading capacity

The encapsulation efficiency (EE) and loading capacity (LC) of CRM-loaded particles and CA-loaded droplets was assessed by ultrafiltration using centrifugal ultrafiltration tubes (Amicon® Ultra-4 filter 10 kDa cut-off, Millipore, Billerica, MA, USA). 1 mL of either the dispersion or emulsion systems was added to the upper chamber of the centrifugal tube and centrifuged at 2,400 rcf for 1 h at room temperature using a SIGMA 3K-30 centrifuge (SciQuip®, UK). The concentration of unentrapped CRM or CA in the filtrate was subsequently determined by measuring the UV-Vis absorbance (Genova Bio Life Science Spectrophotometer, Jenway®, Cole-Palmer, UK) at 425 or 278 nm, respectively. Explicitly for CA, a solvent extraction protocol was followed prior to the absorbance measurements to eliminate any co-absorption interference at the specific wavelength. An aliquot of the filtrate was mixed with pentane at a 1:2 ratio, and the CA-rich pentane phase was then measured to determine the absorbance. The concentration of each model active was determined using calibration curves previously generated, with linearity studied for 0–6 μg/mL and linear regression value of R^2 = 0.9995 for CRM, and linearity of 0–28.7 μg/mL and R^2 = 0.9915 for CA. The EE and LC values were calculated using the following equations:

$$EE = \frac{W_{i.} - W_{u.}}{W_{i.}} \times 100\ (\%) \tag{6.1}$$

$$LC = \frac{W_{i.} - W_{u.}}{W_{l.p.}} \times 100\ (\%) \tag{6.2}$$

where $W_{i.}$ is the amount of active that was initially used during the preparation of the aqueous lipid dispersions or emulsions, $W_{u.}$ is the amount of active measured in the filtrate, and $W_{l.p.}$ is the total amount of the lipid/oil components used in the systems.

6.2.10 *In vitro* release and co-release

In vitro release of curcumin, from curcumin-loaded lipid particle dispersions and particle-stabilised (Pickering) o/w emulsions was performed by diffusion through a dialysis membrane. A known amount of the particle dispersions or the Pickering emulsions was enclosed in a cellulose dialysis membrane (43 mm width, 14 kDa M.W. cut-off, Sigma-Aldrich Company Ltd., Dorset, UK), and the tubing was introduced in the *in vitro* release medium (130 g) consisting of phosphate buffer saline (PBS, pH 7.4) and 1.0% w/w Tween® 80. At predetermined time intervals, 1 mL aliquots of the dissolution medium were collected and analysed by UV-Vis spectrophotometry (Genova Bio Life Science Spectrophotometer, Jenway®, Cole-Palmer, UK). The *in vitro* release of cinnamaldehyde-loaded simple or Pickering emulsion droplets was assessed following the exact same protocol, with a slight modification at the absorbance measurement step, accordingly to what was previously described for the EE and LC determination. The absorbance was measured at 425 nm for CRM and at 278 nm for CA. The release measurements were performed using an Incu-Shake MIDI shaker incubator (Sciquip, UK) operating at 25°C under constant shaking (180 rpm). The dissolution of CRM and CA solutions (at equal concentrations as those used in the dispersion/emulsion systems) prepared using the dissolution medium as solvent was also assessed. The dialysis membranes were soaked in the dissolution medium overnight, prior to usage. Sink conditions were maintained by replacing the sampled aliquots with equal volume of fresh media. The volume correction has been accounted for, in the reported cumulative

release plots. The measurements were conducted in triplicate using independently prepared samples.

For the co-release assessments, the only adaptation in the above-described method was relevant to doubling the volume of aliquots withdrawn, to allow for sufficient quantification volume. For the stability assessments, the co-release measurements were performed immediately after preparation and after 1 month of storage at 4°C.

6.2.11 Modelling of release data

The release data from the CRM-loaded lipid particles either in dispersion or emulsion settings were fitted into the mechanistic model described by Crank [28], to gain further insight regarding the underlying release mechanism. The diffusion coefficient (*D*) was determined as follows:

$$\frac{Q_t}{Q_\infty} = 1 - \frac{6}{\pi^2}\sum_{n=1}^{\infty}\frac{1}{n^2}\exp\left(-\frac{Dn^2\pi^2 t}{r^2}\right) \quad (6.3)$$

where Q_t is the mass of active released at time t, Q_∞ is the total mass of active released when the formulation is exhausted, n is the number of the term in the series, r is the particle radius (calculated using the *Z*-average), and D is the apparent diffusion coefficient of the active within the system.

Regarding the release of actives from within emulsion droplets, two limiting models have been previously described [29,30] and utilised in literature [22,31,32]. According to these, the release of the active is either primarily driven by diffusion through the oil droplet, or it is limited by the presence of an interfacial barrier around the emulsion droplet.

When the former is true, there is no interfacial barrier effect on the diffusion of the active through the oil core, and the release at long times can be approximated by:

$$ln(1-\frac{Q_t}{Q_\infty}) = ln(\frac{6}{\pi^2}) - \frac{\pi^2 D}{r^2}t \quad (6.4)$$

which is the linear form of the following:

$$\frac{Q_t}{Q_\infty} = 1 - \frac{6}{\pi^2}\exp\left(-\frac{\pi^2 D}{r^2}t\right) \quad (6.5)$$

The symbols retain their previous meaning (Equation 6.3), but relevant to the emulsion droplets. For the emulsion radius (r), the $D_{3,2}$ data acquired from the LD measurements was used. Using Equation 6.4 and plotting the $ln(1-Q_t/Q_\infty)$ against time will have a limiting slope of ($\pi^2 D/r^2$), which can be used to calculate the diffusion coefficient D.

For the alternative model, where the active discharge is governed by the transfer across the interfacial barrier and the active is considered to be uniformly distributed within the emulsion droplet at all times, the following long-time approximation equation was used:

$$\frac{r^2}{3}ln(1-\frac{Q_t}{Q_\infty}) = -k_1 t \quad (6.6)$$

which is the linear form of the following:

$$\frac{Q_t}{Q_\infty} = 1 - exp\left(\frac{-3k_1}{r^2}t\right) \quad (6.7)$$

where k_1 is the interfacial rate constant, with all other symbols retaining their meaning. Comparably to the previous model, plotting the natural logarithmic term on the left-hand side of Equation 6.6 against time would provide with a straight line, the slope of which can be used to calculate k_1.

The D values attained here were in the range of 10^{-11}, and thus significantly lower than those calculated using the Stokes-Einstein equation ($D = 1.3\times10^{-7}$ cm^2 s^{-1}) for a small molecule diffusing through sunflower oil. If release was driven by diffusion, it would be expected that the estimated values would be close to that calculated by the Stokes-Einstein equation, but also close to one another, provided that the same oil phase was utilised in all formulations [22,29,31,32]. Therefore, the release should be primarily governed by transfer across the interfacial layer, rather than diffusion, and any k_1 differences should come as a result of having structurally different interfaces. The interfacial barrier-limiting model was further considered for the emulsion release behaviour at longer times ($t \geq 30$ min).

6.2.12 Statistical analysis

Samples were analysed in at least triplicate and averages are reported with standard deviation. Figures depict the calculated average value with error bars showing the standard deviation above and below the average. Comparison of means was conducted by ANOVA analysis followed by an all pairwise multiple comparison test using the Student-Newman-Keuls Method (SigmaPlot 14.5). The differences were considered statistically significant when $p \leq 0.05$.

6.3 Results and discussion

6.3.1 Release from lipid particles

Recently, SLNs and NLCs were utilised as dual functional species, with the intent of simultaneously regulating the encapsulation/release of curcumin (used model hydrophobic active) and acting as Pickering emulsion stabilisers [25,26]. Though the introduction of the particles within the emulsion system was shown to accelerate the release rate compared to that in a dispersion setting, both types of particles were still able to regulate the discharge of curcumin, with overall sustained release profiles being reported (~50% released over 7 days), while maintaining their Pickering stabilisation capacity [26]. Herein, the impact of modifying lipid particle formulation aspects, namely the type of solid lipid used and its combination with a liquid lipid, as well as the type of surfactant employed, on the release behaviour from within both dispersion and emulsion settings will be explored.

6.3.1.1 Lipid particles in dispersions

Prior to introducing the lipid particles within the emulsion systems, their performance in aqueous dispersions is explored to establish how changes to the formulation parameters affect their release regulation ability (Fig. 6.1). Based on previous investigations of the release performance of SLNs and NLCs fabricated with C888 as the solid lipid and MCTs as the liquid lipid, it was proposed that addition of MCTs results in the structural re-organisation of the particles' lipid matrix into a less ordered crystalline state, a phenomenon that in turn decreases the rate of curcumin release [26]. Additionally, the release mechanism was described as diffusion-driven, due to both the overall slow release rate and high EE/LC values for either type of particles, and the low diffusion coefficients (*D*).

Delving further into the influence of modifying the lipid particles' composition, the high melting point solid lipid C888 was substituted by the lower melting point P5, keeping the rest of the formulation aspects unchanged, and the release performance of P5 SLNs and NLCs was investigated (Fig. 6.1B). Compared to their C888 counterparts (Fig. 6.1A), both lipid particle types demonstrate almost identical release profiles and very similar *D* values (Table 6.1). According to previous solubility studies (Chapter 3, [27]), C888 and P5 have comparable CRM solubility thresholds (0.6 and 0.7%, respectively), while their EE and LC values were the same (99.9±0.0% and 0.5±0.0%, respectively). Considering the above, it could be assumed that the localisation of curcumin and/or internal arrangement of the lipid particles, for both the SLNs, but also the NLCs pairs are akin. Several studies have discussed the incapacity of the crystalline lipid structure of SLNs to host active molecules, and the subsequent expulsion/migration of the latter towards the surface of the particles [33–35]. Correspondingly, addition of the liquid lipid component within the solid matrix has been associated with solid/liquid phase separation, particularly for higher liquid lipid concentrations, and concentration-dependent creation of distinct lipid structures [27,36,37]. Once the solid lipids' solubility limit for the liquid component is exceeded, liquid oil nano-compartments can be formed within the matrix, or the liquid lipid can be concurrently expelled towards the surface [33,38]. The formation of these compartments requires that sufficient space is available within the arrangement/packing of the crystalline element. Specifically for C888, when the lipid is crystallised at a cooling rate of 1 °C/min, which is very close to the one used in this work (1.2 °C/min), the co-presence of two lamellae has been reported [39], leading to matrix imperfections [40]. Recently, Galeano *et al*. [35] described the stages of active (paraben) exclusion as the lipid matrix crystallises, towards the MCTs-rich surface of trimyristin NLCs, or in-between the trimyristin crystals and the surfactant (P188) layer in SLNs. In this study, both C888 and P5 are mixtures of variable

triacylglycerols; the former of slightly longer alkyl chains, while the latter of more varied composition (behenic acid and palmitic/stearic acid esters, respectively). Additionally, in both types of NLCs, the prospect of the presence of polymorphs characterised by lower packing densities has been previously discussed (Fig. 6.2A & B) [27], thereby not utterly excluding the possibility of MCTs compartment formation within the NLCs' structure [41,42]. However, taking into account that MCTs is used at a 30% w/w concentration of the total lipid phase, which is likely exceeding the solubility limits of either solid lipid for MCTs, it is expected that the bulk of the liquid lipid component will be contained near the surface of the particles [33,38]. Consequently, given the solubility constrains imposed by the solid lipid crystallisation, it can be hypothesised that CRM will be preferentially located within the MCTs phase (NLCs) or near the surface of the particles (SLNs), at least when it comes to its highest proportion [35,43,44].

The next parameter assessed was the effect of the lipid particle formation in the presence of different surface active species types on the CRM release regulation capability, with both SLNs and NLCs fabricated with P188 as surfactant and C888 as the solid lipid (Fig. 6.1C). Compared to their T80 counterparts, both P188 particle types exhibited faster release. Furthermore, there was almost no difference between the C888/P188 SLN and NLC formulations, as opposed to the slower NLC release recorded for the particles fabricated with T80 for either type of solid lipid. The *D* values calculated for these systems (Table 6.1), although higher than the particles formed with T80, are still significantly lower than values reported in literature for curcumin-loaded SLNs fabricated with stearic acid as the lipid phase and P188 as surfactant [22,45]. Taking into consideration that there are only very small particle size differences (Table 6.2), and the EE/LC values remain the same in all particle types [27], it could be suggested that the discrepancies in the release behaviour are driven by the surfactant substitution. Based on the melting behaviour of the C888/P188 lipid particles where a diminished degree of polymorphism

is observed (Fig. 6.2C), and previous investigations regarding the compatibility between the lipid matrix components [27], T80 appears to participate in a greater extent within the crystalline network (close to the particle surface). Therefore, it could be also postulated that the co-existence of C888/T80 in SLNs or MCTs/T80 in the case of NLCs at the edge of the particles' structure and near the particles' surface is posing an additional barrier for CRM to cross, possibly due to the creation of a favourable hydrophobic environment compared to the dissolution medium, particularly in the latter. Contrary to the potentially denser packing arrangement provided by the smaller T80 molecules, the larger molecular size P188 molecules could not provide an as tightly packed interface, which together with their limited crystalline network participation provided curcumin easier and more extended access to regions much closer to the surface of both SLNs and NLCs [46].

With respect to the quite slow release rate from all 6 lipid particle types (<50% CRM released cumulatively in 7 days), similar trends have been previously reported for SLNs and NLCs encapsulating hydrophobic moieties [47–50]. Such sustained release profiles are usually ascribed to hindered diffusion of the active molecules through the highly ordered crystalline arrangement of the lipid particles, though active partition coefficients and solubility constraints could also contribute to the stunted release percentages and lengthy experimental times [51–54]. Herein, the dissolution medium was selected based on two criteria; firstly, it was prerequisite to have sufficient solubilisation capacity for the amount of active present in the particle dispersions during the release studies (sink conditions), and secondly based on previously reported literature [55,56] and its use in similar systems, it was anticipated that it would not impact on the lipid particles' integrity over the timescales of the measurement, to ensure that the effect of the formulation aspects was adequately represented. However, it should also be noted that the selection of a solvent for which CRM has a higher affinity compared to

the selected lipids, and hence would result in lower partition coefficient [57,58], and/or higher solubility thresholds could potentially lead to much faster release rates. Therefore, the results presented here in terms of the release profiles, but also with regard to the diffusion coefficients should only be approached as a relative measure of the influence of formulation parameter changes.

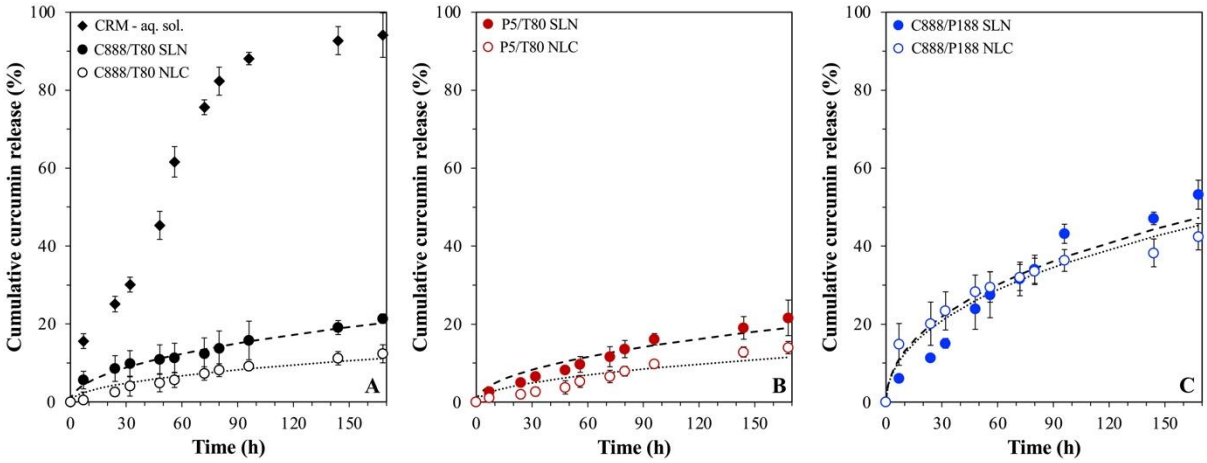

Fig. 6.1. *In vitro* release profile of curcumin-loaded SLN and NLC dispersions formulated with either Tween® 80 (T80) as surfactant and different types of solid lipid (A) Compritol® 888 ATO (C888) and (B) Precirol® ATO 5 (P5), or different surface active species (C) Poloxamer 188 (P188) and C888 as solid lipid. NLCs were fabricated with Miglyol® 812 as the liquid lipid, at 30% w/w of the total lipid phase mass. The release profile from a curcumin solution obtained under the same conditions is also depicted (A). The *in vitro* release kinetic Crank model fitting of curcumin for each SLN (dashed line) and NLC (dotted line) dispersion is also presented. Graph A has been previously shown in [26] and is provided here for comparison purposes.

Table 6.1. Diffusion coefficient (*D*) and coefficient of determination (R^2) describing the fitting into the Crank model of the curcumin release data from lipid particles within dispersion and emulsion systems. Identical lowercase letters indicate no significant differences between samples.

Lipid particle setting	Lipid formulation	$D \times 10^{-20}$ (cm^2 s^{-1})	R^2
Dispersions	**C888/T80 SLN**	45.1±7.9^a	0.98
	C888/T80 NLC	12.1±1.4^a	0.97
	P5/T80 SLN	45.0±3.7^a	0.96
	P5/T80 NLC	6.6±1.2^a	0.91
	C888/P188 SLN	214±34.5^b	0.95
	C888/P188 NLC	178±23.1^b	0.98
Emulsions	**C888/T80 SLN**	213±23.2^b	0.94
	C888/T80 NLC	177±25.4^b	0.97
	P5/T80 SLN	546±45.1^c	0.96
	P5/T80 NLC	171±45.8^b	0.98
	C888/P188 SLN	278±39.0^b	0.99
	C888/P188 NLC	310±51.0^b	0.99

Table 6.2. *Z*-average and polydispersity index (PDI) of different SLN and NLC formulations measured after preparation.

Formulation	*Z*-average (nm)	PDI
C888/T80 SLN	165.1±2.7	0.20±0.02
C888/T80 NLC	163.2±3.8	0.12±0.01
P5/T80 SLN	176.0±9.6	0.28±0.04
P5/T80 NLC	134.4±7.1	0.14±0.04
C888/P188 SLN	139.7±1.9	0.20±0.01
C888/P188 NLC	133.7±2.1	0.18±0.02

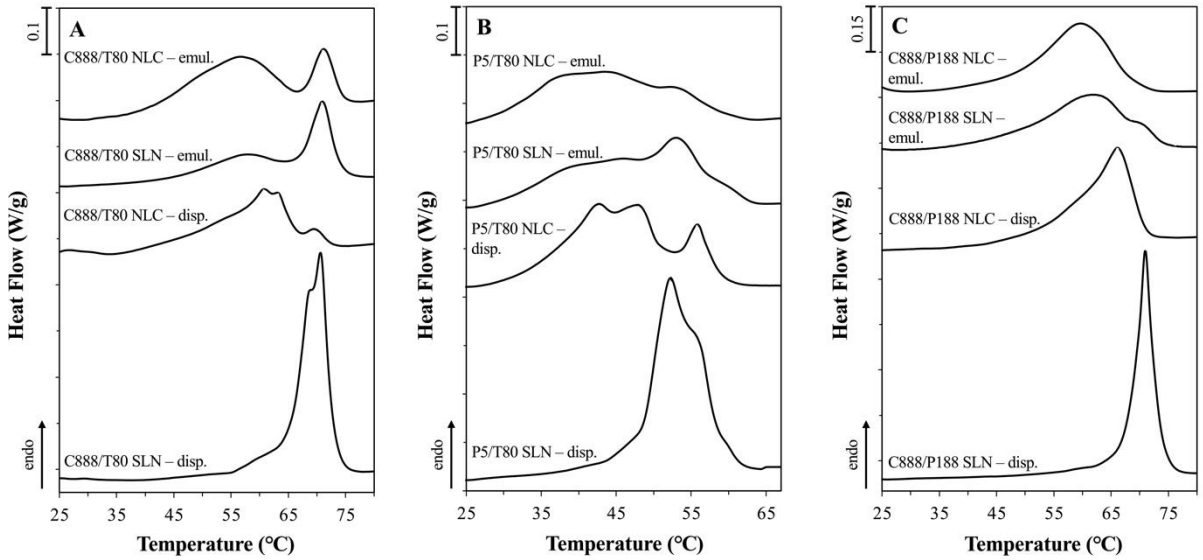

Fig. 6.2. DSC melting thermograms of SLN and NLC dispersions and their respective Pickering emulsions, for lipid particles formulated with either Tween® 80 (T80) as surfactant and different types of solid lipid (A) Compritol® 888 ATO (C888) and (B) Precirol® ATO 5 (P5), or different surface active species (C) Poloxamer 188 (P188) and C888 as solid lipid. NLCs were fabricated with Miglyol® 812 as the liquid lipid, at 30% w/w of the total lipid phase mass. The curves were normalised for the amount of solid matter present in each sample and shifted along the ordinate for better visualisation. Graph A has been previously shown in [26,27] and is provided here for comparison purposes.

6.3.1.2 Lipid particles in emulsions

The dual role of both SLNs and NLCs to act as Pickering stabilisers and in tandem as release regulators of CRM was previously confirmed, using particles fabricated with C888 and T80 [25,26]. Particular focus was placed on the lipid particle and particle-stabilised emulsion properties that can have an effect on the release behaviour, and the underlying mechanism that drives said release. It was suggested that the CRM discharge from particle-loaded Pickering emulsions is the composite of the release from particles remaining dispersed in the continuous phase, and particles adsorbed at the droplet interface [26]. The increased release rate compared to the particle dispersions was attributed to both particle characteristics and emulsion

formation-induced phenomena; more specifically to partial migration of any loosely entrapped curcumin to the oil phase and contribution of crystalline matter loss. Therefore, before probing deeper into the release performance of lipid particles with modified formulation parameters, namely type of solid lipid and surfactant, physical characteristics of both the particle dispersions and the respective particle-stabilised emulsions were scrutinised. This was performed to gain further insight into the microstructural properties of the formed systems, particularly in terms of their Pickering behaviour.

Among these was the interfacial tension reduction capacity of the particles (Fig. 6.3), based on which information regarding the interfacial decoration of the particles can be extracted. It was observed that both P5 fabricated particle types had identical interfacial tension reduction ability with an equilibrium value of 6.3 mN/m, which was at similar degree as that recorded for the C888 NLCs (Fig. 6.3A & B), and higher than the C888 SLNs. Considering that all T80-formed particles have similar sizes and equal amount of surfactant was used, this disparity could be attributed to differences in the lipid composition of the particles affecting the arrangement and packing density of surfactant molecules at their interface. Particles prepared with P188 as the surfactant demonstrated considerably higher equilibrium interfacial tension values, with 15.3 and 14.3 mN/m for the SLNs and NLCs, respectively (Fig. 6.3C). This observation could be stemming from differences in the molecular size of the two surfactants, which in turn could be resulting in different packing arrangements at the particles' interface. T80 seems to instigate a higher interfacial tension reduction compared to P188, possibly owing to a higher and more tightly packed interfacial presence, caused by its smaller molecular size, as supported by the trends of both aqueous surfactant solution curves [59]. The effect of the surfactant molecular size is also reflected in the obtained emulsion droplet sizes. Regardless of the type of solid lipid used or type of lipid particle (SLN/NLC) created, particles fabricated with T80 exhibited almost

identical droplet size distributions (Fig. 6.4A & B), while P188 particles formed droplets that were an order of magnitude larger (Fig. 6.4C). This could be due to the slower movement of P188 molecules to the oil/water interface compared to T80, thus leading to larger droplet sizes.

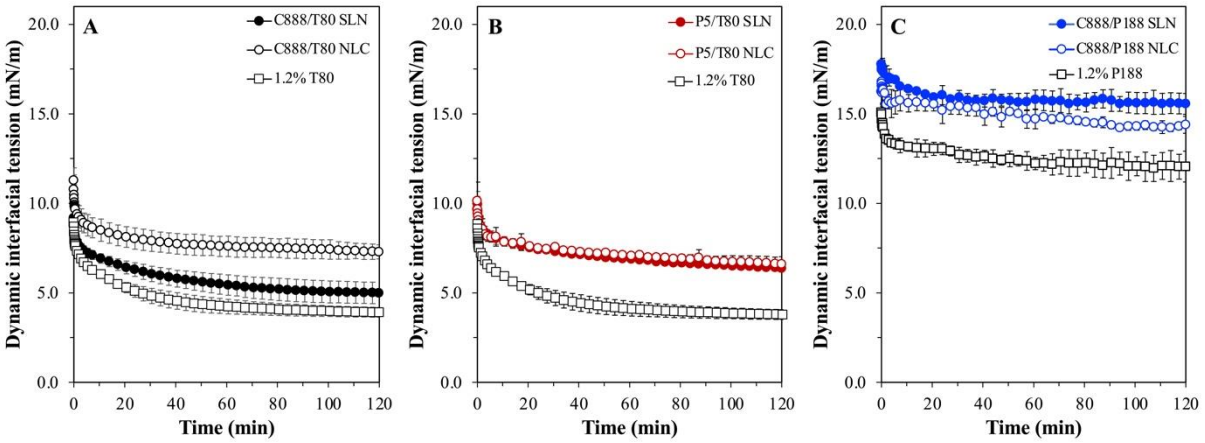

Fig. 6.3. Dynamic interfacial tension of aqueous dispersions of SLN and NLC formulations prepared with either Tween® 80 (T80) as surfactant and different types of solid lipid (A) Compritol® 888 ATO (C888) and (B) Precirol® ATO 5 (P5), or different surface active species (C) Poloxamer 188 (P188) and C888 as solid lipid. NLCs were fabricated with Miglyol® 812 as the liquid lipid, at 30% w/w of the total lipid phase mass. The curves of pure T80 and P188 solutions with similar concentration (1.2% w/w) as of those used for the dispersions are also presented for comparison. Data points are the average of three measurements and error bars represent the standard deviation. Graph A has been previously shown in [25] and is provided here for comparison purposes.

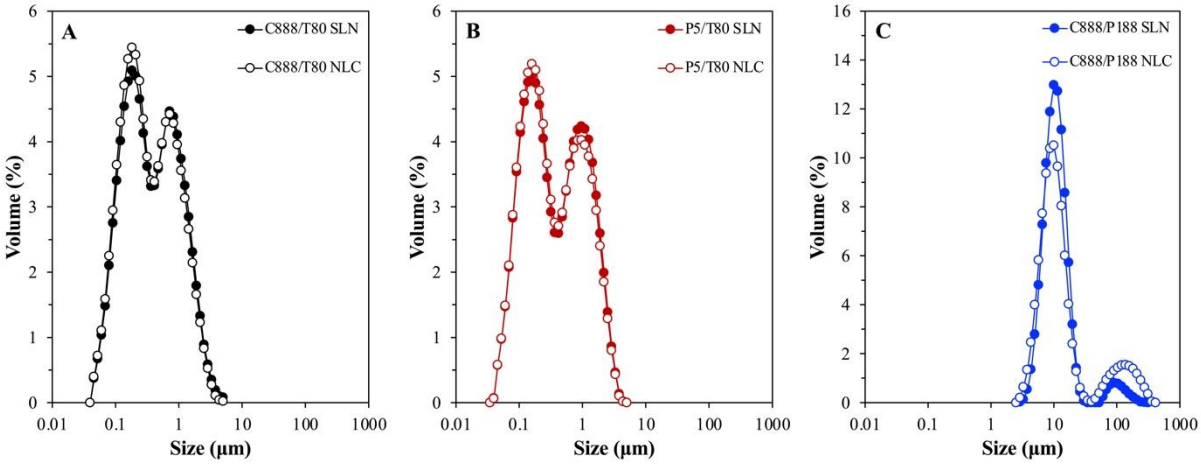

Fig. 6.4. Droplet size distribution of SLN- and NLC-stabilised emulsions, with lipid particles formulated with either Tween® 80 (T80) as surfactant and different types of solid lipid (A) Compritol® 888 ATO (C888) and (B) Precirol® ATO 5 (P5), or different surface active species (C) Poloxamer 188 (P188) and C888 as solid lipid. NLCs were fabricated with Miglyol® 812 as the liquid lipid, at 30% w/w of the total lipid phase mass. Graph A has been previously shown in [25] and is provided here for comparison purposes.

The loss of crystalline matter once the particles are introduced within the emulsion systems was also explored, as this has been suggested as a factor impacting their release behaviour. According to Fig. 6.5, there was a greater loss of crystalline material for the P5/T80 SLNs/NLCs compared to C888 containing particles. As it has already been suggested in literature [26,60,61], the type of lipid source used can play a crucial role in lipid mass transfer phenomena, with surfactant micelles facilitating the transfer of oil molecules from the emulsion droplets to the lipids constituting the particles' lipid core. Such occurrences could either be directly related to particles adsorbed at the emulsion interface or even particles remaining free in the continuous phase. In this instance, it appears that the potentially higher compatibility of P5 (glyceryl palmitostearate) and sunflower oil (containing triglycerides of palmitic and stearic acids), due to their closer chemical composition compared to that between C888 and sunflower oil, could be further aiding dissolution [27,62]. On the contrary, emulsion formation did not cause any losses for the C888/P188 particles, possibly owing to the improved protection

provided by the P188 molecules over such incidents. As mentioned above, besides the type of lipid source, another aspect affecting this event is the formation and presence of surfactant micelles within the continuous phase [63–66]. In this work, the aqueous P188 concentration even before addition to the pre-emulsion used for the particle dispersion production, was a lot lower than its critical micelle concentration (CMC, 17.9 mM) [67]. Therefore, the lack of micelles present in the systems to facilitate any mass transfer, in combination with the usage of a lipid (C888) with very low aqueous solubility [61] has led to no losses compared to the already minimal crystalline matter reduction reported for the C888/T80 particles. Lastly, the fewer particle/oil contact points should be accounted, as the proportion of C888/P188 particles required to cover the oil droplet surface area is a lot less than that of the C888/T80 particles, as a result of the significantly larger emulsion droplet sizes produced with the former (Fig. 6.4).

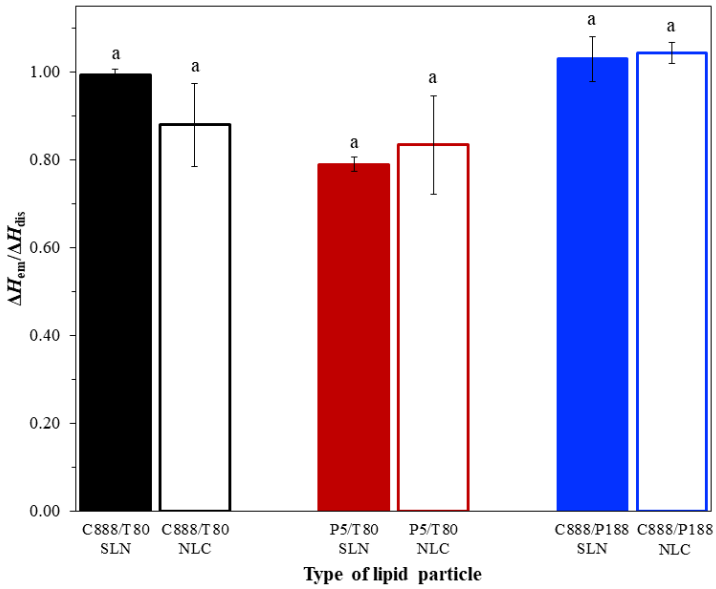

Fig. 6.5. Ratio of the melting enthalpies of the particles within an emulsion environment and those in a lipid particle dispersion setting ($\Delta H^{T}_{em}/\Delta H_{dis}$), representing the amount of crystalline material remaining within the emulsions stabilised by different types of lipid particles. Identical lowercase letters indicate no significant differences between samples.

With regard to their release regulation ability, both particle types prepared with P5 exhibited faster release comparatively to the respective particles fabricated with C888, and same trends in terms of the P5 NLCs showing more sustained release than the P5 SLNs (Fig. 6.6A & B). The greater loss of crystalline matter in the P5/T80 SLNs/NLCs (Fig. 6.5) could account for the higher release rate, particularly in the first half of the measurement (first 90 h). Previous work utilising DSC data of the particle-stabilised emulsions [26] has shown that it is possible to estimate the particle interfacial occupancy by ascribing different melting peaks to particles present at the interface or particles remaining in the continuous phase. More specifically, for C888 SLNs and NLCs the adsorbed particles percentage was approximately 60 and 75%, respectively. Although an estimate of the adsorbed/unadsorbed ratio for either P5/T80 or C888/P188 SLNs/NLCs could not be made, owing to the complex melting behaviour of the particles in the emulsion system (Fig. 6.2B & C), it could be assumed that an excess concentration of them was used, and thus a portion of them is not associated with the droplet interface [25]. Conversely, the CRM release rate from both P188-formed SLNs and NLCs at the emulsion interface was only marginally higher to that exhibited by the particles in an aqueous dispersion setting (Fig. 6.6C). In view of the effect that the surfactant type has on any mass transfer occurrences, whether that is the active or participating lipids, these data come as no surprise. The absence of any micelles available to facilitate any dissolution of solid matter and thereby release of any CRM associated with it, as well as the higher percentage of unadsorbed C888/P188 particles in the continuous phase (due to the lower number required to cover the smaller droplet surface area) rather than "exposed" to the oil phase, can be aiding towards the lack of release profile changes. The *D* values were in the same order of magnitude for all particle-stabilised emulsions (Table 6.1), with only exception the P5/T80 SLNs that were characterised by a significantly higher *D* value, which aligns well with the fact that this was the

particle type with the higher loss of crystalline matter. The EE and LC remained the same as for the dispersions (99.9±0.0% and 0.5±0.0%, respectively).

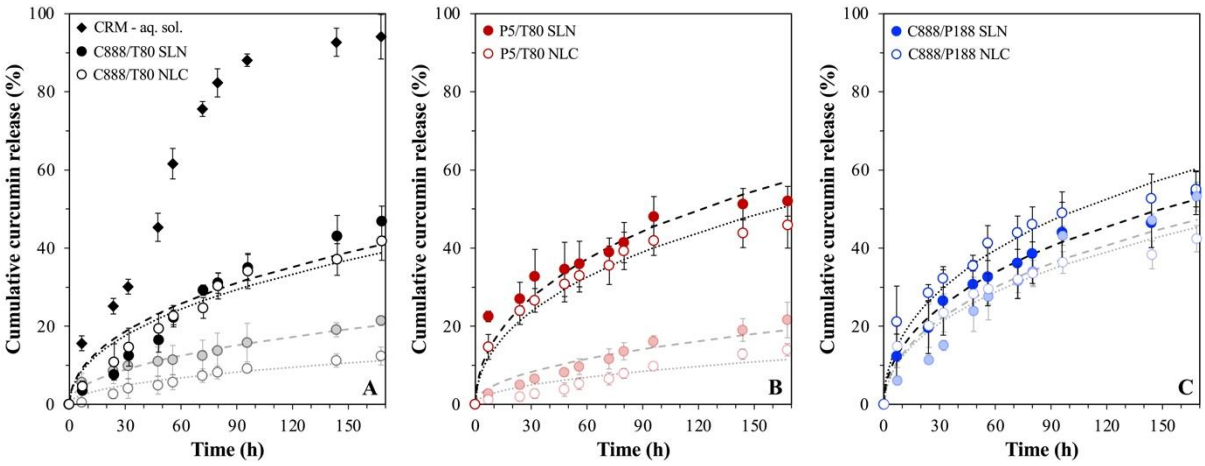

Fig. 6.6. *In vitro* release profile of curcumin-loaded SLN- and NLC-stabilised emulsions formulated with either Tween® 80 (T0) as surfactant and different types of solid lipid (A) Compritol® 888 ATO (C888) and (B) Precirol® ATO 5 (P5), or different surface active species (C) Poloxamer 188 (P188) and C888 as solid lipid. NLCs were fabricated with Miglyol® 812 as the liquid lipid, at 30% w/w of the total lipid phase mass. The *in vitro* release kinetic Crank model fitting of curcumin for each emulsion system stabilised by SLNs (dashed line) or NLCs (dotted line) is also presented. The release profile from a curcumin solution obtained under the same conditions (A), and that of the particles within the dispersion systems are also depicted in each respective graph. Graph A has been previously shown in [26] and is provided here for comparison purposes.

6.3.2 Release from emulsion droplets

Within this work, apart from their active carrying and release regulation ability that was demonstrated above, the lipid particles are also in tandem acting as Pickering emulsion stabilisers. The latter functionality can be equally translated into two aspects; the first being the particles' droplet stabilisation capacity, and the second the level of control they can provide over the release of a secondary active encapsulated within the emulsion droplets. Provided that

there are two rate-limiting factors relevant to the release from within emulsion droplets as has been previously suggested in literature formulations [22,29-32], those being the active's diffusion within the oil droplet and its subsequent transfer across the interfacial barrier surrounding the droplets, the formulation properties of the lipid particles can be influencing said barrier to a varying extent. Therefore, the range of SLNs and NLCs that were previously investigated for their curcumin discharge regulation, were now utilised as blank colloidal species providing Pickering stabilisation to emulsion droplets loaded with cinnamaldehyde, used as a (secondary) model hydrophobic active.

For the purpose of establishing a reference for the impact of the particles' interfacial presence on both the droplets' active carrying and release governing capacity, simple emulsions fabricated with either of the two surface active species used in the lipid particle preparation (T80 or P188) were also studied. Compared to a cinnamaldehyde solution, encasing of the active within the emulsion droplets appears to slow down the release rate to a certain degree, with full discharge achieved within 100 min for the former and a delay of 50 and 150 min recorded for the P188 and T80 stabilised emulsions, respectively (Fig. 6.7A). Properties like the droplet size distribution and EE/LC were also determined, with both emulsions showing bimodal distributions with a main peak at around 1 μm and a smaller at ~0.25 μm (Fig. 6.7B), and no significant differences in the attained EE and LC values (approximately 83% and 7.6×10^{-3} %, respectively) (Table 6.3). In contrast, the presence of the lipid particulates seems to slow down the cinnamaldehyde release rate and overall percentage discharged. Approximately 75% release was reached at 280 min for both C888/T80 and P5/T80 particles, and 40% was released at the same timescale for the C888/P188 counterparts, while almost identical profiles were obtained for SLNs and NLCs with the same formulation characteristics (Fig. 6.8). In terms of the capacity of the particles to improve the amount of active remaining

contained within the droplets, the EE and LC values were in the same range as for the simple emulsions (Table 6.3). This suggests that the active retention within the droplets is predominantly governed by the characteristics of the oil phase, rather than their interfacial decoration.

Even though o/w emulsions represent a suitable and adaptable platform for the encapsulation and delivery of poorly water-soluble actives, owing to their droplets' inherent hydrophobic character and easily tuneable physicochemical characteristics (e.g. type of oil/surfactant, droplet size), the absence of any physical barrier at the droplet interface can lead to burst release and active expulsion overtime [68–71]. Herein, it was shown that differences in the interfacial composition, from surfactant molecules to lipid particles, and even more specifically changes in the structure of the particles themselves, do in fact alter the release kinetics. In literature, complete release from simple emulsions has been shown to occur over varying timescales ranging from a couple of minutes for small hydrophobic solutes such as chlorpromazine from soya oil droplets stabilised with P188 [29], to a couple of hours for the release of dibutylpthalte from polydimethylsiloxane bare droplets [72]. This data aligns well with what is reported here, as any small difference could be related to disparities in the droplet sizes, variations in the partition coefficient values between the used active, oil phase and dissolution medium, and/or altered release measurement methods. Concerning the effect of the particle addition, preliminary studies revealed that the incorporation of cinnamaldehyde does not alter the physical properties of Pickering emulsions. Therefore, required information regarding the droplet sizes to estimate the interfacial rate constant (k_1) values arising from literature models given in Equation 6.6, was used according to Fig. 6.4. The $k_1$values estimated in this work were in the range of 10^{-15} cm^2 s^{-1} for the emulsions stabilised by T80-formed particles and almost three orders of magnitude larger for the C888/P188 SLNs/NLCs-stabilised emulsions (Table

6.3). Similar values to the C888/P188 particle-stabilised emulsions have been described for dimethyl phthalate releasing from emulsions stabilised with SLN prepared using whey protein isolate as the surfactant (3.09×10^{-12} cm^2 s^{-1}) [22], as well as emulsions stabilised by surfactants with Pickering-like characteristics [32]. On the contrary, emulsions stabilised with T80 particles gave values akin to previously reported data for emulsion stabilised by silica particles [69,72] and protein/polysaccharide co-precipitates [31]. Such deviations could be ascribed to disparities in the active partition coefficient and dissolution medium solubility values amongst the various studies. However, despite the much greater k_1 values for the C888/P188 SLNs/NLCs, the experimentally recorded release rate for CA was much slower compared to the T80 counterparts. This could be due to the lower interfacial area owing to their much larger droplet sizes, but also potentially bridging effects or gelling properties of block co-polymers like P188 [73], thereby increasing the viscosity of the continuous phase, and hence leading in slower release rates.

Overall, both SLNs and NLCs were shown to act as effective barriers against the burst release of a model hydrophobic active. The presence of particles at the droplet interface that bear easily malleable characteristics could be potentially utilised as a tool for tuning the interfacial structure according to the desired release performance [74,75].

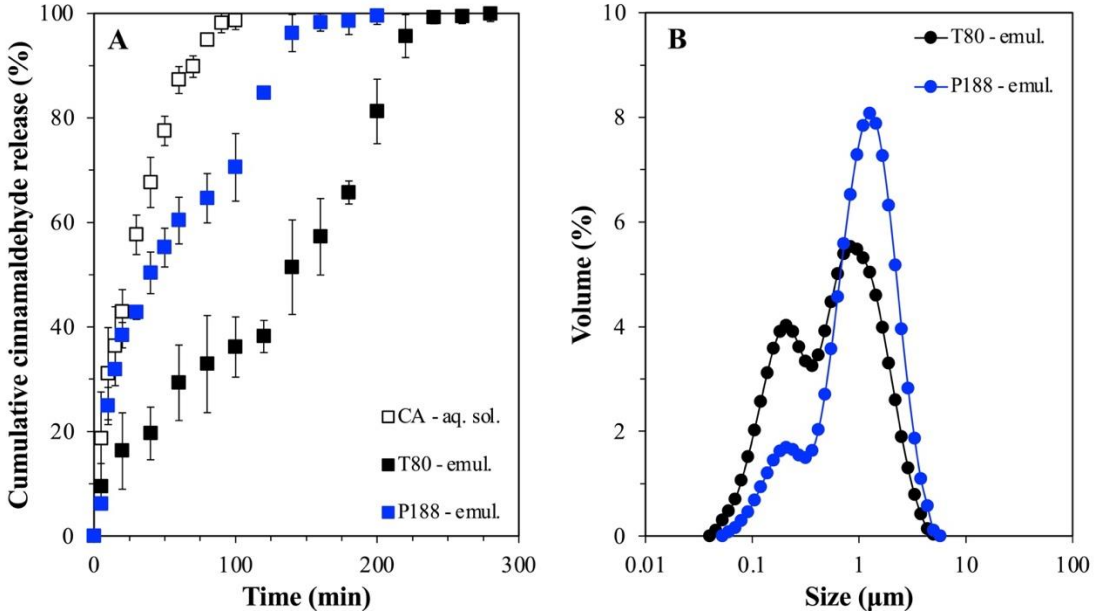

Fig. 6.7. *In vitro* release profile of cinnamaldehyde-loaded emulsions stabilised with either T80 or P188 (A), droplet size distribution of the same systems (B). The release profile from a CA solution obtained under the same conditions is also depicted (A).

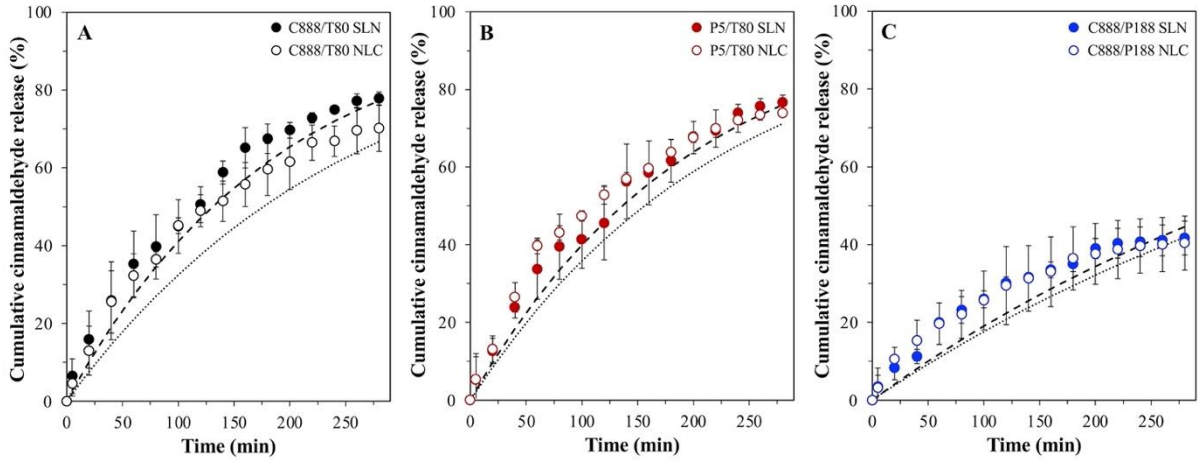

Fig. 6.8. *In vitro* release profile of cinnamaldehyde-loaded emulsions stabilised by SLNs and NLCs formulated with either Tween® 80 (T80) as surfactant and different types of solid lipid (A) Compritol® 888 ATO (C888) and (B) Precirol® ATO 5 (P5), or different surface active species (C) Poloxamer 188 (P188) and C888 as solid lipid. NLCs were fabricated with Miglyol® 812 as the liquid lipid, at 30% w/w of the total lipid phase mass. The interfacial barrier-limited model fitting of cinnamaldehyde for the SLN- (dashed line) and NLC- (dotted line) stabilised emulsions is also presented.

Table 6.3. Encapsulation efficiency (EE), loading capacity (LC), interfacial rate constant coefficient (k_1), and coefficient of determination (R^2) describing the model fitting for the interfacial barrier-limiting model of the cinnamaldehyde release data from emulsion systems. Identical lowercase letters indicate no significant differences between samples.

Formulation	EE (%)	LC × 10^{-3} (%)	k_1 × 10^{-15} (cm^2 s^{-1})	R^2
T80	84.2±1.0^a	7.8±0.0^a	-	-
P188	83.3±2.8^a	7.6±0.0^b	-	-
C888/T80 SLN	80.7±1.1^a	7.7±0.0^c	3.9±1.5^a	0.98
C888/T80 NLC	88.1±3.8^a	8.6±0.0^d	2.6±0.4^a	0.99
P5/T80 SLN	82.9±2.5^a	7.7±0.0^e	2.8±0.6^a	0.99
P5/T80 NLC	83.5±3.3^a	7.9±0.0^f	2.4±0.5^a	0.99
C888/P188 SLN	84.4±1.4^a	8.1±0.0^g	1900±45^b	0.94
C888/P188 NLC	88.0±2.1^a	8.1±0.0^h	1700±53^c	0.94
C888/T80 SLN – 64°C 5 min	80.7±0.9^a	7.7±0.0^c	1.4±0.7^a	0.98
C888/T80 SLN – 64°C 20 min	80.9±0.8^a	7.7±0.0^c	1.4±0.9^a	0.96
C888/T80 SLN – 64°C 60 min	81.0±1.0^a	7.7±0.0^c	2.2±0.5^a	0.94

6.3.2.1 Sintering

To further evaluate the plausibility of controlling the active discharge from within the o/w emulsion droplets by manipulating the lipid particle-laden interfacial architecture, the newly prepared Pickering emulsions were subjected to thermal post-fabrication processing. The occurrence of solid bridge formation between neighbouring fat crystals that are driven by mutual adhesion, also known as sintering, has been previously discussed in literature as a means of controlling the strength of a lipid-based structure and the texture of the resulting products [76]. Thermal sintering has been widely utilised as a preparation method for colloidosomes, thereby creating a robust layer at the oil/water interface that can provide not only improved protection against destabilisation phenomena, but also create microcapsules suitable for

carrying and delivering active molecules [77,78]. To this end, C888/T80 SLN-stabilised emulsions were heated either at 64 or 78°C under mild stirring for varying times and changes in their physical properties and (release) performance were studied.

According to earlier work using the particle-stabilised emulsions [26], the two peaks at ~60 and 70°C observed in their melting thermograms were ascribed to either particles associated with the emulsion interface (adsorbed) or particles remaining free in the continuous phase (unadsorbed), respectively. Therefore, the temperatures selected for this proof-of-concept sintering assessment were based on said melting events, presented in Fig. 6.9A. Heating of the formed SLN-stabilised emulsions at 64°C for increasing timescales (5, 20 and 60 min) caused statistically significant loss of crystalline matter compared to the untreated system, although the loss was overall minimal with all systems maintaining >90% of their initial solid content intact post thermal processing (Fig. 6.9B). When the emulsions were heated at the highest temperature (78°C), the melting profile of the system in terms of the relative intensity of the peaks appeared altered, with the peak at 62°C being more pronounced than the one at 70°C, suggesting decrease in the proportion of particles remaining unadsorbed in the continuous phase. Following the extended heating at 78°C, partial phase separation was observed with a visible oil layer formed at the top of the system. Additionally, droplet size increase was recorded, possibly due to droplet and/or particle aggregation induced by the complete melting of the lipid particles both at the droplet interface and within the continuous phase (Fig. 6.10A). In terms of the release performance, thermally-processed emulsion systems at 64°C displayed a more sustained release profile with no differences observed between them, and around 50% of CA being released within 240 min, as opposed to the 75% achieved with the used-as-prepared emulsion (Fig. 6.10B). Fitting of the interfacial barrier limiting-model gave k_1 values lower than for the unprocessed emulsion (Table 6.3). The release performance of samples

heated at 78°C was not further assessed due to the oil phase separation and discrepancies that this would cause to the calculation of the percentage of active discharging from the remaining physically stable droplets.

To gain further insight regarding the interfacial arrangement of the particles following the thermal treatment, cryo-SEM micrographs were acquired to visualise the emulsion droplets' surface (Fig. 6.11). For comparison purposes, the interface of droplets stabilised by T80 was also examined (Fig. 6.11A). Compared to the particle-stabilised emulsions, the surfactant-decorated interface of the simple emulsion appeared smoother, in accordance with data reported in literature [79]. Conversely, the emulsions stabilised by any of the different SLN types (C888/T80, P5/T80 or C888/P188) showed a rougher surface (Fig. 6.11B, E & F), although a clearly packed particle structure could not be distinguished. Specifically in terms of the impact of heating at 64 and 78°C, the droplet surface roughness appears somewhat reduced compared to the respective unprocessed C888 SLN-stabilised emulsion, albeit no particular observations can be made in regard to the influence of heating temperature (Fig. 6.11C & D). In a study by Yow and Routh [77], the formation of colloidosomes from colloidal poly(styrene-co-butyl acrylate) particles via sintering at varying temperatures and durations, was examined in relation to the release rate of a model active (fluorescein). It was shown that manipulation of the time and temperature provides control over the porosity and roughness of the formed colloidosome shell, with smoother shells providing longer release times. The importance of the sintering conditions when it comes to the tightness and durability of Pickering emulsion-based colloidosomes was also highlighted in another work [80], whereby reduced oil leakage was recorded for tightly packed colloidosome layers at the interface. Correspondingly, Rao *et al*. [81] demonstrated that longer sintering (3 h) of C888 matrices at 80°C led to retarded release rate of ketorolac tromethamine, owing to the increased extent and firmness of the sintered

structure. Overall, the results presented here suggest that a level of particle sintering was attained following the thermal processing of the formed Pickering emulsions, although further work is required to better elucidate the effect of the chosen conditions. Amongst these could be the influence of the occurring interactions and type of bridges formed depending on the composition of the interfacial layer (i.e. co-existence or not of particles and surfactant molecules) [76].

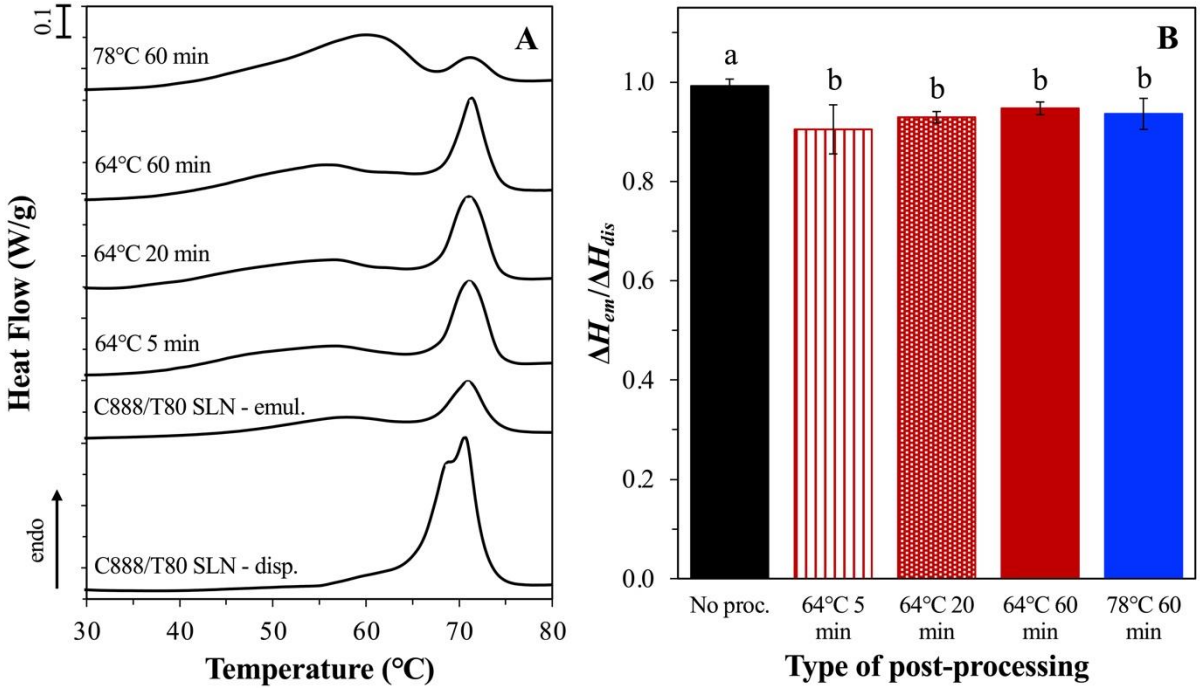

Fig. 6.9. DSC melting thermograms of C888/T80 SLN-stabilised emulsions before and after sintering at 64 and 78°C for varying durations (A). The curves were normalised for the amount of solid matter present in each sample and shifted along the ordinate for better visualisation. The melting curve of the C888/T80 SLN dispersion is also provided for comparison purposes. Ratio of the melting enthalpies ($\Delta H^{T}_{em}/\Delta H_{dis}$) of the emulsion systems presented in graph (A), representing the amount of crystalline material remaining within the emulsions post-processing (B). Identical lowercase letters indicate no significant differences between samples.

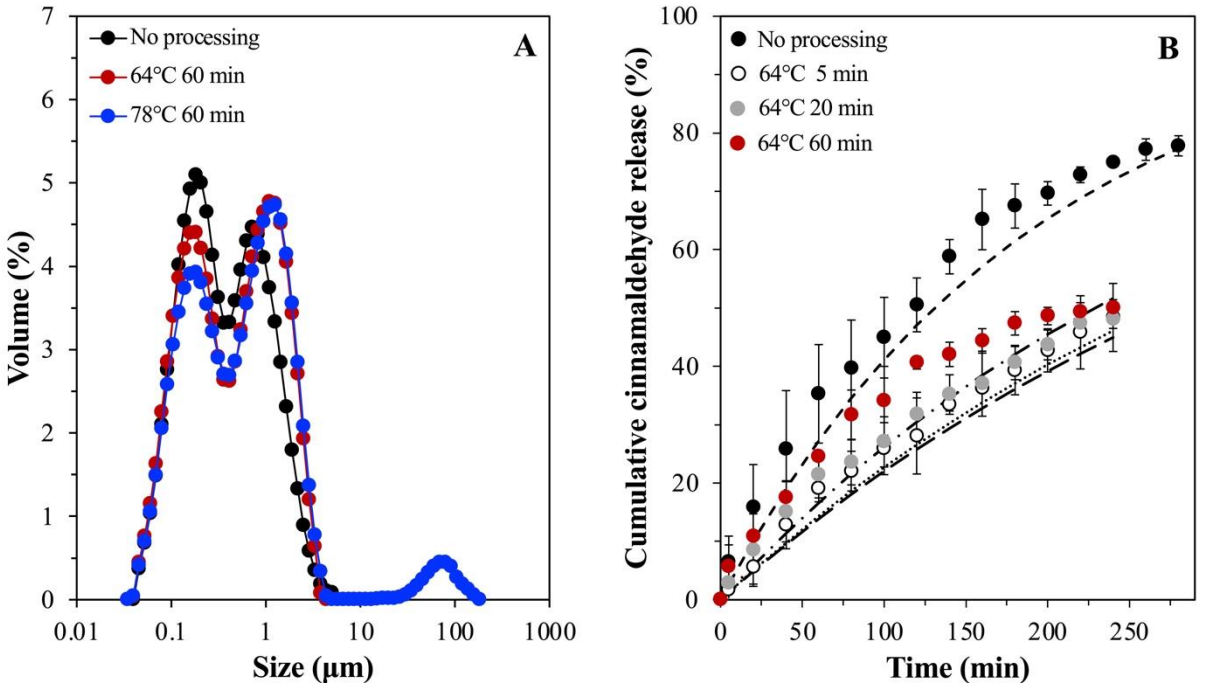

Fig. 6.10. Droplet size distribution of C888/T80 SLN-stabilised emulsions before and after thermal processing at 64 and 78°C for 60 min (A). *In vitro* release profile of cinnamaldehyde-loaded emulsions stabilised by C888/T80-SLNs after being subjected to thermal processing at 64°C for varying durations (B). The profile of the respective emulsion system prior-sintering is also presented for comparison purposes. The interfacial barrier-limited model fitting of cinnamaldehyde for each emulsion system is also presented (- - no processing, ···· 64°C 5 min, — 64°C 20 min, – · 64°C 60 min).

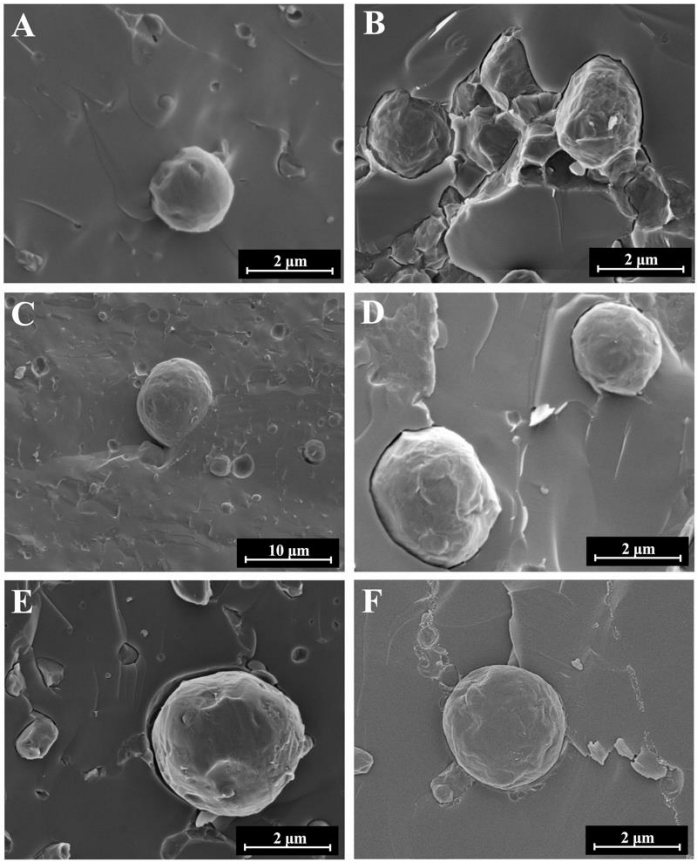

Fig. 6.11. Cryo-SEM micrographs of emulsions stabilised with: (A) Tween® 80, (B) C888/T80 SLN, (C) C888/T80 SLN after thermal treatment at 64°C for 60 min, (D) C888/T80 SLN after thermal treatment at 78°C for 60 min, (E) P5/T80 SLN and (F) C888/P188 SLN.

6.3.3 Co-release from lipid particle-stabilised emulsions

Having established the capability of both lipid particles and lipid particle-stabilised droplets to separately act as effective carriers and delivery systems of model hydrophobic actives, this part of the work is scrutinising whether these performances perpetuate when the lipid-particle stabilised emulsion is utilised as a co-delivery system. Previous work using lipid-particle stabilised emulsions as a co-delivery formulation has provided indications that this type of carrier platform can indeed facilitate the independent co-delivery of actives by separately measuring their release behaviour [22]. Herein, the co-release performance of cinnamaldehyde-

loaded emulsion droplets stabilised by curcumin-loaded C888/T80 SLNs, was assessed by simultaneously acquiring the release profiles of the two actives under the same experimental conditions (Fig. 6.12).

The co-release profiles for both curcumin (releasing from the C888/T80 SLNs) and cinnamaldehyde (discharging from the o/w droplets) showed no significant differences to the profiles that were individually acquired (Fig. 6.12A). As was previously recorded, the highest percentage of cinnamaldehyde releases over 280 min, while curcumin shows a relatively more sustained release rate with approximately 40% being released over the 7 day assessment. The D for CRM and k_1 constant for CA (130×10^{-20} cm^2 s^{-1} and 3.2×10^{-15} cm^2 s^{-1}, respectively) are in accordance with what was reported above for the singly measured release rates. Notably, the co-release behaviour was preserved after 1 month of emulsion storage, with no major disparities being observed in the profiles or release kinetics (D = 250×10^{-20} cm^2 s^{-1} and k_1 = 4.4×10^{-15} cm^2 s^{-1}) (Fig. 6.12B). The co-encapsulation of the two actives did not alter the ability of either compartment in the formulation (i.e. lipid particles and emulsion droplets) to act as an independent active carrier, with no significant differences in the EE and LC values compared to the single encapsulation formulations.

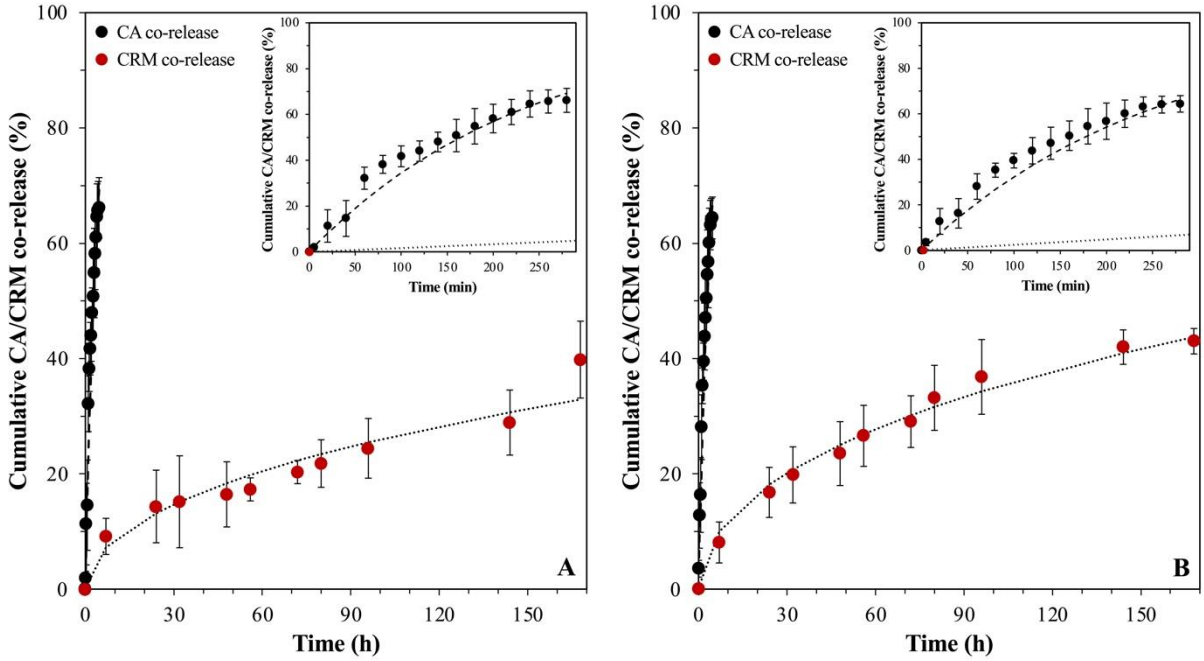

Fig. 6.12. *In vitro* co-release profiles of cinnamaldehyde-loaded emulsion droplets stabilised by curcumin-loaded C888/T80-SLNs measured immediately after preparation (A) and after 1 month of emulsion storage (B). Data are presented at longer (main graph) and shorter (inset graph) timescales to demonstrate differences in the release rates. The diffusion-driven release kinetic model fitting for all curcumin data (dotted lines) and the interfacial barrier-limited model fitting for all cinnamaldehyde curves (dashed lines) are also presented.

6.4 Conclusions

The present study demonstrated the potential of lipid particles to simultaneously regulate the co-release performance of an active encapsulated within the particles themselves, but also for a secondary active contained within the Pickering emulsion droplets. Extending previous work performed on the impact of formulation parameters, namely type of solid lipid and surfactant used, on the properties of SLNs and NLCs dispersions, the release behaviour was now assessed, whereby it is suggested that the release rate of the encapsulated active is predominantly governed by its relative location within the lipid matrix. Following confirmation of the

Pickering stabilisation capacity of the same particles, changes to their release control capability once within the emulsion setting were shown to be related to their formulation characteristics. The compatibility between the particles' solid lipid and emulsion oil and the presence of surfactant micelles were suggested to have an inverse effect on the particles' ability to maintain control over the active discharge. Correspondingly, their influence was perpetuated to the level of release regulation that the particles provide while at the droplet interface to an active encapsulated within the emulsion droplets. Regardless of their composition all particles exhibited improved control compared to surfactant decorated interfaces, although the surfactant properties had a significant effect on the release rate. Attempting to manipulate the permeability of the interfacial layer, a thermal post-fabrication approach was adopted to demonstrate that interfacial sintering of the particles and hence creation of a less permeable layer can impede the droplet release even further. Lastly, it was corroborated that the concurrent co-release for the two model hydrophobic actives was in line with their singly assessed performance. Overall, the results presented here underline the aptitude of the developed Pickering emulsion as a promising system for the compartmentalised co-encapsulation and independently controlled co-delivery of incorporated actives, owing to its tuneable lipid particle-decorated interface. Future work using this system could explore mechanisms to trigger co-release and investigate its response under more biologically-relevant conditions, e.g. gastric pH, presence of bile salts and/or enzymes.

References

[1] N. Kolishetti, S. Dhar, P.M. Valencia, L.Q. Lin, R. Karnik, S.J. Lippard, R. Langer, O.C. Farokhzad, Engineering of self-assembled nanoparticle platform for precisely controlled combination drug therapy, Proc Natl Acad Sci U S A. 107 (2010) 17939–17944. https://doi.org/10.1073/pnas.1011368107.

[2] J. Meng, F. Guo, H. Xu, W. Liang, C. Wang, X. Da Yang, Combination Therapy using Co-encapsulated Resveratrol and Paclitaxel in Liposomes for Drug Resistance Reversal in Breast Cancer Cells in vivo, Scientific Reports 2016 6:1. 6 (2016) 1–11. https://doi.org/10.1038/srep22390.

[3] M.R. Kim, T. Feng, Q. Zhang, H.Y.E. Chan, Y. Chau, Co-Encapsulation and Co-Delivery of Peptide Drugs via Polymeric Nanoparticles, Polymers (Basel). 11 (2019). https://doi.org/10.3390/polym11020288.

[4] S.M. Motevalli, A.S. Eltahan, L. Liu, A. Magrini, N. Rosato, W. Guo, M. Bottini, X.-J. Liang, Co-encapsulation of curcumin and doxorubicin in albumin nanoparticles blocks the adaptive treatment tolerance of cancer cells, Biophysics Reports 2019 5:1. 5 (2019) 19–30. https://doi.org/10.1007/s41048-018-0079-6.

[5] J. Cui, C. Sun, A. Wang, Y. Wang, H. Zhu, Y. Shen, N. Li, X. Zhao, B. Cui, C. Wang, F. Gao, Z. Zeng, H. Cui, Dual-Functionalized Pesticide Nanocapsule Delivery System with Improved Spreading Behavior and Enhanced Bioactivity, Nanomaterials 2020, Vol. 10, Page 220. 10 (2020) 220. https://doi.org/10.3390/nano10020220.

[6] F. Graily Moradi, M.J. Hejazi, H. Hamishehkar, A.A. Enayati, Co-encapsulation of imidacloprid and lambda-cyhalothrin using biocompatible nanocarriers: Characterization and application, Ecotoxicol Environ Saf. 175 (2019) 155–163. https://doi.org/10.1016/j.ecoenv.2019.02.092.

[7] F. Han, D. Luo, W. Qu, D. Chen, Y. Hong, J. Sheng, X. Yang, W. Liu, Nanoliposomes codelivering bioactive peptides produce enhanced anti-aging effect in human skin, J Drug Deliv Sci Technol. 57 (2020) 101693. https://doi.org/10.1016/j.jddst.2020.101693.

[8] Y. Wei, S. Yang, L. Zhang, L. Dai, K. Tai, J. Liu, L. Mao, F. Yuan, Y. Gao, A. Mackie, Fabrication, characterization and in vitro digestion of food grade complex nanoparticles for co-delivery of resveratrol and coenzyme Q10, Food Hydrocoll. 105 (2020) 105791. https://doi.org/10.1016/j.foodhyd.2020.105791.

[9] P.J. Chawda, J. Shi, S. Xue, S. Young Quek, Co-encapsulation of bioactives for food applications, Food Quality and Safety. 1 (2017) 302–309. https://doi.org/10.1093/fqsafe/fyx028.

[10] L. Tavano, R. Muzzalupo, N. Picci, B. de Cindio, Co-encapsulation of antioxidants into niosomal carriers: Gastrointestinal release studies for nutraceutical applications, Colloids Surf B Biointerfaces. 114 (2014) 82–88. https://doi.org/10.1016/j.colsurfb.2013.09.058.

[11] J. Liu, D. Chi, S. Pan, L. Zhao, X. Wang, D. Wang, Y. Wang, Effective co-encapsulation of doxorubicin and irinotecan for synergistic therapy using liposomes prepared with triethylammonium sucrose octasulfate as drug trapping agent, Int J Pharm. 557 (2019) 264–272. https://doi.org/10.1016/j.ijpharm.2018.12.072.

[12] H.G. Lee, Y.S. Park, J.H. Jeong, Y. Bin Kwon, D.H. Shin, J.Y. Kim, Y.S. Rhee, E.S. Park, D.W. Kim, C.W. Park, Physicochemical properties and drug-release mechanisms of dual-release bilayer tablet containing mirabegron and fesoterodine fumarate, Drug Des Devel Ther. 13 (2019) 2459. https://doi.org/10.2147/dddt.s212520.

[13] J. Wang, H. Hao, J.H. Cai, Amphiphilic Drug Delivery Microcapsules via Layer-by-Layer Self-Assembly, Https://Doi.Org/10.1080/00222348.2019.1593640. 58 (2019) 535–550. https://doi.org/10.1080/00222348.2019.1593640.

[14] A. Awad, F. Fina, S.J. Trenfield, P. Patel, A. Goyanes, S. Gaisford, A.W. Basit, 3D Printed Pellets (Miniprintlets): A Novel, Multi-Drug, Controlled Release Platform Technology, Pharmaceutics. 11 (2019). https://doi.org/10.3390/pharmaceutics11040148.

[15] N.A. Helal, H.A. Eassa, A.M. Amer, M.A. Eltokhy, I. Edafiogho, M.I. Nounou, Nutraceuticals' Novel Formulations: The Good, the Bad, the Unknown and Patents Involved, Recent Pat Drug Deliv Formul. 13 (2019) 105–156. https://doi.org/10.2174/1872211313666190503112040.

[16] J. Čejková, F. Štěpánek, Compartmentalized and Internally Structured Particles for Drug Delivery - A Review, Curr Pharm Des. 19 (2013) 6298–6314. https://doi.org/10.2174/1381612811319350007.

[17] N. Li, L. Zhao, L. Qi, Z. Li, Y. Luan, Polymer assembly: Promising carriers as co-delivery systems for cancer therapy, Prog Polym Sci. 58 (2016) 1–26. https://doi.org/10.1016/j.progpolymsci.2015.10.009.

[18] Y. Sun, W. Tang, C. Pu, R. Li, Q. Sun, H. Wang, Improved stability of liposome-stabilized emulsions as a co-encapsulation delivery system for vitamin B2, vitamin E and β-carotene, Food Funct. 13 (2022) 2966–2984. https://doi.org/10.1039/d1fo03617c.

[19] H. Chen, H. Dai, H. Zhu, L. Ma, Y. Fu, X. Feng, Y. Sun, Y. Zhang, Construction of dual-compartmental micro-droplet via shrimp ferritin nanocages stabilized Pickering emulsions for co-encapsulation of hydrophobic/hydrophilic bioactive compounds, Food Hydrocoll. 126 (2022) 107443. https://doi.org/10.1016/j.foodhyd.2021.107443.

[20] F. Spyropoulos, D. Kurukji, P. Taylor, I.T. Norton, Fabrication and Utilization of Bifunctional Protein/Polysaccharide Coprecipitates for the Independent Codelivery of Two Model Actives from Simple Oil-in-Water Emulsions, Langmuir. 34 (2018) 3934–3948. https://doi.org/10.1021/acs.langmuir.7b04315.

[21] L. Han, K. Lu, S. Zhou, S. Zhang, F. Xie, B. Qi, Y. Li, Development of an oil-in-water emulsion stabilized by a black bean protein-based nanocomplex for co-delivery of quercetin and perilla oil, LWT. 138 (2021) 110644. https://doi.org/10.1016/j.lwt.2020.110644.

[22] G.I. Sakellari, I. Zafeiri, A. Pawlik, D. Kurukji, P. Taylor, I.T. Norton, F. Spyropoulos, Independent co-delivery of model actives with different degrees of hydrophilicity from oil-in-water and water-in-oil emulsions stabilised by solid lipid particles via a Pickering mechanism: a-proof-of-principle study, J Colloid Interface Sci. 587 (2021) 644–649. https://doi.org/10.1016/j.jcis.2020.11.021.

[23] D.A. Garrec, S. Frasch-Melnik, J.V.L. Henry, F. Spyropoulos, I.T. Norton, Designing colloidal structures for micro and macro nutrient content and release in foods, Faraday Discuss. 158 (2012) 37–49. https://doi.org/10.1039/c2fd20024d.

[24] S. Frasch-Melnik, I.T. Norton, F. Spyropoulos, Fat-crystal stabilised w/o emulsions for controlled salt release, J Food Eng. 98 (2010) 437–442. https://doi.org/10.1016/j.jfoodeng.2010.01.025.

[25] G.I. Sakellari, I. Zafeiri, H. Batchelor, F. Spyropoulos, Solid lipid nanoparticles and nanostructured lipid carriers of dual functionality at emulsion interfaces. Part I: Pickering stabilisation functionality, Colloids Surf A Physicochem Eng Asp. (2022) 130135. https://doi.org/10.1016/j.colsurfa.2022.130135.

[26] G.I. Sakellari, I. Zafeiri, H. Batchelor, F. Spyropoulos, Solid lipid nanoparticles and nanostructured lipid carriers of dual functionality at emulsion interfaces. Part II: active carrying/delivery functionality, Colloids Surf A Physicochem Eng Asp. 659 (2023) 130787. https://doi.org/10.1016/j.colsurfa.2022.130787.

[27] G.I. Sakellari, I. Zafeiri, H. Batchelor, F. Spyropoulos, Formulation design, production and characterisation of solid lipid nanoparticles (SLN) and nanostructured lipid carriers (NLC) for the encapsulation of a model hydrophobic active, Food Hydrocolloids for Health. (2021) 100024. https://doi.org/10.1016/j.fhfh.2021.100024.

[28] J. Crank, The Mathematics of Diffusion, 2nd Edition, Oxford University Press, London, 1975.

[29] C. Washington, K. Evans, Release rate measurements of model hydrophobic solutes from submicron triglyceride emulsions, Journal of Controlled Release. 33 (1995) 383–390. https://doi.org/10.1016/0168-3659(94)00110-g.

[30] R.H. Guy, J. Hadgraft, I.W. Kellaway, M. Taylor, Calculations of drug release rates from particles, Int J Pharm. 11 (1982) 199–207. https://doi.org/10.1016/0378-5173(82)90038-2.

[31] D. Kurukji, I. Norton, F. Spyropoulos, Fabrication of sub-micron protein-chitosan electrostatic complexes for encapsulation and pH-Modulated delivery of model hydrophilic active compounds, Food Hydrocoll. 53 (2016) 249–260. https://doi.org/10.1016/j.foodhyd.2015.02.021.

[32] F. Spyropoulos, C. Clarke, D. Kurukji, I.T. Norton, P. Taylor, Emulsifiers of Pickering-like characteristics at fluid interfaces: Impact on oil-in-water emulsion stability and interfacial transfer rate kinetics for the release of a hydrophobic model active, Colloids Surf A Physicochem Eng Asp. 607 (2020) 125413. https://doi.org/10.1016/j.colsurfa.2020.125413.

[33] K. Jores, W. Mehnert, M. Drechsler, H. Bunjes, C. Johann, K. Mäder, Investigations on the structure of solid lipid nanoparticles (SLN) and oil-loaded solid lipid nanoparticles by photon correlation spectroscopy, field-flow fractionation and transmission electron microscopy, Journal of Controlled Release. 95 (2004) 217–227. https://doi.org/10.1016/j.jconrel.2003.11.012.

[34] N. Kishore, U.M. Dhanalekshmi, M.D. Raja, S. Bhavani, P.N. Reddy, Design and In Vitro Evaluation of Solid-Lipid Nanoparticle Drug Delivery for Aceclofenac, Journal of Dispersion Science and Technology. 33 (2011) 96–102. https://doi.org/10.1080/01932691.2010.534293.

[35] A. Gordillo-Galeano, A. Ponce, C.E. Mora-Huertas, In vitro release behavior of SLN, NLC, and NE: An explanation based on the particle structure and carried molecule location, J Drug Deliv Sci Technol. 76 (2022) 103768. https://doi.org/10.1016/j.jddst.2022.103768.

[36] K. Jores, W. Mehnert, K. Mäder, Physicochemical investigations on solid lipid nanoparticles and on oil-loaded solid lipid nanoparticles: A nuclear magnetic resonance and electron spin resonance study, Pharm Res. 20 (2003) 1274–1283. https://doi.org/10.1023/a:1025065418309.

[37] V. Jenning, A.F. Thünemann, S.H. Gohla, Characterisation of a novel solid lipid nanoparticle carrier system based on binary mixtures of liquid and solid lipids, Int J Pharm. 199 (2000) 167–177. https://doi.org/10.1016/s0378-5173(00)00378-1.

[38] K. Jores, A. Haberland, S. Wartewig, K. Mäder, W. Mehnert, Solid lipid nanoparticles (SLN) and oil-loaded SLN studied by spectrofluorometry and Raman spectroscopy, Pharm Res. 22 (2005) 1887–1897. https://doi.org/10.1007/s11095-005-7148-5.

[39] J.B. Brubach, V. Jannin, B. Mahler, C. Bourgaux, P. Lessieur, P. Roy, M. Ollivon, Structural and thermal characterization of glyceryl behenate by X-ray diffraction coupled to differential calorimetry and infrared spectroscopy, Int J Pharm. 336 (2007) 248–256. https://doi.org/10.1016/j.ijpharm.2006.11.057.

[40] E.B. Souto, W. Mehnert, R.H. Müller, Polymorphic behaviour of Compritol®888 ATO as bulk lipid and as SLN and NLC, J Microencapsul. 23 (2006) 417–433. https://doi.org/10.1080/02652040600612439.

[41] S. Bertoni, N. Passerini, B. Albertini, Liquid lipids act as polymorphic modifiers of tristearin-based formulations produced by melting technologies, Pharmaceutics. 13 (2021) 1089. https://doi.org/10.3390/pharmaceutics13071089/S1.

[42] J. Macridachis-González, L. Bayés-García, T. Calvet, An Insight into the Solid-State Miscibility of Triacylglycerol Crystals, Molecules 2020, Vol. 25, Page 4562. 25 (2020) 4562. https://doi.org/10.3390/molecules25194562.

[43] S. Anantachaisilp, S.M. Smith, A. Treetong, S. Pratontep, S. Puttipipatkhachorn, U.R. Ruktanonchai, Chemical and structural investigation of lipid nanoparticles: drug–lipid interaction and molecular distribution, Nanotechnology. 21 (2010) 125102. https://doi.org/10.1088/0957-4484/21/12/125102.

[44] M. Shah, Y.K. Agrawal, K. Garala, A. Ramkishan, Solid lipid nanoparticles of a water soluble drug, ciprofloxacin hydrochloride, Indian J Pharm Sci. 74 (2012) 434–442. https://doi.org/10.4103/0250-474x.108419.

[45] W. Tiyaboonchai, W. Tungpradit, P. Plianbangchang, Formulation and characterization of curcuminoids loaded solid lipid nanoparticles, Int J Pharm. 337 (2007) 299–306. https://doi.org/10.1016/j.ijpharm.2006.12.043.

[46] N. Badawi, K. El-Say, D. Attia, M. El-Nabarawi, M. Elmazar, M. Teaima, Development of Pomegranate Extract-Loaded Solid Lipid Nanoparticles: Quality by Design Approach to Screen the Variables Affecting the Quality Attributes and Characterization, ACS Omega. 5 (2020) 21712–21721. https://doi.org/10.1021/acsomega.0C02618.

[47] E. Ugazio, R. Cavalli, M.R. Gasco, Incorporation of cyclosporin A in solid lipid nanoparticles (SLN), Int J Pharm. 241 (2002) 341–344. https://doi.org/10.1016/s0378-5173(02)00268-5.

[48] V. Venkateswarlu, K. Manjunath, Preparation, characterization and in vitro release kinetics of clozapine solid lipid nanoparticles, Journal of Controlled Release. 95 (2004) 627–638. https://doi.org/10.1016/j.jconrel.2004.01.005.

[49] Y.F. Luo, D.W. Chen, L.X. Ren, X.L. Zhao, J. Qin, Solid lipid nanoparticles for enhancing vinpocetine's oral bioavailability, Journal of Controlled Release. 114 (2006) 53–59. https://doi.org/10.1016/j.jconrel.2006.05.010.

[50] L. Hu, X. Tang, C. Correspondence, : X Tang, F. Cui, Solid lipid nanoparticles (SLNs) to improve oral bioavailability of poorly soluble drugs, Journal of Pharmacy and Pharmacology. 56 (2004) 1527–1535. https://doi.org/10.1211/0022357044959.

[51] H. Bunjes, Lipid nanoparticles for the delivery of poorly water-soluble drugs, Journal of Pharmacy and Pharmacology. 62 (2010) 1637–1645. https://doi.org/10.1111/j.2042-7158.2010.01024.x.

[52] H. Salminen, C. Gömmel, B.H. Leuenberger, J. Weiss, Influence of encapsulated functional lipids on crystal structure and chemical stability in solid lipid nanoparticles: Towards bioactive-based design of delivery systems, Food Chem. 190 (2016) 928–937. https://doi.org/10.1016/j.foodchem.2015.06.054.

[53] A. Noack, G. Hause, K. Mäder, Physicochemical characterization of curcuminoid-loaded solid lipid nanoparticles, Int J Pharm. 423 (2012) 440–451. https://doi.org/10.1016/j.ijpharm.2011.12.011.

[54] H. Salminen, T. Helgason, S. Aulbach, B. Kristinsson, K. Kristbergsson, J. Weiss, Influence of co-surfactants on crystallization and stability of solid lipid nanoparticles, J Colloid Interface Sci. 426 (2014) 256–263. https://doi.org/10.1016/j.jcis.2014.04.009.

[55] K. Shahani, J. Panyam, Highly loaded, sustained-release microparticles of curcumin for chemoprevention, J Pharm Sci. 100 (2011) 2599–2609. https://doi.org/10.1002/jps.22475.

[56] W. Zhao, M. Zeng, K. Li, C. Pi, Z. Liu, C. Zhan, J. Yuan, Z. Su, Y. Wei, J. Wen, F. Pi, X. Song, R.J. Lee, Y. Wei, L. Zhao, Solid lipid nanoparticle as an effective drug delivery system of a novel curcumin derivative: formulation, release in vitro and pharmacokinetics in vivo, Pharmaceutical Biology. 60 (2022) 2300–2307. https://doi.org/10.1080/13880209.2022.2136205.

[57] A. zur Mühlen, C. Schwarz, W. Mehnert, Solid lipid nanoparticles (SLN) for controlled drug delivery - Drug release and release mechanism, European Journal of Pharmaceutics and Biopharmaceutics. 45 (1998) 149–155. https://doi.org/10.1016/s0939-6411(97)00150-1.

[58] K.M. Rosenblatt, H. Bunjes, Poly(vinyl alcohol) as emulsifier stabilizes solid triglyceride drug carrier nanoparticles in theα-modification, Mol Pharm. 6 (2009) 105–120. https://doi.org/10.1021/mp8000759.

[59] I. Zafeiri, J.E. Norton, P. Smith, I.T. Norton, F. Spyropoulos, The role of surface active species in the fabrication and functionality of edible solid lipid particles, J Colloid Interface Sci. 500 (2017) 228–240. https://doi.org/10.1016/j.jcis.2017.03.085.

[60] I. Zafeiri, P. Smith, I.T. Norton, F. Spyropoulos, Fabrication, characterisation and stability of oil-in-water emulsions stabilised by solid lipid particles: The role of particle characteristics and emulsion microstructure upon Pickering functionality, Food Funct. 8 (2017) 2583–2591. https://doi.org/10.1039/c7fo00559h.

[61] M. Samtlebe, U. Yucel, J. Weiss, J.N. Coupland, Stability of Solid Lipid Nanoparticles in the Presence of Liquid Oil Emulsions, J Am Oil Chem Soc. 89 (2012) 609–617. https://doi.org/10.1007/s11746-011-1944-3.

[62] G.S. Jamieson, W.F. Baughman, The chemical composition of sunflower-seed oil, J Am Chem Soc. 44 (1922) 2952–2957. https://doi.org/10.1021/ja01433a036.

[63] J. Weiss, D.J. McClements, Mass Transport Phenomena in Oil-in-Water Emulsions Containing Surfactant Micelles: Solubilization, Langmuir. 16 (2000) 5879–5883. https://doi.org/10.1021/la9914763.

[64] D.J. McClements, S.R. Dungan, J.B. German, J.E. Kinsella, Factors which affect oil exchange between oil-in-water emulsion droplets stabilized by whey protein isolate: Protein concentration, droplet size and ethanol, Colloids Surf A Physicochem Eng Asp. 81 (1993) 203–210. https://doi.org/10.1016/0927-7757(93)80247-c.

[65] D.J. McClements, S.R. Dungan, J.B. German, J.E. Kinsella, Evidence of oil exchange between oil-in-water emulsion droplets stabilized by milk proteins, J Colloid Interface Sci. 156 (1993) 425–429. https://doi.org/10.1006/jcis.1993.1133.

[66] D.J. McClements, S.R. Dungan, Factors that affect the rate of oil exchange between oil-in-water emulsion droplets stabilized by a nonionic surfactant: droplet size, surfactant concentration, and ionic strength, Journal of Physical Chemistry. 97 (2002) 7304–7308. https://doi.org/10.1021/j100130A030.

[67] P. Alexandridis, J.F. Holzwarth, T.A. Hatton, Micellization of Poly(ethylene oxide)-Poly(propylene oxide)-Poly(ethylene oxide) Triblock Copolymers in Aqueous Solutions: Thermodynamics of Copolymer Association, Macromolecules. 27 (1994) 2414–2425. https://doi.org/10.1021/ma00087A009.

[68] E. Dickinson, Food emulsions and foams: Stabilization by particles, Curr Opin Colloid Interface Sci. 15 (2010) 40–49. https://doi.org/10.1016/j.cocis.2009.11.001.

[69] S. Simovic, C.A. Prestidge, Nanoparticle layers controlling drug release from emulsions, European Journal of Pharmaceutics and Biopharmaceutics. 67 (2007) 39–47. https://doi.org/10.1016/j.elpbJ.2007.01.011.

[70] J. Frelichowska, M.A. Bolzinger, J.P. Valour, H. Mouaziz, J. Pelletier, Y. Chevalier, Pickering w/o emulsions: Drug release and topical delivery, Int J Pharm. 368 (2009) 7–15. https://doi.org/10.1016/j.ijpharm.2008.09.057.

[71] J. Frelichowska, M.A. Bolzinger, J. Pelletier, J.P. Valour, Y. Chevalier, Topical delivery of lipophilic drugs from o/w Pickering emulsions, Int J Pharm. 371 (2009) 56–63. https://doi.org/10.1016/j.ijpharm.2008.12.017.

[72] C.A. Prestidge, S. Simovic, Nanoparticle encapsulation of emulsion droplets, Int J Pharm. 324 (2006) 92–100. https://doi.org/10.1016/j.ijpharm.2006.06.044.

[73] C. Freitas, R.H. Müller, Effect of light and temperature on zeta potential and physical stability in solid lipid nanoparticle (SLN®) dispersions, Int J Pharm. 168 (1998) 221–229. https://doi.org/10.1016/s0378-5173(98)00092-1.

[74] O.S. Deshmukh, D. Van Den Ende, M.C. Stuart, F. Mugele, M.H.G. Duits, Hard and soft colloids at fluid interfaces: Adsorption, interactions, assembly & rheology, Adv Colloid Interface Sci. 222 (2015) 215–227. https://doi.org/10.1016/j.jcis.2014.09.003.

[75] Y. Ming, Y. Xia, G. Ma, C. Yufei Xia, Aggregating particles on the O/W interface: Tuning Pickering emulsion for the enhanced drug delivery systems, Aggregate. 3 (2022) e162. https://doi.org/10.1002/agt2.162.

[76] D. Johansson, B. Bergenståhl, Sintering of fat crystal networks in oil during post-crystallization processes, J Am Oil Chem Soc. 72 (1995) 911–920. https://doi.org/10.1007/bf02542069.

[77] H.N. Yow, A.F. Routh, Release profiles of encapsulated actives from colloidosomes sintered for various durations, Langmuir. 25 (2009) 159–166. https://doi.org/10.1021/la802711y.

[78] A.D. Dinsmore, M.F. Hsu, M.G. Nikolaides, M. Marquez, A.R. Bausch, D.A. Weitz, Colloidosomes: Selectively permeable capsules composed of colloidal particles, Science (1979). 298 (2002) 1006–1009. https://doi.org/10.1126/science.1074868.

[79] R. Pichot, F. Spyropoulos, I.T. Norton, O/W emulsions stabilised by both low molecular weight surfactants and colloidal particles: The effect of surfactant type and concentration, J Colloid Interface Sci. 352 (2010) 128–135. https://doi.org/10.1016/j.jcis.2010.08.021.

[80] D. Yin, L. Bai, Y. Jia, J. Liu, Q. Zhang, Microencapsulation through thermally sintering Pickering emulsion-based colloidosomes, Soft Matter. 13 (2017) 3720–3725. https://doi.org/10.1039/c7sm00528h.

[81] M. Rao, A. Ranpise, S. Borate, K. Thanki, Mechanistic Evaluation of the Effect of Sintering on Compritol® 888 ATO Matrices, AAPS PharmSciTech 2009 10:2. 10 (2009) 355–360. https://doi.org/10.1208/s12249-009-9211-8.

Chapter 7

Conclusions and Future work

7.1 Conclusions

The work conducted in this thesis considered the design and development of a novel emulsion-based liquid structuring strategy that can enable the segregated co-encapsulation and independent co-delivery of two active ingredients. As discussed throughout this thesis, this research area is still at its infancy, with currently available formulations having yet to overcome shortcomings related to their inability to achieve simultaneous and concurrently individual delivery of each of the encapsulated species, and their microstructural performance having not been fully elucidated. This work addressed these challenges by adopting a Pickering emulsion microstructural approach, with lipid particles comprising the stabilising agents.

In the following sections, the main conclusions deduced from this work are summarised.

7.1.1 Lipid particles as active carriers and delivery systems

A big portion of this study was dedicated to the design and characterisation of solid lipid nanoparticles and nanostructured lipid carriers, specifically in regard to the effect of certain formulation compositional parameters on their crystalline structure properties and subsequent active carrying and release functionalities. Understanding the degree to which these formulation aspects influence said performances, without compromising attributes that enable their Pickering functionality, could ultimately lead to a tool for tuning the particles' behaviour not only within a colloidal dispersion, but also within an emulsion environment.

Solid lipid nanoparticles and nanostructured lipid carrier were fabricated using building materials that were selected following theoretical and experimental screening to identify components that would provide the highest solubilisation capacity for curcumin, which was the

chosen model hydrophobic active. It was found that high encapsulation efficiency and loading capacity values were achieved and maintained during storage (up to 7 months for certain samples), by keeping the amount of active used close to the solubilisation threshold of the selected lipids, as was corroborated by thermal analysis of the bulk lipids and their mixtures. Particles prepared with different combinations of solid/liquid lipids and surface active species in terms of their type and percentage, were shown to be in the nanometer size range, that was confined as a physical marker indicative of Pickering functionality, and were characterised by negative surface charge.

Assessment of the liquid lipid addition impact on the SLNs structural characteristics indicated that there was a liquid lipid concentration-dependent effect, with smaller particle sizes obtained at increased liquid lipid mass ratios (>20% w/w of the total lipid phase), enhanced polymorphic transitions and increased loss of crystallinity. Incorporation of curcumin within the particles led to size enlargement and imparted an effect on their thermal behaviour that was primarily dictated by the level of influence caused by the solid-to-liquid lipid ratio used. Substitution of Tween® 80 with a more hydrophilic, larger molecular size surfactant (Poloxamer 188) highlighted the effect of the compatibility between the lipid components and the surfactant used, for both SLNs and NLCs. Higher crystalline participation of the former resulted in greater lowering of the particles' crystallinity, though smaller sizes were achieved with the latter owing to the thicker interfacial particle layer offering enhanced protection against coalescence during the particle formation stage.

Regarding the lipid particles' behaviour as release regulators for curcumin, both SLNs and NLCs demonstrated overall sustained release rates that remained below 50% over the span of 7 days, irrespectively of the matrix composition. Results from the release assessment further

underlined the potential of attaining varying release profiles, by formulation aspects alteration. It was suggested that the rate of curcumin diffusion is governed by its relative localisation within the lipid matrix, which in turn is controlled by the arrangement of the matrix constituents and their ability to create favourable conditions for the active. More specifically, the presence of the active near the particles' surface in SLNs fabricated with Tween® 80 prompted faster discharge rates compared to the respective NLCs, where the active is better contained/distributed within the lipid matrix. In these structures, the liquid hydrophobic environment bestowed by the presence of the liquid lipid near the particles' surface, together with the higher surfactant participation in the same regions, creates a more fitting environment for the active. These results were consistent for particles fabricated with both a high (Compritol® 888 ATO) and a low (Precirol® ATO 5) melting point solid lipid, underlying the significant contribution of the type of surface active species used. Conversely, weaker curcumin retention and faster release for both SLNs and NLCs was observed when Poloxamer 188, a more hydrophilic and bulkier surfactant was utilised, that could not provide an as-tightly-packed interfacial arrangement, along with a more limited crystalline network compatibility.

7.1.2 Lipid particles as species of dual functionality

The potential of curcumin-loaded lipid particles to concurrently exhibit the dual functionality of acting as Pickering emulsion stabilisers and as active carrier/delivery systems was explored by forming o/w emulsions in their presence. This objective was dissected into two parts; these were designed to initially elucidate the impact of certain formulation parameters on the Pickering stabilisation aptitude of the lipid particles, and consequently verify that the lipid nanostructures could retain their previously defined properties, particularly their active carrying/release regulation ability while at the droplet interface. The particles utilised

throughout this assessment were fabricated with the high melting point lipid Compritol® 888 ATO, Miglyol® 812 as the liquid lipid and Tween® 80 as the surfactant.

For the Pickering stabilisation capacity evaluation, blank lipid particles used as produced but also following dialysis to remove any unadsorbed surfactant were employed. According to experimental surface/interfacial tension measurements and theoretical approximations relevant to the amount of excess surfactant remnant from the fabrication step of the lipid particle dispersions, it was shown that NLCs were generally able to entrap a higher proportion of the available surfactant. This was attributed to both their smaller particle sizes and hence larger surface area available compared to SLNs, and their less ordered crystalline network, allowing for superior trapping of surfactant molecules. Assessment of the physicochemical characteristics of the lipid particles post-removal of excess surface active species revealed small changes in their particle size and surface charge, though no differences were observed in their crystallinity. Interfacial tension and wettability measurements suggested that both types of particles, irrespective of their solid-to-liquid lipid mass ratio and surfactant decoration could effectively stabilise o/w emulsion droplets, albeit particles with higher liquid lipid content were characterised by relatively higher hydrophilicity. That was indeed confirmed following emulsion droplet formation, where regardless of the presence or absence of remnant surfactant in the aqueous carrier phase, both SLNs and NLCs exhibited close association with the emulsion interface, as was also confirmed by microscopy observations. Despite the larger droplet sizes obtained when dialysed lipid particles were utilised, all particle-stabilised emulsions showed no loss of emulsion integrity over a storage period of 12 weeks.

The lipid particles' fate within the emulsion setting was investigated both in terms of their physical stability and the degree of their interfacial presence. According to thermal behaviour

analysis and calculation of the ratio between the melting enthalpy of the particles within emulsions and within dispersions, it was suggested that the extent of dissolution phenomena (i.e. loss of particles) is directly impacted by the hydrophilicity of the particles and presence of excess surfactant in the continuous phase. Despite that, both SLNs and NLCs appeared to preserve the greatest fraction of their crystalline matter. To estimate the ratio between interfacially adsorbed and unadsorbed particles, a methodology was adopted, whereby the melting profiles of the particles within the emulsion systems were deconvoluted into two peaks corresponding to each of the two possibilities; particles in the continuous phase and particles at the interface. In correspondence to data reported earlier, the effect of the lipid particles' characteristics (i.e. size, surface charge, morphology) was inferred as a dictating factor when it comes to the particles' interfacial occupancy; although no changes were observed over a storage period of 12 weeks.

Encapsulation of curcumin within SLNs and NLCs did not compromise the interfacial properties and Pickering stabilisation capacity of either lipid particles. Regarding the curcumin discharge regulation ability of the particles while in an emulsion setting, it was proposed that the release profiles are the combination of the release from particles remaining free in the continuous phase and interfacially adsorbed particles. Although an increase in the discharge rate was observed compared to that of particles in an aqueous dispersion (this was ascribed to the creation of a change-inducing potential due to oil addition), the particles release regulation ability was shown to persist within the emulsions. This potential was further intensified in the stripped-from-excess-surfactant particles, assigned to the additional processing stage of dialysis. Lastly, perpetuation of the particles release performance was demonstrated even after prolonged storage of both the particle dispersions prior to emulsification, and newly formed particle-stabilised emulsion systems.

7.1.3 Lipid particles as interfacial entities

Particles formulated with varying solid lipid and surfactant types, that were previously evaluated for their curcumin discharge regulation within dispersions, were used to form o/w emulsions and the microstructural properties of the formed systems were studied. This assessment aimed to provide further insight on the degree to which certain formulation elements affect the dual role and functionality of the lipid particles, as Pickering stabilisers and active carriers/release regulators, prior to the utilisation of the lipid particle-stabilised emulsion as a co-encapsulation/co-delivery system.

According to interfacial tension, droplet size distribution and loss of crystalline matter measurements, both formulation elements were suggested to impact the performance of the particles at the droplets' interface, alongside the structural characteristics of the obtained emulsions. The characteristics of the solid lipid employed were shown to prompt deviations to the packing arrangement of the surfactant molecules at the particles' interface, as well as varying extent of crystalline matter losses. Similarly, the type of surfactant used with respect to its hydrophilicity, molecular size and concentration was also revealed to contribute to such incidents. Notably, SLNs and NLCs prepared with Precirol® ATO 5 instead of Compritol® 888 ATO as the solid lipid, exhibited a greater loss of crystalline matter that was attributed to enhanced dissolution phenomena, arising from the closer chemical composition between the former crystalline matrix lipid and the oil of the emulsion droplets. On the contrary, such losses were negligible for particles fabricated in the presence of Poloxamer 188, that was ascribed to the absence of any micellar content, to facilitate mass transfer between droplets and particles. Although, droplets of one order of magnitude larger were attained compared to particles prepared with Tween® 80 owing to the larger molecular size of Poloxamer 188 molecules.

These attributes further proffered their effect on the particles release performance while at the droplets' interface, with increased solid matter losses and presence of surfactant micelles accelerating the release rate compared to that of particles within dispersions.

7.1.3.1 Release regulation through the interfacial architecture

The role of the interfacial architecture provided by the presence of the particles at the droplets' interface as a barrier hindering the release of an additional hydrophobic active (cinnamaldehyde) encapsulated within the oil droplets was also scrutinised. Compared to a simple emulsion, stabilised by either surfactant used in the particle preparation, both SLNs and NLCs were able to halt the discharge of the encapsulated active, though no further increase was observed in the encapsulation efficiency/loading capacity. The particles' characteristics were again shown to affect the permeability of the formed interfacial barrier and hence the release rate, with particles formed with Poloxamer 188 resulting in a more sustained rate, that was attributed to the surfactant properties. Efforts to manipulate the permeability of the interfacial layer through sintering of the particles at the interface, revealed that a level of release impediment could be additionally provided following thermal post-fabrication processing. However, the temperature that the sintering is carried out, as well as the duration of the sintering step were indicated to impact the emulsion stability.

7.1.4 Lipid particle-stabilised emulsions as co-encapsulation/co-delivery microstructures

Having examined the interfacial characteristics of lipid particles fabricated with varying formulation parameters, the co-encapsulation and co-release capacity of the developed

Pickering system was explored, utilising one of the previously studied formulations. Concurrent encapsulation of cinnamaldehyde within the emulsion droplets and curcumin within the lipid particles, that were already separately examined for their sole entrapment within the respective carriers, did not compromise the encapsulation efficiency/loading capacity for either active. Evaluation of the simultaneous co-release confirmed that the active co-encapsulation bears no significant effect on the vehicles' behaviour. In addition, the formed system was able to maintain its performance over a storage period of 1 month, further supporting its potential as a promising co-encapsulation/co-delivery formulation.

7.2 Areas for future work

In line with the conclusions presented above and aiming to extend the understanding and characterisation of the novel Pickering emulsion co-encapsulation and co-delivery vehicle developed in this thesis, there are certain areas that provide motivation for future work.

Investigation and visualisation of the lipid particle internal structure and arrangement at the emulsion droplet interface

As discussed throughout this manuscript, particularly in Chapters 3 and 6, the lipid particles' structural features both in terms of their compositional elements and the arrangement of these constituents within the particle matrix, can greatly affect their active encapsulation and delivery performance. This is an impact that is not only imparted while the particles are within the dispersions, but also persists when the particles are introduced in the emulsions. Although the lipid particles consist of a seemingly simple core, comprising of the lipid building blocks,

surface active species and the encapsulated active, the components assembly within the lipid matrix is not yet fully elucidated.

Attempts have been previously made to understand how incorporation of the liquid lipid at increasing concentration in the NLCs microstructure influences the particles' properties and visualise its distribution within the particle matrix, using a range of different characterisation techniques [1–4]. However, it has not been possible still to capture the exact structural arrangement, possibly due to the small size of the particles and the added complexity of the active incorporation. Recently, a form of confocal microscopy that offers much faster acquisition times and three-dimensional imaging, known as coherent anti-Stokes Raman scattering (CARS), was employed for the visualisation of solid lipid microparticles [5]. Combination of CARS with electron microscopy allowed imaging of the particles' internal structure and distribution of the encapsulated protein within the matrix. Therefore, it could be proposed that implementation of these techniques for the systems developed in this work could provide insight on the components' positioning within the particles' matrix, and whether any migration can be observed during storage, alongside the timescales/rates involved in that. Taking this a step further it would also be compelling to investigate how this arrangement changes once the particles are residing at the emulsion droplet interface, immediately after preparation and over time. This sort of information could enable a more rationalised design and development of microstructures tailored to specific applications.

Devising approaches to trigger the release from particles and particle stabilised-emulsions

In this work, the approach taken regarding the evaluation of the lipid particles and lipid particle-stabilised emulsions release behaviour was confined to the fundamental discernment of the

vehicles' performance, without the contribution of external stimuli. Considering the end application of these carriers as a pharmaceutical product, and the plethora and complexity of different environments that these systems would be exposed to once administered, studying their response at varying conditions would be an integral part of their characterisation. Apart from gaining information about the fate of the systems under the specific environmental factors (e.g. pH, temperature, enzymatic presence), such knowledge could also be employed to modify the structural composition of the formulation in such a way that would ultimately constitute a means of tuning the release performance. An example of this would be the investigation of lipid particles and particle-stabilised emulsions under different temperatures according to previous work in this area [6], whereby understanding the systems' response to this stimulus could inform the selection of lipid wall materials with the desired response (i.e. partial or full melting).

Utilising a standardised dissolution apparatus

Although the technique employed to quantify the active release in this work proved to be an adequate approach in understanding the performance of the active carriers, it would certainly be appropriate to adopt a standardised and more industrially-acceptable/relevant apparatus in future experiments. Usage of a universally acceptable method of assessing dissolution, that is able to mimic physiochemical conditions and mechanical forces experienced by pharmaceutical products in the gastrointestinal tract, could potentially provide more representative active release results. An example of such dissolution apparatuses could be the ones used for dissolution testing as per the United States Pharmacopeia (USP), or equivalent.

Tailoring towards a more application-oriented system

A natural next step, following the characterisation of the system and the findings of the present work, would be the customisation of the formulation to the requirements of a specific purpose. Though there are copious application possibilities and active ingredient combinations that such a formulation could be utilised to serve, owing to its easily tuneable properties, one of the areas that this system could be tested for its suitability would be the development of a palatable oral liquid formulation [7,8]. On the basis of being able to facilitate the independently controlled and at different timescales delivery of multiple active molecules, one of the encapsulated species could be a taste-masking active (water-insoluble flavouring agents e.g. fruit essences) that could be releasing fast and in response to the oral physiological conditions, to mask the bitter/unpleasant taste of the secondary active. Though certain level of structural tuning and characterisation would be required, such formulation could significantly aid surmounting palatability and treatment adherence hurdles in paediatric, geriatric and other patient populations that require oral intake of liquid formulations.

Extending to more than two active ingredients

Attempting to harness the full potential of this truly modular system, it could be possible to co-encapsulate more than two actives within its compartmentalised structure, as previously accomplished employing multicompartmental triple emulsions [9]. The approach taken to achieve such an endeavour would be to develop two independently formulated types of lipid particles that would encase two different active ingredients, that would then both be used to stabilise emulsion droplets encasing a third active. Provided that detailed elucidation of the vehicles' properties and performance would be performed, the particles' characteristics could be even controlled to trigger three independently controlled active release profiles.

References

[1] K. Jores, W. Mehnert, K. Mäder, Physicochemical investigations on solid lipid nanoparticles and on oil-loaded solid lipid nanoparticles: A nuclear magnetic resonance and electron spin resonance study, Pharm Res. 20 (2003) 1274–1283. https://doi.org/10.1023/a:1025065418309.

[2] K. Jores, A. Haberland, S. Wartewig, K. Mäder, W. Mehnert, Solid lipid nanoparticles (SLN) and oil-loaded SLN studied by spectrofluorometry and Raman spectroscopy, Pharm Res. 22 (2005) 1887–1897. https://doi.org/10.1007/s11095-005-7148-5.

[3] K. Jores, W. Mehnert, M. Drechsler, H. Bunjes, C. Johann, K. Mäder, Investigations on the structure of solid lipid nanoparticles (SLN) and oil-loaded solid lipid nanoparticles by photon correlation spectroscopy, field-flow fractionation and transmission electron microscopy, Journal of Controlled Release. 95 (2004) 217–227. https://doi.org/10.1016/j.jconrel.2003.11.012.

[4] N. Izza, N. Watanabe, Y. Okamoto, K. Suga, Y. Wibisono, N. Kajimura, K. Mitsuoka, H. Umakoshi, Dependence of the Core-Shell Structure on the Lipid Composition of Nanostructured Lipid Carriers: Implications for Drug Carrier Design, ACS Appl Nano Mater. 5 (2022) 9958–9969. https://doi.org/10.1021/acsanm.2c02214.

[5] P.C. Christophersen, D. Birch, J. Saarinen, A. Isomäki, H.M. Nielsen, M. Yang, C.J. Strachan, H. Mu, Investigation of protein distribution in solid lipid particles and its impact on protein release using coherent anti-Stokes Raman scattering microscopy, Journal of Controlled Release. 197 (2015) 111–120. https://doi.org/10.1016/j.jconrel.2014.10.023.

[6] S.M. Dieng, N. Anton, P. Bouriat, O. Thioune, P.M. Sy, N. Massaddeq, S. Enharrar, M. Diarra, T. Vandamme, Pickering nano-emulsions stabilized by solid lipid nanoparticles as a temperature sensitive drug delivery system, Soft Matter. 15 (2019) 8164–8174. https://doi.org/10.1039/c9sm01283d.

[7] A. Cram, J. Breitkreutz, S. Desset-Brèthes, T. Nunn, C. Tuleu, Challenges of developing palatable oral paediatric formulations, Int J Pharm. 365 (2009) 1–3. https://doi.org/10.1016/j.ijpharm.2008.09.015.

[8] H.K. Batchelor, J.F. Marriott, Formulations for children: problems and solutions, Br J Clin Pharmacol. 79 (2015) 405. https://doi.org/10.1111/bcp.12268.

[9] X.W. Chen, X.Y. Ning, X.Q. Yang, Fabrication of Novel Hierarchical Multicompartment Highly Stable Triple Emulsions for the Segregation and Protection of Multiple Cargos by Spatial Co-encapsulation, J Agric Food Chem. 67 (2019) 10904–10912. https://doi.org/10.1021/acs.jafc.9b03509.